ENERGY EFFICIENT CONTROL AND OPTIMISATION TECHNIQUES FOR DISTILLATION PROCESSES

Funmilayo Nihinlola OSUOLALE

A thesis submitted for the degree of Doctor of Philosophy

School of Chemical Engineering and Advanced Materials
Newcastle University
United Kingdom

July, 2015

ABSTRACT

Distillation unit is one of the most energy intensive processes and is among the major CO_2 emitter in the chemical and petrochemical industries. In the quest to reduce the energy consumption and hence the environmental implications of unutilised energy, there is a strong motivation for energy saving procedures for conventional columns. Several attempts have been made to redesign and heat integrate distillation column with the aim of reducing the energy consumption of the column. Most of these attempts often involve additional capital costs in implementing. Also a number of works on applying the second law of thermodynamics to distillation column are focused on quantifying the efficiency of the column. This research aims at developing techniques of increasing the energy efficiency of the distillation column with the application of second law using the tools of advanced control and optimisation. Rigorous model from the fundamental equations and data driven models using Artificial neural network (ANN) and numerical methods (PLS, PCR, MLR) of a number of distillation columns are developed. The data for the data driven models are generated from HYSYS simulation. This research presents techniques for selecting energy efficient control structure for distillation processes. Relative gain array (RGA) and relative exergy array (REA) were used in the selection of appropriate distillation control structures. The viability of the selected control scheme in the steady state is further validated by the dynamic simulation in responses to various process disturbances and operating condition changes. The technique is demonstrated on two binary distillation systems. In addition, presented in this thesis is optimisation procedures based on second law analysis aimed at minimising the inefficiencies of the columns without compromising the qualities of the products. ANN and Bootstrap aggregated neural network (BANN) models of exergy efficiency were developed. BANN enhances model prediction accuracy and also provides model prediction confidence bounds. The objective of the optimisation is to maximise the exergy efficiency of the column. To improve the reliability of the optimisation strategy, a modified objective function incorporating model prediction confidence bounds was presented. Multiobjective optimisation was also explored. Product quality constraints introduce a measure of penalization on the optimisation result to give as close as possible to what obtains in reality. The optimisation strategies developed were applied to binary systems, multicomponents system, and crude distillation system. The crude distillation system was fully explored with emphasis on the preflash unit, atmospheric distillation system (ADU) and vacuum distillation system (VDU). This study shows that BANN models result in greater model accuracy and more robust models. The proposed

techniques also significantly improve the second law efficiency of the system with an additional economic advantage. The method can aid in the operation and design of energy efficient column.

DEDICATION

This thesis is dedicated to the glory of God the Father, Son and Holy Spirit my help in ages past and my hope for years to come.

To my daughters Tolu, Temi and Tobi for their hopes and aspirations

ACKNOWLEDGMENT

I appreciate my able and dynamic supervisor Dr. Jie Zhang for his timely suggestions, guidance and encouragement. I count myself fortunate to be learning from someone of great expertise and embodiment of knowledge as he. I am indebted to Dr. Lv of the Institute of Process Control,Department of Automation,Tsinghua University,China for his help on the HYSYS simulation. Mention must also be made of staff member and students of the school of Chemical Engineering, Newcastle University for their immeasurable input directly or indirectly in seeing to the success of this work. May God bless you all.

I am also grateful to the Commonwealth scholarship commission in the United Kingdom for sponsoring this research and my home University, Ladoke Akintola University of Technology, Ogbomoso, Nigeria for granting me study leave.

I cannot but extend my appreciation to my husband Mike and my girls TOluwanimi, Temitayo and Oluwatobi for their supports and sacrifice of love and having to cope with an absentee wife and mum. We shall all live to enjoy the better years ahead. I appreciate my loving parents Rev Dr. and Evang. (Mrs) Amuda for loving me and cheering me on to attain great heights in life. May you live to eat and enjoy the fruits of your labours.

And now most importantly, to God the author and the giver of life, my help in ages past and my hope for years to come who has for now blessed me with these be glory, honour and adoration.

TABLE OF CONTENTS

LIST OF FIGURES

LIST OF TABLES

NOMENCLATURES

A, B	Pure component density correlation constants
C	Total number of component
CO	Controller output
e	Control error
Ex	Exergy rate, $kJhr^{-1}$
F_j	Feed rate to the *jth* stage
$G(s)$	Transfer function
h	Specific enthalpy, $kJkmol^{-1}$
h_i^L	Liquid pure component specific enthalpy
h_i^v	Vapour pure component specific enthalpy
h_j	Liquid enthalpy from stage *j*, $kJkmol^{-1}$
$\bar{h}_{0i}$	Partial specific enthalpy of the component at reference conditions, $kJkmol^{-1}$
H_j	Vapour enthalpy from stage *j* $kJkmol^{-1}$
H_{vap}	Heat of vapourisation,
I	Irreversibility. $kJhr^{-1}$
K_c	Controller gain
K_i	Equilibrium constant for component *i*
K_{ji}	Equilibrium constant for component *i* on the *jth* stage
L_j	Liquid rate from jth stage
m	Molar flow, $kmolhr^{-1}$
M_L	Molecular weight of liquid mixture, (lb/lbmol)
M_i	Molecular weight of pure component, (lb/lbmol)
M_j	Liquid hold up on the jth stage
N	Total number of stages

P	Total pressure, kpa
p_{ci}	Critical pressure of component i, (psia)
p_i^{sat}	Saturated pressure for component i
P	System pressure, (psia)
P_0	Reference pressure, kpa
P_U	Ultimate period
Q_z	Net heat transferred, $kJhr^{-1}$
R	Ideal gas constant, $kJkmol^{-1}K^{-1}$
s	Specific entropy, $kJkmol^{-1}K^{-1}$
$\bar{s}_{0i}$	Partial specific entropy of the component at reference conditions, $kJkmol^{-1}K^{-1}$
t	time, s
T	System temperature, ^oR
T_{ci}	Critical temperature of component i , ^oR
T_j	Temperature on the *jth* stage
T_0	Reference temperature, K
T_r	Reduced temperature
ΔU	Change in manipulated variable
u_i	Weighted input to a neuron
V_j	Vapour rate from *jth* stage
w_i	Aggregated network weight for BANN
W^b	Network weight for bootstrap sample
W_s	Net external work transferred
x_i	Neural network input
X	Predictor variables
y_i	Mole fraction of component *i* in the vapour state
y_{ji}	Mole fraction of ith component in the vapour state on stage *j*
Δy	Change in the controlled variable

Y	Response variables
Z_j	Mole fraction of component j

Greek Letters

α_{ij}	Relative volatility
β	Coefficients of predictor variables
θ	Model parameter
ϑ	Neuron output
μ	Ultimate gain
π	Constant
ρ_i	Pure component liquid density, lb/ft^3
ρ_L	Density of liquid mixture, lb/ft^3
v_{ji}	Vapour flow rate of ith component from *jth* stage
σ	Entropy production
τ_i	Integral time
τ_D	Derivative time
φ	Exergy efficiency, %
$\overline{\emptyset}_{iL}$	Partial fugacity coefficient of a specie in a mixture *i* liquid state
$\overline{\emptyset}_{iv}$	Partial fugacity coefficient of a specie in a mixture *i* liquid state
Φ	Neuron activation function
χ_i	Mole fraction of component *i* in the liquid state
χ_{ji}	Mole fraction of ith component in the liquid state on stage *j*
γ_i	Activity coefficient
ω_c	Critical frequency
ω_i	Accentric factor

Subscripts

chem	Chemical
$0i$	component *i* at reference conditions
0	Reference conditions
i	Component *i*, controlled variable *i* or neural network input variable *i*
ij	Component *i* on tray *j*
iL	Component *i* in liquid state
n	counter
phy	Physical
iv	Component *i* in vapour state

Superscripts

sat	Saturated
L	Liquid state
V	Vapour state
-	Partial condition

ABBREVIATIONS

ADU	Atmospheric distillation unit
AGO	Atmospheric gas oil
ANN	Artificial neural network
BANN	Bootstrap aggregated neural network
BLS	Batch least square
BP	Bubble point
CDU	Crude distillation unit
COT	Coil outlet temperature
DMC	Dynamic matrix control
DOE	Department of energy
DRGA	Dynamic relative gain array
EEF	Exergy ecoefficiency factor
ERGA	Effective relative gain array
FUG	Fenske-Underwood-Gilliland
GA	Genetic Algorithm
GCC	Grand composite curve
HGO	Heavy gas oil
HIDC	Heat integrated distillation column
MAC	Model algorithm control
MIMO	Multi-input multi-output
MLR	Multiple linear regression
MPC	Model predictive control
NAICS	North America Industry Classification System
PCA	Principal component analysis
PCR	Principal component regression

PLS	Partial least square
REA	Relative exergy array
REDA	Relative exergy destroyed array
RGA	Relative gain array
RNGA	Relative normalized gain array
RTO	Real time optimization
SR	Sum of rates
SHRT	Self-heat recuperation technology
VDU	Vacuum distillation unit
VLE	Vapour liquid equilibria

CHAPTER 1: INTRODUCTION

1.1 Preamble

The most widely used separation technique (contrary to predictions of being superseded by other separation technique) in the chemical and petrochemical industry is distillation. It is however a highly energy intensive process and contributes significantly to the capital investment in chemical and petrochemical industries. Of all the industries, the refinery industry is one of the most highly energy intensive industries with the cost of energy for heat and power accounting for 40% of the operating costs (White, 2012) and 3 % of the world energy consumption (Humphrey and Siebert, 1992). Crude in its original state is of limited value until it is separated into its constituents which may be further processed and distillation processes are used extensively in achieving this separation, thus make refinery processes an energy intensive processes. According to the North America Industry Classification System (NAICS), the petroleum refineries consumed 3.1 quadrillion Btu in 2002, almost 20% of the fuel energy consumed by the U.S. About 35% of this is consumed in two types of distillation processes in the refinery, the atmospheric crude distillation unit (ADU) and vacuum distillation unit (VDU) (Sankaranarayanan *et al*., 2010). It can be concluded that operating costs of distillation column are often a major part of the total operating cost of the refinery. Developing effective and reliable system for the efficient operation of the distillation unit is therefore of paramount importance.

Process intensification of distillation unit has always attracted the interest of researchers and quite a number of publications have been focused on ways to reduce the energy consumption of distillation processes via alternate energy efficient arrangements. Of note amongst these are the petyluk column (Amminudin *et al.*, 2001), heat integrated distillation column (HIDC) (Nakaiwa *et al.*, 2003, Amiya, 2010), thermally coupled dividing wall column and intensified distillation column (Errico et al., 2009, Vazquez–Castillo *et al*., 2009). Conventional distillation column sequences with minimum energy consumption has also been studied (Aguirre *et al.*, 1997). The column configuration that will consume the least total energy was studied and a number of examples were presented to substantiate the proposed methodology. Heat integration has also been the focus of some researchers with emphasis on where to place or not place side reboilers or side condensers (Bandyopadhyay, 2007, Mascia *et al*., 2007), exchange of heat between crude distillation unit and delay coking unit of a refinery (Plesu *et al.*, 2003) and focus on the self-heat recuperation for a crude distillation unit (Kansha *et al.*, 2012).

Furthermore, attempts at understanding the happenings within the column that could lead to increased energy efficiency has led to the application of first and second laws of thermodynamics to the analysis of the column. Previous works on the thermodynamic efficiency of the crude distillation unit revealed a high energy and exergy loss of the column with the overall efficiency of the column ranging from 5-23% (Rivero *et al*., 2004, Al-Muslim *et al*., 2003, Al-Muslim and Dincer, 2005). This shows that there is a lot of room for improvement of the energy efficiency of distillation columns and indicates a high entropy generation within the column is making the irreversibility of the column to be highly significant. In the past, there have been efforts at devising methods of minimising entropy production rate in distillation columns. (Mullins and Berry, 1984, Ogunnaike and Ray, 1994, Ratkje *et al*., 1995, Aguirre *et al*., 1997, de Koeijer *et al*., 2002). One of such attempts is targeted at diabatic binary distillation systems (de Koeijer *et al*., 2002). The issue of energy conservation in distillation processes has always been important in both academia and industry. Ways of minimising energy usage have been studied extensively in recent years. These include the use of self-heat recuperation technology (SHRT) (Kansha *et al*., 2012, Matsuda *et al.*, 2011). In this method, two compressors are installed in the overhead for the reflux stream and the overhead product stream. The authors suggested that SHRT was able to reduce the energy consumption of the column significantly. Nakkash (2011) demonstrated that a 20% saving in total energy consumption was possible in multicomponent distillation by using a heat pump with and without split tower techniques. An energy saving of about 12.6% in the condenser duty by introducing the vapour feed into the upper stages of distillation column was proposed by (Arjmand *et al.*, 2011). The proposal was conducted on an industrial case of crude distillation unit using ASPENHYSYS for simulation.

Efficient operation of the distillation unit cannot be over emphasised. A slight improvement in thermal efficiency of the unit can make a large difference in profitability. It has been observed that a 10% energy saving in distillation column is equivalent to about 100,000 barrels of petroleum per day (Fitzmorris and Mah, 1980). Energy generation leads to release of greenhouse gas (GNG) especially in developing countries that are just coming up industrially leading to environmental pollution and thus defeating the concept of sustainable development (Dincer and Rosen, 1998, Dincer, 1998). Improved efficiency of chemical processes is one of the ways of reducing the GNG. Also, improved efficiency of distillation column will result in better yield of

product and improved product quality. It will also reduce the consumption of energy and thereby lengthen the depleting energy reserve.

1.2 Motivation

Although distillation process has been extensively studied by researchers, the issue of energy efficiency still remains an unresolved. Determination of minimum energy requirements for a distillation process is useful in the design stage. This is because a high energy requirement in distillation column culminates in a high number of stages and increases the complexity and subsequently the cost of the column. An initial understanding of the minimum energy for a separation process gives room for the understanding of its cost implication as there is a direct relationship between the minimum energy and the diameter and length of the column. The basic question therefore is how can a column's minimum energy requirement be determined right from the design stage? How can this minimum energy requirement be actualised in the operation of the column especially for the special case of multicomponent non ideal system?

There is a need to develop a model that will evolve methods of column improvement which will incorporate the principle of second law analysis in determining points of inefficiency in the column, bring about a control mechanism of the unit to achieve the optimum energy efficiency and develop optimization procedures aimed at minimising the inefficiencies without compromising the qualities of the products.

This research work is focused on novel methods of increasing the efficiency of distillation units either in the simple binary system or the complex crude distillation system of the refinery by the application of second law principle using the tools of advanced control and optimisation. This increased efficiency can then translate to reduction in the energy requirements of the column.

1.3 Aim and Objectives

The main aim of this research work is to develop energy efficient operating techniques for distillation columns.

Briefly, the objectives can be itemised as

- Develop rigorous and data driven models of distillation columns

- Develop methodology for energy efficient control structure selection of distillation columns
- Develop methods of incorporating exergy analysis in optimising the energy efficiency of distillation columns
- Investigate, compare and further improve the reliability of the optimisation procedures

1.4 Contributions

In this thesis, the contribution is on developing methods to bring about the application of second law analysis to improve the energy efficiency of various forms of distillation columns. Past studies in examining the second law analysis of distillation columns has been majorly focused on quantifying its energy and exergy efficiency and pinpointing the area of the column with most exergy loss. This study goes a step further to use exergy analysis not only as an analytical tool but also a retrofitting and a design tool in improving the exergy efficiency of the distillation unit.

In selection of energy efficient control structures for distillation columns, relative exergy array (REA) has been used in some past work. However, detailed analysis of the control structure in the steady and dynamic state is lacking. This study presents methods of selecting energy efficient control structures in the steady state and validating the methods in the dynamic state.

This study also presents an optimisation framework based on exergy analysis to improve the energy efficiency of distillation column. Bootstrap aggregated neural network (BANN) is presented in this study for enhanced model accuracy. This is in lieu of artificial neural network (ANN) which has been commonly used in past studies. The presented techniques were applied on a wide range of columns from the simple binary system to more complex crude distillation systems with remarkable results.

Usually, to improve the process unit, design and process engineers often use advance control and optimisation in lieu of designing new processes because of its cost implications. This study introduces a new way of controlling and optimising the column using the second law of thermodynamics.

The contributions in each chapter that make up the thesis are outlined in the next section.

1.5 Structure of the thesis

In Chapter 2, the knowledge gap on energy efficiency of chemical processes, distillation systems and application of thermodynamics analysis is highlighted. The theory on which the research is based on and a general review of literatures related to the research is presented.

Chapter 3 is focused on modelling and the choice of the models used in this research. Rigorous models and dynamic models of distillation column are presented as well as method of solution of the models. Linear data driven models such as multiple linear regression (MLR), principal component regression (PCR) and partial least square (PLS) are discussed. Artificial neural network model are also discussed extensively.

In Chapter 4, energy efficient control strategies based on relative gain array (RGA) and relative exergy array (REA) was discussed. The developed method incorporates energy efficiency in control structure selection. Detailed analysis of the control structures in the steady and dynamic states is reported. Application of the methods to binary distillation systems was highlighted.

In Chapter 5, a neural network based strategy for the modelling and optimisation of distillation columns incorporating the second law of thermodynamics was discussed. Neural network models for exergy efficiency and product compositions are developed from simulated process operation data and are used to maximise exergy efficiency while satisfying product quality constraints. Applications to binary and multicomponent systems demonstrate the effectiveness of the method. Bootstrap aggregated neural network (BANN) is introduced

In Chapter 6, Bootstrap aggregated neural network (BANN) was further elaborated for enhanced model accuracy. Multiobjective optimisation of the column based on BANN was developed. Application to a complex system of crude distillation unit (comprising of atmospheric distillation unit and vacuum distillation unit) was discussed. A further study on effect of preflash unit (preflash drum and preflash column) on the crude distillation unit was also made.

Chapter 7 is focused on highlighting the conclusions from the research and recommendations for further work.

1.6 Publications

Published journal papers

1. Funmilayo Osuolale and Jie Zhang (2015), "Distillation control structure selection for energy efficient operations", *Chemical Engineering and Technology*, Vol.38, No.5, 907-916, (DOI): 10.1002/ceat.201400707

2. Funmilayo Osuolale and Jie Zhang (2015), "Energy efficiency optimisation for distillation column using artificial neural network models", *Energy*, (submitted for publication)

3. Funmilayo Osuolale and Jie Zhang (2015), "Energy Efficient Optimisation Techniques For Crude Distillation Systems. Part I : Atmospheric Distillation Unit" (submitted for publication)

4. Funmilayo Osuolale and Jie Zhang (2015), "Energy Efficient Optimisation Techniques For Crude Distillation Systems. Part II : Crude Distillation Unit" (submitted for publication)

Conference peer reviewed papers

1. Funmilayo Osuolale and Jie Zhang (2014) "Energy efficient control and optimisation of distillation column using artificial neural network" Chemical Engineering Transactions, vol 39, 37-42.

2. Funmilayo Osuolale and Jie Zhang (2015) "Multiobjective optimisation of atmospheric crude distillation system operations based on bootstrap aggregated neural network models" Computer aided chemical engineering, vol 37, 671-676.

3. Funmilayo Osuolale and Jie Zhang (2015) "Exergetic Optimisation of Atmospheric and Vacuum Distillation System Based on Bootstrap Aggregated Neural Network Models" To be published.

Conference presentations

1. Funmilayo Osuolale and Jie Zhang (2013) Energy efficient operations of binary distillation column", Northern Postgraduate Chemical Engineering Conference (NPCEC), 8-9, August, Newcastle University, UK

2. Funmilayo Osuolale and Jie Zhang (2013) "Energy efficient control of distillation process", 13AIChE Annual meeting, November 3-8, San Francisco, California, USA

3.Funmilayo Osuolale and Jie Zhang (2014) " Energy efficient control and optimization of distillation process using artificial neural network", 21st International Congress of Chemical and Process Engineering CHISA 2014 Prague 17th Conference on Process Integration, Modelling and Optimisation for Energy Saving and Pollution Reduction PRES 2014 , 23-27 August 2014 Prague, Czech Republic

4. Funmilayo Osuolale and Jie Zhang (2015) "Exergetic optimization of atmospheric and vacuum distillation system based on bootstrap aggregated neural network models" The seventh international exergy, energy and environment symposium, IEEES7, 27-30, April, Valenciennes, France

5. Funmilayo Osuolale and Jie Zhang, (2015) "Multiobjective optimization of atmospheric crude distillation system operations based on bootstrap aggregated neural network models" 12th PSE and 25th ESCAPE joint conference, 31May - 4th June, Copenhagen, Denmark.

CHAPTER 2: LITERATURE REVIEW

2.1 Distillation processes

Distillation is the separation of a mixture into its different constituents due to boiling point difference. The process could be batch or continuous. In batch distillation the feed is fed to the distillation tower, the products are removed one at a time until the distillation process is ended. Continuous distillation on the other hand separates large quantities of mixture such as those found in the chemical and petrochemical industries. The feed are fed continuously to a distillation tower and the products or fractions are withdrawn continuously at the same time from the different stages of the tower. A distillation process that separates only two distinct products is said to be binary distillation while multicomponent distillation has at least three products from the separation process.

Crude oil distillation is a multicomponent, continuous distillation process. Crude oil is made up of a mixture of different hydrocarbons and sometimes referred to as fractions. The separation of these fractions based on boiling point differences is referred to as fractionation. The distillation process does not produce a product of a distinct boiling point rather it produces fraction based on a boiling point range. Each fraction can be further separated into a number of components. For example the naphtha product from the top of the Atmospheric distillation (ADU) column of the refinery can be separated to liquefied petroleum gas (LPG) such as propane, butane etc. while the residue from the bottom can be further distilled to more products in the Vacuum distillation unit. A distillation tower is a series of distillation process with tray such as sieve and bubble gas stacked on each other or with a series of packings such as Raschig ring and Berl saddle. The feed is introduced to the column at its flash point where a portion of the feed vaporises. The portion above the flash zone is the rectifying section and the lower part is the stripping section. Figure 2.1 shows a schematic diagram of a distillation column. At the onset of separation process within the distillation tower, the openings on each tray allows the vapour to travel up the column and as the vapour comes in contact with the liquid, the heavier part of the vapour are condensed back to the liquid state and the lighter part move up the column. The tray is built with weirs that allow liquid to be retained; liquid that overflows the weirs flows into the downcomer and moves down the column. The heavier fractions that may still be retained in the upper part of the column are condensed by the external reflux to give a higher purity of product while the lighter fraction in the bottom of the column are vaporised by the reboiler.

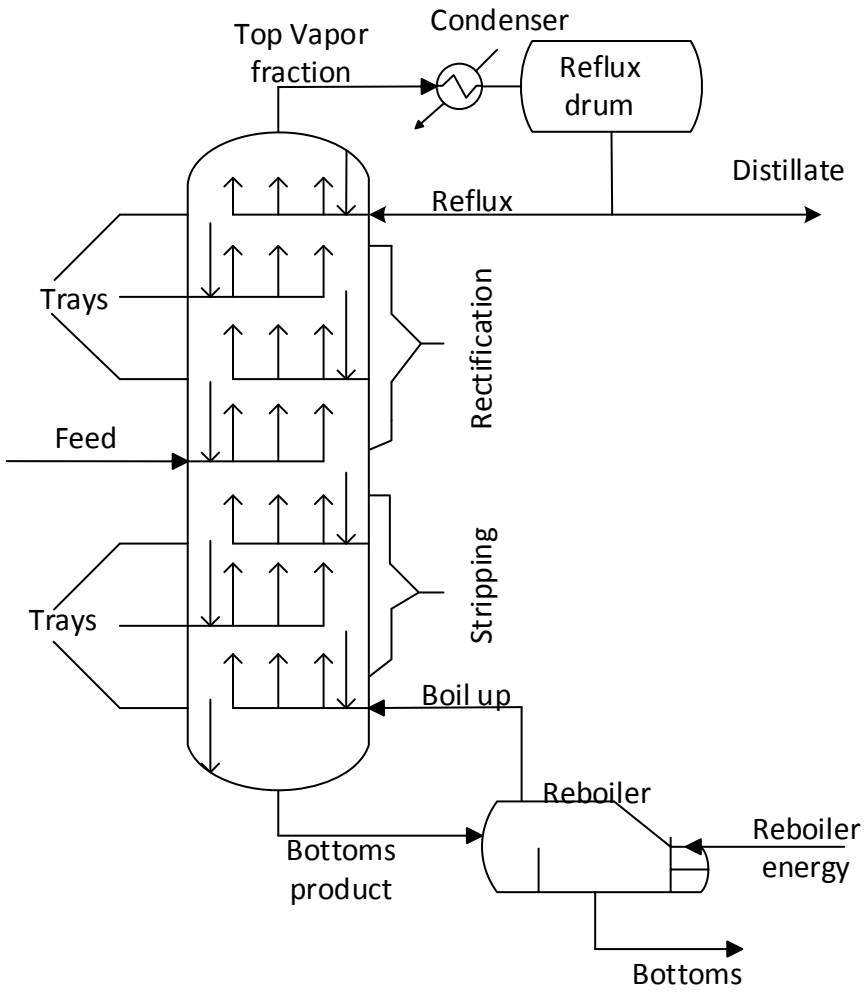

Figure 2.1 : Schematic diagram of a distillation column

2.2 Vapour liquid equilibrium (VLE) and distillation

Processes such as distillation bring phases of different compositions into contact. When the phases are not in equilibrium, mass transfer between the phases alters the composition. The rate of change of compositions in different phases depend largely on the deviation from equilibrium hence the equilibrium temperature, phase composition and pressure is of great importance. The tendency for given chemical species to co-exist in the liquid and vapour phase is defined as its equilibrium ratio.

Equilibrium ratio is the ratio of vapour to liquid phase of mole fraction of species. The constant for the expression of this ratio is K

$$K_i = \frac{y_i}{\chi_i} \qquad 2.1$$

Where K_i is the equilibrium constant, y_i is the mole fraction of species i in the vapour state and χ_i is the mole fraction of species i in the liquid state

For an ideal mixture, Raoult's law applies

$$P = \sum \chi_i p_i^{sat} \qquad 2.2$$

Where P is the total pressure and p_i^{sat} is the saturated pressure for component i

$$P = \frac{1}{\sum y_i / p_i^{sat}} \qquad 2.3$$

If constant relative volatility applies,

$$\alpha_{ij} = \frac{K_i}{K_j} = \frac{y_i/\chi_i}{y_j/\chi_j} \qquad 2.4$$

For non ideality of the liquid phase, a more rigorous VLE data is required in terms of activity coefficient and it is given as

$$K_i = \frac{\bar{\emptyset}_{iL}}{\bar{\emptyset}_{iV}} \qquad 2.5$$

where $\emptyset_{iL} = \frac{\bar{f}_{iL}}{\chi_i P}$ and $\bar{f}_{iL} = \gamma_{iL}\chi_i f_{iL}^0$

$\gamma_{iL} \equiv \frac{a_{iL}}{\chi_i}$

$a_{i \equiv \frac{\bar{f}_i}{f_i^0}}$

$\bar{\emptyset}_{iL}$ implies partial fugacity coefficient of a specie in a mixture

$\bar{f}_{iL}$ implies partial fugacity

γ_{iL} activity coefficient

a_i is the activity

For a simplified system where the pressure is low (<150psia) and the vapour phase is close to ideal, it can be safely assumed that

$$y_i P = \gamma_i \chi_i P_i^{sat} \qquad 2.6$$

The liquid activity coefficient will be modelled by a correlating equation such as Wilson, Van Laar, NRTL, or UNIQUAC (Gmehling and Onken, 1991).

Pure component pressure will be modelled from Antoine equation.

2.2.1 Enthalpy

Usually enthalpy of the vapour and liquid stream should be calculated as functions of temperature, pressure and composition of each stream. However, because liquid are incompressible and if low to moderate pressure system is assumed, then the enthalpy is calculated as function of temperature and composition based on a linear fit of heat capacity with temperature.

$$h_i^L = A_i^L T + B_i^L T^2 \quad 2.7$$

$$h_i^v = A_i^v T + B_i^v T^2 + \Delta H_i^v \quad 2.8$$

h_i^L , h_i^v implies liquid and vapour pure component specific enthalpy

A, B implies the correlation constants

ΔH_i^v implies pure component heat of vapourisation at reference temperature (0^oF in this case)

For multicomponent systems, mixing rule applies. The molar average of the pure component enthalpy is the vapour enthalpy while for liquid enthalpy, non idealities is accounted for by heat of mixing.

$$h_{mix}^L = -RT^2 \sum_i \chi_i \frac{\partial ln\gamma_i}{\partial T} \quad 2.9$$

Vapour and liquid enthalpy for mixture therefore is given as

$$h^v = \sum_i y_i h_i^v$$

$$h^L = \sum_i \chi_i h_i^L + h_{mix}^L$$

2.2.2 Liquid Density

Pure component liquid density is given as

$$\rho_i = AB^{-(1-T_r)^{2/7}} \quad 2.10$$

$$\rho_L = M_L / \left(\sum_i \frac{\chi_i M_i}{\rho_i}\right) \quad 2.11$$

Where ρ_i = pure component liquid density (lb/ft^3)

ρ_L = density of liquid mixture (lb/ft^3)

M_L = molecular weight of liquid mixture (lb/lbmol)

M_i = molecular weight of pure component (lb/lbmol)

T_r = reduced temperature

A, B = Pure component density correlation constants

Francis weir equation for liquid hydraulics is given as

$L_n = C\rho_n^L w_{len} H_{ow}^{1.5}$ (C is a constant for unit conversion) 2.12

Method for accurate prediction of equilibrium constant is of great interest in the correct modelling of a crude distillation unit (Tarighaleslami *et al.*, 2011). There are many approaches to obtaining the K value. This could be from experimental measurements, use of correlations (empirical) such as nomographs and use of Equation of state (EOS).

Methods based on EOS and empirical correlations are explored further. Correlations that could be applicable for the predictions of K value for crude mixtures at low pressure and high pressure include but not limited to the following.

Wilson correlation (Wilson, 1968)

$$K_i = \frac{p_{ci}}{P} exp[5.37(1 + \omega_i)(1 - T_{ci}/T)] \quad 2.13$$

Where p_{ci} is the critical pressure of component i (psia)

T_{ci} is the critical temperature of component i (^{o}R)

ω_i is the acentric factor of component i

T is the system temperature (^{o}R)

P is the system pressure (psia)

Whitson and Torp modified Wilson correlation to allow for composition induced effects at high pressure by incorporating the convergence pressure P_k (Whitson and Torp, 1983).

$$K_i = \left(\frac{p_{ci}}{P_k}\right)^{A-1} \frac{p_{ci}}{P} exp[5.37A(1 + \omega_i)(1 - T_{ci}/T)] \quad 2.14$$

where

$$A = 1 - \left(\frac{p-14.7}{p_k-14.7}\right)^{0.6}$$

Almehaideb further modified Whitson and Torp to give (Almehaideb *et al*., 2001, Almehaideb *et al.*, 2003)

$$K_i = \left(\frac{p_{ci}}{P_k}\right)^{A-1} \frac{p_{ci}}{P} exp[A \times K_i^*] \qquad 2.15$$

Where $K_i^* = \frac{a_{T1}}{T^2} + \frac{a_{T2}}{T} + a_{T3} + a_{p1} lnp + \frac{a_{p2}}{p^2} + \frac{a_{p3}}{p} + \frac{a_w}{w}$

$a_{T1}, a_{T2}, a_{T3}, a_{p1}, a_{p2}, a_{p3}$ are constants

Almehaideb et al., (2003) opined that the correlation based on PVT analysis of crude oil supersedes that of Wilson, Whison and Torp, and Peng-Robinson. He concluded that the K values from Wilson correlation were underestimated for C4 to C7+ and overestimated for N2. Also, the Whitson and Torp correlation underestimated the K values for C7+ and overestimated the K values of non-hydrocarbon (Mittal *et al.*, 2011).

For low pressure of under 100psia, Standing correlation and Wilson correlation were considered in the work of Almehaideb and were found to compare relatively well with the extracted K values from the new work.

To determine K value, some Hydrocarbon properties need to be determined. These properties include critical temperature, critical pressure, acentric factor etc. Several methods of estimating parameters for the evaluation of K value are available in the literatures. Of note is the methods of Riazi and Daubert; and Edmister (Edmister, 1938, Riazi and Daubert, 1987).

The VLE data are of paramount importance in the modelling of distillation unit because it has great impact on the accuracy of the model.

2.3 Thermodynamics

Thermodynamics is a concept derived from the two words thermo and dynamics, which means heat in motion. It was limited to heat engines of which the steam engine was an example but now is applicable in determining heat and work effects associated with processes in terms of obtainable maximum work from a process or minimum work required for processes. It is also applicable in describing relationships among variables for a process in equilibrium. The history of thermodynamics could be dated back to the 18th century when James Watts in 1769 built the first steam engine and thus starting the

development of heat engines (Wall, 2009). In 1824, Sadi Carnot claimed that the efficiency of a heat engine depends on the temperature only, the so-called Carnot factor (Smith *et al*., 2005, Holman, 1980). Thermodynamics developed out of a desire to increase the efficiency of the steam engine. Carnot introduced two ideas in his analysis of heat engines. The first was the idea of a cycle; a process which occurs through several stages but which leads back to the same conditions of temperature, pressure and volume. The second was that the cycle could be reversible if equilibrium is maintained in the system at all times. Carnot's ideas were later brought to limelight by Claypero (Szargut *et al*., 1988). Joule in his experiments in the 1840's showed that heat is a form of energy that can be conserved (Smith *et al*., 2005, Szargut *et al*., 1988). Joule's and Carnot's theories formed the basis of the first and second laws of thermodynamics. In 1854, William J. R. Rankine started to use what he called "thermodynamic function" in his calculations. This was shown to be identical to the concept of entropy formulated in 1865 by Clausius which was an important aid to the theory of thermodynamics (Modell and Reed, 1974, Holman, 1980, Smith *et al*., 2005).

In 1873-1878, Gibbs presented his phase rule which increased the usability of thermodynamics into new areas. He also established a basis for the exergy concept (Sciubba and Wall, 2004). Boltzman in 1877 suggested that probability order is linked to entropy diagram. He is perhaps the most significant contributor in the kinetic theory as he introduced many of the fundamental concepts in the theory. Shannon in 1948 verified the relation between entropy and probability which linked thermodynamics to information theory through statistical mechanics (Wall, 2009). In I953 Rant proposed the word exergy (Wall, 2009, Sciubba and Wall, 2007, Hinderink *et al*., 1996, Cornelissen, 1997).

The science of thermodynamics is built primarily on two fundamental laws known as the first and second laws. The first law is simply an expression of the conservation of energy principle. The law has been proved for many mechanical motions from Newton's laws but its generalisation to all forms of energy was slowly established by several people including Joule (1843), William Grove (1846) and Herman Helmoholtz (1847). It asserts that energy is a thermodynamic property and that during an interaction, energy can change from one form to another but the total amount of energy remains constant. The second law of thermodynamics asserts that energy has quality, and actual processes occur in the direction of decreasing quality of energy. The second law relates to spontaneous change. It originates from Carnot's cycle but the main

advance was introduced by Clausius in 1850. The attempts to quantify the quality or "work potential" of energy in the light of the second law of thermodynamics has resulted in the definition of the properties of entropy and exergy (Dincer and Cengel, 2001).

2.3.1 First law of thermodynamics

The law of conservation and conversion of energy is the fundamental general law of nature. It is also referred to as the first law of thermodynamics. It states that energy cannot be created or destroyed but can only be changed from one form to the other. Consider an open system depicted in figure 2.2, the first law balance can be written as (Perry, 2008)

$$input - output = accumulation \qquad 2.16$$

Considering the system and surrounding, the first law can be also written as (Smith *et al*., 2001, Kyle ,1992)

$$\Delta(Energy\ of\ the\ system) + \Delta(Energy\ of\ surroundings) = 0 \qquad 2.17$$

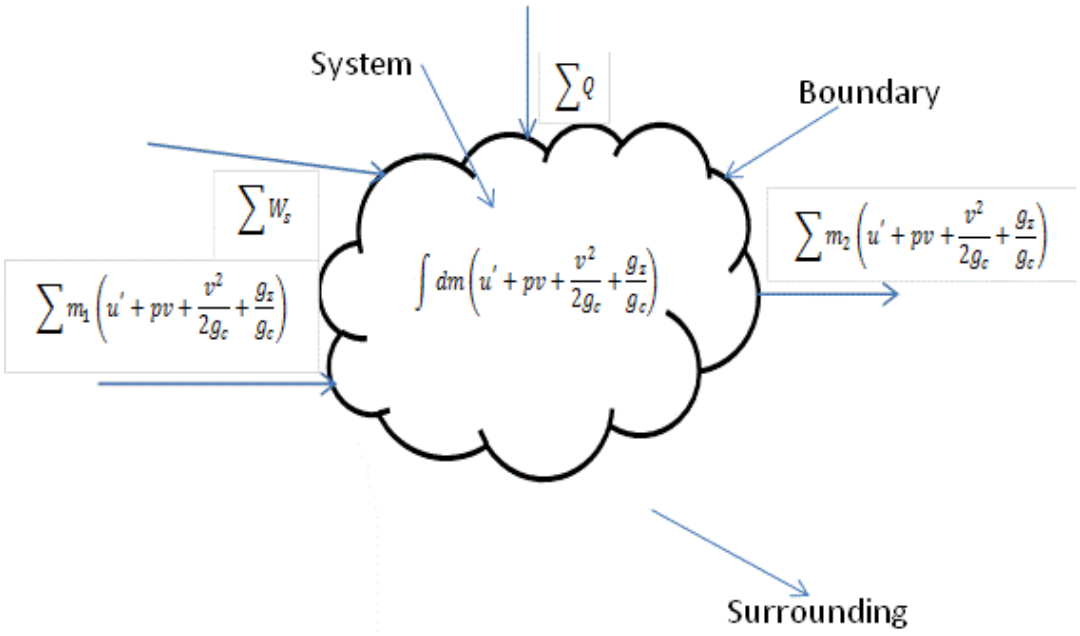

Figure 2.2: Energy flow for a process

The energy input or the energy of the system consists of all the net heat transferred, $\sum Q$; all the net external work transferred, $\sum W_S$, and the energy brought into the system as a result of mass entering,

$$\sum m_1\left(u' + pv + \frac{\upsilon^2}{2g_c} + \frac{g_z}{g_c}\right)_1$$

where u' is the internal energy of the mass at inlet conditions per units mass relative to some reference level, pv is the energy per unit mass as a result of flow, called flow energy, $\frac{\upsilon^2}{2g_c}$ is the kinetic energy of unit mass relative to some reference body, $\frac{g_z}{g_c}$ is the gravitational or potential energy of unit mass relative to some datum level and m_1 is the mass flow per unit time at inlet and subscript 1 denotes inlet condition.

The energy output or the energy of the surrounding is the energy associated with the mass leaving the system and is

$$\sum m_2\left(u' + pv + \frac{\upsilon^2}{2g_c} + \frac{g_z}{g_c}\right)_2$$

where m_2 is the mass flow per unit time at exit and subscript 2 signifies exit condition. The energy that is accumulated in the system is given by

$$\int dm\left(u' + pv + \frac{\upsilon^2}{2g_c} + \frac{g_z}{g_c}\right)$$

Substituting all the terms into Equation (2.16) we have

$$\sum Q + \sum W_S + \sum m_1\left(u' + pv + \frac{\upsilon^2}{2g_c} + \frac{g_z}{g_c}\right)_1 = \sum m_2\left(u' + pv + \frac{\upsilon^2}{2g_c} + \frac{g_z}{g_c}\right)_2 +$$

$$\int dm\left(u' + pv + \frac{\upsilon^2}{2g_c} + \frac{g_z}{g_c}\right) \qquad 2.18$$

Equation 2.18 represents the general energy balance equation for an open system. If the open system is operating at steady state conditions then the accumulation term is zero for equation 2.16 and for 2.18, the energy of the system equals the energy of the surrounding. For the special case of steady state flow and neglecting the changes in kinetic and gravitational energy, Equation (2.18) becomes.

$$\sum Q + \sum W_S = \sum m_2\left(u' + pv\right)_2 - \sum m_1\left(u' + pv\right)_1 \qquad 2.19$$

The specific enthalpy h is defined by

$$h = u' + pv \qquad 2.20$$

Therefore the general equation for the steady state open system becomes

$$\sum Q + \sum W_S = \sum m_2 h_2 - \sum m_1 h_1 \qquad 2.21$$

The sigma summation sign takes care of the fact that there may be more than one entrance and exit stream. Here the convention that heat and work entering the system be taken as positive is used.

The first law of thermodynamics defines internal energy as a state function and provides a formal statement of the conservation of energy. However, it provides no information about the direction in which process can spontaneously occur. The first law is deficient in evaluating the efficiency of a process and the conclusions drawn from the first law are limited because it does not distinguish the various energy forms. Fortunately with the second law of thermodynamics, it is possible to determine true thermodynamic performance of a process.

2.3.2 The second law of thermodynamics

The first law of thermodynamics gives a quantitative measure of the energy conversion in a process. The second law of thermodynamics however gives the qualitative side of these conversions. It imposes restrictions on the quality of energy and the direction of energy transformations (Smith *et al*., 2005).

The second law of thermodynamics establishes the difference in quality between different forms of energy. The second law is often defined in terms of entropy. An ideal process is a reversible process that has the total entropy of streams entering the process equal to that leaving the process. Real processes often have the entropy leaving the process greater than the entropy entering the process because of the generation of entropy within the process. It is the entropy rise that drives the process and thus makes real process having elements of irreversibility in them (Jin *et al*., 1997)

Entropy being a state of disorderliness of a system is at a maximum when the system is at thermodynamic equilibrium. Hence for a system to proceed to a high degree of efficiency, the entropy generation must be as low as possible in order to convert the useful energy of the system to work.

Some proposals of the second law of thermodynamics have been made. Clausius in1850 proposed that "heat cannot pass spontaneously from a body of lower temperature to a body of higher temperature". Thomson in 1851 proposed that "It is impossible by means of an inanimate material agency to derive mechanical effect from any portion of matter by cooling it below the temperature of the coldest of the surrounding objects". Kelvin in 1851 arrived at the same conclusion but expressed the law in a different form. "It is impossible to construct an engine which when working in a complete cycle will produce no effect other than the exchange of heat with a reservoir and the performance of an equivalent amount of heat". This is modified as perpetual motion machine of the second kind is impossible (Granet and Bluestein, 2014, Alattas *et al*., 2011, Holman, 1980).

Clausius in 1854 gave a detailed analysis of the Carnot cycle and represented it mathematically as

$$\frac{q_h}{T_h} + \frac{q_c}{T_c} = 0 \qquad 2.22$$

It states that the heat given out to the cold reservoir divided by its temperature is equal to the heat received at the hot reservoir divided by its temperature.

For a cycle operating reversibly and with various temperature changes,

$$\int \frac{dq}{T} = 0 \qquad 2.23$$

For an irreversible cycle,

$$\int \frac{dq}{T} > 0 \qquad 2.24$$

Clausius later introduced the concept of entropy in 1865. This led to a more general statement that the entropy production in any system must be greater than or equal to zero. This statement can be written mathematically for an open system as (Holman, 1980):

$$Entropy\ production = Entropy\ outflow - Entropy\ inflow + Entropy\ accumulation \qquad 2.25$$

The entropy outflow is given by $m_2 s_2$, where s_2 is the entropy per unit mass flow at exit. The entropy inflow consists of the entropy inflow from mass transport, $m_1 s_1$, and the entropy inflow from heat transfer at boundary of the control volume, $\sum \frac{Q}{T_0}$. The entropy accumulation is given by $\int (d(ms))$. Substituting all the terms into equation 2.25 we have

$$\sum m_2 s_2 - \left(\sum m_1 s_1 + \sum \frac{Q}{T_0} \right) + \int d(ms) > 0 \qquad 2.26$$

Assuming steady state operation, the accumulation term becomes zero. Also quantifying the entropy production by the identity σ and rewriting equation 2.26, we have

$$\sum m_2 s_2 - \sum m_1 s_1 - \sum \frac{Q}{T_0} = \sigma \qquad 2.27$$

Rearranging and solving for $\sum Q$,

$$\sum Q = \sum T_0 m_2 s_2 - \sum T_0 m_1 s_1 - T_0 \sigma \qquad 2.28$$

2.4 Concept of Exergy

Exergy is a concept, which follows from a combination of the first and second laws of thermodynamics. It is a key aspect of providing better understanding of the process; quantifying sources of inefficiency and distinguishing quality of energy used (Rosen and Dincer, 1997). It corresponds to the maximum available work, which can be obtained when taking a system through reversible process with the environments. Szargut (1988) defined exergy as "*the amount of work obtainable when some matter is brought to a state of thermodynamic equilibrium with the common components of the natural surroundings by means of reversible processes, involving interaction only with the abovementioned components of nature*". In real processes, irreversibilities always occur. These lead to loss of exergies or loss of available energy. Exergy is then the energy that is available to be used. After the system and surroundings reach equilibrium, the exergy is zero. During a process, exergy is not conserved but it is destroyed due to irreversibility. For a real process, the exergy input always exceeds the exergy output; this imbalance is due to irreversibilities, which some have referred to as exergy

destruction or anergy or exergy loss as shown in figure 2.3 (Dincer and Al-Muslim, 2001, Szargut *et al*., 1988).

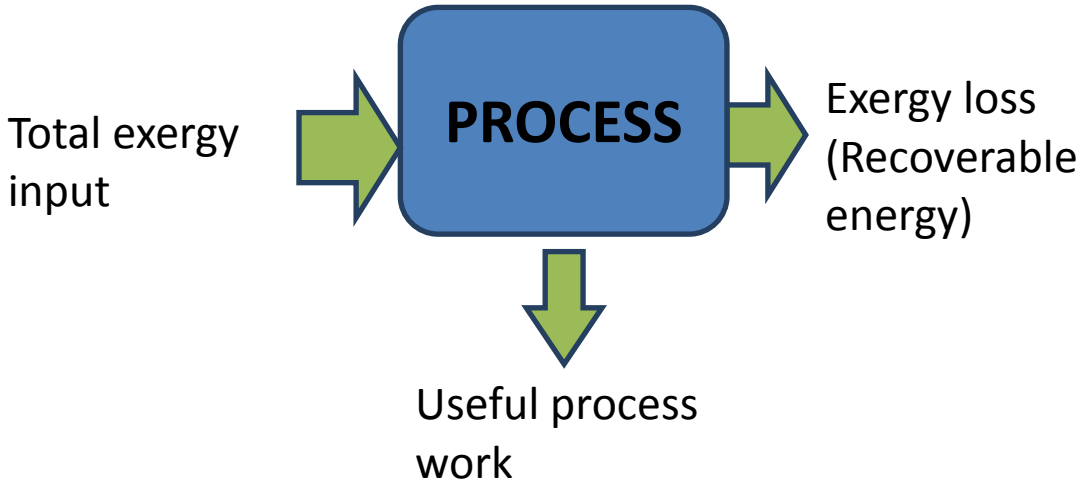

Figure 2.3: Exergy flow of a process

Exergy analysis is a tool for assessing quality of energy and quantifying sources of inefficiency and recoverable energy. Exergy analysis evaluates quality of energy lost and distinguishes between recoverable and non recoverable energy. It is a tool for determining how energy efficient a process is. Exergy analysis of processes gives insights into the overall energy usage evaluation of the process, potentials for efficient energy usage of such processes can then be identified and energy usage improving measures of the processes can be suggested (Asada and Boelman, 2004). It also provides a supplementary tool in identifying design and operation modification targets for processes (Cornelissen, 1997).

The basis of the exergy concept was laid almost a century ago but was introduced as a tool for process analysis in the 1950s by Keenan and Rant (Dincer and Al-Muslim, 2001, Cornelissen, 1997, Hinderink *et al*., 1996). Szargut introduced the concept of chemical exergy and its associated reference states in 1986 (Cornelissen, 1997). It is common to use ambient pressure and temperature as P_0 = 101.325 kPa and T_0 = 298.15 K (Dincer and Rosen, 2012).

2.4.1 Derivation of the exergy function

The first law energy balance given by equation 2.21 and the second law entropy balance given by equation 2.28 are combined by eliminating $\sum Q$ in the two equations to obtain

$$\sum T_0 m_2 s_2 - \sum T_0 m_1 s_1 - T_0\sigma + \sum W_S = \sum m_2 h_2 - \sum m_1 h_1 \qquad 2.29$$

Rearranging further we have.

$$\sum m_1 (\ h_1 - T_0 s_1\ ) + \sum W_S = \sum m_2 (\ h_2 - T_0 s_2\ ) + T_0\sigma \qquad 2.30$$

For a steady state flow operation, $\sum m_1 = \sum m_2$.

Considering the case of a reversible process $T_0\sigma = 0$ and equation (2.11) becomes

$$\left(\sum W_S\right)_{rev} = \sum m(h_2 - T_0 s_2) - \sum m(h_1 - T_0 s_1) \qquad 2.31$$

Or $\sum W_{S\,rev} = \sum m(h_2 - h_1) - T_0(s_2 - s_1)$

$$= \sum m(\Delta h - T_0 \Delta s)$$

Dropping the summation sign

$$W_{S\,rev} = m(\Delta h - T_0 \Delta s) = m(\Delta ex) = \Delta Ex = \Delta H - T_0 \Delta S \qquad 2.32$$

$\Delta h - T_0 \Delta s$ is a thermodynamic function called exergy. It is the minimum work requirement or the maximum work obtainable depending on whether the process requires or produces work in bringing the system to its dead states, that is, equilibrium with the environment.

2.4.2 Exergy calculation

Exergy is the amount of useful work that a system can provide when moving reversibly from the reference environment. It always decreases or at least remains constant when the process is reversible. If the system is a closed system, exergy will be calculated as:

$$Ex = (U - U_0) + P_0(v - v_0) - T_0(s - s_0) \qquad 2.33$$

Or if the system is an open system

$$Ex = (h - h_0) - T_0(s - s_0) \qquad 2.34$$

2.4.3 Forms of exergy

Excluding the nuclear, magnetic, electrical and interfacial effects, the exergy of a stream of matter has four different forms which include:

i. Kinetic exergy

ii. Potential exergy

iii. Physical (Thermo-mechanical) exergy

iv. Chemical exergy

Physical exergy is the work obtainable by taking the substance reversibly from an initial temperature and pressure to the reference temperature and pressure of the environment. Chemical exergy is the work obtainable by taking the substance in chemical equilibrium with the reference level components of the environment. Kinetic exergy is the exergy when the velocity of a stream is considered relative to the surface of the earth while potential exergy is evaluated with respect to the average level of the earth surface. The total exergy of a stream is

$$Ex_{Total} = Ex_{kinetic} + Ex_{potential} + Ex_{physical} + Ex_{chemical} \quad 2.35$$

Kinetic exergy and potential exergy though often neglected in analysis can be calculated as

$$Ex_k = m(\upsilon^2/2) \quad 2.36$$

$$Ex_p = mg_z \quad 2.37$$

2.4.4 Physical exergy

It can also be defined as the state that can be obtained from taking it to physical equilibrium (of temperature and pressure) with the environment (Rivero, 2001).

Physical exergy can be calculated as:

$$Ex_{phy} = m\big((h - h_0) - T_0(s - s_0)\big) \quad 2.38$$

where h denotes enthalpy, s connotes entropy, T connotes temperature and the subscript 0 connotes reference condition.

For a perfect gas with constant specific heat (C_p)

$$Ex_{phy} = m\left(c_p(T - T_0) - T_0\left(ln\frac{T}{T_0} - RT_0 ln\frac{P}{P_0}\right)\right) \quad 2.39$$

2.4.5 Chemical exergy

It is the maximum amount of work obtainable when the system under consideration is brought from the environmental state (T_0, P_0) to the dead state (T_o, P_0 and μ_0) by processes in heat transfer and exchange of substance only with the environment. It can also be defined as the maximum work (useful energy) that can be obtained from it in taking it to chemical equilibrium (of compositions) with the chemical environment (Rivero *et al.*, 2004). Similar to physical exergy, chemical exergy depends on the temperature and pressure of a system as well as its composition. Depending on the process, the amount of chemical exergy may be negligible or large. For instance, a binary, non reactive distillation system, the chemical exergy might be quite negligible because distillation here is basically a physical process. Different substances have different ways of chemical exergy calculation.

Chemical exergy of most mixtures is calculated as

$$Ex_{chem} = m\left(h_0 - \sum z_i \bar{h}_{0i} - T_0(s_0 - \sum z_i \bar{s}_{0i})\right) \quad 2.40$$

where z_i is the mole fraction of the ith component, $\bar{h}_{0i}$ and $\bar{s}_{0i}$ are the partial specific enthalpy and entropy of the component at reference conditions respectively, h is the specific enthalpy, s is the specific entropy, T_0 is the reference temperature, h_0 and s_0 are specific enthalpy and entropy measured at reference conditions.

For a crude stream which is of high interest here, standard molar chemical exergy is calculated from the standard molar chemical exergies of all identified components and pseudo-components as:

$$Ex_{chem} = m\left[\sum b_{qi} + \sum b_{chi} + RT_0 \sum lna_i\right] \quad 2.41$$

Where

b_{chi} is the chemical exergy for component,

b_{qi} is the chemical exergy for pseudo component, and

a_i is the activity coefficient of component i.

The standard chemical exergy for pseudo-components can be determined from heuristic empirical expression as a function of the elementary composition and their heating values (Szargut *et al*., 1988).

$$b_{qi} = \vartheta_i C_i \qquad 2.42$$

where ϑ_i is the regression equation to express the ratios H/C, N/C, O/C and S/C for pseudo-component i,

C_i is the net calorific heating value of the pseudo-component i.

$$\text{where} \quad \vartheta_i = 1.0401 + 0.1728\frac{Z_{H2}}{Z_C} + 0.0432\frac{Z_{O2}}{Z_C} + 0.2169 \qquad 2.43$$

$$Ex_{chem} = m\left[\sum C_i(1.0401 + 0.1728\frac{Z_{H2}}{Z_C} + 0.0432\frac{Z_{O2}}{Z_C} + 0.2169\ ) + \sum b_{chi} + RT_0 \sum lna_i\right] \qquad 2.44$$

Equation 2.44 is used for the calculation of chemical exergy streams in chapter 6 of this thesis.

2.4.6 Evaluation of work equivalent

If Q_z is a heat source at an absolute temperature T_z and if T_0 is the ambient temperature, then the work equivalent of heat is given by

$$W_{\max} = \frac{(T_z - T_0)Q_z}{T_z} \qquad 2.45$$

This is the absolute theoretical maximum work recoverable.

2.4.7 Exergetic efficiency

A criteria of performance based on exergy analysis is known as exergetic efficiency. Exergetic efficiency is used to compute the degree of thermodynamic perfection of a process.

The second law efficiency is a measure of performance relative to the optimal possible performance of a system and hence provides insights to the quality of performance of a system relative to what could be in ideal situations. It is never greater than 1 because it is defined with reference to limitation imposed by the second law of thermodynamics.

Thermodynamic efficiency of an operation or an entire process depends on its goal and the work lost in accomplishing that goal. The efficiency of a process can be calculated as follows

1. Simple efficiency

This is mathematically represented as:

$$\varphi = \frac{\sum Ex_{out}}{\sum Ex_{in}} \quad 2.46$$

2. Rational efficiency

This is mathematically represented as:

$$\varphi = \sum \frac{Ex_{Dout}}{Ex_{Din}} \quad 2.47$$

Where Ex_{Dout} implies total exergy desired out and Ex_{Din} implies total exergy desired in.

Rational efficiency can be applied to any system except a dissipative system.

3. Transiting exergy efficiency

This form of efficiency subtracts the untransformed component from the incoming and outgoing streams. It is mathematically represented as

$$\varphi = \frac{Ex_{out} - Ex_{trans}}{Ex_{in} - Ex_{trans}} \quad 2.48$$

The efficiency calculations in this study are based on simple efficiency.

2.4.8 Comparison between energy and exergy

The concept of energy and exergy can be expressed in the following simple terms:

i. Energy is motion or ability to produce.

ii. Exergy is work or ability to do work.

The laws of thermodynamics can be expressed in the following ways:

i. Energy is always conserved in a process (1st law of thermodynamics).

ii. Exergy is always conserved in reversible process but always consumed in an irreversible process (2nd law of thermodynamics or exergy law) (Wall, 2009).

Exergy is a better measure of the quality of energy than energy because it only accounts for the energy that can be converted into work (DOE, 1998). Also, the majority of the causes of thermodynamic imperfection of thermal and chemical processes cannot be detected by means of an energy balance. For example, 1,000 kW/hour of low-pressure steam would compare equally with 1,000 kW/hour of electricity in terms of energy measurement. In reality, the amount of usable energy from the low-pressure steam is less than a third of that represented by the electricity, because the energy quality of the low-pressure steam is much lower. Quantifying the quality of energy and hence determining its irreversibility can only be made possible with exergy analysis (DOE, 2000). Generally, table 2.1 shows the main characteristics of exergy and energy.

Table 2.1: Main characteristics of Exergy and Energy

S/N	**Energy**	**Exergy**
1.	It is subject to law of conservation.	It is exempt from law of conservation.
2.	It is a function of the state of the matter under consideration.	It is a function of the state of the matter under consideration and of the matter in the environment.
3.	Increases with increase in temperature.	For isobaric processes reaches a minimum at the temperature of the environment; at lower temperature, it increases as the temperature drops.
4.	May be calculated on the basis of any assumed state of reference.	The state of reference is imposed by the environment, which may vary
5.	In the case of ideal gas, does not depend on pressure.	Always depends on pressure

Source: (Szargut *et al.*, 1988)

2.5 Process control

There has been a considerable improvement in the development of software for the modelling of distillation processes but in the art of control and optimisation of the process, there is still much to be done. Hence there is a need for resource or methods for the operation, design and troubleshooting of distillation process control system. In this thesis the emphasis will be on the continuous distillation column in lieu of batch. Stage column as well as rigorous rate based columns will be considered.

Control of a process basically contains three steps; to measure, compare and adjust. In this regards, variables which are factors that can change the condition of the process are used. Control systems could be single loop, multi loop or multivariable. Single loop control refers to the situation where there is only one controlled variable which can be either controlled by a feed forward or a feedback controller loop. In multi-loop control, there are more than one controlled variables which are paired with the corresponding manipulated variables. In multivariable control, all the manipulated variables are used to control all the controlled variables through advanced control technology such as model predictive control.

The control of crude distillation units has always been of particular interest to researchers. Advanced process control is usually implemented through the traditional chemical engineering approach of multiple control loops and the measurements of flows, temperature, pressure and heat and mass balances (Simpson *et al.*, 2010). Model predictive control was later developed to meet the specialised control needs of the petrochemical industries with the objective of driving the outputs as close as possible to the set points (Qin and Badgwell, 2003).

The online estimation and optimisation of products is another control issue that is of great interest (Kumar *et al.*, 2001, Simpson *et al.*, 2010). In this respect, inferential estimation models of product quality from different crude feeds was developed by some authors (Zhou *et al.*, 2012) while others considered developing soft sensor model for estimation and control of products (Ujević *et al*., 2011, Rogina *et al*., 2011, Bolf *et al*., 2010).

Energy efficiency of the crude distillation unit is a very important aspect of the control of the crude distillation process but surprisingly not much work has been devoted to it. A number of authors have tackled the control of energy efficiency of the crude distillation unit via fouling and corrosion control (Kim *et al*., 2011, Kumana *et al*.,

2010). It has however been observed from the second law analysis of the crude distillation unit that the inefficiency of the column is from the entropy generation within the column (Al-Muslim and Dincer, 2005, Al-Muslim *et al*., 2003, Rivero *et al*., 2004). A method of control of distillation columns based on minimising entropy generation within the column will be of paramount importance. This work is set to develop energy efficient control strategies for the distillation unit from the angle of the second law analysis of the process and hence provide a novel way of controlling the distillation unit.

2.5.1 Control structure selection

Process control is the active changing of a process based on the result of process monitoring. It is desirable to have rapid response to changes in set point and rapid return to set point in the face of any disturbance. Usually in processes three levels of control that are of great importance are the composition control, level control and pressure control. For a distillation column, the composition of the products are affected by the reflux ratio (fractionation) and the feed splits (specified products quantities). Pressure is usually held constant in distillation columns except for cases where a change in pressure will aid in effective fractionation. This is because sudden decrease in pressure will lead to excessive vaporisation of the liquid and thereby causing flooding of the column while sudden increase in pressure can cause low vapour rate in the column that will result in the weeping of the column.

Though the control strategies for distillation systems varies in cost and complexity, valves and sensor systems to which they are connected largely influence the effectiveness of these strategies. A careful selection of the valve and sensor system is therefore of paramount importance. Some of the column control sensor issues include sensor location (the required separation the column is expected to maintain has an influence on the location of the sensor that will facilitate the control system), sensor sensitivity, sensor consistency and sensor reliability (Luyben, 1992). The column control valve issues include range (how large an adjustment for the control system), resolution (how small an adjustment), size, dynamics and plant wide implication of each valve.

The design of a control structure for a distillation system involves the selection of controlled and manipulated variables. Usually for a binary distillation process, the manipulated variables are reflux flow rate, reboiler heat load, distillate flow rate,

bottoms flow rate and cooling water flow rate. The controlled variables are often distillate compositions, bottom composition, reflux drum level, reboiler level and pressure (Luyben, 1990).

The aim of control structure synthesis is to develop mechanism that can bring about the realisation of the objectives of the plant and account for interactions associated with the expected multivariate nature of the plant. Most works on the control structure selection of chemical process could be majorly classified into two. The first is based on rule of thumb or simple controllability indicators resulting from process experience and judgement (Luyben *et al.,* 1997, Luyben, 1998). Using this approach some authors employ the concept of partial control such that the control of dominant variables identified stabilizes the entire system results (Price *et al.*, 1994). In a related work, the concept of finding the self optimising control variables was introduced (Skogestad, 2000). Groenendijk *et al*., (2000) proposed the application of linear control theoretic analysis such as relative gain array, singular value decomposition and disturbance gain. Most of these approaches are without consideration to the energy efficiency of the control structures. This work is set to present a methodology that corrects this deficiency. The method has the advantages of not requiring quantitative information and can be easily applied to large scale problems such as plant wide control problem.

The second involves systematic methodology using classical mathematical formulation based on dynamic system theory, optimisation and control to identify the most promising super structures. This method is accurate within the limit imposed from the mathematical models and mathematical programming techniques used. It however suffers from model convergence problems and guaranteed only local optimality. The following researchers have presented mathematically oriented approach among others (Assali and McAvoy, 2010, Bansal *et al.*, 2000, Kookos, 2005) . A review of the two methods is presented by Larsson and Skogestad (Larsson and Skogestad, 2000). In the past control of processes were done via instrumentation approach which is a qualitative method that is based on practice and intuition. Recently there have been advances in systematic choice of optimal control structure using inverse model and mixed integer quadratic programming (Yelchuru and Skogestad, 2012, Sharifzadeh and Thornhill, 2012). The optimization framework for the control structure selection are economically based, hence there is still a need for a structure that will encompass the optimal energy usage.

2.5.1.1 Relative gain array

Relative gain array (RGA) was introduced in 1966 by Bristol (Bristol, 1966). It has been widely used to assess process interaction in multi-input multi-output (MIMO) control loops. Loops that exhibit large interaction can then be discarded for further consideration. In a RGA matrix, the following properties hold true (Seborg, 1989). The sum of the elements in each row or column is one; the permutation of rows and columns in the matrix results in the same permutation in the RGA; and the RGA elements are dimensionless. Shinskey (Shinskey, 1988) popularised the use of RGA by applying it to a number of examples including blending, distillation and energy conservation. RGA is advantageous in that it requires minimal process information, it is simple to calculate and it does not depend on process disturbances and control system tuning (Mc Avoy et al., 2003). However, the fact that RGA does not consider dynamics may lead to incorrect loop parings. A number of authors have modified RGA to have application in the dynamic state (Jain and Babu, 2012, Huang *et al*., 1994). There are different possibilities for RGA analysis of process systems. The following are some of the possibilities and their interpretations.

1. α_{ij} = 1. Manipulated variable u_j affects the controlled variable y_i but has no interaction with other control loops.
2. α_{ij}= 0. Manipulated variable u_j has no effect on the controlled variable y_i.
3. α_{ij}= 0.5. There is a high degree of interaction. The other control loops have the same effect on the controlled variable y_i as the manipulated variable u_j
4. 0.5 < α_{ij}< 1. There is interaction between the control loops. However, this would be the preferable pairing as it would minimise interactions.
5. α_{ij}> 1. The interaction reduces the effect gain of the control loop. Higher controller gains are required.
6. α_{ij}> 10. The pairing of variables with large RGA elements is undesirable.
7. α_{ij}< 0. Care must be taken with negative RGA elements. Negative off-diagonal elements can indicate the control loop is unstable for any feedback controller (integral instability).

Only conditions 1, 4 and 5 are advised for possible pairings

2.5.1.2 Relative exergy array

Relative exergy array (REA) is defined analogous to RGA. It is the extension of exergy analysis in the calculation of RGA. It gives the exergetic efficiency of pairing the control variable with the manipulated variable (Montelongo-Luna *et al*., 2011). REA

can be directly determined by placing the exergy concept in place of the control gain. As RGA can be calculated from the steady state gain matrix, REA can also be obtained from the steady state generic exergy gain matrix (Munir *et al.*, 2012b). RGA and REA have been used to assess interactions and exergy efficiency of control loops for processes such as CSTRs and distillation columns (Letcher, 2015, Munir *et al.*, 2012b) . The application has been extended to processes with recycle streams as well.

A number of other tools based on REA have been introduced for determining the exergy efficiency of control loop while expanding the boundary of interactions. This include relative exergy destroyed (REDA) (Munir *et al*., 2012c) and exergy eco-efficiency factor (EEF) (Munir *et al*., 2013b, Munir et al., 2012a). These tools have been extended to include processes with recycle streams as well (Munir *et al.*, 2013a, Munir *et al.*, 2012b).

However, the fact that REA is based on steady state system introduces a measure of unreliability especially when the system is operated in the dynamic state. Since most chemical processes are operated in the dynamic state, the application of REA to all processes might be limited. This work presents the application of REA analysis both in the steady and the dynamic state. This is with a view to remove the limitation imposed by the steady state analysis.

The interpretations of REA for a number of possible values are defined as follows

$\beta_{ij} = 1$ exergy efficiency is not affected by other loops interaction. A good pairing because maximum change in exergy is neither increased nor decreased by the loop interaction

$\beta_{ij} > 1$ exergy changes for open loop are larger than the changes caused by loop interaction. The interaction of the variable is decreasing the changes in exergy

$\beta_{ij} < 1$ Exergy changes due to loop interactions are larger than the exergy changes when all the loops are opened.

2.5.2 Control of distillation unit

Distillation column control varies a great deal. The control system could be proportional integral derivative (PID) or model based algorithm. Some control strategies use distributed control system (DCS) while others may use conventional electronic and pneumatic control devices.

PID control is the most widely used practical control strategy. Three basic controller actions that determines the controller output in a PID controller are proportional, integral and derivative actions (Luyben, 1990, Ogunnaike and Ray, 1994, Robbins, 2011).

Proportional action is the action of the controller that is proportional to the error between the controlled process variables and the set point.

It is given as $CO = bias \pm K_c\, e$ 2.49

Where CO is controller output, K_c is the controller gain and $e\ is\ the\ control\ error = setpoint - controlled\ variable$

Integral action moves the control valve based on the time integral of the error. It eliminates offset error at steady state.

$$CO = bias + \frac{1}{\tau_i}\int edt \qquad 2.50$$

τ_i is the integral time or the reset time

Derivative action anticipates where the process is heading by looking at the time rate of change of the controlled variable. It responds to the rate of change of error.

$$CO = bias + \tau_D \frac{de}{dt} \qquad 2.51$$

The three actions could be used individually or combined. Hence we have proportional integral (PI), proportional integral derivative (PID) and proportional (P) controllers. A diagrammatic expression of the PID is given in figure 2.4.

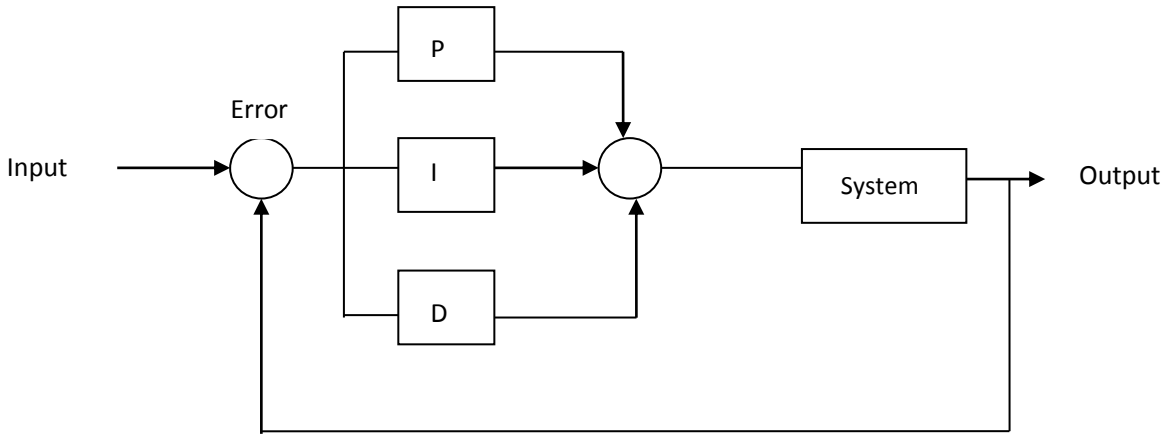

Figure 2.4: Schematic diagram of a conventional PID controller

The traditional way of process control is to compare the variables being controlled after measurement with its desired value or set point and feed the difference to a controller that will drive the controlled variable to its desired level by changing the manipulated variable. This mode of controller which is frequently used in the process industry is termed feedback controller. In the feed forward controller, the disturbance is detected as it enters the process, the controlled variable is then kept constant by appropriate change in the manipulated variable. The control of crude distillation with multiple pumparounds has for a long time been difficult because of a number of reasons. These include interaction between circulating refluxes as a result of line up in crude preheat train leading to slow control circulating reflux return temperature and difficulty in achieving closed loop quality control due to linkage in the heat and material balances. The difficulty has been addressed with multivariable column tray temperature; multivariable quality constraint control and circulating pumparound return temperature control (van Wijk and Pope, 1992). The payoff between yield and energy efficiency of the column is another important strategy which is yet to gain wide spread recognition.

2.5.3 Tuning strategy in controller

Many process control loops are tuned by trial and error which consists of changing one or more of the proportional, integral and derivative. This method, though has the merits of returning the controller back to the initial values and the re-use of existing equipment suffers in its requirement of a long learning curve and the difficulty of a beginner to pick the change in response of variables (Robbins, 2011). Also, each of the settings of K_C, τ_R and τ_D can be varied from 0.01 to 100 and considering the fact that various lags and delays associated with process plant are often large, trial and error tuning will be cumbersome (Love, 2007). This has resulted in the proposal of many PID controller tuning methods in the literature. Two of such methods are discussed here (Love, 2007, Robbins, 2011, Coughanowr and LeBlanc, 2009).

2.5.3.1 Continuous cycling method

This method tuned the controller as installed rather than as designed. The process consist of setting the system up with proportional only control by setting the integral time to infinity and the derivative time to zero. The gain of the controller is altered until the smallest gain that forces the loop into self sustained oscillation of constant amplitude is obtained as shown in figure 2.5. This is the ultimate gain μ. The period of these constant oscillations known as ultimate period P_U is also evaluated (Robbins, 2011). Then the critical frequency is

$$\omega_c = \frac{2\pi}{P_U} \qquad 2.52$$

The values of μ and P_U obtained are substituted in the Zeigler and Nichols formulae given in table 2.2 to determine the optimum settings for the controller. A flow chart for the procedure is given in figure 2.6.

Ziegler and Nichols formulae was first published in 1941 (Love, 2007) and has been used extensively in the industry. However, the formula do not predict the optimum settings precisely (often within 10% of the optimum) and further tuning of a trial and error may be required. In this study, biggest modulus tuning (BLT) is combined with Ziegler Nichols tuning for the controllers in chapter four.

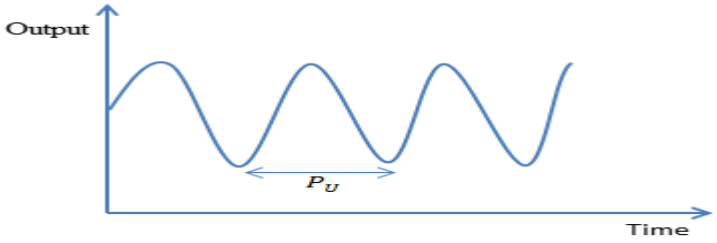

Figure 2.5: Response at ultimate gain

Table 2.2: Ziegler and Nichols formulae

Controller type	**Controller gain**	**Reset**	**Derivative**
P	$\frac{\mu}{2}$		
PI	$\frac{\mu}{2.2}$	$\frac{P_u}{1.2}$	
PID	$\frac{\mu}{1.7}$	$\frac{P_u}{2}$	$\frac{P_u}{1.8}$

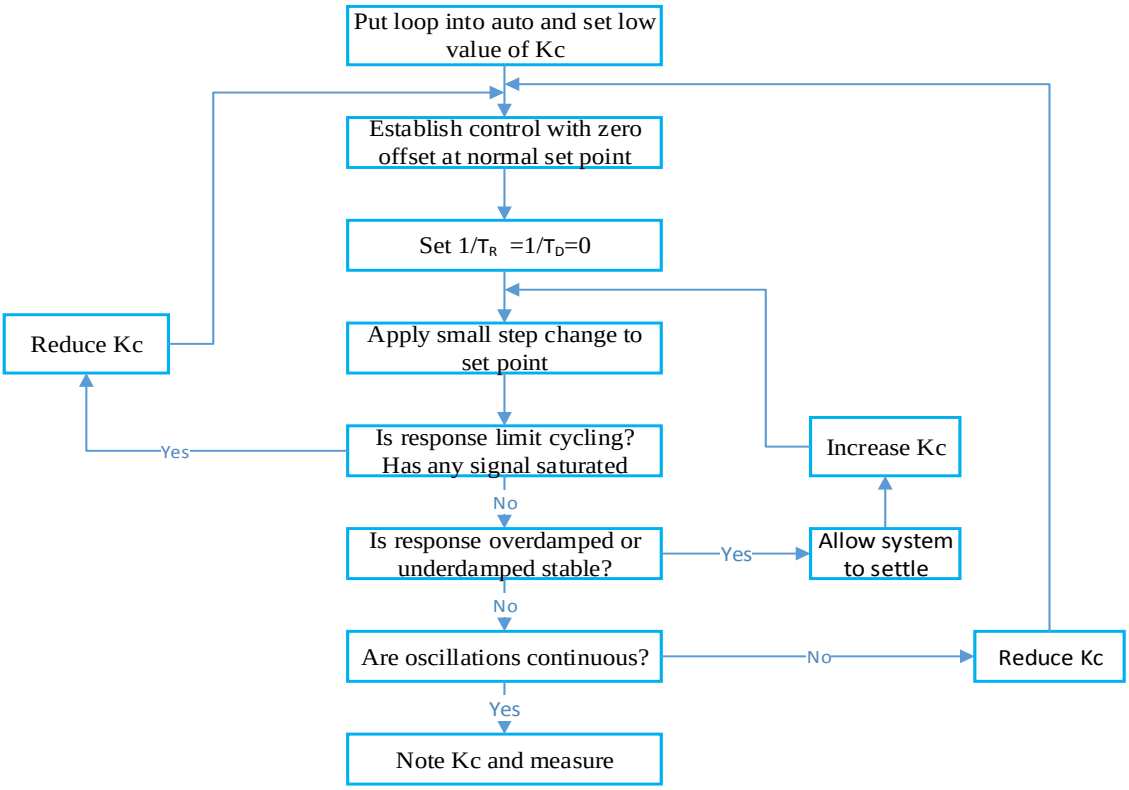

Figure 2.6: Continuous cycling method
Source: (Love, 2007)

2.5.3.2 Reaction curve method

This is an open loop method of controller tuning. The system is allowed to reach equilibrium, while the controller is in a manual mode. The open loop response of the process to a step change in the manipulated variable U as shown in Figure 2.6 is measured and recorded. Since y_2 is the steady state effect of the open loop elements operating on the step change U the steady state gain can be obtained from the ratio $K_c = \frac{\Delta y}{\Delta U}$. Then drawing a tangent to the curve at the point of inflexion and finding its intersection with the asymptote and the time axis as shown in figure 2.7, the values of Ts and Td can be determined. The values are substituted in table 2.3 to determine the Gain G.

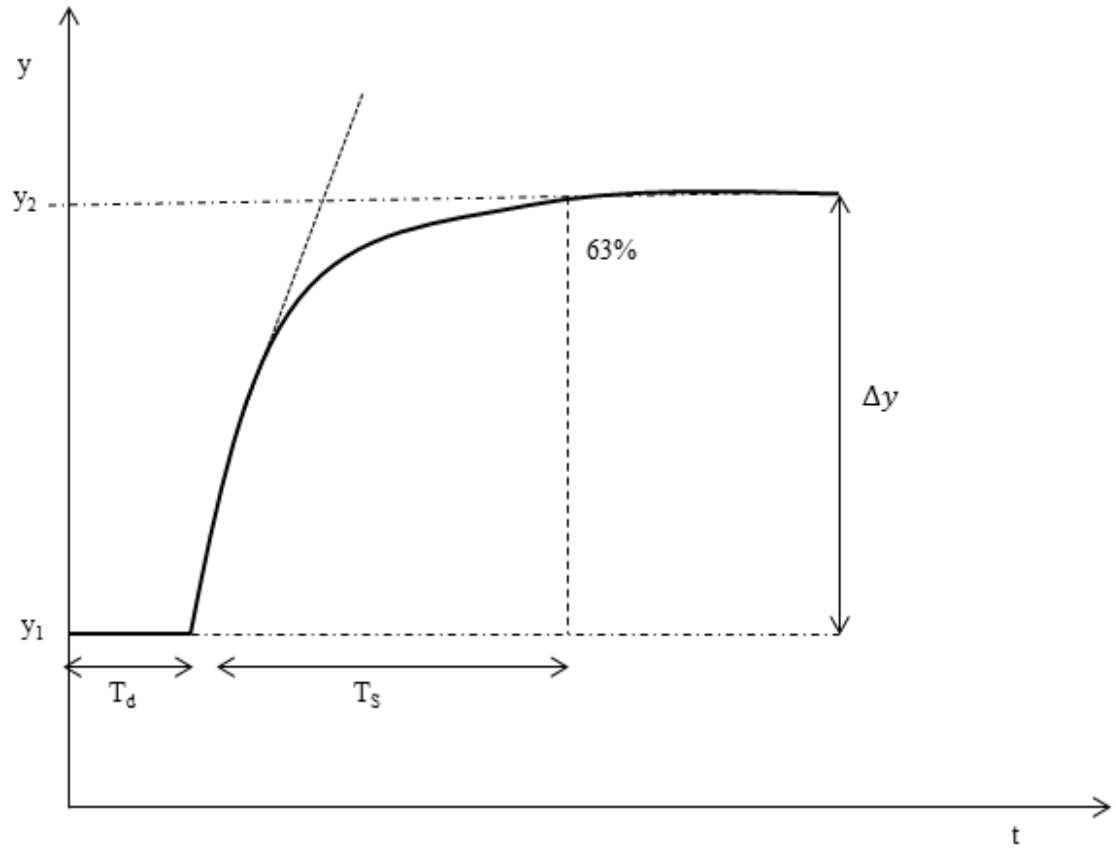

Figure 2.7: Open loop response to a step change in manipulated variable

Table 2.3: Tuning rules using slope and intercept I

Controller type	**Controller gain**	**Reset**	**Derivative**
P	$\frac{Ts}{Td}$		
PI	$\frac{0.9Ts}{Td}$	$3.3Td$	
PID	$\frac{1.2Ts}{Td}$	$2.0Td$	$0.5Td$

The gain calculated here is

$$G = \mu * K_c \qquad 2.53$$

Where μ is the controller setting gain and K_c is the steady state gain. The controller setting gain is then obtained from table 2.4.

Table 2.4: Tuning rules using slope and intercept II

Controller type	Controller gain	Reset	Derivative
P	$\frac{Ts.\Delta U}{Td.\Delta y}$		
PI	$\frac{0.9Ts.\Delta U}{Td.\Delta y}$	$3.3Td$	
PID	$\frac{1.2Ts.\Delta U}{Td.\Delta y}$	$2.0Td$	$0.5Td$

This method however has the disadvantage of being prone to disturbances. It is often difficult to insulate the system from disturbance's long enough to obtain the curve (Love, 2007) and also it doesn't work well for complex processes (Robbins, 2011).

Other methods have since evolved and this includes internal model control and neural networks based methodologies (Hultmann Ayala and dos Santos Coelho, 2012, Vijayan and Panda, 2012).

2.5.4 Model predictive control

The control of processes has evolved from the simple closed loop control to a more advanced control technologies in response to the drive by industries for more consistent attainment of high product quality, more efficient energy usage and increasing strict environmental and safety policies. This has led to the development of Dynamic matrix control (DMC) and model algorithm control (MAC) both of which can be classified as Model predictive control (MPC) (Ogunnaike and Ray, 1994).

One of the main process control technique in the process industries is model predictive control. It is the prediction of future control action and trajectories based on the knowledge of current input and output variables and future control signals (Kumar and Ahmad, 2012). It is a form of control obtained by solving an online optimal control problem in the open loop and using the current state of the plant as the initial state to yield a mathematical programming problem. Predictive control utilises sampled data of system responses for its model unlike dynamic matrix control that utilises sampled data of step responses as its predictive model (Mingjian *et al.*, 2007).

Model predictive control could be based on linear or non-linear models. Non-linear MPC has been the focus of quite a number of authors. It has been applied on a number

of processes such as cryogenic process, continuous stirred tank reactors CSTR), evaporator and distillation processes (Chen *et al.,* 2010, Rivotti *et al*., 2012, Rewagad and Kiss, 2012, Cao, 2005). For most chemical and petrochemical industries however, linear MPC has always been the focus (Darby and Nikolaou, 2012, Porfírio and Odloak, 2011, Porfírio *et al.,* 2003). The idea of multiprogramming and model reduction method was combined in model predictive control (Rivotti *et al.*, 2012).

The first element of a model predictive control is reference trajectory specification. This simply is the desired target trajectory which could be a step to the new set point value. The next is an appropriate model which is used to predict the process output over a period of time. Then the model is used in calculating a sequence of control moves that could minimise the deviation of the predicted output from target subject to some specified process constraints. Finally, the real plant measurement is compared with the model prediction an the error obtained is used to update future predictions (Darby and Nikolaou, 2012, Ogunnaike and Ray, 1994). A diagrammatic representation of the elements in a predictive control is represented in figure 2.8.

Model predictive control has been applied in a large number of industries especially the petrochemical industries because of its ability to cope well with hard constraints on control and states (Dua *et al.*, 2008). In their review of commercially available model predictive technology for both non-linear and linear systems, Qin and Badgwell (2003) concluded that most products use multiple steps signals for test and requires the close attention of experienced engineers for the test; error identification algorithm are mostly of the least squares type; and most has uncertainty estimate though most do not use uncertainty bound in control design.

MPC is advantageous in that it could handle multivariable control problems, could simultaneously take the effects of manipulated variables to all controlled variables and allows operation with input and output constraints (Porfírio *et al.*, 2003).

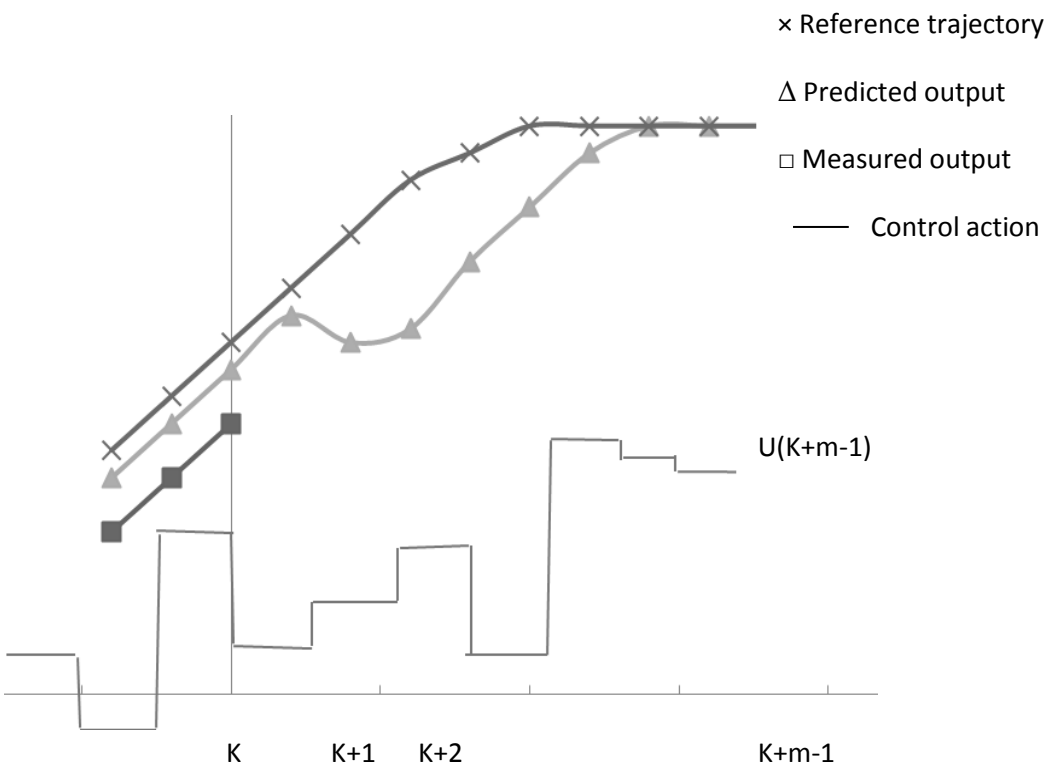

Figure 2.8: Elements in model predictive control

2.6 Optimisation

The control and optimisation of processes especially in the refineries overlap and may be difficult to actually separate. Three basic technology of this application are : Real time optimisation (RTO) based on non-linear steady state model sending steady state targets to a linear MPC controller, a non-linear steady state model setting the gains of an adaptive model predictive controller (MPC), and a non-linear empirical dynamic models (neural network) for control and optimisation.

In a process system with varying disturbances such as feed composition and feed flow rate, a method that deals with the most effective way of operating a process under such frequent disturbances is real time optimisation (RTO) (Adetola and Guay, 2010). RTO involves components for steady state detection, data acquisition and validation, process model updating, optimisation calculation and optimal operating policies transfer to advanced controllers. Multilayer approach of RTO is usually in three layers. In the upper layer RTO optimises equipment constraints, product specification and operating conditions at steady state; optimum values of these input and output are passed to an intermediate layer. Feasible targets of these input and output are then recomputed and fed to the dynamic layer that contains the model predictive controller (Ying and Joseph, 1999).

However, the approach of multilayer may not be feasible if different disturbances alter the optimum operating points and the typical sampling time of the RTO may be of several hours. Dynamic real time optimisation with a non-linear dynamic model or non-linear MPC with economic objective may be appropriate (Adetola and Guay, 2010, Hosen *et al.*, 2011). The demerits notwithstanding, RTO has been proved useful especially in the refinery and has been applied in the ethylene plant, toluene distillation system, fluid catalytic cracking and olefins production (Porfírio and Odloak, 2011, Diehl *et al.*, 2002, Geddes and Kubera, 2000). RTO identifies and continually adapts optimal operating points within a process while control system keep the plant as close as possible to the optimal point and minimises economic losses. The optimisation of crude distillation unit using RTO is not yet popular (Basak *et al.*, 2002). It is expected that the methods to be developed from this study could be adapted for real time optimisation of distillation process in future work.

Optimisation of chemical processes involve solving a number of non linear constrained problems with conflicting objectives (Edgar, 2001). A number of algorithms are available for solving optimisation problem. Most of the methods these algorithms used especially for solving non linear problems are based on trust region (Jorge and Sorensen, 1983). In this study, two of such algorithms are used. Sequential quadratic programming algorithm was used for the optimisation of constrained single objective distillation process and goal attainment method for the multi objective process.

2.6.1 Sequential quadratic programming

Sequential Quadratic Programming (SQP) has become the most successful method for solving nonlinearly constrained optimization problems. It was found to outperform every other compared method in terms of accuracy, efficiency and percentage over a range of test problems (Schittkowski, 1986)

Usually, the nonlinear programming problem to be solved is of the form

$$\min_{X} J(x)$$

$$\text{Subject to}: \begin{cases} h(x) = 0 \\ g(x) \leq 0 \end{cases} \qquad 2.54$$

Where h and g are define constraints and J is linear or quadratic.

SQP is not a feasible point method. This gives the method an edge over others because finding a feasible point especially for non linear constraint as found in distillation

processes may be nearly as hard as solving the optimisation problem itself. Also SQP method depends on the existence of accurate algorithm for solving quadratic programs (Boggs and Tolle, 1995). One of such algorithms fmincon is used for the optimisation problems in this study.

In previous studies, SQP has been augmented with a lagragian line search function (Schittkowski, 1983) and hybridised with harmony search algorithm (Fesanghary *et al*., 2008).

2.6.2 Goal attainment method

This method uses a set of objectives $J = \{J_1(x), J_2(x), \dots J_m(x)\}$ with a set of design goals $F = \{F_1(x), F_2(x), \dots F_m(x)\}$. The degree of over or under achievement of goals is controlled by a set of weighting factor $W = \{W_1, W_2, \dots W_m\}$.

The problem can be expressed as

$$\min_{x,\delta} \delta$$

Such that $J_i(x) - W_i\delta \leq F_i,\ i = 1, \dots m.$ 2.55

The weighting factor introduces a measure of slackness to the problem and allows for trade off between the objectives.

If there are a number of constraints to be satisfied, the problem becomes

$$\min_{x,\delta} \delta \begin{cases} J(x) - weight.\delta \leq goal \\ c(x) \leq 0 \\ ceq(X) = 0 \\ A.x \leq b \\ Aeq.x = beq \\ lb \leq x \leq ub \end{cases} \quad 2.56$$

Weight, goal b and beq are vectors, A and Aeq are matrices, and c(x), ceq(x) and F(x) are functions that return vectors. F(x), c(x) and ceq(x) can be non linear functions. X, lb and ub can be passed as vectors or matrices. Aeq is matrix of linear equalities constraints, beq is vector of linear equality constraint, lb is vector of lower bound and ub is vector of upper bound

This minimization is supposed to be accomplished while satisfying all the constraints. Some study on evolutionary based multi objective optimisation techniques are given in the literatures (Coello Coello, 1999, Deb, 2001)

2.7 Summary

Distillation column is one of the unit operations in chemical and petrochemical industries with a high potential for energy efficiency improvement. Economic, ecological and environmental benefit for such improvement is an enough incentive to seek for alternative ways of operating the column to bring about the desired change. Process control and optimisation of the column and alternative design of the column are some of the ways the column has been targeted for energy efficiency improvement in the past. This study is aimed at controlling and optimising the column albeit in terms of second law of thermodynamic application. It is novel ways of retrofitting existing columns for improve energy efficiency.

CHAPTER 3: MODELING AND OPTIMISATION OF DISTILLATION PROCESS

3.1 Introduction

Modelling and simulation is an insightful and productive process engineering tool. A model is a mathematical representation of the systems of a process while simulation is the computerised version of the model that gives a good understanding of the interaction of the model parameters. However, models are never a complete representation of reality as there will always be factors that cannot be included in the abstraction. The word model itself implies simplification and idealisation. A model simplifies and approximates reality and hence will not reflect all reality (Burnham and Anderson, 2002). However, the most influential factors must be included in the model. Models are conditional on available information and with enough data; imperfections in a model can be detected. Perhaps the aphorism "all models are wrong but some are useful" (Box and Norman, 1987) might be another way of saying models cannot be 100% accurate. There will always be some elements of approximations and simplifications. Calling a model right or wrong is therefore a matter of perspective.

Modelling provides the ability to base important engineering decisions on proven and tested numerical data, it helps to screen design alternatives without having to go through costly and time consuming experiments. It also synchronise the research and development with the industries, offering useful suggestions on ways of improving or designing processes and transferring knowledge and understanding between different groups involved in the development of a process. Models can be used in the design of a process with the particular specifications of the designer such as product quality and economy. It can also be used in the effective operation and improvement of an existing design. It equally finds relevance in the control of system design and could solve plant-wide operability problems. Modelling of chemical processes allows for further insights of the processes. This can aid in further analysis and optimal operation of the process to respond to increasing performance demands.

A number of approaches have been developed to model distillation columns. These approaches can be broadly classified as rigorous models and reduced models (Ochoa-Estopier *et al*., 2014). Reduced models can be divided into simplified or short cut models and data driven models. A number of simplified models of distillation columns have been studied. Pashikanti and Liu (2011) considered a predictive model of the

FCCU of the refinery. The model was used on an excel sheet with Aspen plus. A model to describe the effects of crude blending on the energy, emission and economic profit E3 was described and implemented in the HYSYS environment (Xu *et al.*, 2011). The model was for the crude and vacuum distillation units of the refinery. In another study, a refinery planning model was developed (Alattas *et al.*, 2011). Some other authors have presented works based on short cut models (Kumar *et al.*, 2001, Mahalec and Sanchez, 2012, Mizoguchi *et al*., 1995). This chapter however focuses extensively on rigorous model and data driven models

The choice of model to be used for a distillation column depends on a number of factors. In control and optimisation which is the focus of this thesis, factors such as accuracy, simulation time and robustness need to be considered. In this wise, the strengths and weaknesses of a number modelling technique are outlined and some examples where they have been used are given. The choice of modelling methods used in this thesis is also presented against the pros and cons of other existing models. The chapter is divided as follows. Section 3.2 presents rigorous models both in the steady and dynamic state and their methods of solution. In section 3.3, linear data driven models such as multiple linear regression (MLR), principal component regression (PCR) and partial least square (PLS) are presented. Non linear data driven model in form of artificial neural network (ANN) and bootstrap aggregated neural network (BANN) is presented in section 3.4. Section 3.5 concludes the chapter with a brief summary.

3.2 Rigorous Models

Models of distillation system have always assumed equilibrium cases for the stages. Models could be classified as equilibrium or non-equilibrium model. Non-equilibrium models are either rate based or stage by stage. Non-equilibrium models however involve large number of variables, leading to distillation models with differential equations that may exhibit high differential index and could generate stiff dynamics (Bonilla *et al*; 2012). Modelling of a process and in particular distillation system could be done in the steady state mode or dynamic mode.

3.2.1 Steady state modelling and simulation

Mathematical model of distillation unit vary from simple to complex depending on the nature of assumptions used in formulating the model. Usually the model equations for

the equilibrium stage of a distillation column is represented by the MESH equations, that is, mass balance, equilibrium, summation and enthalpy equations.

A distillation column with N equilibrium separation stages and C chemical species can be modelled with N(C+2) non-linear ordinary differential equations. Previously proposed models of crude distillation unit include the one by Naphtali and Sandholm (1971) which used N(2C+1) model where the independent variables are $l_{ji}, v_{ji}\ and\ T_j$, with N representing the no of trays and C representing the number of components. The mole fractions 2NC and total flow rates 2C were reduced to component flow rates. Therefore N(2C+3) stage variables were reduced to N(2C+1). Tomich (1970) had a variation of N(C+2) variables with the independent variable being $l_{ji}, V_j\ and\ T_j$ while Russel (1983) and Kumar *et al*., (2001) used N(C+3) variables with $l_{ji}, L_j, V_j and\ T_j$ as the independent variables. The explicit defined variables for each case were unique to each author.

Often, columns are simulated in the steady state for energy consumption analysis of the column, parametric analysis, developing energy saving methodology and environmental analysis of the column's operation. There have also been considerable efforts in simulating steady state operations of the distillation column for the determination of some online properties. Kumar *et al.,(*2001) focused on the model of a crude distillation unit for predicting the products from different specifications of crudes. The model was concluded to be suitable for production planning and scheduling, for online control and optimization and for process analysis and design. Online determination of the true boiling point (TBP) curve of the crude with a view to optimising the process were considered and steady state models for achieving the aim were developed (Dave *et al*., 2004, Dave *et al.*, 2003, Basak *et al.*, 2002). The authors claimed that economic optimisation and quality control of products is possible when online data are available and hence the need for steady state online model of the distillation process.

Most of these works are focused on predicting product qualities and composition of products. The need however arises to incorporate the dynamism of process energy efficiency and product qualities in the model of online predictions.

So far, the steady state cases considered were equilibrium based model. Non-equilibrium or rate based model are also of great importance because of additional insights to physical phenomenon in the column that can be gleaned from them. In this regard, the mass transfer rate equations and energy transfer rate equation for the liquid

and vapour phases were added to the MESH equations of each stage in the column. A procedure for solving each equation simultaneously using Newton's method was outlined by Krishnamurthy and Taylor and was applied to a set of binary systems (Krishnamurthy and Taylor, 1985, Luyben, 2006). Lee and Dudukovic (2011) however claimed that the homotopy continuation method is superior to the Newton-Raphson method in the solution of the non-equilibrium model. This approach has been applied to reactive distillation column and binary column but application to multicomponent system like crude distillation unit is a difficult task. This is because of the interaction between the process heat and mass transfer as well as the interaction between the components.

3.2.2 Dynamic modelling and simulation

As much as steady state simulation of processes finds relevance in the chemical and petrochemical industries, dynamic simulation is more useful in practice. Dynamic simulation is a useful tool in the study of the behaviour of processes and it serves to explore proper control strategy for the process. It can be used in investigating optimisation options of a process, start up and shut down procedures. It also finds applications in the quantitative and effective design of safety system in the column as a result of its accurate response time (Luyben, 2012).

In the dynamic simulation of a distillation column, a number of assumptions are made to simplify the models. Rarely can it be found in literature where rigorous dynamic models are made without simplifying assumptions (Van De Wal and De Jager, 2001). The assumptions fall under the categories of simplification to the vapour dynamics, the liquid dynamics and the energy balance.

Assumption on vapour dynamics: Neglecting the vapour holdup on each stage. This assumption is valid when the vapour component hold up can be neglected compared to liquid phase. It is however invalid for volatile components, column with high pressure and for cryogenic substances.(Luyben, 1990, Robbins, 2011) Another assumption is to fix pressure and neglect vapour hold up or include vapour hold up.

Assumption on energy balance: This include neglecting changes in energy hold up and changes in liquid enthalpy and assuming equal vapour flows up the column

Assumption on liquid dynamics: This is assuming a constant liquid hold up in the column. An often acceptable option is to linearize the dynamics of the column by using expressions such as Francis weirs equation.

Several authors have reported their findings on the dynamic modelling and simulation of the crude distillation unit (Goncalves *et al*., 2010, Kreul *et al.*, 1999). Most of these efforts are directed at studying the dynamic responses of the crude unit to step disturbances.

3.2.3 Methods of solution of models

Earlier before the advent of computer systems, approximate methods for making preliminary design and optimisation of crude distillation unit are the Kremser method, Edmister method and Fenske-Underwood-Gilliland (FUG) method (Green and Perry, 2006). Kremser method uses absorption factor method to provide algebraic solutions for equilibrium cascades. FUG method estimates reflux, number of tray and feed tray for design of a new column.

Solution methods for multicomponent require detail determination of pressure, temperature, flow rate, compositions and heat transfer on each tray of the column. This determination is made by solving the material balance equation, energy equations, equilibrium equations and summation equations (MESH). For a complex column like the crude distillation unit having a great number of stages and numerous numbers of components, equations to be handled are not only large in number but are nonlinear with strong interactions. Early attempts of solving these equations resulted in stage by stage and equation by equation attempts of Matheson (1932) and Thiele-Geddes (1933). Amundson and Pontinen (1958) solved the MESH equations component by components. Friday and Smith (1964) modified Amundson and Pontinen approach for components of similar volatility and termed it the bubble point (BP) method (Green and Perry, 2006). In the BP method, all but the Material balance (M) equations are solved sequentially while the M equations are solved for each component with the use of tridiagonal matrix technique. The BP method failed for components of wide volatility high boiling point difference and hence the sum of rates method (SR) was suggested. Because of the limits of the BP and SR methods, a simultaneous correction procedure that uses Newton Raphson method was developed. Other methods which have gained popularity are the Newton-Raphson method and the inside out method (Green and Perry, 2006).

3.2.4 Concluding Remarks

Rigorous models are often considered appropriate for simulation of distillation columns. This is because they provide accurate stage by stage information making them ideal for the design of distillation columns and for monitoring real time operations of the columns. Rigorous models are however computationally demanding and might not be feasible for real time optimisation. They are often not robust enough to accommodate disturbances that significantly deviate from initial guesses and the complexity of rigorous models often limits networking the distillation system with other heat integrated systems (Ochoa-Estopier et al., 2014). Another complication of rigorous models is their numerical complexity and the difficulty of describing the physiochemical phenomena such as thermodynamics driving VLE in a distillation column (Bachnas *et al.*, 2014).

3.3 Linear Data Driven Models

3.3.1 Multiple Linear Regression

Multiple linear regression (MLR) is an extension of simple linear regression. It is a linear regression model that contains more than one predictor variable and could be more than one response variable. MLR models the relationship between two or more predictor variables and one or more response variable by fitting a linear equation to observe the data.

A set of predictor variables X and response variables Y can be represented by equations 3.1 and 3.2

$$X = x_1 , x_2, \dots x_n \quad 3.1$$

$$Y = y_1 , y_2, \dots y_p \quad 3.2$$

Taking the case of having a response variable y with several predictor variables x_n, there will be an error on the measured value of y as given by equation 3.3

$$y = \beta_0 + \beta_1 x_1 + \beta_2 x_2 + \cdots + \beta_n x_n + \varepsilon \quad 3.3$$

Where β_0 is the intercept, $\beta_1, \beta_2 \dots \beta_n$ are the coefficients and $x_1, x_2 \dots x_n$ are the predictor variables. There is a need to estimate the various β coefficients. From a set of empirical data, a collation in matrix form can be obtained as given in equation 3.4

$$\begin{bmatrix} y_1 \\ y_2 \\ \vdots \\ y_p \end{bmatrix} = \begin{bmatrix} 1 & x_{11} & x_{12} & \dots & x_{1n} \\ 1 & x_{21} & x_{22} & \dots & x_{2n} \\ \vdots & \vdots & \vdots & \ddots & \vdots \\ 1 & x_{p1} & x_{p2} & \dots & x_{pn} \end{bmatrix} \begin{bmatrix} \beta_0 \\ \beta_1 \\ \beta_2 \\ \vdots \\ \beta_n \end{bmatrix} + \begin{bmatrix} \varepsilon_1 \\ \varepsilon_2 \\ \vdots \\ \varepsilon_p \end{bmatrix} \quad 3.4$$

The general form of the equation 3.4 is given in equation 3.5

$$Y = X.\underline{\beta} + \underline{\varepsilon} \quad 3.5$$

Where Y and $\underline{\varepsilon}$ are $(p \times 1)$ vector, X is $(p \times (n+1))$ matrix and $\underline{\beta}$ is a $((n+1) \times 1)$ vector. MLR model parameter is obtained from equation 3.6

$$\theta = (X^T X)^{-1} X^T Y \quad 3.6$$

Equation 3.6 is the so called batch least squares (BLS) solution.

Model prediction can then be calculated as

$$Y_p = X\theta \quad 3.7$$

Model prediction residual is calculated as

$$e = Y - Y_p \quad 3.8$$

Addition of more predictor variables creates more relationship among the variables. The predictor variables are related to response variable and potentially related to one another (Love, 2007). This is called multicolineraity. The ideal in applying MLR is for all the predictor variables to be correlated with the response variable and not with each other. Adding too many variables account for more variance and may not add to the model but might result in over fitting. Some preparation works are needed for MLR to be quite effective. This includes

- checking the relationship among the predictor variables using the scatter plots and correlations
- checking the relationship between each response variable and the predictor variable using the scatter plots and correlations
- use the non redundant predictor variable in the analysis to find the best fitting model
- Use the best fitting model to make predictions about the response variable.

In many chemical systems especially for distillation processes which are being considered here, most of the variables are correlated and highly non linear. To overcome the co linearity in the regression variables, principal component regression (PCR) or partial least squares (PLS) models are used to obtain the linearised models (Geladi and Kowalski, 1986).

3.3.2 Principal Component Regression

PCR overcomes the co-linearity problem by finding uncorrelated principal components of the original predictor variables and then used MLR to regress the principal component scores (PCi) against the independent variable(s) Y. PCR incorporates PCA (principal component analysis) with a regression model.

Assuming there is a set of predictor variables X and a response variable Y

$$X = x_1, x_2, x_3 \qquad 3.9$$

In figure 3.1, the PCA analysis of the X plane extracts the most variation of the data set yielding a representation of the sample in a space of fewer dimensions than the initial. A linear regression between the sample scores and the most collated factors in Y results in equation 3.10. Instead of using all the predictor variables for regression, the selected principal components are used

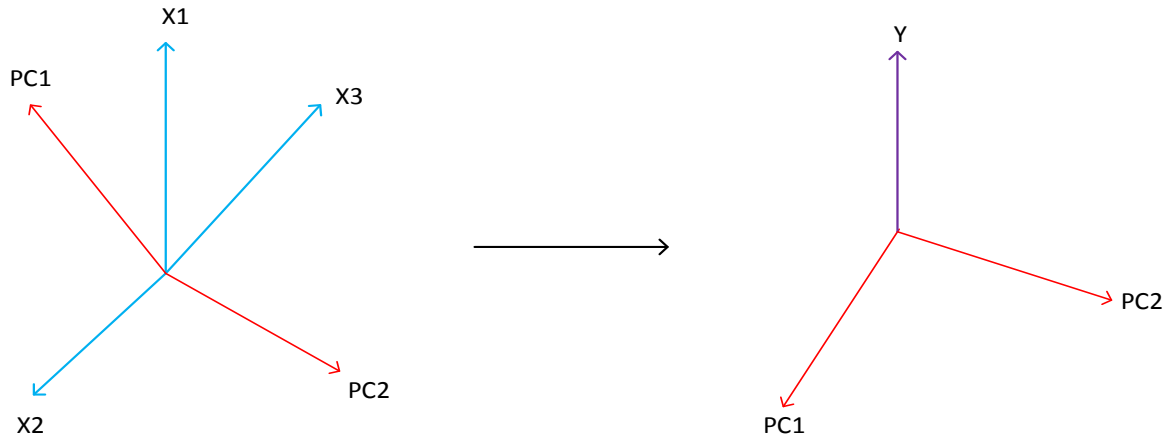

Figure 3.1: Description of PCR

$$Y = \beta_0 + \beta_1 PC1 + \beta_2 PC2 \qquad 3.10$$

One major use of PCR lies in overcoming the collinearity. PCR can aptly deal with such situations by excluding some of the low-variance principal components in the regression

step. In addition, by usually regressing on only a subset of all the principal components, PCR can result in dimension reduction. This can be particularly useful in settings with high-dimensional covariates. Also, through appropriate selection of the principal components to be used for regression, PCR can lead to efficient prediction of the outcome based on the assumed model.

3.3.3 Partial Least Squares

Partial least squares regression extends multiple linear regression without imposing the restrictions employed by discriminant analysis, principal components regression, and canonical correlation. Partial least squares regression has become a standard tool for modeling linear relations between multivariate measurements (de Jong, 1993).

In PLS, the outer decomposition of both the X and Y data matrices are performed. This is to maximize the covariance between X and Y.

Figure 3.2 shows a description of PLS

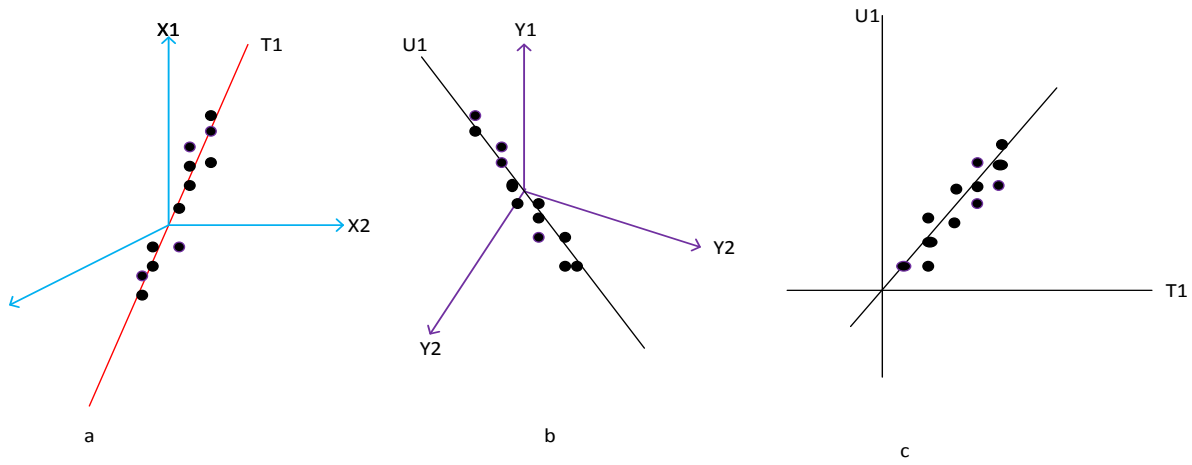

Figure 3.2: Description of PLS

Outer decomposition on X is as given in Figure 3.2(a) and is represented by the following equations

$$X = TP' + E \qquad 3.11$$

PCA on Y is as given in Figure 3.2(b)

$$Y = UQ' + F \qquad 3.12$$

T and U are scores of X and Y respectively while P' and Q' are loadings. The PLS inner relation is as given in Figure 3.2(c).

Principal components regression and partial least squares regression differ in the methods used in extracting factor scores. While, principal components regresses the covariance structure between the predictor variables, partial least squares regresses the covariance structure between the predictor and response variables.

PLS is advantageous in that it deals with colinearity, takes the X and Y axis data structure into account, provides great visual result that helps in interpreting the data, and can model several response variables at the same time taking their structure in to account.

3.3.4 Concluding remarks

Distillation system even in its simplest form of binary distillation are highly non linear. When the modelling of the system involves system interaction and thermodynamic analysis as being considered in this report, linear models as discussed above might be highly inadequate to predict the outcome of the model and might give fictitious and unreliable results. Application of these linear models in the simplest case of distillation system-binary distillation is discussed in Chapter 5.

3.4 Neural network model

An artificial neural network is an information processing system using computing techniques that are analogous to the human processes of thought and reasoning. Neuro-computing techniques has been in existence since around 1950s but has only be utilized for practical problem solving in the 1990s. They have been recognized as powerful tools for handling non linear problems especially when the relationships among variables are unknown.

3.4.1 Neural network structure

A neural network is made up of a number of interconnecting information processing elements called neurons. In figure 3.3, a typical multi layer neural network is given. Each of the input is connected to a neuron in the input layer and the input neurons are connected to the output neurons. Each connection link (known as synapses) has associated weights which determine the characteristics of the neural network. The prediction ability of the network is further enhanced by a hidden layers of neurons

between the input and output layers. The structure of a neural network is identified by its number of hidden layers and number of hidden neurons. Bias are added to the layers to improve the network's approximation capability. In figure 3.3 is a feed forward structure of a neural network with two hidden layers. In feed forward neural network, information propagates from the input to the output in a forward direction. It is the most commonly used form of neural network due to its effectiveness and simplicity. In this thesis, a single hidden layer feed forward neural network is used.

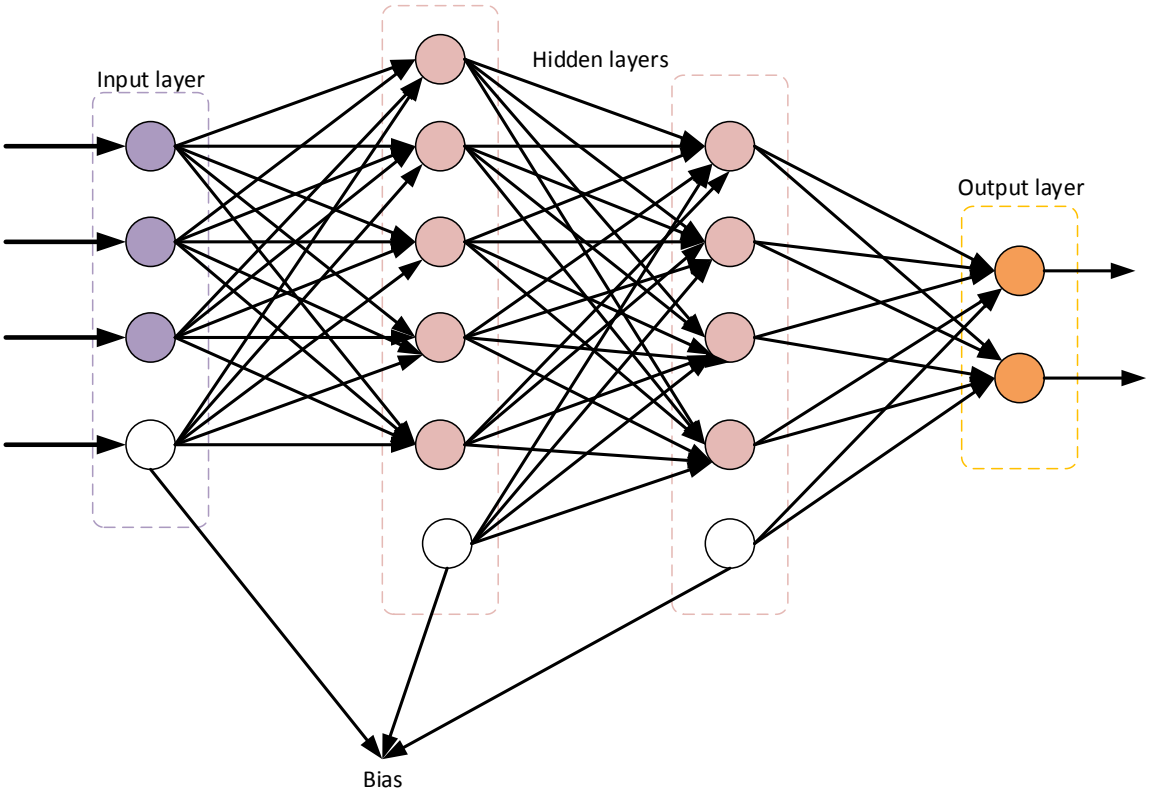

Figure 3.3: A three layer feed forward neural network

All neurons in the hidden layer are identical apart from the weight associated with their input and output. Figure 3.4 shows a single neuron in the hidden layer. Weighted inputs to the neuron are summed together as given in equation 3.13

$$u = w_1 x_1 + w_2 x_2 + \ldots + w_i x_i \qquad 3.13$$

A neuron activation function Φ is applied to the sum to get the neuron output in equation 3.14.

$$\vartheta = f(u) \qquad 3.14$$

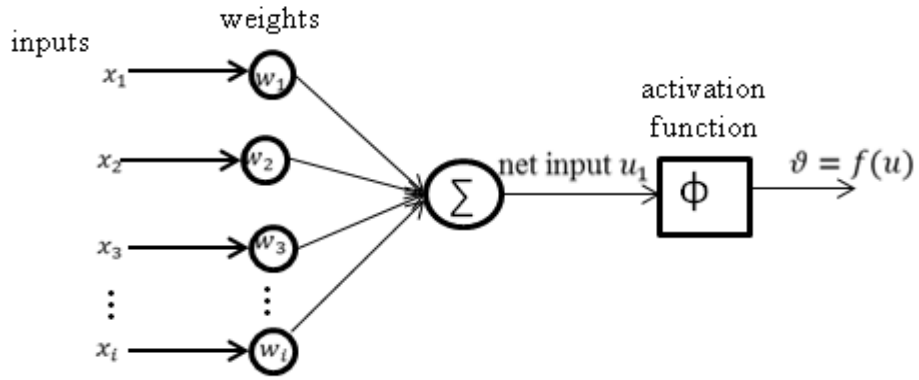

Figure 3.4: An artificial neuron

Some neuron activation function includes sigmoid function, linear functions, hyperbolic tangent and hard limiter. In this study the sigmoid activation function is used. The function models the non-linearity relationships in the input and scales the output between 0 and 1 as given in equation 3.15 and figure 3.5. If positive and negative outputs are required, the function can be rescaled into interval (+1, -1). The sigmoid activation function is commonly used in multilayer networks that are trained using the back propagation algorithm partly because they are differentiable (Martin, 2014).

$$\vartheta = \frac{1}{1+e^{-u}} \qquad 3.15$$

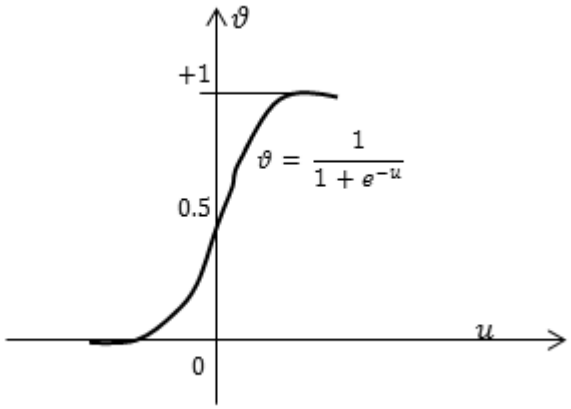

Figure 3.5: Sigmoid activation function

The objective of a neural network is to predict the output given a set of valid inputs. In figure 3.6, is a network with an input layer of p neurons ($i = 1 \rightarrow p$), a single hidden layer of h neurons ($k = 1 \rightarrow h$) and an output layer with a single neuron. The sum of the weighted inputs at the first neuron u_1 is given in equation 3.16

$$u_1 = w_{101} + w_{111}.x_1 + w_{121}.x_2 + w_{131}.x_3 + \ldots + w_{1p1}.x_p \quad 3.16$$

$$u_1 = w_{101} + \sum_{i=1}^{p} w_{1i1}.x_i \quad 3.17$$

For the kth neuron in the hidden layer

$$u_k = w_{10k} + \sum_{i=1}^{p} w_{1ik}.x_i \quad 3.18$$

Using the sigmoid activation function, the hidden layer output from the kth neuron is

$$\vartheta_k = \frac{1}{1+e^{-uk}} = \frac{1}{1+e^{-(w_{10k}+\sum_{i=1}^{p} w_{1ik}.x_i)}} \quad 3.19$$

The final output from the output layer is the sum of the weighted outputs from the hidden layer and given in equation 3.20

$$y = w_{001} + \sum_{k=1}^{h} w_{0k1}.\vartheta_k \quad 3.20$$

It can be clearly seen that without the activation function, the output reduces to that of a multiple linear regression

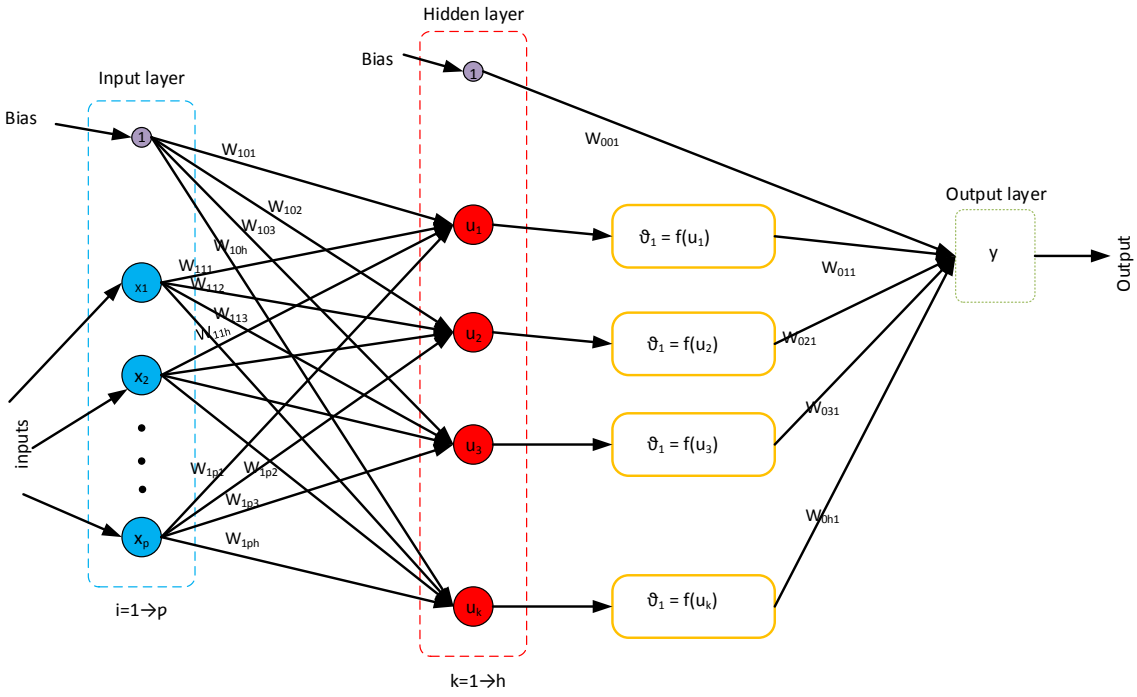

Figure 3.6: Detailed description of inputs, neuron and synapses

3.4.2 Neural network training

The objective of neural network training is to find appropriate network weights such that the relationship between model inputs and outputs presented in a data set can be well mimicked. The process of finding such sets of appropriate weight is termed neural network training. During training, the values of the weights and biases are tuned to optimize the network performance. The objective of the training is to minimize sum of squared differences between the targets output and the network outputs as represented in equation 3.21.

$$J = \frac{1}{n}\sum_{i=1}^{n}(y(i) - y'(i))^2 \qquad 3.21$$

y' is the target output, y is the neural network output and n is the number of training data. There are a number of network training methods. Levenberg- Marquardt optimisation algorithm is used in this thesis. This is because it improves training speed by using approximate Hessian matrix to determine the weight adaptation step size. The steps required in building neural network models are pictorially given in figure 3.7.

In the recent past a number of authors performed the steady state simulation of the distillation unit using some commercially available simulators such as Aspen Hysys and ProII (Mittal *et al.*, 2011, Arjmand *et al*., 2011, Anitha, 2011, Haydary, 2009).

In the design of process control and monitoring systems, considerations for energy and material costs in addition to process quality and throughput and demand for robust, fault-tolerant systems have introduced extra needs for effective process modelling techniques. In this regard, artificial neural network (ANN) has been recognised as a powerful tool that can facilitate the effective development of models for nonlinear, multivariable static and dynamic systems for both control and optimisation of process systems (Al Seyab and Cao, 2008, Cao *et al*., 2008). ANN can learn complex functional relations for a system from the input and output data of the system, hence serving as a black box model of the system (Liptak, 2006).

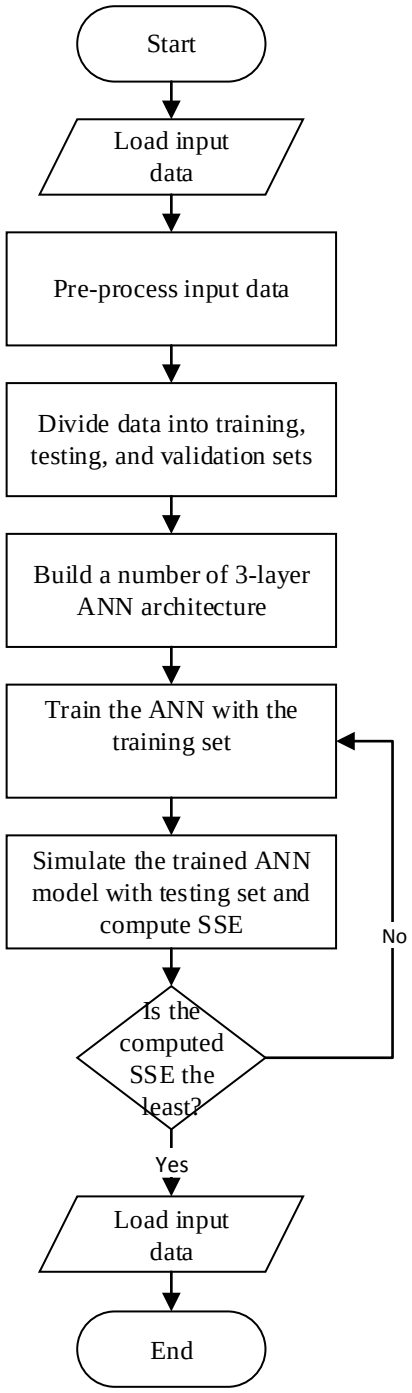

Figure 3.7: Building steps of neural network model

In the recent past a number of authors performed the steady state simulation of the distillation unit using some commercially available simulators such as Aspen Hysys and ProII (Mittal *et al.*, 2011, Arjmand *et al.*, 2011, Anitha, 2011, Haydary, 2009).

In the design of process control and monitoring systems, considerations for energy and material costs in addition to process quality and throughput and demand for robust, fault-tolerant systems have introduced extra needs for effective process modelling techniques. In this regard, artificial neural network (ANN) has been recognised as a

powerful tool that can facilitate the effective development of models for nonlinear, multivariable static and dynamic systems for both control and optimisation of process systems (Al Seyab and Cao, 2008, Cao *et al*., 2008). ANN can learn complex functional relations for a system from the input and output data of the system, hence serving as a black box model of the system (Liptak, 2006).

Distillation unit poses a great challenge to control engineers because of its complexity. It comes in varieties of configurations with different operating objectives, significant interactions among the control loop and specialised constraints. These result in distinct dynamic behaviours and different operational degree of freedom that will necessitate the need for specialised control configurations in order to optimize energy usage. Artificial neural network has found applications in distillation process from simple binary system to complex crude distillation system. This includes process control, process monitoring, system identification, process optimization and process sensors. Some of these are enumerated in the following subsections.

3.4.3 ANN in Binary Systems

Most neural networks for distillation process are based on feed forward neural network with back propagation learning algorithm. (Amit *et al*., 2013) used two neural network : a feed forward neural network (FFNN) and recurrent neural network (RNN) for a binary system of methanol-water. The network is a two layer with a hyperbolic tangent sigmoid function as activation function in the first layer and pure linear function in the second layer. The data for the training, testing and validation were acquired experimentally. The input to the neural network are reflux flow rate, feed flow rate, first tray temperature, reboiler duty, reflux drum top pressure and reboiler bottom pressure. The output of the neural network is the distillate composition.

In another previous work, the model of a methanol water system is considered. The network model a pilot plant distillation column which consist of 15 trays, a reboiler and a condenser. The feed is on the 8^{th} tray, and temperatures at trays 2, 6, 10 and 14 were measured under different reflux flow rates and reboiler heat inputs. The input to the network are reflux rate, reboiler heat input, reboiler temperature, condenser temperature and the 4 tray temperatures mentioned earlier and the outputs are top and bottom compositions. The FFNN was trained by the Levenberg-Marquardt optimisation algorithm. Hidden neurons used the sigmoid activation function and the output layer neurons used the linear activation function. The number of hidden neurons were

determined through trial and error of the network with the least sum of square error (SSE) (Abdullah *et al*., 2011).

A pilot scale binary distillation system for the separation of acetone and isopropyl alcohol is considered in (Osman and Ramasamy, 2010). Partial least square method (PLS) was used to determine the importance of the input variables. Two neural networks were trained and compared. One uses the feed forward network and the other is non-linear autoregressive with exogenous input (NARX). Both networks have three layers, input, hidden and output layers. Levenberg -Marquardt back propagation with momentum technique was used as training method. Pureline and tan sigmoid activation function were used in the output and hidden layers respectively for the two networks. The input variables are reboiler steam flow rate, reflux flow rate, column top pressure, column bottom temperature and tray temperatures along the column. The output is the mole fraction of acetone at the top. The neural network can be used in inferential closed loop control of the pilot plant distillation column.

An adaptive learning approach using a multi-layer feed forward neural network for composition control was the focus of another work. The neural network has two hidden layers. Activation function used was hyperbolic tangent function. The computer simulation shows the performance of the neural network controller as satisfactory (Yu, 2003).

In (González *et al*., 1999), LV control problem in binary column is addressed. The control was for composition set points in the distillate and the bottom. Two on-line trained feedforward neural networks were used to estimate unknown parameters and the closed loop behaviour of the system was illustrated in numerical simulations.

Model predictive control for a binary system of propylene and propane separation is presented in (Paraschiv *et al.*, 2009). The column is simulated in HYSYS and the control structure is implemented in MATLAB. The top and bottom compositions, feed flow and feed compositions are sent from HYSYS to the control structure. LB control is implemented here and the control variables reflux flow and bottom product flow are computed and sent at each sampling time to the process. The dynamic behaviour of the system in terms of composition set points, disturbances and controllers tuning parameters were analysed. The paper presented model based predictive control technique having the sampling time, prediction horizon, control variable horizon output and control variable weight as the tuning parameters.

3.4.4 Neural networks applied to multicomponent distillation

Neural networks have been applied to the control of industrial distillation column either directly or used in model predictive control. In (Bahar *et al*., 2004), inferential control of product compositions through temperature measurements using ANN is presented. A multi input multi output (MIMO) model predictive control (MPC) is used with the ANN estimator for the dual composition control of a multicomponent distillation column. It was concluded that the controller using ANN estimator is as good as the controller using direct composition method. A multilayer back propagation training algorithms was used. The inputs to the system are the temperatures of the selected trays, top and bottom compositions.

A soft sensor was developed for the monitoring of debutaniser column compositions (Fortuna *et al*., 2005). The neural network based sensor was developed from a set of historical data of a refinery. The sensors have been implemented and currently being used to monitor the production process.

A dynamic model of non-ideal distillation column using differential equations, algebraic equations and Newton-type recursions equations to calculate tray temperatures was developed in (XiaoOu and Wen, 2011). The model was identified using neural network. Based on the neural network identifier, a local optima controller is then designed. A numerical simulation of a 5 components distillation column with 15 trays was used to illustrate the effectiveness of the approach.

3.4.5 Applications of neural network in crude distillation unit

A steady state model from material and energy balance equations, phase equilibrium equations and summation equations was used to simulate a crude distillation unit. A multi-objective optimization problem was addressed. The decision variables which were varied within operability range were the four side strippers drawn flow rates, the four pump around flow rates, the reflux flow rate and the coil outlet temperature which determines the temperature of the feed to the CDU. The side stripper flow rate and reflux flow were varied by +_10% and the pump around flows by +-20%. The optimisation objectives were to maximise profit and minimise energy cost, maximise total distillate produced and minimise energy cost and maximise profit and minimise property deviation. The properties considered were specific gravities of products, flash point of product and % recovery of HGO at 366C.A new optimal operating conditions

was determined from the optimisation results. This was pegged to increase profit at the same energy costs.(Inamdar *et al*., 2004)

Steady state optimisation of a crude distillation system was studied in (Basak *et al*., 2002). Online optimisation was done using a tuned model and a back calculated TBP (true boiling point). The optimised control parameters include product draw rates, pump around flow rates, reflux flow rates and coil outlet temperature (COT). A code was developed in FORTRAN for the maximising of product properties and profit. Care must be taken to ensure that the model is in tune with plant operation by back calculating the crude TBP and tuning the model parameter (stage efficiencies) online using measured temperatures and other column parameters before applying the online optimisation. The cases investigated show potentials for yearly profit.

The maximisation objective used in (Liau *et al*., 2004) is the oil production rates subject to the market needs. Hence kerosene flow ratio, diesel flow ration and AGO flow ratio were optimised independently. ANN model which can predict oil product qualities with respect to the system input variables was built from a practical CDU operating condition. The ANN is a feed forward network with hidden layers using error back propagation training. Design of experiment (DOE) method was used to evaluate effect of each input variable on the quality of the product. The expert system was found to predict the optimal conditions for the various objective functions considered.

The approach taken in (Monedero *et al.*, 2012) is to optimize the energy efficiency including the production rate with required product quality while minimising the reboiler energy usage. The data generated from a practical crude distillation unit was pre-processed and modelled with SPSS modeller.

In the study (Ochoa-Estopier *et al*., 2013), a crude distillation system is simulated in HYSYS. ANN model is a feed forward back propagation network consisting of three layers. Hyperbolic tangent function was used for hidden layer and a linear transfer function for the output layer. The inputs to the system are the duty and temperature drop of the pump around and the flow rates of products. The outputs are variables that describe product quality (5 and 95% TBP) and minimum energy requirements variables such as enthalpy change, supply and target temperatures of process streams. The column was optimized to maximise profit and minimise energy requirements. Minimum energy requirements are calculated using the grand composite curve (GCC). Cost model were used to determine the product income and operating costs. Simulated annealing

optimization algorithm was used to solve the non-linear programming problem formulated.

An ANN model of a crude distillation unit with inputs as operating variables such as feed flow rate and temperature and the output as the product qualities is reported in (Motlaghi *et al*., 2008). The ANN model is a multilayer feed forward network trained with the Levenberg-Marquardt training method. The product quality was optimised using Genetic Algorithm (GA). The optimisation result yielded optimal operating conditions for the unit.

3.4.6 Bootstrap Aggregated Neural Network

The objective in neural network modelling is to build a network that can generalise. That is, it can give excellent performance on the training data as well as unseen testing data. This however is not always the case in neural network training. When building neural network models from the same data set, there is possibility that different networks perform well in different regions of the input space. Hence, prediction accuracy on the entire input space could be improved when the multiple neural networks are combined instead of using a single neural network. In a bootstrap aggregated neural network model, several neural network models are developed to model the same relationship. Individual neural network models are developed from bootstrap re-sampling replications of the original training data. Instead of selecting a single neural network that is considered to be the "best", several networks are combined together to improve model accuracy and robutsness. These models can be developed on different parts of the data set.

The data for building neural network models are re-sampled using bootstrap techniques. Distribution of the data that is obtained through bootstrap resampling is similar to the original data distribution. The idea of bootstrap resampling is to suppose that a cumulative distribution function (CDF) $\overline{F}$ calculated from an observed sample $x_1, \ldots x_n$ is sufficiently like the unknown CDF F such that a calculation performed based on $\overline{F}_n$ can be used as an estimate of the calculation to be performed based on F. In this thesis, for the BANN modeling in chapters 5 and 6, 30 data sets were obtained through bootstrap resampling of the original data. Each data are then divided to form several pairs of training, testing and validation data sets. A neural network model is then developed from each pair of training and testing data sets.

Predictions from the individual neural networks are combined to give the final model predictions. This overall output is a weighted combination of the individual neural network outputs. This is represented by equation 3.22

$$f(x) = \sum_{i=1}^{n} w_i f_i(x) \quad 3.22$$

where $f(x)$ is the aggregated neural network predictor, $f_i(x)$ is the *i*th neural network, w_i is the aggregating weight for combining the *i*th predicted neural network, n is the number of neural networks and x is a vector of neural network inputs.

The aggregating weight w_i needs to be properly determined for enhanced model prediction and performance. Since the neural networks are highly correlated, appropriate aggregating weight can be obtained through PCR (Zhang, 1999).

If y is the expected model ouput for a neural network and $\overline{y}$ be a vector of the predictions from the ith neural network predictor: predictions from a set of n predictors can be put in a matrix form as given in equation 3.23

$$\overline{Y} = [\overline{y}_1 \ \overline{y}_2 \ldots \overline{y}_n] \quad 3.23$$

Each column in equation 3.24 corresponds to an individual predictor. The vector of prediction from BANN model $\overline{y}_B$ can then be represented as

$$\overline{y}_B = \overline{Y}w = w_1\overline{y}_1 + w_2\overline{y}_2 + \cdots w_n\overline{y}_n \quad 3.24$$

The matrix $\overline{Y}$ can be decomposed through principal component decomposition into the sum of series of rank one matrices as

$$\overline{Y} = t_1 p_1^T + t_2 p_2^T + \ldots + t_n p_n^T \quad 3.25$$

Where t_1 is the ith score vector and p_1 is the loading vector. The loading vector defines the direction of the greatest variability and the score vector represents the projection of each column of $\overline{Y}$ onto p_1. Through PCR, the BANN model output is obtained as a linear combination of the first few principal components of $\overline{Y}$. If the first few principal components used are denoted by T_k and T_k is expressed as

$$T_k = \overline{Y}P_k \quad 3.26$$

Where $P_k = [p_1 \ p_2 \ \ldots p_k]$

Then the BANN model can be represented as

$$\overline{y}_B = T_k\theta = \overline{Y}P_k\theta \quad 3.27$$

The least square estimation of θ is

$$\overline{\theta} = (T_k^T T_k)^{-1} T_k^T y = \left(P_k^T\ \overline{Y}^T \overline{Y} P_k\right)^{-1} P_k^T \overline{Y}^T y \quad 3.28$$

The aggregating weight calculated through PCR is

$$w = P_k\theta = P_k \left(P_k^T\ \overline{Y}^T \overline{Y} P_k\right)^{-1} P_k^T \overline{Y}^T y \quad 3.29$$

BANN has the advantage of model prediction confidence bounds.

The prediction confidence bounds can be calculated as described below

Having generated n samples, each drawn with replacements from m training observations as

$$\{(x_1, y_1), (x_2, y_2), \dots, (x_m, y_m)\} \quad 3.30$$

If the bth sample is denoted by

$$\left\{\left(x_1^b, y_1^b\right), \left(x_2^b, y_2^b\right), \dots, (x_m^b, y_m^b)\right\} \quad 3.31$$

For each bootstrap sample $b = 1, 2, \dots, n$, a neural network model is trained. The weights of the resulting neural network model is denoted by W^b

Then the standard error of the ith predicted value can be given by

$$\sigma_e = \left\{\frac{1}{n-1} \sum_{b=1}^{n} [y(x_i; W^b) - y(x_i;)]^2\right\}^{\frac{1}{2}} \quad 3.32$$

where $y(x_i) = \sum_{b=1}^{n} y(x_i; W^b)\ /n$ and n is the number of neural networks.

The 95% prediction confidence bounds can be calculated as $y(x_i;) \pm 1.96\sigma_e$.

To demonstrate the procedure outlined, an example is given as follows.

For example, Assuming data sample were generated from the equation

$$y = \text{cosine}(x) \quad 3.33$$

where x was generated as random numbers between 1 and 10 with an increment of 0.2. 46 data points were generated to build the neural network model. 24 of the data points were selected randomly for training, 14 for testing and 8 for validation. Figure 3.8

shows the training, testing and validation data sets. A number of network with different number of hidden neurons were studied. Network were trained on the training data set and appropriate network structure is selected after testing with the testing data sets. During the training, the sum of square error (SSE) is continously checked on the testing data set and the network that gives the least SSE is considerd as having the appropriate number of hidden neurons. In table the SSE for training, testing and validation for different number of hidden neuron is shown. The network structure with 3 hidden neuron has the least SSE.

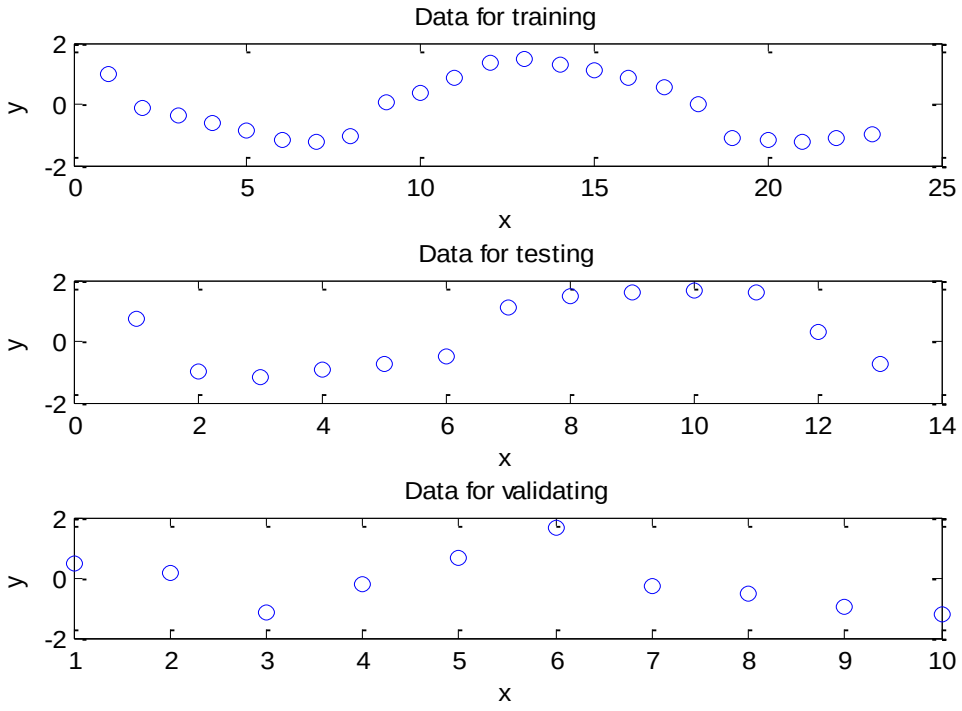

Figure 3.8: Training, testing and validation data sets.

Table 3.1: SSE for a number of neural networks

No of hidden neuron	SSE training	SSE testing	SSE validation
2	1.2671	1.5560	0.2921
3	0.00094	0.3195	0.0054
4	0.00099	0.3471	0.0066
5	0.00097	0.3241	0.0054
6	0.0017	0.3714	0.0075
7	0.1331	0.3246	0.0230
8	0.00099	0.3468	0.0064

A BANN model containing 30 networks was developed. Training data for each network was obtained from bootstrap resampling of the original training data. Levenberg Marquardt algorithm was used for the training and network aggregating weights were obtained through PCR. An example code for implementing this in MATLAB is given in Appendix B. The SSE for the training, testing and validation data sets for the BANN model are 0.0023, 0.0042 and 0.0012 respectively. The model accuracy can be seen to be significantly improved using BANN model.

3.4.7 Neural network and optimsation

Since ANN can learn complex relationships from the input and output data and hence can adequately predict unknown process variables then there is a scope of harnessing ANN for optimising the values of such variables. The optimised values can then be used as input to a real time optimiser. Figure 3.8 shows the structure of using a neural network for the optimisation.

Real time optimisation of distillation columns based on mechanistic models is often infeasible due to the effort in model development and the large computation effort associated with mechanistic model computation. This issue can be addressed by using neural network models which can be quickly developed from process operation data. The application of data driven process modelling in the optimisation of binary distillation column, multicomponent distillation column and crude distillation units are explored further in the chapters 5 and 6 of this thesis.

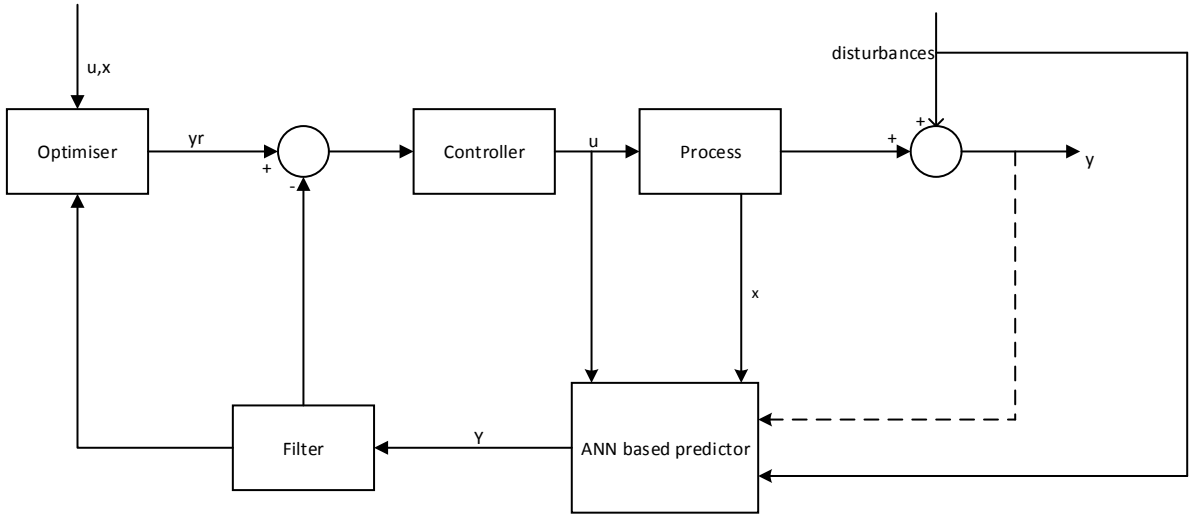

Figure 3.9: Structure of neural network for optimisation
Source: (Love 2007)

3.4.8 Concluding remarks

Data driven models like ANN and BANN have a wide range of application in the process industries. They are more robust, computationally less time consuming than rigorous models and are able to accommodate complexities in processes. However, the fact they are data driven suggests the need for the accuracy of the data on which they are trained. They might also be found unsuitable for processes that deviate significantly from the original data and thus limit their versatility.

3.5 Summary

Rigorous models and data driven models of distillation column has been extensively discussed in this chapter. Rigorous model gives accurate stage by stage information on distillation column and are essential for the design of the column. Rigorous models are however significantly limited for process optimisation. This is because they are sensitive to initial guesses and hence are generally not robust to significant changes. Also convergence of the model can be very slow especially for complex distillation column like the crude distillation unit. Linear data driven models perform better in terms of robustness, convergence and time. They are however not able to adequately model the non-linearity nature of the column and hence are not appropriate for distillation column. Non-linear data driven models (ANN and BANN) are extremely robust with a very short computation time. This makes them ideal for real time optimisation and model predictive control of the column. However caution must be taken to ensure correct, quality and accurate data are used for the modelling. This is because the quality of the model depends on the quality of the data. Also it is not advisable to use the model on data beyond the range of the data used for regression. This is because the model is not based on physical principles and hence might not hold true for every columns that significantly deviate from the base column for the modelling.

CHAPTER 4: DISTILLATION CONTROL STRUCTURE SELECTION FOR ENERGY EFFICIENT OPERATIONS

This chapter is based on the paper published in Chemical Engineering and Technology

4.1 Introduction

There have been several studies aimed at improving the energy efficiency of distillation processes which has led to evolving distillation schemes different from the conventional ones. These include but not limited to vapour recompression (Kim, 2012), heat integrated distillation columns (Kiss *et al*., 2012) and dividing wall columns (Chun and Kim, 2013). The operation of distillation systems irrespective of whether conventional or heat integrated columns can be better improved with appropriate control schemes. Distillation has in fact been identified as the unit operation that could be significantly improved with good control with an estimate of about 15% reduction of energy if proper column control were in use (Dartt, 1985). One of the three issues identified by Skogestad and Morari (Skogestad and Morari, 1987) in the control of distillation columns is the control structure selection. Take for example, the control of a typical binary distillation system is usually viewed as a 5×5 control problem with 5! = 120 possible combinations of control loop pairings. Each of the configurations has different degrees of control loop interactions and disturbance sensitivities making the design of distillation control systems a difficult venture. Methods of selection of controlled variables for processes such as evaporator and exothermic reactor has been discussed extensively in the literatures (Umar *et al*., 2014).

Relative gain array (RGA) is commonly used for the selection of the best control structure (Skogestad *et al*., 1990, Skogestad and Morari, 1987, Xiong *et al*., 2005, He *et al*., 2009). The steady state RGA however contains no information on the dynamic and disturbance on which distillation is hinged. This has led to the modifications of the RGA technique by different researchers to evolve techniques such as dynamic relative gain array (DRGA), effective relative gain array (ERGA) and relative normalized gain array (RNGA) (He *et al*., 2009, Xiong *et al*., 2005, Mc Avoy *et al*., 2003).

However, despite all the modifications, control loop interaction analysis is no longer sufficient for the selection of the best control strategy in the context of sustainable chemical industry. This is because of the cost and environmental implications of energy and the need to incorporate minimum energy usage in the selection of the control structure (Munir *et al.,* 2012d). In this wise a number of tools based on application of

thermodynamics in the process control regime have been developed. These include relative exergy array (REA), exergy ecoefficiency factor (EEF), and relative exergy destroyed array (REDA) (Munir *et al.*, 2012a, Munir *et al*., 2013c, Munir *et al*., 2012c, Montelongo-Luna *et al.*, 2011). These methods are all based on steady state and have not been validated in the dynamic state. This chapter aims at using thermodynamics analysis in addressing the important issue of control structures selection for distillation columns. This is with a view of identifying the best energy efficient control strategies from a number of alternatives and validating the methods in the dynamic states. This will then lead to an optimum control structure that will serve the dual purpose of achieving good product quality and minimum energy usage. A full detailed thermodynamic analysis of the control structures in the steady state with the aim of gaining insights into the exergy efficiency and exergy loss of each control structure is also given. The viability of the selected control scheme in the steady state is further validated by the dynamic simulation in responses to various process disturbances and operating condition changes. This is to show the performance of the control structure in terms of composition control and energy efficiency.

This chapter is organised as follows. Section 4.2 describes the distillation systems and their modelling. The systems are modelled from the fundamental equations and HYSYS simulation. Section 4.3 gives an overview of the control structure selection in terms of RGA and REA. In Section 4.4, application to methanol-water system is described while Section 4.5 presents the application to benzene-toluene system. Section 4.6 gives the conclusion of the chapter.

4.2 Binary distillation systems and modelling

4.2.1 Binary distillation columns

A simple binary distillation system is shown in figure 4.1 and it consists of a reboiler, a condenser, a single feed stream, a distillate product stream and a bottom product stream. Methanol-water separation and benzene-toluene separation were considered in this study. The methanol-water system contains 50% methanol to be continuously rectified at 1 atm and at a rate of 4320kg/h to provide a distillate containing 99% methanol and a residue containing 1% methanol (by weight). The number of stages in the column is 16, and the feed is on the 4^{th} tray with bottom up numbering.

For the benzene–toluene mixture, a continuous fractionating column is used to separate 30,000 kg/hr of a mixture with 44% benzene and 56% toluene at 95°C into an overhead product containing 95% benzene and a bottom product containing 5% benzene at a

pressure of 1 atmosphere and actual reflux ratio of 3.5. The relative volatility of the mixture is given as 2.5. The number of stages is 11 with the feed on the 5th stage numbering from bottom up.

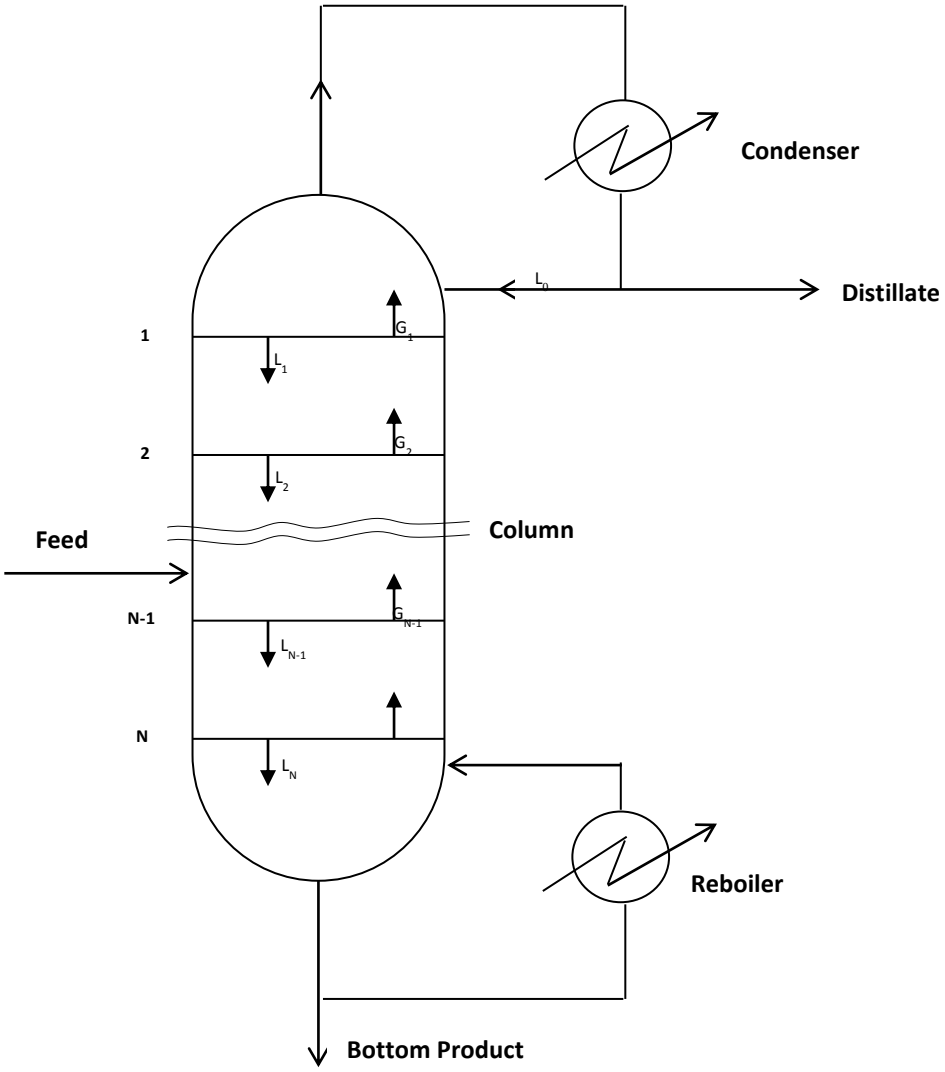

Figure 4.1: Schematic diagram of a binary distillation system

4.2.2 Modelling of distillation columns

The mathematical model of a distillation column is an aggregation of individual theoretical stages. Figure 4.2 shows a generic stage.

Component continuity equation:

$$\frac{d(M_j\chi_{j,i})}{dt} = L_{j+1}\chi_{j+1,i} + V_{j-1}y_{j-1,i} + F_j^l\chi_{j,i} + F_j^v y_{j,i} - L_j\chi_{j,i} - V_j y_{j,i} \qquad 4.1$$

where M_j is the liquid hold up in the *j*th stage, $\chi_{j,i}$ is the composition of *i*th component in the liquid at the *j*th stage, $y_{j,i}$ is the composition of *i*th component in the vapour at the *j*th stage, L_j is the liquid flow rate leaving from the *j*th stage, V_j is the vapour flow rate

leaving from the *j*th stage, F_j^l is the liquid feed rate, F_j^v is the vapour feed rate, and *t* is time.

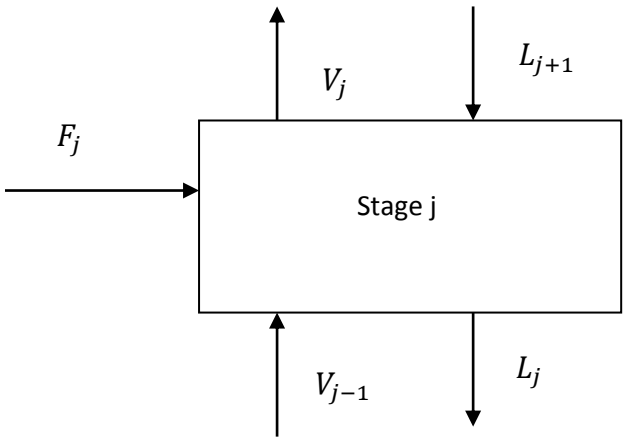

Figure 4.2: Diagrammatic representation of an equilibrium stage

The dynamic state equations for a general stage are given below.

Total continuity equation:

$$\frac{d(M_j)}{dt} = L_{j+1} + V_{j-1} + F_j^l + F_j^v - L_j - V_j \qquad 4.2$$

Energy equation:

$$\frac{d(M_j h_j)}{dt} = L_{j+1}h_{j+1} + V_{j-1}H_{j-1} + F_j^l h_j + F_j^v H_j - L_j h_j - V_j H_j \qquad 4.3$$

where h_j is the liquid enthalpy from the *j*th stage and H_j is the vapour enthalpy from the *j*th stage.

Equilibrium equations:

$$y_{j,i} = K_{ji}\chi_{j,i} \qquad 4.4$$

$$\chi_{j,i} = \frac{l_{ji}}{L_j} \qquad 4.5$$

$$y_{j,i} = \frac{v_{ji}}{V_j} \qquad 4.6$$

where K_{ji} is the equilibrium constant for the *i*th component on the *j*th stage, l_{ji} is the liquid flow rate of the *i*th component from the *j*th stage, and v_{ji} is the vapour flow rate of the *i*th component from the *j*th stage.

Liquid summation equation:

$$L_j = \sum_{i=1}^{C} L_{ji} \quad 4.7$$

where *C* is the total number of components and *C*=2 for the case of binary distillation.

Vapour summation equation:

$$V_j = \sum_{i=1}^{C} V_{ji} \quad 4.8$$

Usually dynamic simulations of distillation systems are made with some assumptions to simplify the model (Skogestad, 1997). The assumptions made for the dynamic modelling and simulation of the two distillation columns considered here are:

- Equilibrium between the liquid and vapour on each stage
- Neglecting hold up in the gas phase
- The liquid stream was modelled using linearised tray hydraulics incorporating activity coefficient equations (Wittgens and Skogestad, 2000).
- Antoine's equation was used for the vapour pressure model

If the specific liquid enthalpy is assumed to be a function of the specific heat capacity C_p, then

$$h_{L,j} = C_p(\Delta T) \quad 4.9$$

The specific vapour is assumed to be

$$h_{V,j} = h_{L,j} + H_{vap} \quad 4.10$$

where H_{vap} is the heat of vaporisation.

4.3 Distillation control structure selection

Generally, variables that are needed to be controlled for a binary distillation column are composition of the distillate χ_D, composition of the bottom product χ_B, liquid level in the reflux drum, liquid level in the base drum and pressure in the column. Usually, the manipulated variables are reflux flow, *L*, reboiler vapour flow, *V*, distillate flow, *D*, bottom product flow, *B*, and condenser duty. Column pressure is usually controlled by the condenser duty and various distillation column control configurations refer to the

pairing of other controlled and manipulated variables. Some typical distillation column control schemes include *LV*, *DV*, and *LB* control configurations.

In the *LV* control configuration, the top product composition is regulated by adjusting the reflux flow *L* and the bottom product composition is controlled by adjusting the reboiler's energy which is equivalent to reboiler vapour flow *V*. Distillate rate is used to control the condenser level and bottom product rate *B* is used to control the reboiler level. Similarly for the *DV* control configuration, *L* is used to control the condensor level and *D* is used to control the top composition while the reboiler level is controlled by *B* and the bottom product composition is controlled by *V*.

4.3.1 RGA analysis

A multi-input multi-output (MIMO) system usually has interactions among the control loops. For better control of a process, control loop interactions should be minimised as a high degree of loop interaction makes the control difficult. Relative gain array (RGA) proposed by Bristol (Bristol, 1966) is a tool that can be used to quantify control loop interactions. Relative gain is the ratio of the steady state gain when the loops are open to the steady state gain with all other loops closed.

The relative gain between the *i*th controlled variable and the *j*th manipulated variable is represented mathematically as

$$\alpha_{ij} = \frac{\left(\frac{\Delta y_i}{\Delta u_j}\right)_{all\ loops\ open}}{\left(\frac{\Delta y_i}{\Delta u_j}\right)_{all\ loops\ closed\ except\ the\ u_j\ loop}} \qquad 4.11$$

$$= \frac{open\ loop\ gain}{closed\ loop\ gain}$$

RGA is then obtained when the relative gains for all the pairing combinations in a multi-loop control system are calculated and put in an array.

$$RGA = \begin{bmatrix} \alpha_{11} & \alpha_{12} & \dots & \alpha_{1n} \\ \alpha_{21} & \alpha_{22} & \dots & \alpha_{2n} \\ \vdots & \vdots & \ddots & \vdots \\ \alpha_{n1} & \alpha_{n2} & \dots & \alpha_{nn} \end{bmatrix} \qquad 4.12$$

A relative gain of 1 on the diagonal of RGA indicates that there are no control loop interactions. The strategy is then to match the controlled and manipulated variables when α_{ij} is nearest to 1 and to avoid the pairings with close to zero or negative relative gains.

4.3.2 Thermodynamic analysis

Exergy is from a combination of the 1st and 2nd laws of thermodynamics. It is a key aspect of providing better understanding of the process and quantifying sources of inefficiency and distinguishing quality of energy used (Jin *et al*., 1997, Rosen and Dincer, 1997, Doldersum, 1998). Exergy analysis is a measure of the quality of energy and is the maximum work produced or the minimum required depending on whether the system produces or requires work in bringing the system through reversible process with the environment. It is a tool for determining how efficient a process is (Dhole and Linnhoff, 1993, Demirel, 2004).

Exergy represents the part of energy, which can be converted into maximum useful work. It is used to establish criteria for the performance of engineering devices (Asada and Boelman, 2004). Unlike energy, exergy is not conserved and gets depleted due to irreversibilities in the processes (Sengupta *et al*., 2007). The greater the extent of irreversibilities is, the greater the entropy production is. Therefore, entropy can be used as a quantitative measure of irreversibilities associated with a process. Minimization of irreversibility in processes implies increase in energy efficiency of such process. Exergy analysis of processes gives insights into the overall energy usage evaluation of the process, potentials for efficient energy usage of such processes can then be identified and measures for improving energy usage of the processes can be suggested.

The total exergy of a stream is calculated as

$$Ex_{total} = Ex_{phy} + Ex_{chem} + Ex_{mixing} \quad 4.13$$

$$Ex_{phy} = H - H_0 - T_0(S - S_0) \quad 4.14$$

$$Ex_{phy} = \Delta H - T_0 \Delta S \quad 4.15$$

$$\Delta Ex_{chem=} \sum n_i b_{chi} + RT_0 \sum n_i ln\gamma_i \quad 4.16$$

In the above equations, b_{chi} is the chemical exergy for component i, γ_i is the activity coefficient of component i, H is the total enthalpy, S is the total entropy, T_0 is the reference temperature, H_0 and S_0 are enthalpy and entropy respectively measured at reference conditions.

For a heat source such as the reboiler, if Q_z is a heat source at an absolute temperature, T_z, and if T_0 is the ambient temperature, then the work equivalent of heat is given by (Dincer and Rosen, 2012)

$$W_Z = \int_{intial}^{final} \left(1 - \frac{T_0}{T_Z}\right) \partial Q_Z \quad 4.17$$

where ∂Q_Z is an incremental heat transfer at absolute temperature T_Z and the integral is from initial state to final state.

If the temperature of the heat source is constant, the work equivalent of heat is given by (Dincer and Rosen, 2012)

$$W_{\max} = \frac{(T_z - T_0)Q_z}{T_z} \quad 4.18$$

This is the absolute theoretical maximum work recoverable. Equation 4.18 is used in calculating the exergy of the reboiler and the condenser.

Exergy efficiency of a system is calculated as

$$\varphi = \frac{\sum Ex_{out}}{\sum Ex_{in}} \quad 4.19$$

While the exergy loss of a system is given as

$$I = \sum Ex_{in} - \sum Ex_{out} \quad 4.20$$

It takes a good engineering judgement to determine the streams that are qualified as in and those that are qualified as out.

For a binary distillation system the total exergy in and total exergy out are given as

$$Total\ Ex_{in=} Ex_{feed} + Ex_{Reboiler} \quad 4.21$$

$$Total\ Ex_{out} = Ex_{Distillate} + Ex_{Bottoms} \quad 4.22$$

In the above equations, Ex_{feed}, $Ex_{Reboiler}$, Ex_{Reflux}, Ex_{Boilup}, $Ex_{Distillate}$, and Ex_{Bottom} are, respectively, the exergy in the feed stream, reboiler, reflux stream, boil up stream, distillate product stream, and bottom product stream.

4.3.3 Relative exergy array

Relative exergy gain is defined as "the ratio of the gain change in the steady state exergy of the controlled stream with respect to that of the manipulated stream when all loops are open to the gain change in the steady state exergy of the controlled stream with respect to that of the manipulated stream when all other loops are closed and in perfect control" (Montelongo-Luna *et al.*, 2011). This is given in equation 4.23.

$$\beta_{ij} = \frac{\left(\frac{\Delta Ex(y_i)}{\Delta Ex(u_j)}\right)_{all\ loops\ open}}{\left(\frac{\Delta Ex(y_i)}{\Delta Ex(u_j)}\right)_{all\ loops\ closed\ except\ the\ u_j\ loop}} \quad 4.23$$

REA is based on the RGA concept by replacing relative gain with relative exergy gain. The exergy gain ratio is usually calculated after a step input change in the manipulated variable. It gives the amount of exergy change in the controlled variable resulting from the exergy change in the manipulated variable and hence provides information on the thermodynamic efficiency of the pairing. This permits a good insight to the energy efficiency of a process right from the design stage and allows for the choice of optimum combination of loops.

Putting all the relative exergy gains in an array gives the relative exergy array:

$$REA = \begin{bmatrix} \beta_{11} & \beta_{12} & \cdots & \beta_{1n} \\ \beta_{21} & \beta_{22} & \cdots & \beta_{2n} \\ \vdots & \vdots & \ddots & \vdots \\ \beta_{n1} & \beta_{n2} & \cdots & \beta_{nn} \end{bmatrix} \quad 4.24$$

REA indicates the exergy efficiency effects of pairing each of the manipulated variables to each of the controlled variables. It is defined analogous to the relative gain array. If the value of a relative exergy gain on the diagonal of REA is equal to 1, then it indicates the thermodynamic efficiency of the control loop under consideration is not affected by the other control loops (Montelongo-Luna *et al*., 2011, Munir *et al.*, 2013c, Munir *et al*., 2012b). This control loop pairing will be good in terms of thermodynamic efficiency. The value of a relative exergy gain greater than 1 implies that the exergy change from the open loop is much more pronounced. In this case, interaction from the variables in the process will decrease the process exergy change. The value of a relative exergy gain less than 1 indicates the exergy change due to open loop is less and hence an increase in exergy changes when the loops are closed. If the sign is negative, closing the control loop will improve the thermodynamic efficiency of the process but if on the other hand the sign is positive, this shows that the thermodynamic efficiency of the process will be decreased by the control loop. In control structure selection, a control loop paring with relative exergy gain close to one is preferred.

4.4 Application to methanol-water separation column

The methanol-water system was simulated from the fundamental first principle model in MATLAB. Three control configurations, LV, DV and LB, are considered for the

system. The open loop responses of the controlled variables (distillate and bottom compositions) to step changes in their corresponding manipulated variables for each of the configurations are shown in Figure 4.3 to Figure 4.5 for the methanol-water system
The transfer function of a first order system is given by

$$G(s) = \frac{Y(s)}{X(s)} = \frac{K_c}{1+\tau s} \quad 4.25$$

$$K_c = \frac{\Delta y}{\Delta U} \quad 4.26$$

Where K_c is the process gain

τ is process time constant

$Y(s)$ is the response of the process

$X(s)$ is the process input

Δy is the change in the controlled variable

ΔU is the change in the manipulated variable.

Transfer function models are identified from the open loop step response data and are shown as follows.
Transfer function matrix of the LV configuration for methanol-water separation:

$$G(s) = \begin{pmatrix} \frac{0.259}{1+5.21s} & -\frac{1.109}{1+5.14s} \\ \frac{0.114}{1+5.31s} & -\frac{2.196}{1+4.42s} \end{pmatrix} \quad 4.27$$

Transfer function matrix of the DV configuration for methanol-water separation:

$$G(s) = \begin{pmatrix} \frac{-2.42}{1+3.61s} & +\frac{1.36}{1+3.96s} \\ \frac{-1.19}{1+4.04s} & -\frac{1}{1+3.03s} \end{pmatrix} \quad 4.28$$

Transfer function matrix of the LB configuration for methanol-water separation:

$$G(s) = \begin{pmatrix} \frac{1.45}{1+3.88s} & +\frac{1.08}{1+6.01s} \\ \frac{-1.1}{1+4.65s} & +\frac{2.19}{1+3.63s} \end{pmatrix} \quad 4.29$$

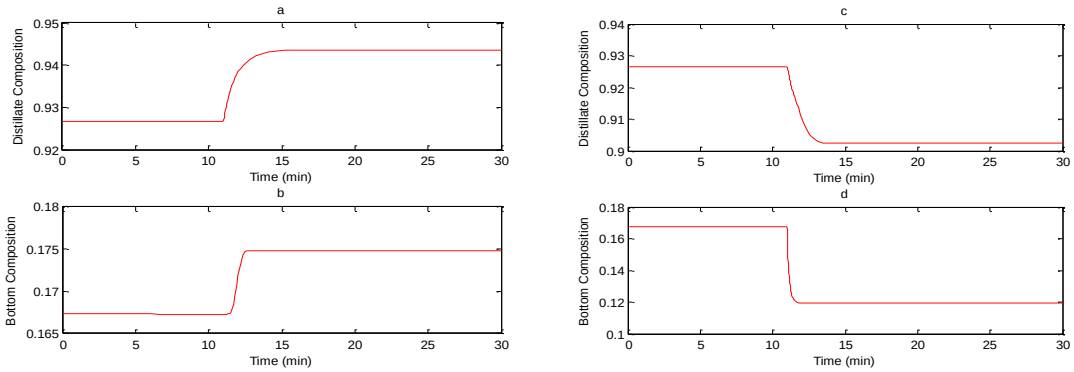

Figure 4.3: Open loop step responses for the LV configuration in the methanol-water separation column, (a) and (b): change in reflux rate, (c) and (d): change in reboiler energy

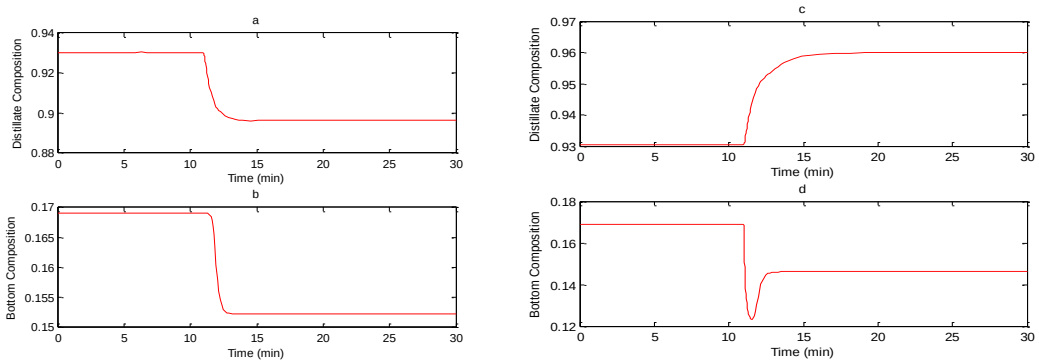

Figure 4.4: Open loop step responses for the DV configuration in the methanol-water separation column, (a) and (b): change in distillate flow rate, (c) and (d) : change in reboiler energy

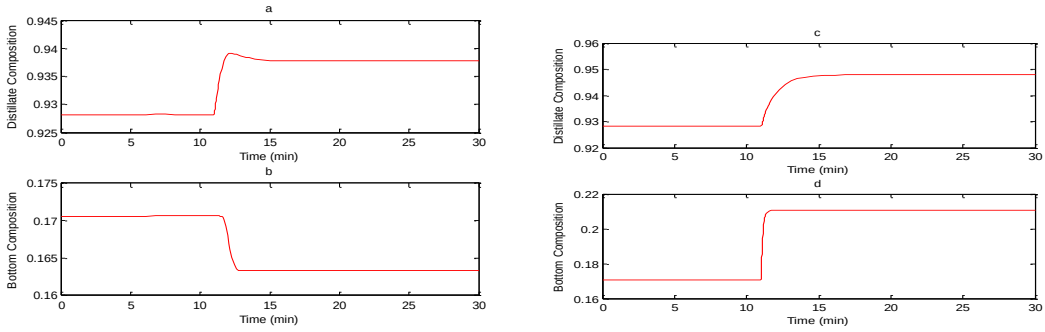

Figure 4.5: Open loop step responses for the LB configuration in the methanol-water separation column, (a) and (b): change in reflux rate, (c) and (d): change in reboiler energy

The RGA and REA results from the steady state analysis are shown in table 4.1. Table 4.2 shows the open loop simulation results under the three control configurations for the methanol-water system.

The RGA values obtained for the methanol-water system, for all the considered control configurations are quite good. In terms of good control, any of the structures will be usable judging from RGA. If RGA value is greater than 0.5 but less than 1, this will be the preferred loop as it will minimise interaction (Ogunnaike and Ray, 1994). Hence LB and DV will be good choices. For RGA greater than 1 as found in LV, higher controller gain will be required. This was confirmed in the closed loop dynamic simulation. The controller gain for LV is much higher than for the other structures. This however is not ruling LV structure out as regards to good control. In terms of REA however, when the relative exergy gain is equal to 1, it is the preferred choice as the exergy efficiency is not affected by the control loop interactions (Montelongo-Luna *et al.,* 2011). For the three control structures considered, the relative exergy gain for the LB control structure is closer to 1 than the other two control structures. The LB control structure will be the preferred choice with respect to thermodynamic efficiency. The steady state analysis of the control structures shows LB as the preferred control structure in terms of controllability and thermodynamic efficiency.

Table 4.1: Results for RGA and REA analysis (methanol-water)

Control structures	**RGA**	**REA**
LV	$\begin{bmatrix} 1.2858 & -0.2858 \\ -0.2858 & 1.2858 \end{bmatrix}$	$\begin{bmatrix} 1.3056 & -0.3056 \\ -0.3056 & 1.3056 \end{bmatrix}$
DV	$\begin{bmatrix} 0.5992 & 0.4008 \\ 0.4008 & 0.5992 \end{bmatrix}$	$\begin{bmatrix} 0.6088 & 0.3912 \\ 0.3912 & 0.6088 \end{bmatrix}$
LB	$\begin{bmatrix} 0.7277 & 0.2723 \\ 0.2723 & 0.7277 \end{bmatrix}$	$\begin{bmatrix} 0.7331 & 0.2669 \\ 0.2669 & 0.7331 \end{bmatrix}$

The open loop simulation results for the methanol water system show some inconsistencies. For example, the exergy efficiency of LB structure for methanol-water system is not always the highest as predicted from the REA and RGA analysis. The overall decisions regarding a controller design should not be based on the steady state

analysis alone (Skogestad *et al.*, 1990). There is a strong need for a detailed dynamic simulation analysis.

In order to validate the steady state analysis results in the dynamic state, the closed loop response of each of the control structures to disturbances in the feed flow rate and changes in the setpoints of the distillate and bottom compositions were studied. Multi-loop PI controllers were used on each of the control configuration. The controllers were tuned using Ziegler-Nichols tuning combined with the BLT tuning method (Luyben, 1992). The controllers were first tuned using the Ziegler-Nichols tuning as if they are for single input and single output systems without control loop interactions and then detuned using the BLT tuning method to account for control loop interactions. An example for this calculation is given in Appendix A.

Figure 4.6 to Figure 4.8 show the responses of the various control configurations to changes in distillate and bottom product setpoints for methanol-water system. The corresponding exergy analysis and reboiler energy usage are shown in Table 4.3.

Table 4.2: Open loop results for the methanol-water system

Control configuration and operating conditions	**Exergy efficiency (%)**	**Exergy loss (kJ/hr)**	**Reboiler exergy (kJ/hr)**	**Reboiler energy (kJ/hr)**	χ_D	χ_B
			LV			
Steady state	74.6	1.27×10^{7}	1.26×10^{4}	2.92×10^{4}	0.9266	0.167
Step change in reflux rate	72.2	1.43×10^{7}	1.26×10^{4}	2.92×10^{4}	0.9436	0.175
Step change in reboil energy	77	1.16×10^{7}	1.36×10^{4}	3.13×10^{4}	0.9023	0.119
			DV			
Steady state	74.04	1.31×10^{7}	1.26×10^{4}	2.92×10^{4}	0.9303	0.169
Step change in distillate rate	79	9.87×10^{6}	1.27×10^{4}	2.92×10^{4}	0.8962	0.152
Step change in reboil energy	68.8	1.68×10^{7}	1.35×10^{4}	3.14×10^{4}	0.960	0.146
			LB			
Steady state	74.6	1.28×10^{7}	1.26×10^{4}	2.90×10^{4}	0.9282	0.171

Control configuration and operating conditions	**Exergy efficiency (%)**	**Exergy loss (kJ/hr)**	**Reboiler exergy (kJ/hr)**	**Reboiler energy (kJ/hr)**	χ_D	χ_B
Step change in reflux rate	72.8	1.39×10^7	1.29×10^4	2.97×10^4	0.9377	0.163
Step change in bottom rate	72.7	1.36×10^7	1.17×10^4	2.71×10^4	0.9479	0.211

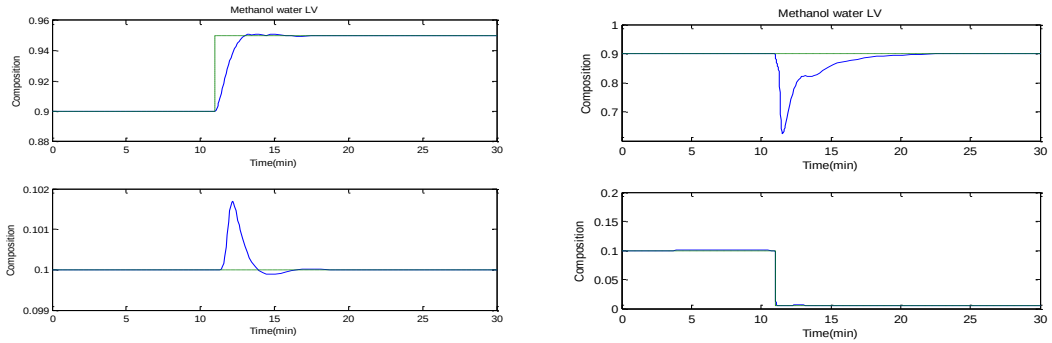

(a) (b)

Figure 4.6: Responses to setpoint changes in top composition (a) and bottom composition (b) for the LV structure in the methanol-water system

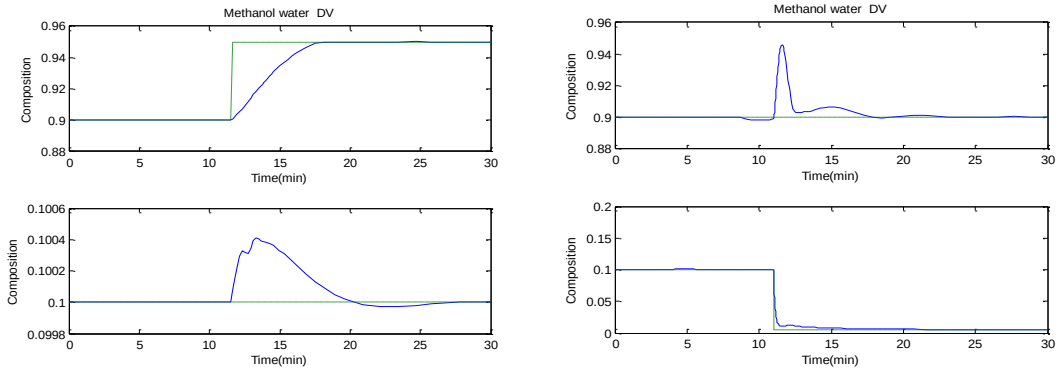

(a) (b)

Figure 4.7: Responses to setpoint changes in top composition (a) and bottom composition (b) for the DV structure in the methanol-water system

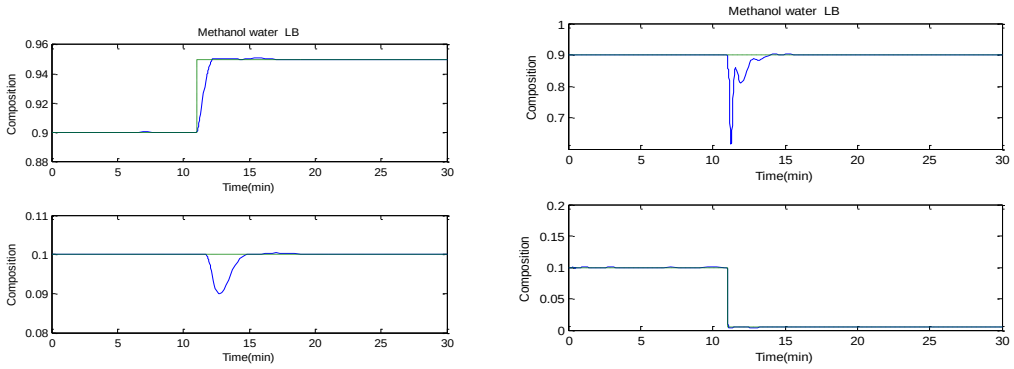

(a) (b)

Figure 4.8: Responses to setpoint changes in top composition (a) and bottom composition (b) for the LB structure in the methanol-water system

Table 4.3: Closed loop simulation results for the methanol-water column

Control configurations and operating conditions	**Exergy eff (%)**	**Exergy loss (kJ/hr)**	**Reboiler exergy (kJ/hr)**	**Reboiler energy (kJ/hr)**
		LV		
Nominal steady state (X_D= 0.99; X_B = 0.01)	37.83	6.84×10^7	2.60×10^4	6.04×10^4
-0.5% change in feed	37.97	6.54×10^7	2.46×10^4	5.72×10^4
+0.5% change in feed	38.36	7.01×10^7	2.73×10^4	6.33×10^4
X_D at 0.95 and X_B at 0.01	45.16	4.90×10^7	2.42×10^4	5.60×10^4
X_D at 0.90 and X_B at 0.005	32.81	8.98×10^7	3.24×10^4	7.48×10^4
X_D at 0.95 and X_B at 0.005	30.38	1.01×10^8	3.31×10^4	7.66×10^4
		DV		
Nominal steady state (X_D= 0.99; X_B = 0.01)	37.99	6.87×10^7	2.59×10^4	6.03×10^4
-0.5% change in feed	37.41	6.71×10^7	2.47×10^4	5.72×10^4
+0.5% change in feed	38.52	7.04×10^7	2.72×10^4	6.33×10^4
X_D at 0.95 and X_B at 0.01	44.39	5.04×10^7	2.43×10^4	5.62×10^4

Control configurations and operating conditions	**Exergy eff (%)**	**Exergy loss (kJ/hr)**	**Reboiler exergy (kJ/hr)**	**Reboiler energy (kJ/hr)**
X_D at 0.90 and X_B at 0.005	32.26	9.35×10^7	3.25×10^4	7.50×10^4
X_D at 0.95 and X_B at 0.005	30.06	1.04×10^8	3.30×10^4	7.64×10^4
		LB		
Nominal steady state (X_D= 0.99; X_B = 0.01)	41	5.58×10^7	2.53×10^4	5.94×10^4
-0.5% change in feed	42.42	4.97×10^7	2.29×10^4	5.33×10^4
+0.5% change in feed	37.31	6.93×10^7	2.91×10^4	6.76×10^4
X_D at 0.95 and X_B at 0.01	46.12	4.58×10^7	2.37×10^4	5.47×10^4
X_D at 0.90 and X_B at 0.005	34.76	7.65×10^7	3.19×10^4	7.36×10^4
X_D at 0.95 and X_B at 0.005	34.99	7.45×10^7	3.01×10^4	6.97×10^4

Close loop dynamic simulations were used to confirm the preferred choice from RGA and REA analysis. For the methanol-water system closed loop simulation results in Table 4.3 , the exergy efficiency for the LB control structure is higher than those for the other two control structures except for increase in feed rate. And as expected, the exergy loss is lower under the LB control structure than under the other two control structures. This shows that the LB control structure is thermodynamically more efficient than the LV and DV control for the methanol-water system. The responses of all the control structures to setpoint changes further confirm the controllability of the structures and show that any of the structure could be used to bring about desired separation specification. To achieve it with the minimum usage of energy however, the LB control configuration will be the optimum choice.

A dual composition control is used here because it yields less variation in downstream units and a more uniform quality of the final products. The large disparity in the exergy efficiency of the control structures in the open loop steady state to that in the closed loop as revealed in table 4.2 and table 4.3 for methanol-water system is a result of the composition specifications for the two cases due to the setpoint changes in the closed

loop response. This shows that high purity distillation is at a cost of energy. A cut in purity specification for example from 0.99 and 0.01 to 0.94 and 0.17 for top and bottom compositions respectively could result in as much as 30% more of exergy efficiency and a reduction in exergy loss. Also, the results in Table 4.3 for different setpoint changes show the LB control configuration as more energy efficient for distillate setpoint changes and bottom product setpoint change. In addition, the LB control configuration favours an increase in feed rate disturbance in terms of exergy efficiency as compared to other control configurations. These observations reveal the need to incorporate thermodynamic analysis to aid the decision of energy efficient control configuration selection for distillation column operations. This will be a valuable tool in choosing control configuration for design and operation of distillation systems. Overall, the LB control configuration has a lower exergy loss and improved exergy efficiency than other control configurations. This information is quite revealing and shows the potential for bringing about energy efficient control operation of distillation processes. The reboiler exergy for each of the configuration at different variations considered also reveals the LB configuration as the structure with the least consumption of exergy.

4.5 Application to benzene-toluene separation column

The benzene-toluene system was simulated using HYSYS. The parameters for the simulation are given in Table 4.4. These parameters were used for the steady state simulation of the systems. For the dynamic simulation, the trays for each column were sized and parameters such as weir height, tray space, tray diameter and tray height were determined.

Table 4.4: Parameters for simulation of Benzene-toluene system in HYSYS

Parameters	value
Feed Temperature(^{0}C)	95
Feed pressure (KPa)	101.3
Feed rate(kmol/hr)	350
Reflux ratio	3.5
No of trays	11
Feed tray	7
Distillate rate (kmol/hr)	153.4

The condenser and reboiler were sized using equation 4.30 and assuming the residence time to be 10min and liquid level volume to be 50% at residence time.

$$Vessel\ volume = \frac{Total\ liquid\ exit\ flow \times residence\ time}{Liquid\ level} \quad 4.30$$

Three control configurations LV, LB and DB are considered. The open loop responses of the controlled variables (distillate and bottom compositions) to step changes in their corresponding manipulated variables for each of the configurations are shown in figure 4.9 to figure 4.11 for the benzene-toluene system. Transfer function identified for the system from the open loop response are given in equations 4.31-4.33

Transfer function matrix of the LV configuration for benzene-toluene system:

$$G(s) = \begin{pmatrix} \frac{1.608}{1+1.1s} & -\frac{9.9}{1+0.34s} \\ \frac{2.372}{1+3.3s} & -\frac{2.5}{1+0.9s} \end{pmatrix} \quad 4.31$$

Transfer function matrix of the DV configuration for benzene-toluene system:

$$G(s) = \begin{pmatrix} \frac{-4.35}{1+1.42s} & +\frac{8.49}{1+2.13s} \\ \frac{-1.03}{1+1.7s} & -\frac{7.6}{1+1.67s} \end{pmatrix} \quad 4.32$$

Transfer function matrix of the LB configuration for benzene-toluene system:

$$G(s) = \begin{pmatrix} \frac{1.34}{1+1s} & +\frac{2.16}{1+3.35s} \\ \frac{1.07}{1+4.23s} & +\frac{2.83}{1+5.6s} \end{pmatrix} \quad 4.33$$

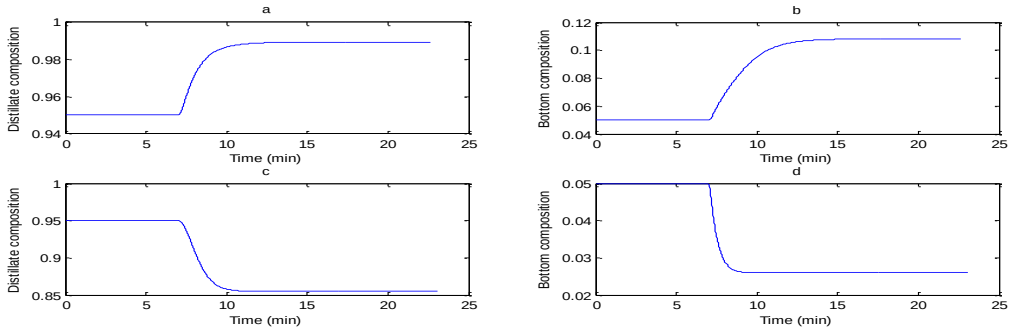

Figure 4.9: Open loop step responses for the LV configuration in the benzene-toluene separation column, (a) and (b): change in reflux rate, (c) and (d): change in reboiler energy

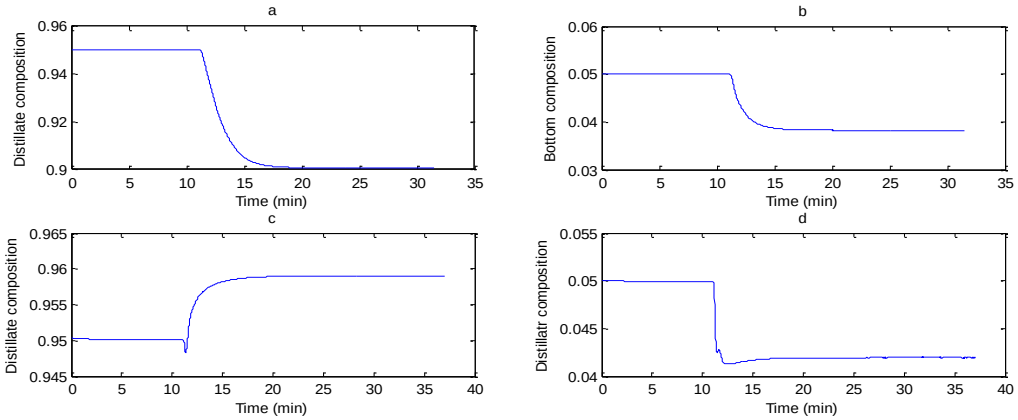

Figure 4.10: Open loop step responses for the DV configuration in the benzene-toluene separation column, (a) and (b): change in distillate flow rate, (c) and (d): change in reboiler energy

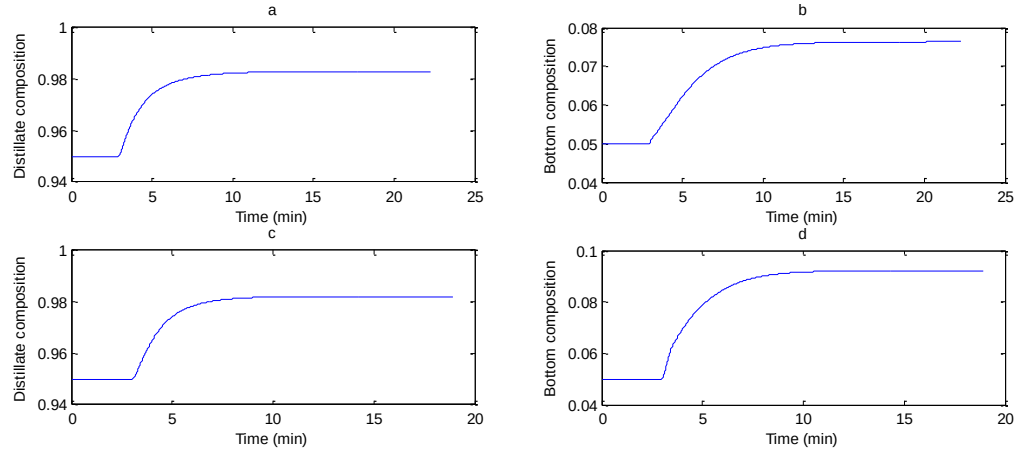

Figure 4.11: Open loop step responses for the LB configuration in the benzene-toluene separation column, (a) and (b): change in reflux rate, (c) and (d): change in bottom product flow rate

The RGA and REA results from the steady state analysis are shown in table 4.5 for benzene-toluene systems. Table 4.6 shows the open loop simulation results under the three control configurations for the methanol-water system and benzene toluene system respectively.

In table 4.5 the control structures for the benzene-toluene system show marked variations in terms of RGA and REA. The diagonal RGA values for LV control structure are less than zero and those for the LB control structure are much higher than 1. Negative diagonal elements in RGA indicate that closing the loop will change the sign of the effective gain. These structures may not be considered. RGA value for the DV control structure is greater than 0.5 but less than 1. The DV control structure therefore will be the preferred control structure. Considering the REA values, the LB

and DV control structures could be chosen. However, though the LB control structure looks good for energy efficiency, it is eliminated by its RGA if both controllability and energy efficiency are considered. The tool could aid in decision making and gives opportunity for consideration of design options. The steady state analysis of the benzene-toluene system shows DV as the control structure of choice.

Table 4.5: Results for RGA and REA analysis (benzene-toluene)

Control structures	**RGA**	**REA**
LV	$\begin{bmatrix} -0.2065 & 1.2065 \\ 1.2065 & -0.2065 \end{bmatrix}$	$\begin{bmatrix} 0.0007 & 0.9993 \\ 0.9993 & 0.0007 \end{bmatrix}$
DV	$\begin{bmatrix} 0.7908 & 0.2092 \\ 0.2092 & 0.7908 \end{bmatrix}$	$\begin{bmatrix} 0.8290 & 0.1710 \\ 0.1710 & 0.8290 \end{bmatrix}$
LB	$\begin{bmatrix} 2.5606 & -1.5606 \\ -1.5606 & 2.5606 \end{bmatrix}$	$\begin{bmatrix} 1.0349 & -0.0349 \\ -0.0349 & 1.0349 \end{bmatrix}$

The open loop simulation results for benzene-toluene separation column behaved unpredictably. The exergy efficiency of DV structure is not always the highest as predicted from the REA and RGA analysis. This further confirms just like methanol-water system that the overall decisions regarding a controller design should not be based on the steady state analysis alone (Skogestad *et al.*, 1990). There is a strong need for a detailed dynamic simulation analysis.

Table 4.6: Open loop results for the benzene-toluene system

Control configuration and operating conditions	**Exergy efficiency (%)**	**Exergy loss (kJ/hr)**	**Reboiler exergy (kJ/hr)**	**Reboiler energy (kJ/hr)**	χ_D	χ_B
			LV			
Steady state	47.75	1.57×10^7	9.72×10^6	1.28×10^7	0.950	0.050
Step change in reflux rate	48.12	1.55×10^7	9.73×10^6	1.282×10^7	0.9894	0.011
Step change in	46.29	1.75×10^7	1.07×10^7	1.39×10^7	0.855	0.145

Control configuration and operating conditions	**Exergy efficiency (%)**	**Exergy loss (kJ/hr)**	**Reboiler exergy (kJ/hr)**	**Reboiler energy (kJ/hr)**	χ_D	χ_B
reboil energy						2
			DV			
Steady state	47.75	1.57×10^7	9.72×10^6	1.28×10^7	0.950	0.050
Step change in distillate rate	47.79	1.57×10^7	9.723×10^6	1.28×10^7	0.9501	0.049
Step change in reboil energy	46.63	1.73×10^7	1.05×10^7	1.39×10^7	0.959	0.041
			LB			
Steady state	47.75	1.57×10^7	9.72×10^6	1.28×10^7	0.950	0.050
Step change in reflux rate	47.69	1.60×10^7	9.96×10^6	1.31×10^7	0.982	0.018
Step change in bottom rate	48.81	1.46×10^7	9.29×10^6	1.23×10^7	0.982	0.017 9

For the benzene-toluene system, response to setpoint change in distillate and bottom compositions are shown in Figure 4.12 to Figure 4.14. The exergy efficiencies of the responses setpoint changes and changes in feed rate are shown in Table 4.7. For all the 4 cases of deviations from the nominal steady state considered, exergy efficiencies for the DV control structure are greater than those for the LV control structure and greater than those for two cases in the LB control structure. This trend follows that predicted from steady state REA analysis. Reboiler exergy differs from the reboiler energy because exergy analysis is a tool for assessing quality of energy and quantifying sources of inefficiency and recoverable energy in a system. Exergy analysis also takes into account entropy generation in a system and hence indicates "useful energy" of a system. The change in reboiler exergy per time at the closed loop simulation is shown in figures 4.15 to 4.18 for each of the control structures. It can be seen that the DV control structure overall has less reboiler exergy than the other control structures. A full detailed analysis of the performance of the control structure should be supplemented with a detailed dynamic analysis as presented. This will give a measure of confidence on a preferred control structure and as well quantifies its exergy consumption.

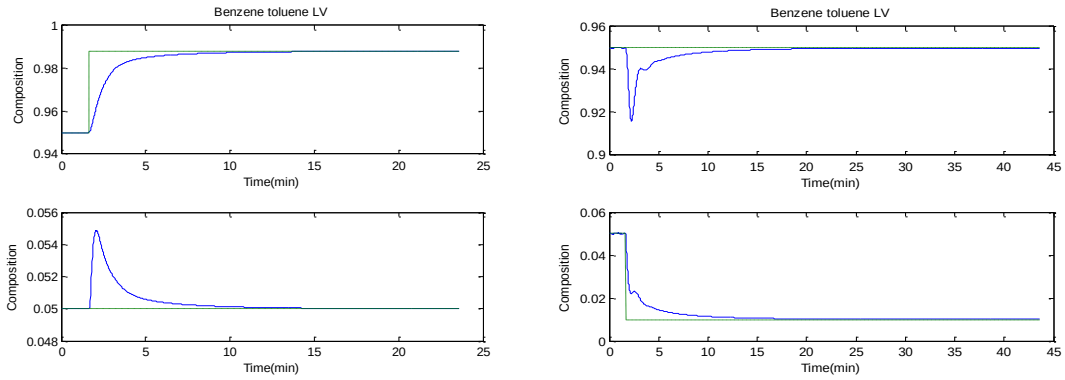

(a) (b)

Figure 4.12: Responses to setpoint changes in top composition (a) and bottom composition (b) for the LV structure in the benzene-toluene system

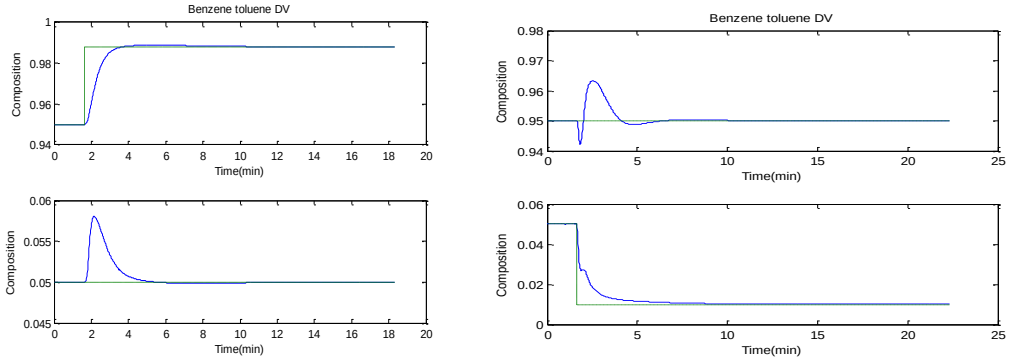

(a) (b)

Figure 4.13:Responses to setpoint changes in top composition (a) and bottom composition (b) for the DV structure in the benzene-toluene system

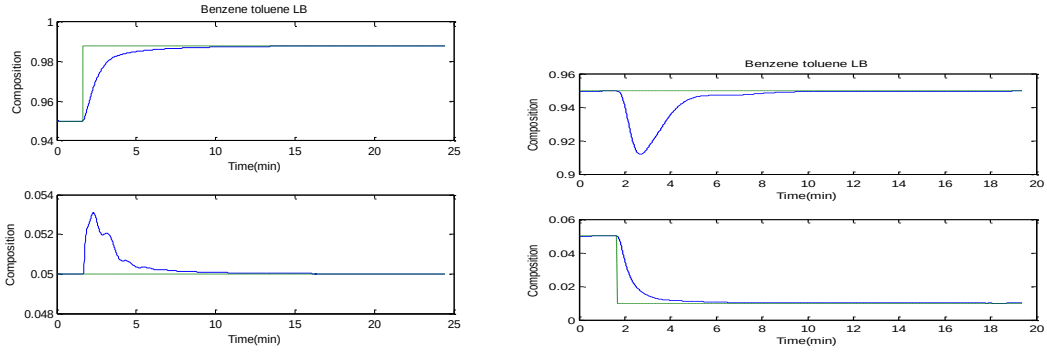

(a) (b)

Figure 4.14: Responses to setpoint changes in top composition (a) and bottom composition (b) for the LB structure in the benzene-toluene system

Table 4.7: Closed loop simulation results for the benzene-toluene system

Control configuration	**Exergy eff. (%)**	**Exergy loss (kJ/hr)**	**Reboiler exergy (kJ/hr)**	**Reboiler energy (kJ/hr)**
		LV		
Nominal steady state (X_D= 0.95; X_B = 0.05)	47.75	1.57×10^7	9.72×10^6	1.28×10^7
-7.5% change in feed	47.18	1.48×10^7	9.11×10^6	1.18×10^7
+7.5% change in feed	47.89	1.68×10^7	1.06×10^7	1.38×10^7
X_D at 0.988and X_B at 0.05	44.7	2.07×10^7	1.24×10^7	1.60×10^7
X_D at 0.95 and X_B at 0.01	40.58	3.24×10^7	1.81×10^7	2.33×10^7
		DV		
Nominal steady state (X_D= 0.95; X_B = 0.05)	47.75	1.57×10^7	9.72×10^6	1.28×10^7
-7.5% change in feed	47.58	1.45×10^7	8.88×10^6	1.17×10^7
+7.5% change in feed	48.16	1.66×10^7	1.04×10^7	1.37×10^7
X_D at 0.988and X_B at 0.05	44.74	2.09×10^7	1.22×10^7	1.60×10^7
X_D at 0.95 and X_B at 0.01	42.08	3.01×10^7	1.77×10^7	2.33×10^7
		LB		
Nominal steady state (X_D= 0.95; X_B = 0.05)	47.75	1.57×10^7	9.72×10^6	1.28×10^7
-7.5% change in feed	47.44	1.47×10^7	8.96×10^6	1.18×10^7
+7.5% change in feed	48.15	1.66×10^7	1.05×10^7	1.37×10^7
X_D at 0.988 and X_B at 0.05	44.93	2.05×10^7	1.22×10^7	1.60×10^7
X_D at 0.95 and X_B at 0.01	40.82	3.22×10^7	1.78×10^7	2.33×10^7

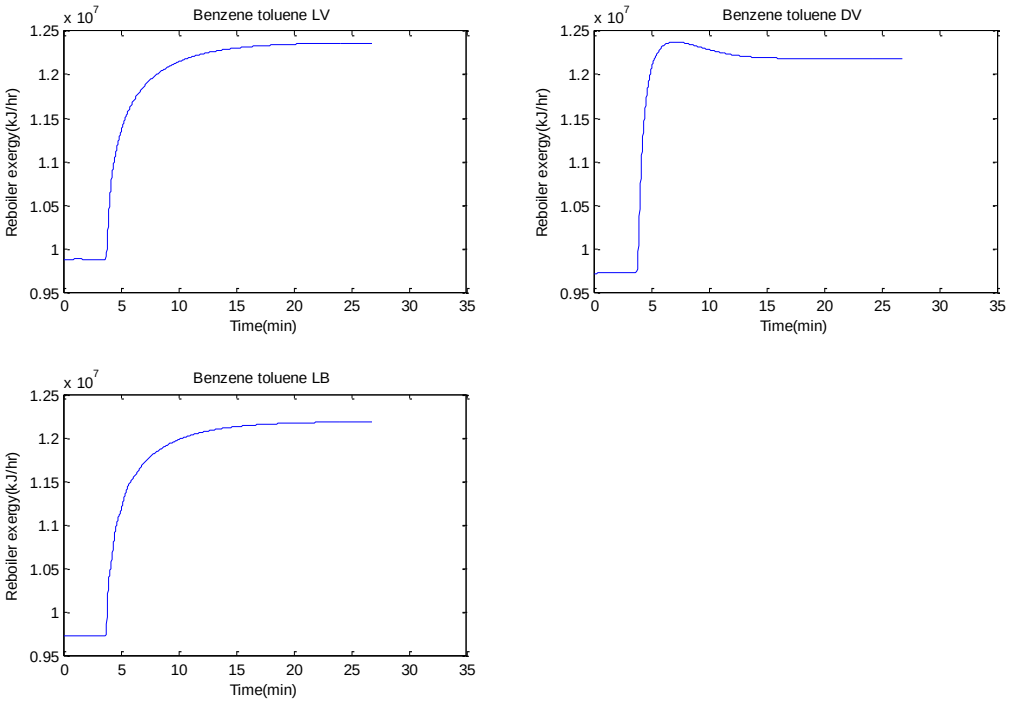

Figure 4.15: Reboiler exergy per time for change in distillate composition

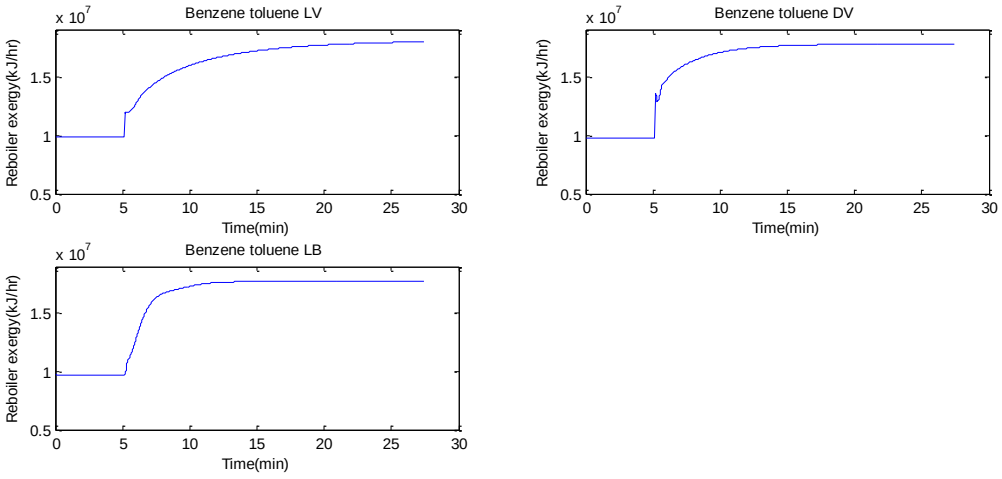

Figure 4.16: Reboiler exergy per time for change in bottom composition

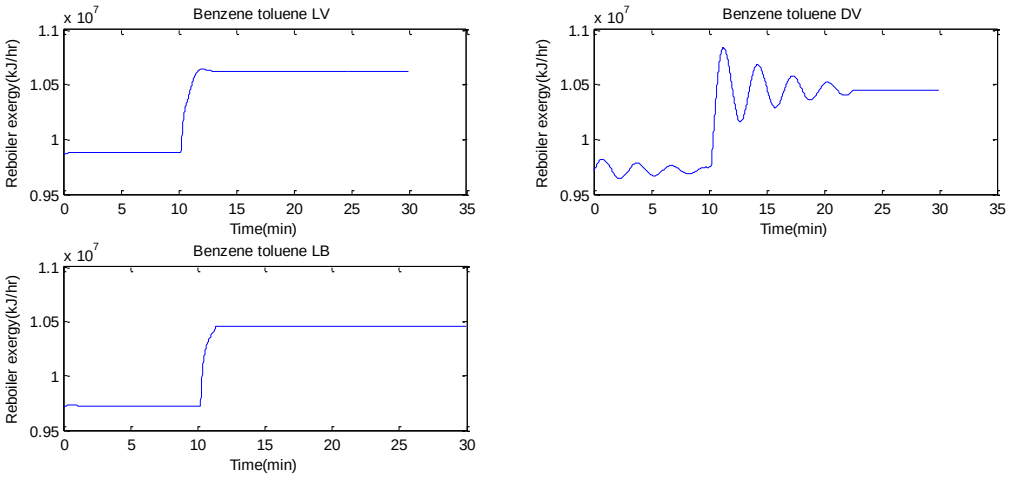

Figure 4.17: Reboiler exergy per time for increase in feed rate

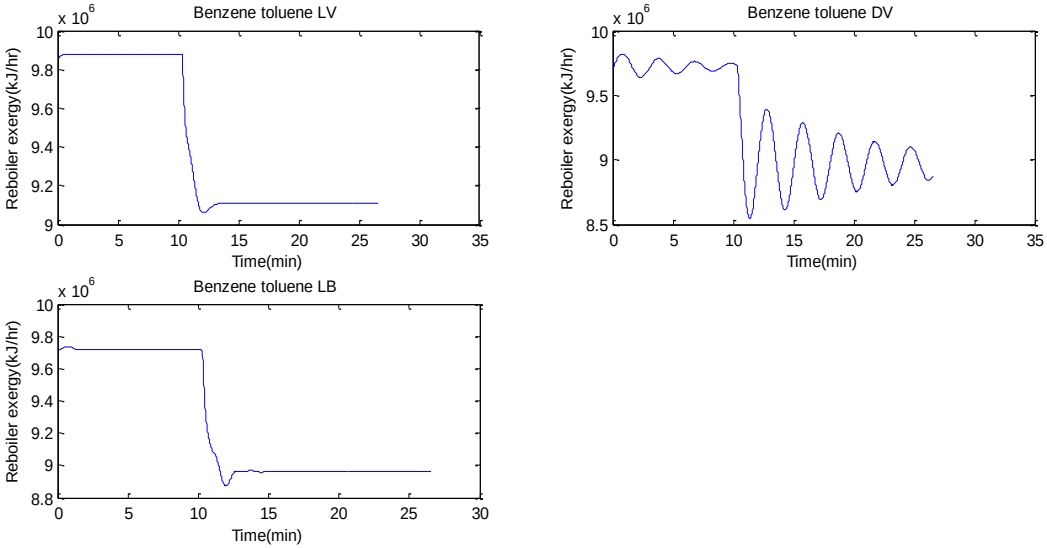

Figure 4.18: Reboiler exergy per time for decrease in feed rate

4.6 Conclusions

In this chapter both RGA and REA were used in the selection of appropriate distillation control structures. The preferred distillation control structure should have good operability based on RGA analysis and high exergy efficiency based on REA analysis. The effectiveness of the method was demonstrated by dynamic simulation. It should be stressed here that the decisions regarding the controller should be based on the dynamic simulations in addition to the steady state REA and RGA analysis. The simulation results were found to confirm the control structure selection results. RGA as a tool for selecting control structure should be supplemented with REA to determine an energy efficient control structure. The tools when combined can help in choosing from various design alternatives. It will therefore aid in choosing an optimum structure right from the

design stage. It could equally be effective tool in selecting optimum operations of distillation system. The tool as presented here is limited to the distillation unit. An overall energy analysis of the whole plant might be made to determine the effectiveness of the method on the plant as a whole.

CHAPTER 5: OPTIMISATION OF ENERGY EFFICIENCY: APPLICATION TO BINARY AND MULTICOMPONENT SYSTEMS

This chapter is based on PRES conference paper published in Chemical Engineering Transactions and the paper under review in Energy journal

5.1 Introduction

Distillation units pose a great challenge to control engineers because of its complexity. It comes in varieties of configurations with different operating objectives, significant interactions among the control loops, and specialised constraints. These result in distinct dynamic behaviours and different operational degree of freedom that necessitate the need for specialised control configurations in order to optimize energy usage. Usually the order of economic importance in the control of distillation columns is product quality, process throughput, and utility reductions. Often trade off between them has to be made. Optimisation of distillation column operations is essential in order to achieve energy efficiency while meeting product quality constraints.

Optimisation of distillation columns requires accurate process models. A number of distillation process models are available in the published literatures but the complexity of distillation processes has led to a number of assumptions that might limit the universality of the models (Ochoa-Estopier *et al.*, 2014). Most of the mechanistic models of distillation systems have assumed equilibrium cases for the stages. Such models deviate from the reality and will not give a true representation. To overcome this, non-equilibrium stages are assumed (Liang *et al*., 2006). Non-equilibrium models however involve large number of variables, leading to distillation models with differential equations that may exhibit high differential index that could generate stiff dynamics. Furthermore, such mechanistic models are computationally demanding making them not suitable for real-time optimisation. To overcome these problems, data driven models such as artificial neural network (ANN) models can be utilised (Uzlu *et al*., 2014). ANN has been recognised as a powerful tool that can facilitate the effective development of data-driven models for highly nonlinear and multivariable systems (Osuolale and Zhang, 2014). ANN can learn complex functional relations for a system from the input and output data of the system. Furthermore, their evaluation is much less computationally demanding making them suitable for real-time optimisation.

Most neural network applications to distillation systems target at modelling the product specification as the model output (Ochoa-Estopier *et al.,* 2013). Often the economic objective in terms of profitability is the focus in the optimization of such distillation processes (Amit *et al.,* 2013). However, with the issues of global warming, green house gas (GHG) effects, and depleting fossil energy resources, the issue of energy efficiency of processes has been brought to the limelight. The need therefore arise to focus on energy efficiency of the column especially focusing on second law of thermodynamics (exergy analysis) in lieu of first law of thermodynamics. Application of thermodynamics for process energy improvement especially in terms of pinch analysis has been widely reported (Ochoa-Estopier and Jobson, 2015). However, pinch analysis is restricted to analysing for minimum utility consumption and or minimum number of heating units for heat exchange equipment. Exergy analysis overcomes this restriction and encompasses the total energy systems in processes. This chapter attempts to model the exergy efficiency of distillation column using ANN. Previously ANN has been used to model distillation column, but there is a need for robust and accurate model to represent the column within an optimisation frame work irrespective of the complexities of the column. Bootstrap aggregated neural network is introduced in this study to improve the prediction accuracy and reliability of the model. The model is then used for the optimisation of exergy efficiency of the distillation column to reduce the energy consumption while satisfying product quality specifications. Past studies on the exergy analysis of distillation column has been limited to pinpointing and quantifying sources of inefficiencies in the column (Oni and Waheed, 2015). A further step away from the usual is to use exergy analysis as a retrofit tool to present several practical options for process energy improvement rather than as an analytical tool. This chapter develops an optimisation based methodology incorporating exergy analysis for improving the energy efficiency of the column.

Most often, distillation columns are optimised in terms of energy usage without paying particular attention to the reduction of entropy generation within the column (Kamela *et al.,* 2013). There is therefore a strong need to focus on reducing column's irreversibility by applying the second law of thermodynamics in column efficiency improvement.

In this chapter, an attempt is made at improving the energy efficiency of distillation columns using the tool of applied thermodynamics to determine the optimum operating conditions of the column with consideration to energy efficiency and product quality. The energy efficiency is however on the basis of reduction in the irreversibility of the

column. Exergy analysis and optimisation are the major qualitative and quantitative tools that are used in the decision making.

This chapter is organised as follows. Section 5.2 gives the description and exergy analysis of a typical binary column. Data driven models such ANN, BANN and linear models are presented in Section 5.3. Application of the models to two binary systems and their subsequent optimisation are presented in Section 5.4. Section 5.5 presents the special case of a multicomponent system, its modelling, modification and optimisation and Section 5.6 concludes the chapter.

5.2 Thermodynamic Analysis

The total exergy of the material stream is calculated from equations 4.13 -4.16. The exergy of the energy stream is calculated from equation 4.18. For a typical binary distillation system as shown in figure 5.1

$$\sum Ex_{in} = Ex_{feed} + Ex_{reboiler} \quad 5.1$$

$$\sum Ex_{out} = Ex_{distillate} + Ex_{bottoms} + Ex_{condenser} \quad 5.2$$

The irreversibility of the system is calculated as:

$$\varphi = \frac{\sum Ex_{out}}{\sum Ex_{in}} \quad 5.3$$

Efficiency of the system is then given as

$$I = \sum Ex_{in} - \sum Ex_{out} \quad 5.4$$

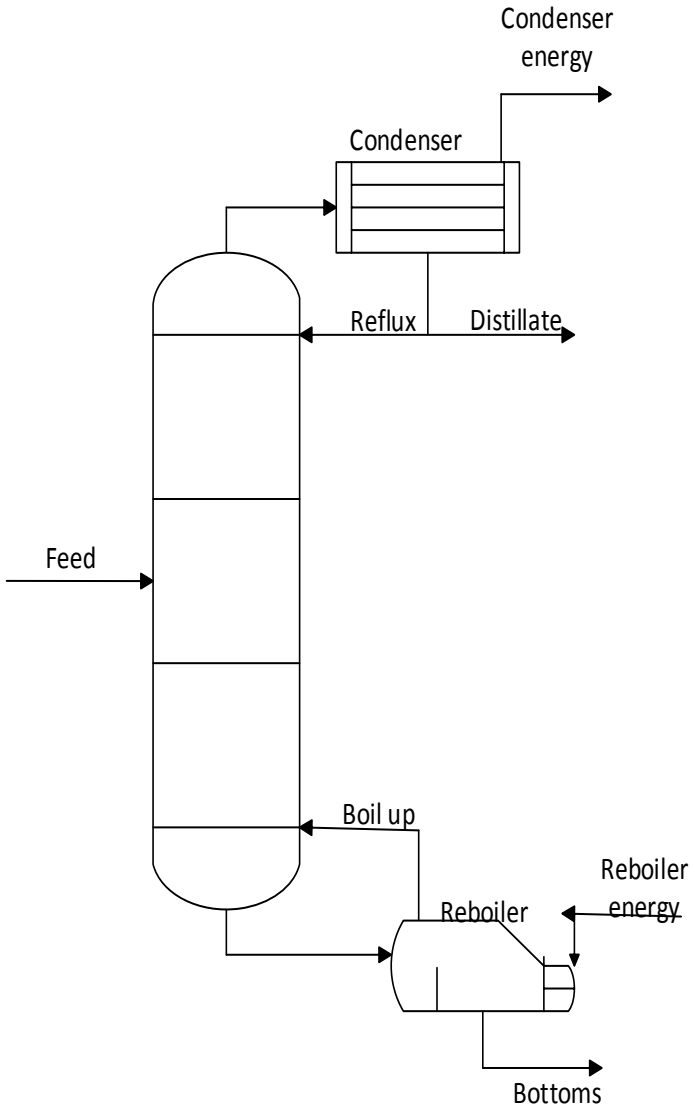

Figure 5.1: A typical binary distillation column with the in and out streams

5.3 Modelling of Exergy Efficiency

5.3.1 Artificial neural network modelling

Mechanistic models have been traditionally used in the past for control and optimisation studies. However developing mechanistic models for complex processes especially to incorporate the second law energy efficiency could be very difficult and time consuming. These difficulties can be readily circumvented by developing neural network models (Morris *et al.,* 1994). Neural networks have been proved to be capable of approximating any continuous non-linear functions. Here neural networks are used to model exergy efficiency and product composition. The neural networks models are then used for exergy efficiency optimization subject to product quality constraints. Data for

neural network modelling are generated from simulation. The neural network model for exergy efficiency is of the following form:

$$y = f(x_1, x_2, x_3 \ldots x_n) \qquad 5.5$$

where y is exergy efficiency, x_1 and x_2 are feed rate and feed temperature respectively, while x_3 …x_n are the most volatile composition in each of the outlet stream. Neural network models for the product compositions use the same model inputs. Single hidden layer feed forward neural networks are used to model exergy efficiency and product compositions. The quality of the neural network is dependent on the training data and the training method (Zhang, 1999). The data were divided into training data (50%), testing data (30%), and unseen validation data (20%). The training data is used for network training and the testing data is used for network structure selection (number of hidden neurons) and "early stopping" in network training. With the "early stopping" mechanism, neural network prediction errors on the testing data are continuously monitored during training and training is terminated when the prediction errors on the testing data do not futher reduce. The number of hidden neurons was determined by building a number of neural networks with different numbers of hidden neurons and testing them on the testing data. The network giving the lowest sum of squared errors (SSE) on the testing data is considered as having the appropriate number of hidden neurons. The final developed neural network model is then evaluated on the unseen validation data. The data for the network training, validation and testing were scaled to the range [-1 1] because of the different magnitudes of the model inputs and outputs. Levenberg-Marquardt training algorithm was used to train the networks. For the pupose of comparison, linear models are also built using partial least square (PLS) regression.

However, conventional neural networks can lack generalisation capability when applied to unseen data due to over-fitting noise in the data (Zhang, 2004). The objective in neural network modelling is to build a network which can generalise and not to build a network which simply memorise the training data. Several techniques have been reported for the enhancement of neural network model generalisation capability such as Bayesian learning, regularisation, training with dynamic and static process data, early stopping and combining multiple networks, and bootstrap aggregated neural networks (Mukherjee and Zhang, 2008).

5.3.2 Bootstrap aggregated neural network

When building neural network models from the same data set, there is possibility that different networks perform well in different regions of the input space. Hence, prediction accuracy on the entire input space could be improved when the multiple neural networks are combined. In a bootstrap aggregated neural network model, several neural network models are developed to model the same relationship. Individual neural network models are developed from bootstrap re-sampling replications of the original training data. Instead of selecting a single neural network that is considered to be the "best", several networks are combined together to improve model accuracy and robutsness. These models can be developed on different parts of the data set. A diagram of a bootstrap aggregated neural network is shown in figure 5.2. A bootstrap aggregated neural network can be represented mathematically as

$$f(x) = \sum_{i=1}^{n} w_i f_i(x) \qquad 5.6$$

where $f(x)$ is the aggregated neural network predictor, $f_i(x)$ is the *i*th neural network, w_i is the aggregating weight for combining the *i*th predicted neural network, n is the number of neural networks and x is a vector of neural network inputs. The overall output of bootstrap aggregated network is a combination of the weighted individual neural network output.

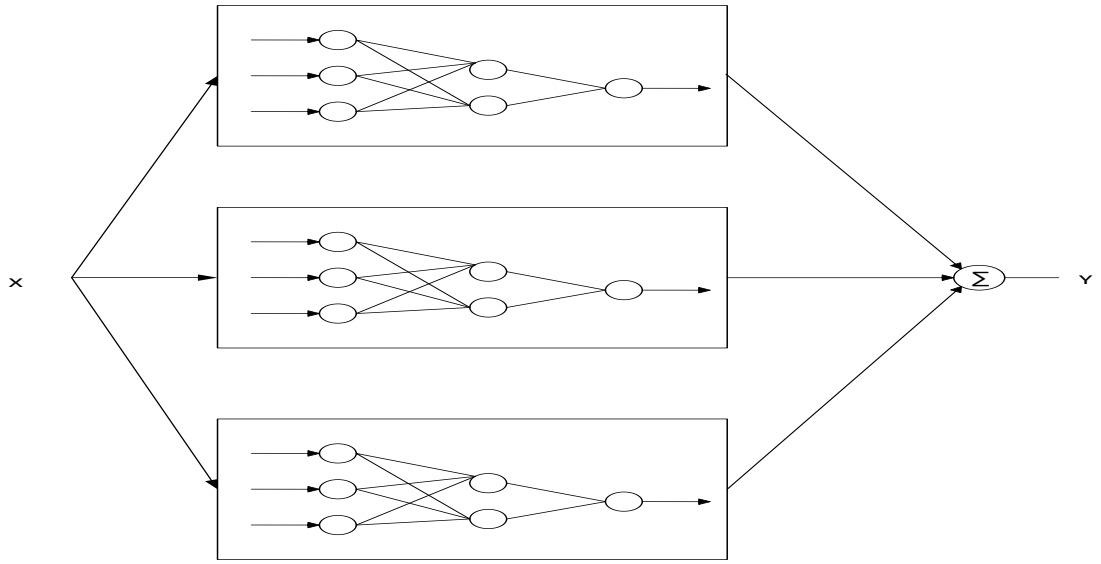

Figure 5.2: A bootstrap aggregated neural network

The boostrap aggregated neural network can also be used to calculate model prediction confidence bounds from individual network predictions. The standard error of the *i*th predicted value is calculated as

$$\sigma_e = \left\{\frac{1}{n-1}\sum_{b=1}^{n}[y(x_i; W^b) - y(x_i;)]^2\right\}^{\frac{1}{2}} \quad 5.7$$

where $y(x_i) = \sum_{b=1}^{n} y(x_i; W^b)/n$ and n is the number of neural networks. The 95% prediction confidence bounds can be calculated as $y(x_i;) \pm 1.96\sigma_e$. A narrower confidence bounds indicates the reliability of the associated model prediction.

5.4 Application to Binary Distillation Systems

5.4.1 Modelling of the distillation systems

Two binary distillation systems of methanol-water and benzene-toluene separations were considered. The methanol-water system was to be rectified into a distillate containing 90% methanol and a residue containing 5% methanol. The Benzene-toluene system is to be separated to 95% benzene in the distillate and 5% benzene in the residue. The nominal parameters for simulation are as given in table 5.1 (McCabe and Smith, 2005, Treybal, 1980). At the steady state, based on the data generated in HYSYS, exergy analyses of the streams were performed using equations 4.13, 4.14 and 4.16. Exergies of the reboiler and condenser were calculated using equation 4.18. This is because the data in HYSYS were obtained at the steady state and the temperature can safely be assumed to be constant at the prevailing operating conditions. The temperature, pressure, enthalpy and entropy of each stream were generated in HYSYS. Careful considerations were made to compute the exergy of each stream both at the prevailing operating conditions and at reference states. The total exergy in and out of the system were calculated using equations 5. 1 and 5.2 respectively. Exergy efficiency was calculated from equation 5.3 and irreversibility was calculated from equation 5.4.

Tables 5.2 and 5.3 give the data for the streams in and out of the methanol-water system and benzene-toluene system respectively. The exergy efficiency and the irreversibility of the system were calculated using equations 5.3 and 5.4. The exergy efficiencies are 83.9% and 82.3% for methanol-water system and benzene-toluene system respectively while the exergy loss / irreversibility are 7.21610^5 and 3.691×10^6 respectively for methanol-water system and benzene toluene system. This is revealing that there is room for improvement of the separation processes.

Table 5.1: Nominal parameters for simulation

	Methanol water	**Benzene toluene**	**Unit**
Feed temperature	53	105	^oC

	Methanol water	Benzene toluene	Unit
Feed pressure	1	1	atm
Feed rate	216.8	350	kmol/h
Reflux ratio	1.03	3.5	
Number of trays	8	11	
Feed tray	5	7	
Distillate rate	88.9	151.8	kmol/h

Table 5.2: Simulated data for exergy analysis of methanol-water system

	h_0(kJ/ kmol)	s_0(kJ/ kmol°C)	h(kJ/kmol)	s(kJ/ kmol°C)	m(kmol /h)	Ex(kJ/h)
Feed	-2.66×10^5	26.57	-2.64×10^5	46.21	216	4.53×10^5
Distillate out	-2.42×10^5	11.16	-2.39×10^5	42.83	88.93	1.39×10^5
Bottom out	-2.83×10^5	29.89	-2.77×10^5	71.86	127.06	5.54×10^5
Reflux	-2.42×10^5	11.16	-2.39×10^5	42.82	49.67	7.78×10^4
Boilup	-2.73×10^5	28.58	-2.28×10^5	175.73	138.44	5.63×10^6
Reboiler						4.03×10^6
Condenser						3.07×10^6

Table 5.3: Simulated data for exergy analysis of benzene-toluene system

	h_0(kJ/ kmol)	s_0(kJ/ kmol°C)	h(kJ/kmol)	s(kJ/ kmol°C)	m(kmol /h)	Ex(kJ/h)
Feed	29022.4	-103.73	73150.8	40.76	350	14181516
Distillate out	47908.7	-122.42	55163.2	-83.96	151.75	954911.8
Bottoms out	14566.9	-96.59	28547.7	-29.08	198.24	2437092
Reflux	47908.7	-122.42	55163.2	-83.96	497.9	3133213
Boil up	16856.3	-97.11	63541.8	55.11	261.2	11201230
Reboiler						6722074
Condenser						13820882

The emphasis here is to increase exergy efficiency and increase profitability of existing plants rather than plant expansion. Parametric analysis of the column was conducted to investigate the impacts of a number of variables on the exergy efficiency of the column. To each variable $\pm 15\%$ of its initial value was added. The initial exergy efficiencies are 83.9% for methanol water and 82.3% for benzene toluene as given for the base cases of the systems. The desired purity specification of the distillate was maintained for all the variations. The exergy of the material streams and energy streams were calculated at each variation, the corresponding exergy efficiency and reboiler exergy were also calculated. Tables 5.4 and 5.5 show the sensitivity analysis of the two systems under consideration. For most cases considered, improve exergy efficiency translates to reduction in reboiler energy. However, exception is noticed for condenser pressure and the feed rate in tables 5.4 and 5.5. This is possibly because there is a significant change in the reboiler energy at these variations without corresponding significant change in the exergy of the streams.

Table 5.4: Sensitivity analysis of the Methanol-water system

	-15% of initial values			**+15% of initial values**		
	Exergy eff (%)	Reboiler duty (kJ/h)	Reboiler exergy (kJ/h)	Exergy eff (%)	Reboiler duty (kJ/h)	Reboiler exergy (kJ/h)
Reflux rate	82.15	5.320×10^6	3.905×10^6	85.20	5.700×10^6	4.183×10^6
Feed rate	83.93	4.675×10^6	3.432×10^6	83.93	6.325×10^6	4.643×10^6
Feed temperature	84.14	5.632×10^6	4.135×10^6	83.66	5.367×10^6	3.940×10^6
Reboiler duty	97.5	4.675×10^6	3.430×10^6	77.32	6.325×10^6	4.640×10^6
Condenser pressure	80.92	5.459×10^6	4.008×10^6	86.37	5.536×10^6	4.064×10^6
Reboiler pressure	85	5.417×10^6	3.905×10^6	83.12	5.574×10^6	4.152×10^6
Condenser temperature	Not feasible			Not feasible		
Reboiler	99.9	2.970	2.042×10^6	Not		

	-15% of initial values			+15% of initial values		
temperature		$\times 10^6$		Feasible		
Distillate rate	97	4.684×10^6	3.335×10^6	Not feasible		
Bottoms rate	Not feasible			98	4.366×10^6	3.081×10^6

From the tables, it can be seen that feed temperature and distillate and bottom compositions greatly affect the exergy efficiency of the systems. Some of the variables fail to give a converged solution at the steady state when changed from their initial values. They however gave converged solutions in the dynamic state when the distillate and bottom compositions are controlled to be at their reference values. These variables are considered not feasible because the data to be generated for ANN training are to be taken from the steady state. For most of the variables of the methanol-water system, the change in variable values alters the composition of the bottoms from the initial reference value. This was not seriously considered as the main focus of the sensitivity analysis is to check out the variables that have noticeable impact on the overall exergy efficiency of the column. Reflux rate and reboiler energy even though have effect on the exergy efficiency were not considered. This is because of the impact they have in the composition control of the column (Skogestad, 2007). The feed rate has no effect on the exergy efficiency of the column but influences the reboiler energy. It has been previously considered as input in the simulation of distillation column (Amit *et al*., 2013).

The variables that were then considered are the controlled variables (distillate and bottom compositions) and external input variables which can be regulated (feed rates and feed temperatures). Subsequently, data for neural network training were generated by varying these independent variables within their upper and lower bounds. Corresponding values of the exergy efficiency and irreversibility were calculated based on equations 5.3 and equation 5.4.

Table 5.5: Sensitivity analysis of the benzene-toluene system

	-15% of initial values			+15% of initial values		
	Exergy eff (%)	Reboiler duty	Reboiler exergy	Exergy eff (%)	Reboiler duty (kJ/h)	Reboiler exergy

	-15% of initial values			+15% of initial values		
		(kJ/h)	(kJ/h)			(kJ/h)
Reflux rate	83.95	5.959×10^{6}	4.568×10^{6}	82.10	1.121×10^{7}	8.676×10^{6}
Feed rate	82.34	7.393×10^{6}	5.704×10^{6}	82.34	1.01×10^{7}	7.721×10^{6}
Feed temp.	91.53	1.435×10^{7}	1.107×10^{7}	82.01	8.491×10^{6}	6.551×10^{6}
Reboiler duty	82.86	7.4×10^{6}	5.694×10^{6}	74.47	1.00×10^{7}	7.7296×10^{6}
Condenser pressure	80.07	8.596×10^{6}	6.632×10^{6}	84.14	8.823×10^{6}	6.807×10^{6}
Reboiler pressure	82.48	8.224×10^{6}	6.22×10^{6}	82.24	9.11×10^{6}	7.124×10^{6}
Condenser temp.	Not feasible			Not feasible		
Reboiler temp.	Not feasible			Not feasible		
Distillate rate	85.66	4.477×10^{6}	3.414×10^{6}	Not feasible		
Bottoms rate	Not feasible			86.9	3.640×10^{6}	2.768×10^{6}

5.4.2 Linear models

Partial least square (PLS), principal component regression (PCR) and multiple linear regression (MLR) were used to build the linear models in this study. In PLS models, it was found that 4 latent variables give the smallest SSE on the testing data and, hence, 4 latent variables should be used in the PLS models. Plots of model prediction error (top left), model prediction error versus fitted values (top right), histogram of prediction error (bottom left), and normal probability plots (bottom right) from the two PLS models are given in figures 5.3 and 5.4. These plots indicate the linear model prediction errors of the two systems are not normally distributed indicating that the models are not adequate. Table 5.6 gives the SSE, Mean square error (MSE), and the coefficient of determination (R^2) for PLS models. The very large SSE and MSE values of the linear models and their low R^2 values indicate that there could be strong non-linearity in the relationship between exergy efficiency and process operating conditions. This justifies the need to build nonlinear models using ANN.

Figures 5.5 and 5.6 show the PCR models errors for the systems. The figures show the model error for different principal components. Keeping 4 principal components reduces the model for the two systems as compared to using less than 4. This follows the same trend as the PLS models where four latent variables give the smallest SSE. Since there are 4 input for the model, it follows that the PLS, PCR and MLR model will have the same performance. The MLR model performance for the training, testing and validation data sets for the systems are given in figures 5.7 and 5.8. The predicted and actual values for the model deviate significantly showing the models are not true representation of the actual and hence can not be deemed fit for use.

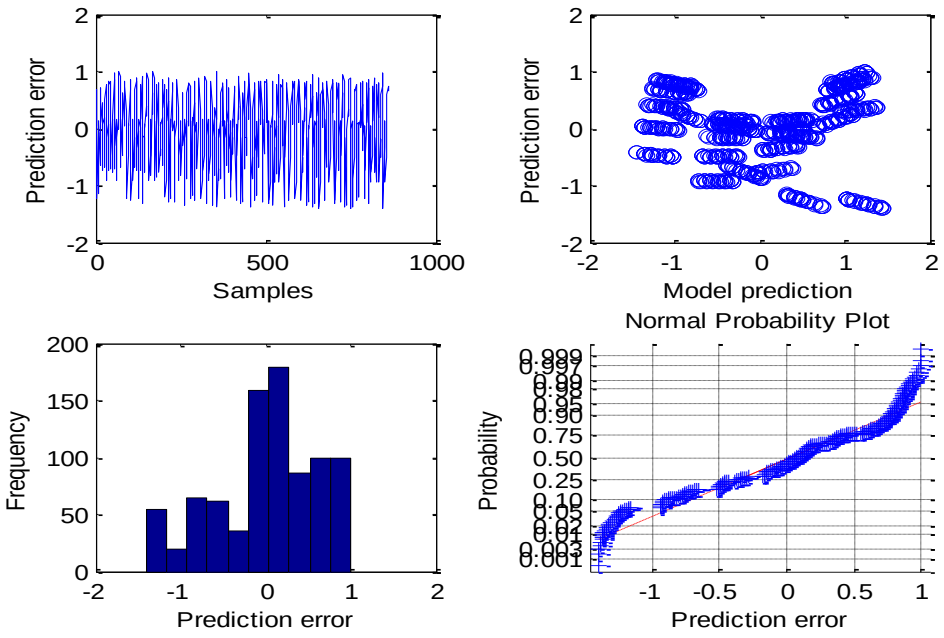

Figure 5.3: PLS model validation for the methanol-water system

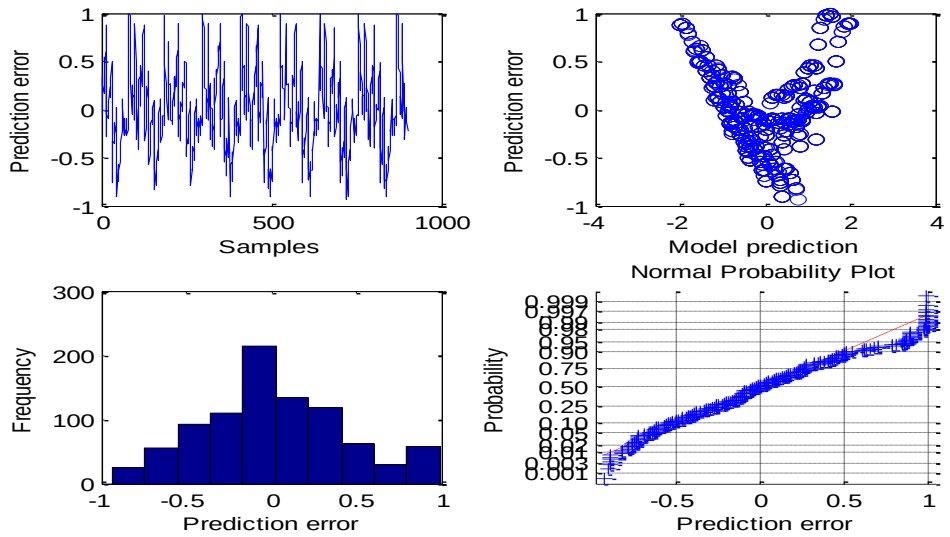

Figure 5.4: PLS model validation for the benzene-toluene system

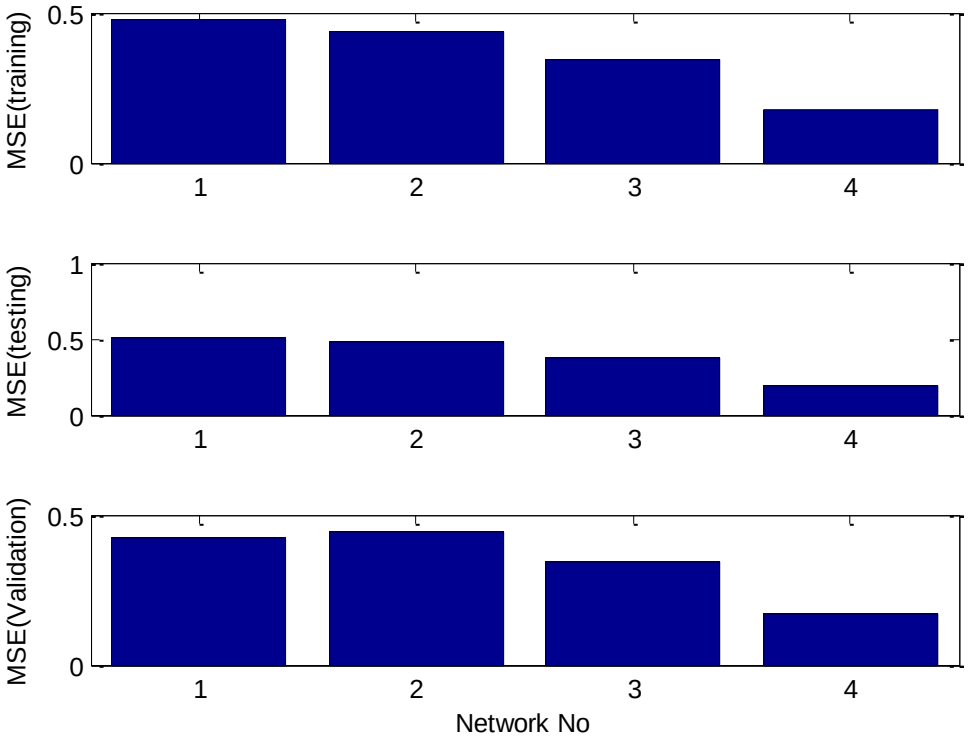

Figure 5.5: PCR Model error for methanol water

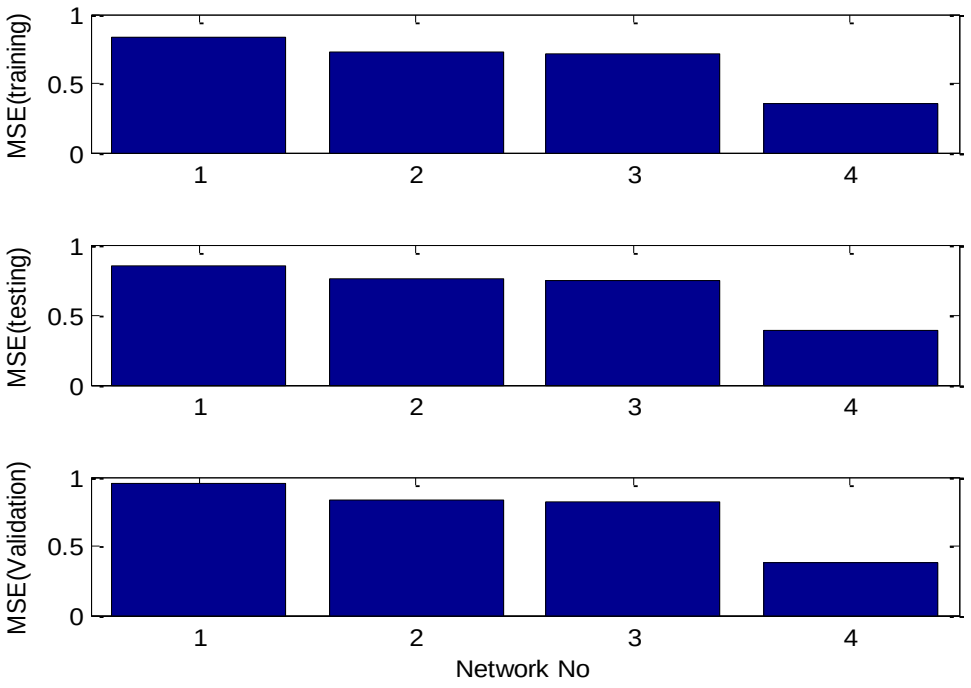

Figure 5.6: PCR model error for benzene toluene system

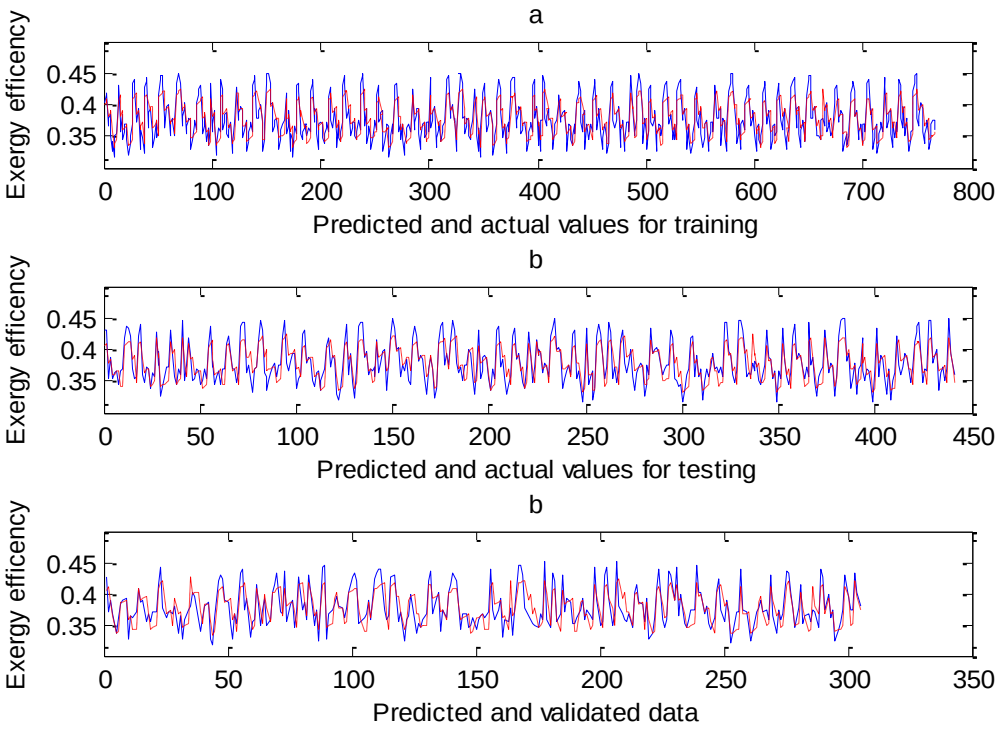

Figure 5.7: MLR model for methanol water

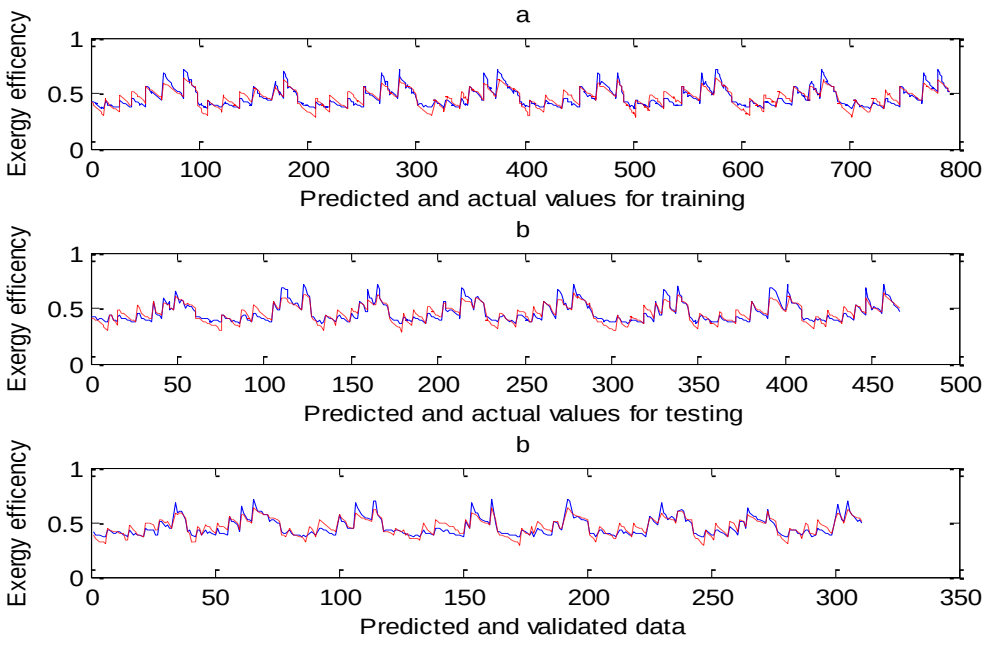

Figure 5.8: MLR model for benzene toluene

Table 5.6: Model performance indicators for PLS models

	Methanol-water			**Benzene-toluene**		
	Training	Testing	Validation	Training	Testing	Validation
SSE	186.68	63.86	50.41	109.82	43.42	37.11
MSE	0.4050	0.3414	0.3680	0.1489	0.1336	0.1405
R^2	0.4701	0.3934	0.4871	0.6880	0.6215	0.6908

5.4.3 ANN models

The performance of ANN is dependent on the data, the network structure and the training method. The trained network is as described in Section 5.3.1. Figures 5.9 and 5.10 show the actual exergy efficiencies (solid curves, blue) and neural network predictions (dashed curves, red) on the training, testing, and unseen validation data sets for the methanol-water column and the benzene-toluene column respectively. The SSEs on the training, testing and unseen validation data sets are given in table 5.7. The numbers of hidden neurons that gave the least SSE on the testing data are 17 for methanol-water and 18 for benzene-toluene. The results in figures 5.9 and 5.10 and table 5.7 show that the ANN models give excellent prediction performance. The models

can be conveniently used to determine the exergy efficiencies of the distillation processes at different operating conditions. Usually in the calculation of exergy efficiency, the enthalpies and entropies of all streams involved must be determined. The ANN models can be used to predict the exergy efficiencies without the rigours of calculating the enthalpies and entropies of the streams. This will be a valuable tool in the hand of process design engineers and operators in determining the effects of different operating conditions on the exergy efficiency of the distillation process.

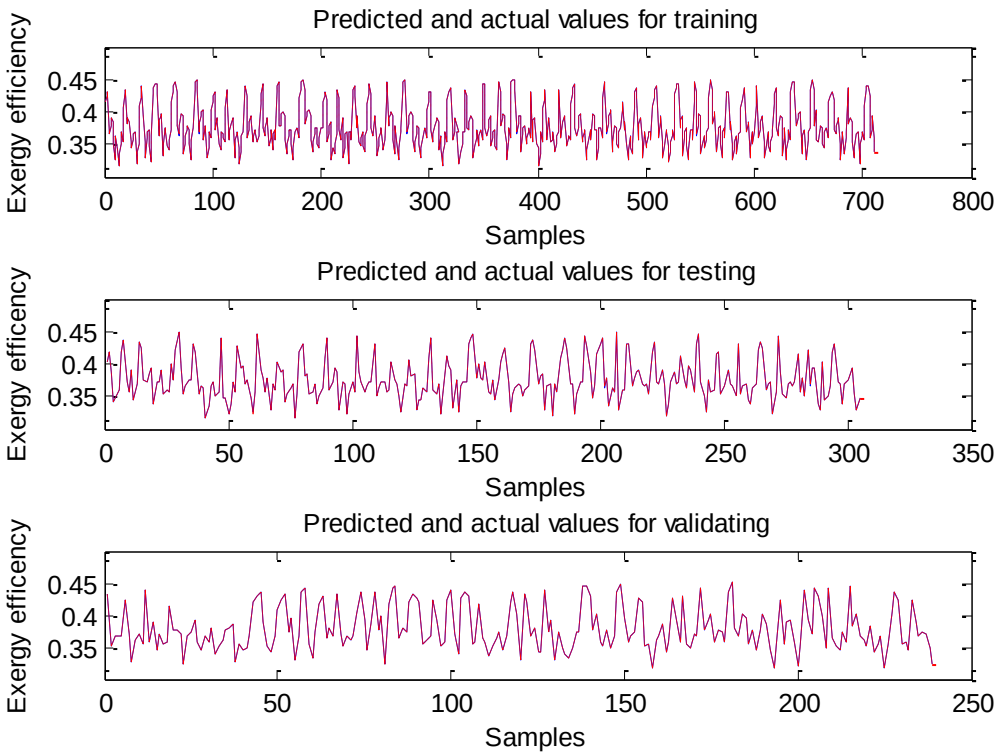

Figure 5.9: Actual and ANN model predicted exergy efficiency for the methanol-water column

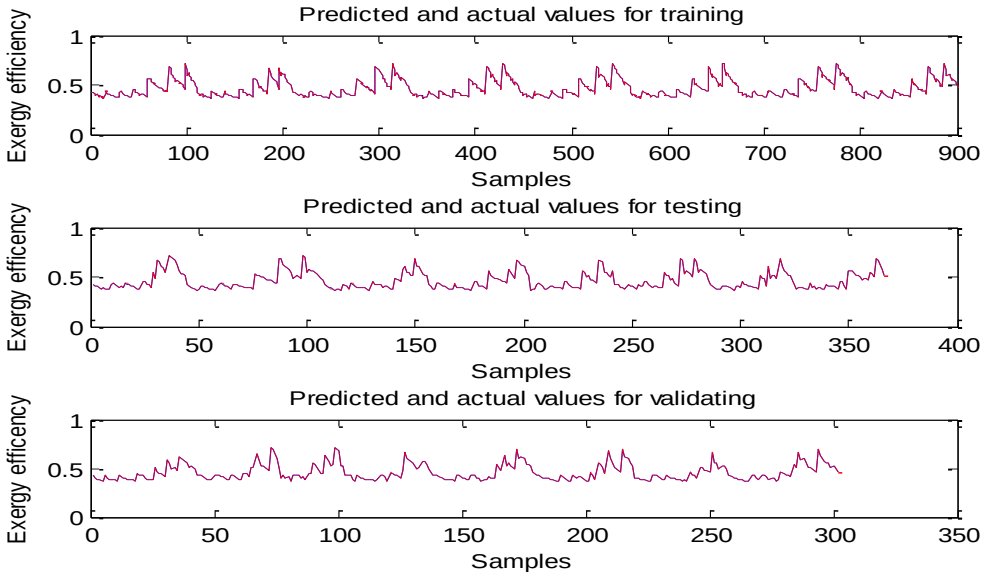

Figure 5.10: Actual and ANN model predicted exergy efficiency for the benzene-toluene column

Table 5.7: Model performance indicators for single ANN models

	Methanol-water			**Benzene-toluene**		
	Training	Testing	Validation	Training	Testing	Validation
SSE	0.0089	0.0039	0.0026	0.0011	0.0010	0.0007
MSE	8×10^{-6}	7×10^{-6}	1.35×10^{-6}	2.95×10^{-6}	4.15×10^{-6}	4.66×10^{-5}
R^2	0.9990	0.9988	0.9987	0.9976	0.9913	0.9913

5.4.4 Bootstrap Aggregated Neural Network

A bootstrap aggregated neural network (BANN) containing 30 neural networks was developed to predict the exergy efficiency of each system. Each individual network has one hidden layer. The Levenberg-Marquardt training algorithm was used to train the networks. Training data for the individual networks differs. This is due to bootstrap re-sampling to ensure that different individual networks are obtained and their combination lead to that the entire input space being well predicted. A problem in neural network is over-fitting which means a trained neural network can give excellent performance on the training data but performs poorly when applied to unseen validation data. A combination of multiple non-perfect models improves the prediction accuracy on the

entire input space. Figures 5.11 and 5.12 show the MSE of individual network on training, testing and validation data sets. It can be seen that the performances of individual networks on different data sets are inconsistent. A network with low MSE on the training data could have a large MSE on the validation data. This shows the non-robust nature of a single neural network. The MSE values for the aggregated neural networks with different numbers of consistent networks are shown in figures 5.13 and 5.14 for the methanol-water column and the benzene-toluene column respectively. The MSE for BANN models on training and validation data sets are 1.38×10^{-6} and 1.59×10^{-6} respectively for the methanol-water system and 8.78×10^{-6} and 1.0×10^{-5} respectively for the benzene-toluene system. This is an improvement on the minimum MSE for the single neural networks given in table 5.7. The model accuracy is seen to be improved by using bootstrap aggregated neural network model.

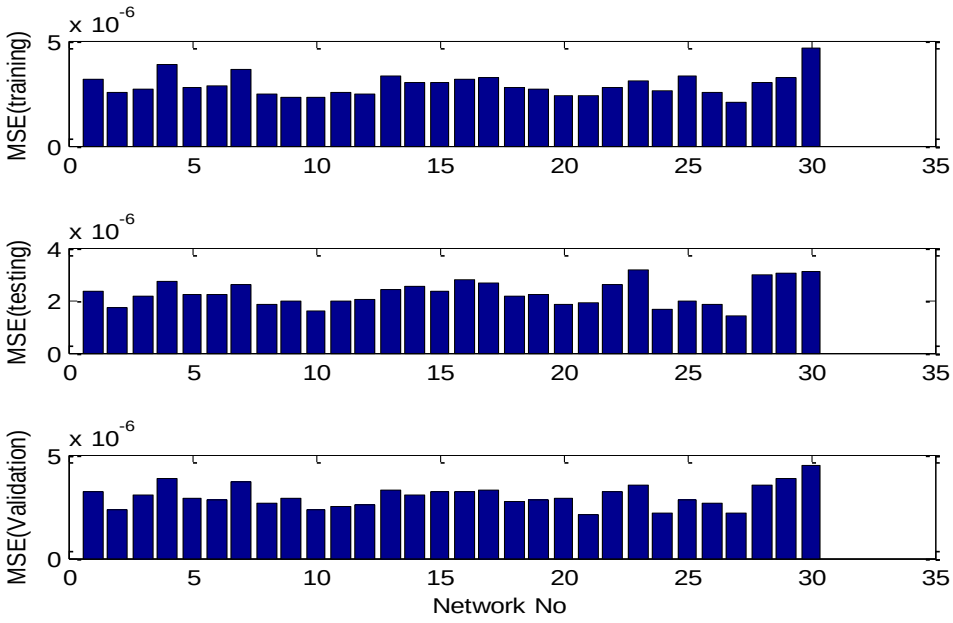

Figure 5.11: Model errors of individual networks for methanol-water system

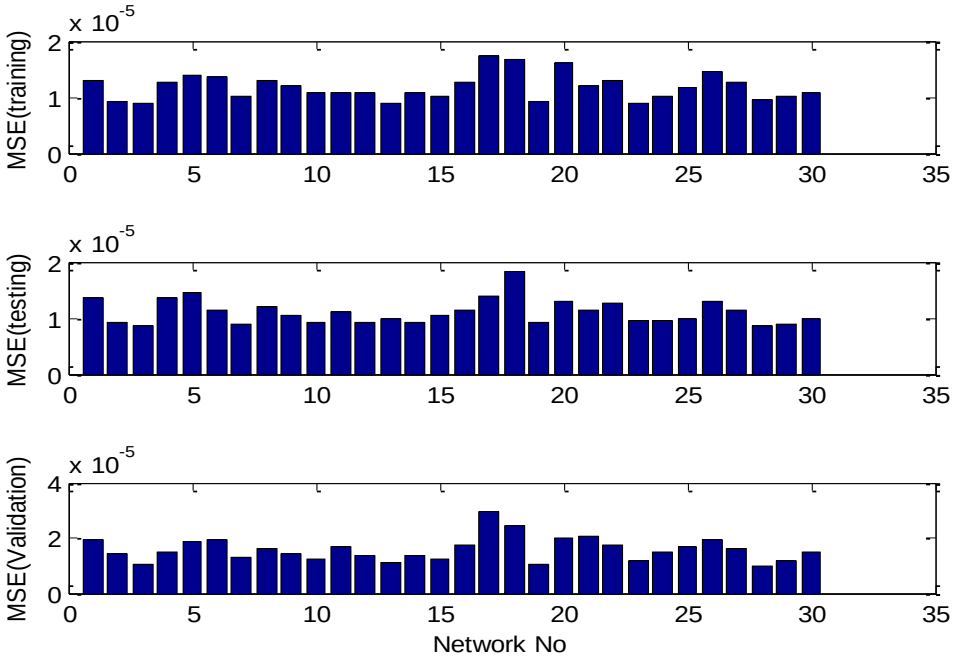

Figure 5.12: Model errors of individual networks for benzene-toluene system

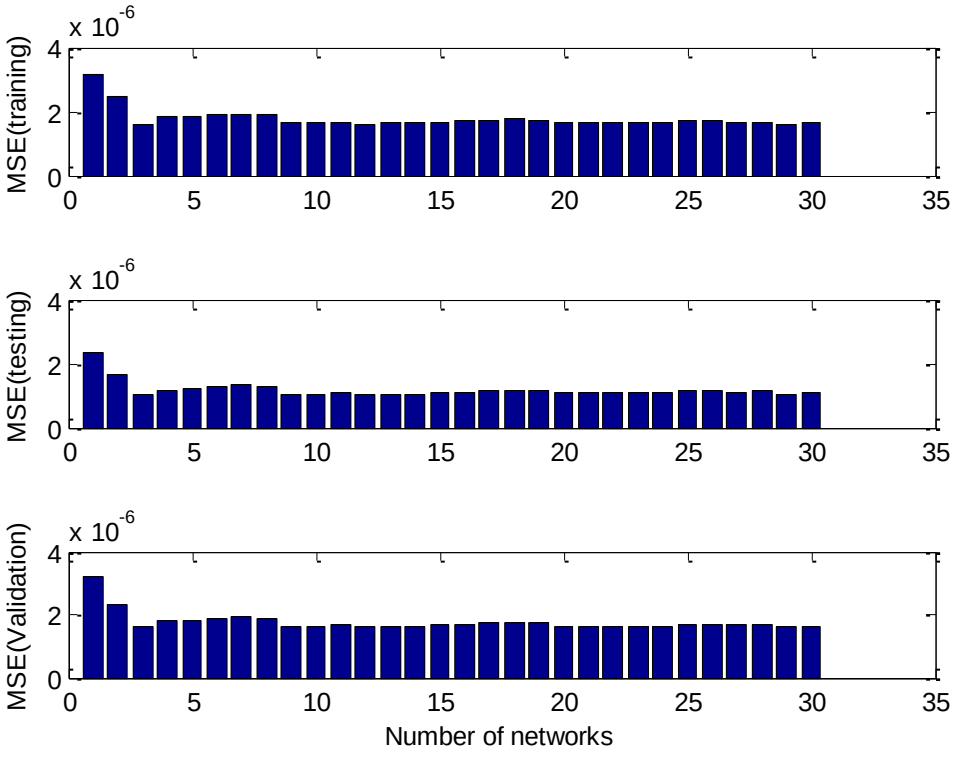

Figure 5.13: Model errors of aggregated networks for methanol-water system

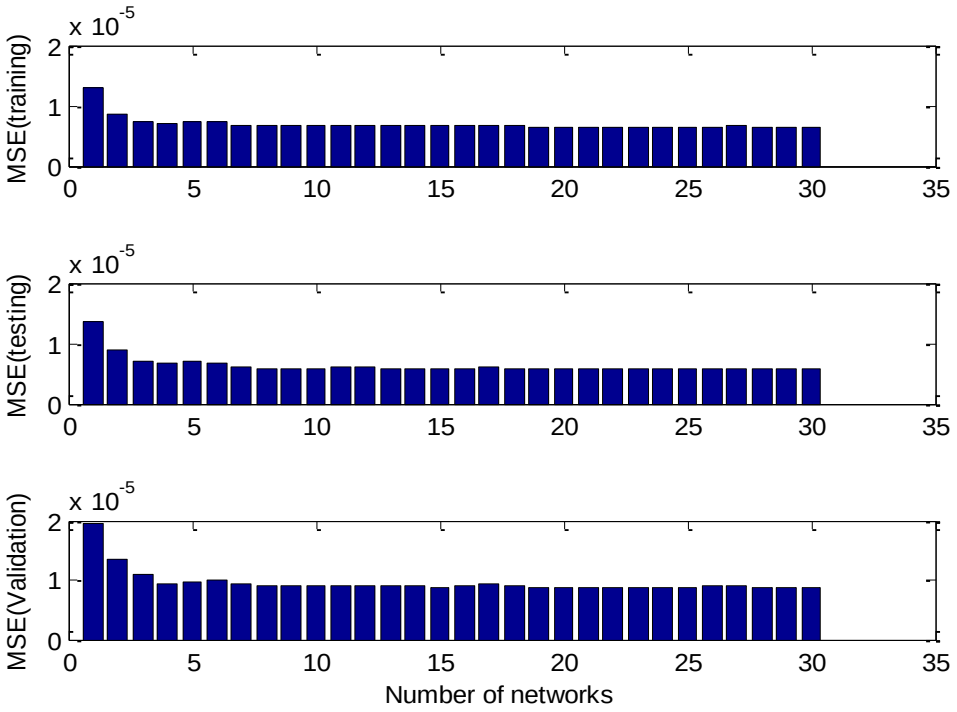

Figure 5.14: Model errors of aggregated networks for benzene-toluene system

5.4.5 Optimization of exergy efficiency

The optimization problem can be stated as

$$\min_{x} J = -\varphi \qquad 5.8$$

s.t.

$$\varphi = f(x_1, x_2, x_3, x_4)$$

$$0.8 \le x_3 \le 0.99$$

$$0.01 \le x_4 \le 0.1$$

where J is the objective function, x=[x_1,x_2,x_3,x_4] is a vector of neural network model inputs which are feed rate, feed temperature, distillate composition and bottom composition respectively; and φ is the exergy efficiency. As changing feed temperature would require pre-heating of the feed which can have impact on the overall energy efficiency, in this study the feed temperature is kept constant, i.e. removed from decision variable list.

The sequential quadratic programming (SQP) method was used for the optimization. The exergy efficiency is maximised subject to the distillate and bottom composition

constraints. Tables 5.8 and 5.9 give the results of the optimisation procedure for the two systems. The optimum conditions and the base case conditions are shown. The optimum exergy efficiency at different distillate and bottom compositions for the two systems are also shown.

In Tables 5.8 and 5.9, case 1 refers to the solution of equation 5.8. It can be seen that exergy efficiency is improved with the bottom composition at its upper bound. When the bounds on the product composition are altered (cases 2 and 3), the optimal exergy efficiencies increases when the bounds are narrowed and it reduces when the bounds are widen. However, there is a limit for the purity specification of the products beyond which increasing the exergy efficiency has the added clause of increase in energy of the reboiler. This is shown in case 4 and gives a caution on placing consideration on the exergy efficiency while specifying the product purity.

Table 5.8: Summary of optimization results for methanol-water system

	Base case	**Optimum case 1**	**Optimum case 2**	**Optimum case 3**	**Optimum case 4**
Feed rate (kmol/h)	216.8	216.8	216.79	180.7	216.79
Feed temp.(^oC)	53	53	53	53	53
Distillate composition	0.90	0.90	0.90	0.90	0.92
Bottom composition	0.05	0.1	0.08	0.01	0.05
ANN predicted efficiency (%)	83.95	93.28	89.77	74.98	85.59
HYSYS validated efficiency (%)	83.93	93.31	89.29	77.9	85.59
Reboiler energy (kJ/hr)	5.5×10^6	5.02×10^6	5.23×10^6	6.74×10^6	5.77×10^6
Reboiler exergy(kJ/hr)	4.04×10^6	3.61×10^6	3.78×10^6	5.05×10^6	4.24×10^6
Utility cost ($/yr)	1.70×10^4	1.56×10^4	1.62×10^4	2.09×10^4	1.79×10^4

Table 5.9: Summary of optimization results for benzene-toluene system

	Base case	**Optimum case 1**	**Optimum case 2**	**Optimum case 3**	**Optimum case 4**
Feed rate (kmol/h)	350	350	350	350	350
Feed temp.(^oC)	105	105	105	105	105

	Base case	Optimum case 1	Optimum case 2	Optimum case 3	Optimum case 4
Distillate composition	0.95	0.95	0.90	0.90	0.97
Bottom composition	0.05	0.1	0.08	0.01	0.05
ANN predicted efficiency (%)	82.34	83.82	83.22	80.86	82.88
HYSYS validated efficiency (%)	82.34	83.86	83.15	81.78	83.25
Reboiler energy (kJ/hr)	8.712×10^6	6.05×10^6	6.92×10^6	1.87×10^7	2.07×10^7
Reboiler exergy(kJ/hr)	6.72×10^6	4.64×10^6	5.31×10^6	1.44×10^7	1.71×10^7
Utility cost ($/yr)	2.94×10^4	2.11×10^4	2.38×10^4	3.04×10^4	3.68×10^4

The optimum efficiency as given in each case is showing that there is a reduction of entropy generation within the systems at these operating conditions and that is why there are corresponding increases in the exergy efficiencies of the systems. The distillate and bottom compositions were not compromised for the first case showing that the desired purity can be maintained with a corresponding increase in the exergy efficiency of the system. This increment translates to an increase in the energy efficiency of the systems considering the fact that there is a decrease in the reboiler energy even though the feed rate is maintained. Other varying compositions specifications were shown with their corresponding exergy efficiencies.

Taking the optimum case 1 as an example, the improvement in the exergy efficiency of the system is 11.16% for methanol water and 1.79% for benzene toluene when compared to the base case. The utility cost of the cases based on the assumption of 8600h per year are calculated and shown in tables 5.8 and 5.9. For the optimum case 1, the increase in exergy efficiency translates to 8.9% reduction in utility cost for methanol water and 28.2% reduction in utility cost for benzene toluene over a year period. The cumulative effect of this could be of great economic value.

The optimum operating conditions given by the optimisation procedures were simulated in HYSYS. It can be seen from tables 5.8 and 5.9 that actual (HYSYS simulated) exergy efficiencies are very close to the BANN model predicted values. This shows that the optimal predicted conditions of the BANN model can give the optimum of the actual process. This further demonstrates the suitability of the Bootstrap aggregated models at the modelling and optimisation of the exergy efficiency of the distillation columns. The method as applied on the binary system might seem non trivial but the

accuracy of the predictability of BANN model of the exergy efficiency cannot be over emphasised. For a more complex system, the relevance of the method will be much more pronounced.

As seen in tables 5.8 and 5.9, BANN model is able to predict what the exergy efficiency of the system will be at different quality specifications. In a processing plant, the relevance of this cannot be over emphasised especially in the area of decision making for the most energy efficient operating conditions of the system. This could serve as guide for process operators and process engineers. It could also find relevance in the design of a new system. The cautions in the application are firstly that the system to be investigated should be fully trained. A BANN model for a particular system, might not work for another. Also cost of increasing the temperature of the feed should be weighed against the use of reboiler energy. It will be much profitable if the temperature of the feed is raised with dissipated heat from the system which could have been discarded to the environment.

In order to compliment the results from the data driven models, HYSYS optimizer was used to show the optimum conditions that will improve exergy efficiency for the two systems. Table 5.10 shows the result for the methanol-water system and table 5.11gives the results for the benzene-toluene system. The predicted optimum operating conditions for the methanol –water system for all cases considered are close to the global optimum from HYSYS optimizer. This gives a measure of confidence on the optimum conditions found from the proffered method. Benzene-toluene system also follows the same trend except for case 2 that has a deviation of about 1.5% for the feed rate and 1.7% for the exergy efficiency. The deviation notwithstanding, the optimum conditions from the model can be found reliable. Hence the method can still be deemed appropriate for the design and operation of energy efficient distillation columns.

Table 5.10: Summary of optimization results for methanol-water system using HYSYS optimizer

	Base case	**Optimum case 1**	**Optimum case 2**	**Optimum case 3**	**Optimum case 4**
Feed rate (kmol/h)	216.8	217.9	216	216	216
Feed temp.(ºC)	53	53	53	53	53
Distillate composition	0.90	0.90	0.90	0.90	0.92
Bottom composition	0.05	0.1	0.08	0.01	0.05
HYSYS optimizer efficiency (%)		93.31	89.28	77.9	85.59

Table 5.11: Summary of optimization results for benzene-toluene system using HYSYS optimizer

	Base case	**Optimum case 1**	**Optimum case 2**	**Optimum case 3**	**Optimum case 4**
Feed rate (kmol/h)	350	344.8	344.8	350	350
Feed temp.(°C)	105	105	105	105	105
Distillate composition	0.95	0.95	0.90	0.90	0.97
Bottom composition	0.05	0.1	0.08	0.01	0.05
HYSYS optimizer efficiency (%)		83.86	81.75	81.76	82.89

5.5 Application to multicomponent system

5.5.1 The system

A multicomponent system as depicted in figure 5.15 (Green and Perry, 2006) is simulated in HYSYS. The 3 products from the fractionation process are a vapor distillate rich in C_2 and C_3, vapor side stream rich in nC_4 and bottoms rich in nC_5 and nC_6. SRK equation of state was used for the K values and enthalpy departure. The system was simulated in HYSYS. The enthalpy and entropy at the stream conditions and at reference conditions are shown in table 5.10. The system being a multi-component system with 5 components necessitates the calculation of the chemical exergy of each stream to determine the contribution of the chemical exergy to the total exergy the stream. Equation 5.9 was used in calculation of the chemical exergy. Exergy of the component at reference states of 298K and 101.325kPa are taken from the literature for each of the component (Szargut *et al*., 1988).

$$Ex_{chem} = m\left(h_0 - \sum z_i \bar{h}_{0i} - T_0\left(s_0 - \sum z_i \bar{s}_{0i}\right)\right) \qquad 5.9$$

where z_i is the mole fraction of the ith component, $\bar{h}_{0i}$ and $\bar{s}_{0i}$ are the partial specific enthalpy and entropy of the component at reference conditions respectively, h is the specific enthalpy, s is the specific entropy, T_0 is the reference temperature, h_0 and s_0 are specific enthalpy and entropy measured at reference conditions and m is the flow rate of the stream under consideration.

The physical exergy of the inlet and outlet streams as calculated using equation 4.13-4.18 are shown in table 5.12.

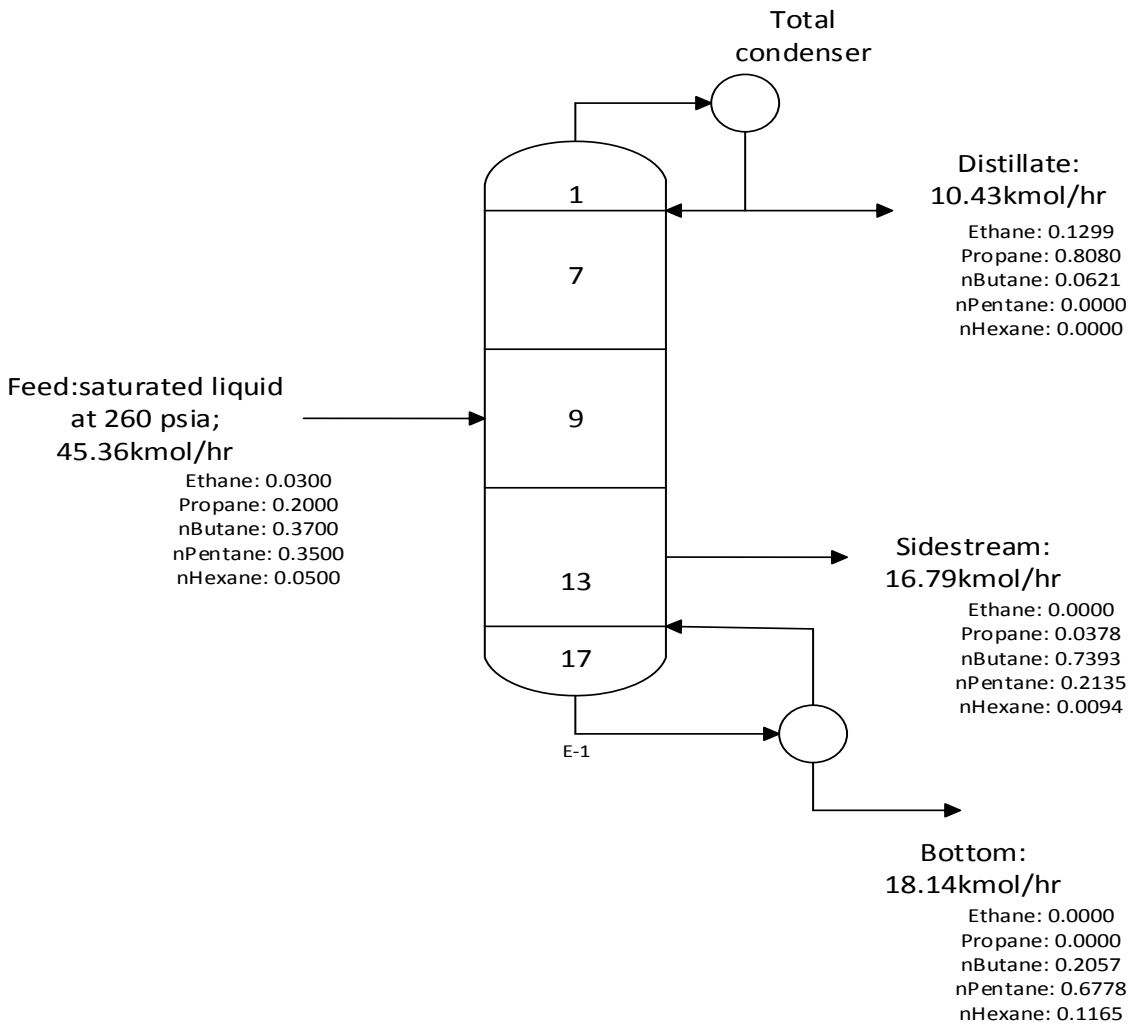

Figure 5.15: The multicomponent separation system

Consider the multicomponent system

$$\sum Ex_{in} = Ex_{feed} + Ex_{reboiler} \quad 5.10$$

$$\sum Ex_{out} = Ex_{distillate} + Ex_{bottoms} + Ex_{sidestream} + Ex_{condenser} \quad 5.11$$

Each stream exergy is a sum of the physical and chemical exergy. The exergy efficiency and the irreversibility of the unit is calculated using equations 5.3 and 5.4.

In table 5.11, the exergy efficiency, exergy loss and the reboiler energy of the unit is shown. Two measures of efficiency are presented. Efficiency 1 is based on the physical exergy of the stream and efficiency 2 is a combination of the physical and chemical exergy of the stream. As can be seen in table 5.13, the reboiler energy, reboiler exergy and exergy loss for the two measured efficiencies are the same. The contribution of the chemical exergy to the total exergy of the unit is 0.5%. This is attributed to the fact that

the distillation process as described here is a physical process. A reactive distillation column might possibly have a significant contribution from the exergy efficiency. The contribution of chemical exergy to this process can be reasonably assumed to be negligible (Anozie *et al*., 2009)

Table 5.12: Simulated data for exergy analysis of multicomponent system

	h_0(kJ/hr)	**s_0(kJ/hr0C)**	**h(kJ/hr)**	**s(kJ/hr^{0}C)**	**m(kmol/hr)**	**Ex(kJ/hr)**
Feed	-129865	160.51	-150891	84.11	45.36	81814.24
Distillate	-102864	168.96	-115493	104.36	10.44	59638.84
Side stream	-130216	141.88	-121966	139.39	16.78	122795.73
Bottom	-171395	74.98	-147889	143.99	18.14	82326.64
Reflux	-102864	168.96	-115493	104.36	68.27	377275.10
Boilup	-160416	96.11	-129710	177.29	117.26	1019346.26
Reboiler duty						1.865×10^6
Condenser duty						9.932×10^5

Table 5.13: Exergy analysis of the multicomponent system

	Efficiency 1(%)	**Efficiency 2(%)**
	64.3	64.6
Reboiler energy (kJ/hr)	1.983×10^6	1.983×10^6
Reboiler Exergy (kJ/hr)	1.865×10^6	1.865×10^6
Exergy loss (kJ/hr)	6.940×10^6	6.885×10^6

As discussed in Section 5.4.1, the input variables for the ANN training are the feed temperature, the feed rate and the key component in each of the product stream which are propane in the distillate, npentane in the bottom and nbutane in the side stream. These variables were varied in their upper and lower bounds and the corresponding exergy analysis of the inlet and outlet streams were calculated both at the prevailing

operating conditions and at reference conditions. Subsequently data generated in HYSYS are used in the ANN modeling of the column. The software generated data can be easily replaced with plant operating data over a period of time for an industrial column. The methodology as developed here is generic.

5.5.2 Bootstrap aggregated neural network modelling of the multicomponent

A bootstrap aggregated neural network is developed from process operational data based on the simulated data in HYSYS. The neural network contained 30 neural networks for predicting the exergy efficiency of the system. Each individual network has a single layer with 30 hidden neurons. Hidden neurons use sigmoid activation function and the output neuron uses the linear activation function. Levenberg-Marquardt training algorithm was used to train the individual networks. Figure 5.16 gives the predicted exergy efficiency for the training, testing and validation data sets. The results clearly show the ability of BANN to accurately model the exergy efficiency. The prediction error within -4×10^{-3} and 6×10^{-3} as shown in figure 5.17. Figure 5.18 shows the predicted and actual values of the exergy efficiency as well as the confidence bounds. Another advantage of BANN model is that it can offer model prediction confidence bound. With increasing decision variables, the complexities of the method increases. BANN has additional advantage of inclusion of confidence bounds in the optimisation criteria. A narrower confidence bounds indicates the reliability of the associated model prediction.

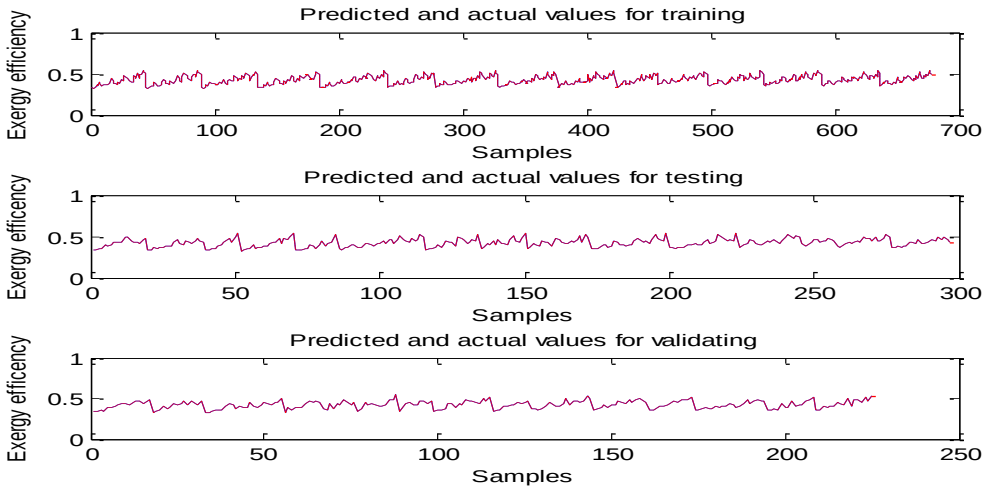

Figure 5.16: BANN model of the multi-component system

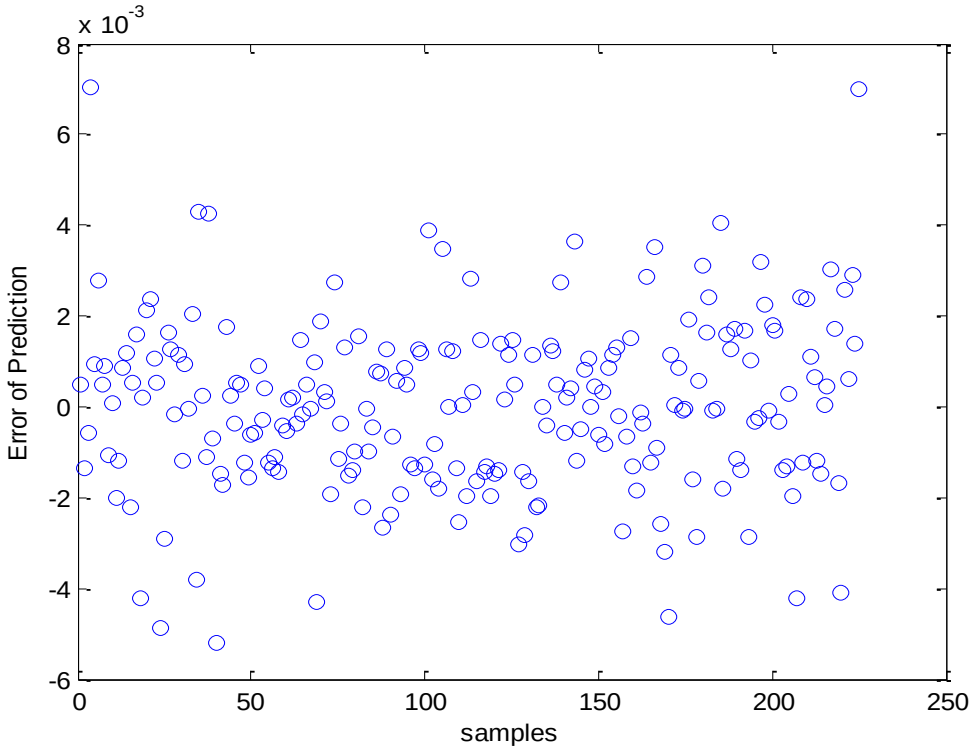

Figure 5.17: Error of prediction of muticomponent BANN model

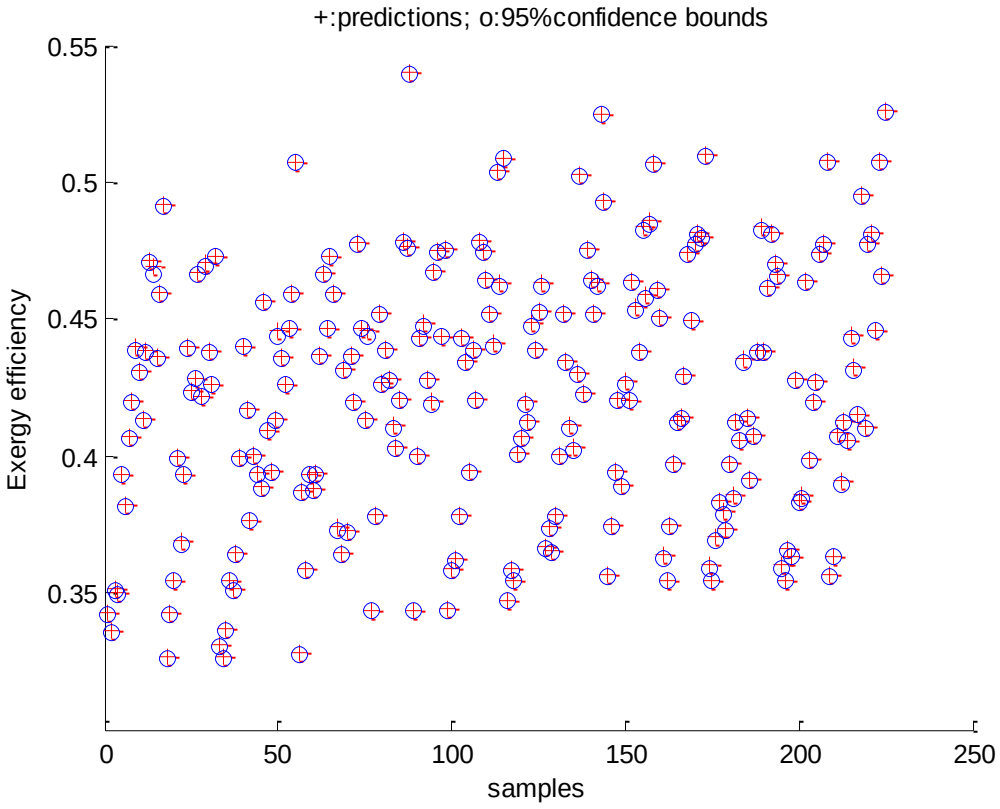

Figure 5.18: Predictions, and confidence bounds of multicomponent BANN model

5.5.3 BANN model of the modified multicomponent system

A further modification of the system was made based on the given specification in Figure 5.19. The number of stages was increased to 25, the feed stage at stage 7 and the sidestream was drawn from stage 17. The modifications were intended for a change in the design of the column to investigate the contribution it will have on the exergy efficiency.

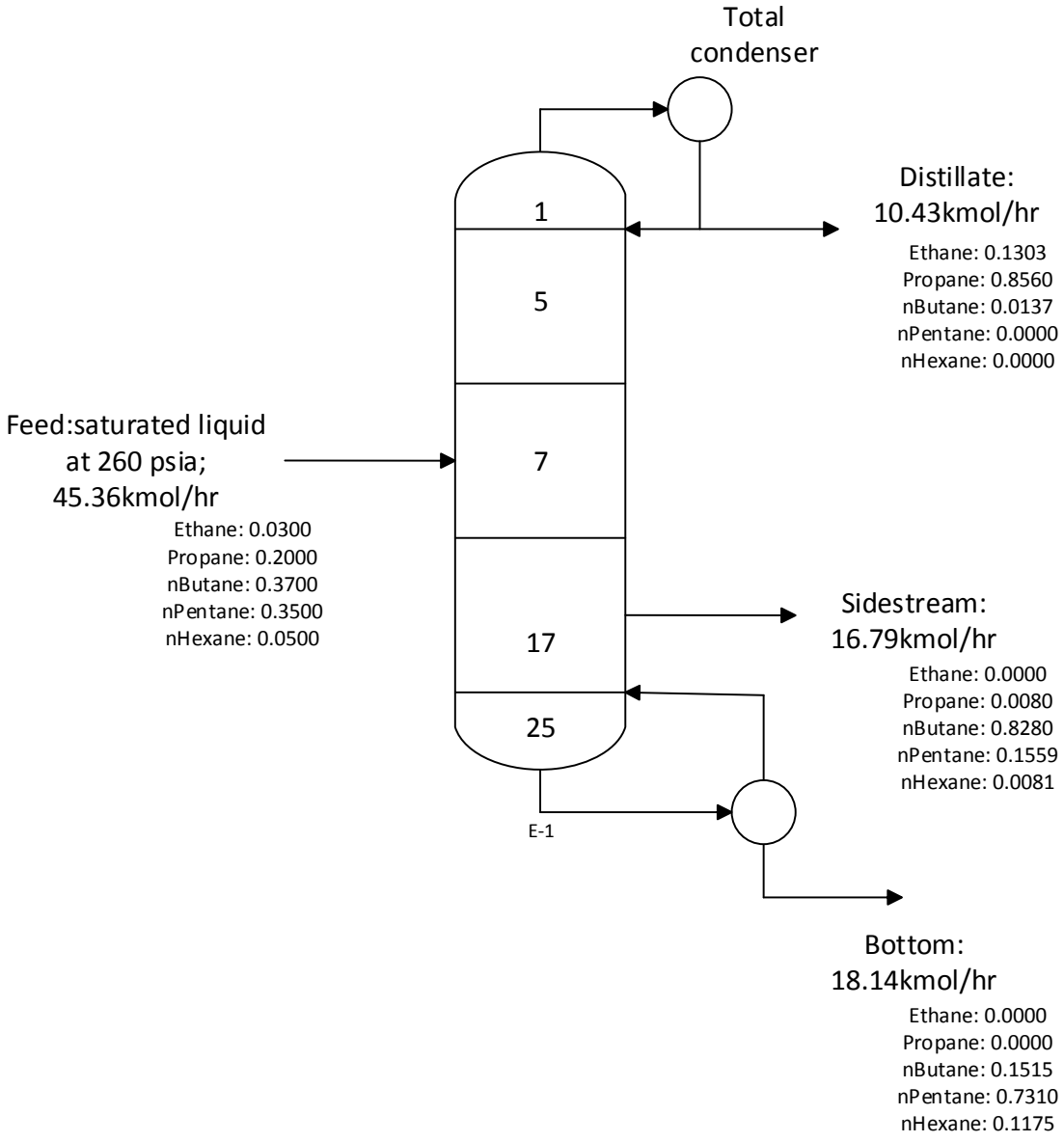

Figure 5.19: Modified multicomponent system

The subsequent thermodynamic analysis of the modified system was made as described in Section 5.5.1. Table 5.14 shows the simulated data and the exergy calculation of the streams in and out of the modified system. Exergy efficiency, exergy loss and reboiler exergy of the system are shown in table 5.15. As was the case for the previous multicomponent system, the reboiler exergy and exergy loss for the two measured

efficiencies are the same. The contribution of the chemical exergy to the total exergy of the system is 0.4% and hence can be considered negligible here as well. There is an increment in the exergy efficiency of the modified system by 2% corresponding to an improvement of 5.3% as compared to the initial system. There is a corresponding decrease in the reboiler energy and the exergy loss of the system. This signifies a reduction in entropy generation within the column resulting from increasing the stage number. It should however be noted that the improvement in efficiency comes with the added expenses of capital cost.

Table 5.14: Simulated and thermodynamic data of the modified system

	h_0(kJ/hr)	s_0(kJ/hr0C)	h(kJ/hr)	s(kJ/hr^{0}C)	m(kmol/hr)	Ex(kJ/hr)
Feed	-129865	160.51	-150891	84.12	45.36	81814.25
Distillate	-102864	168.96	-115491	104.36	10.44	71209.26
Side stream	-130216	141.88	-121965	139.38	16.78	153814.2
Bottom	-171395	74.98	-147889	143.99	18.14	56800.36
Reflux	-102864	168.96	-115491	104.36	68.36	454774.8
Boilup	-160416	96.11	-129710	177.30	117.33	767273.4
Reboiler duty						1957834
Condenser duty						1048452

Table 5.15: Exergy analysis of the modified multicomponent system

	Efficiency 1(%)	**Efficiency 2(%)**
	66.5	66.8
Reboiler energy (kJ/hr)	2.072×10^6	2.072×10^6
Reboiler Exergy (kJ/hr)	1.949×10^6	1.949×10^6
Exergy loss (kJ/hr)	6.788×10^5	6.733×10^5

BANN model of exergy efficiency as a function of the products composition, feed temperature and feed rate was developed. The structure of the BANN is as discussed in Section 5.3.2. Figure 5.20 shows the BANN model of the modified multicomponent system. The system can be seen to be perfectly represented by the model. The actual and the predicted exergy efficiency are more or less superimposed showing a quite good correlation. The model prediction of the system showing the 95% confidence bounds is shown in Figure 5.21. Figure 5.22 shows the plot of the training, testing and validation data for the predicted and actual exergy efficiency of the system.

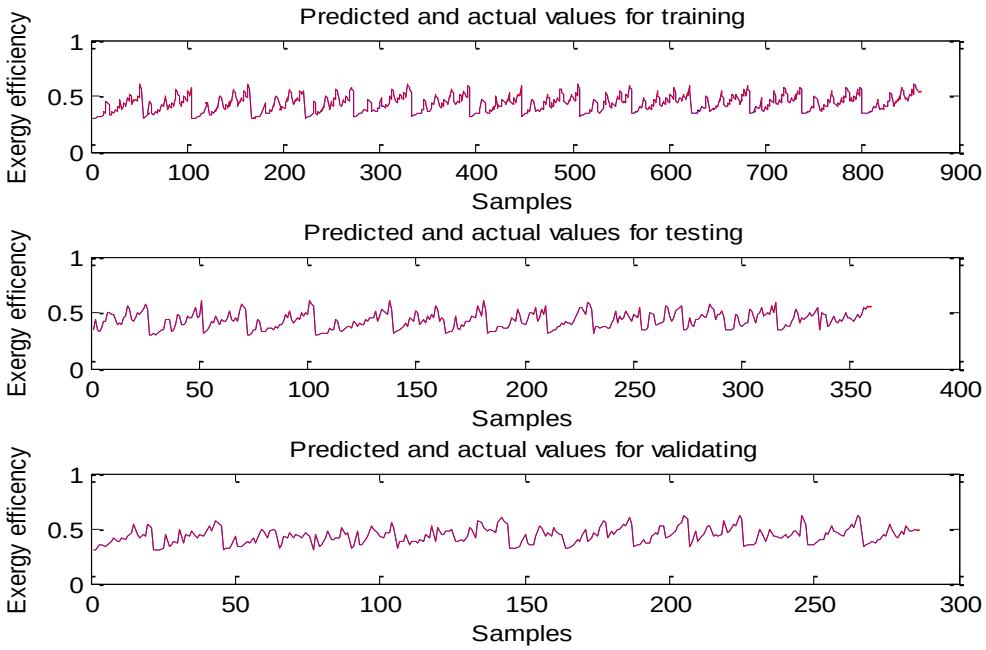

Figure 5.20: BANN model of the modified multicomponent system

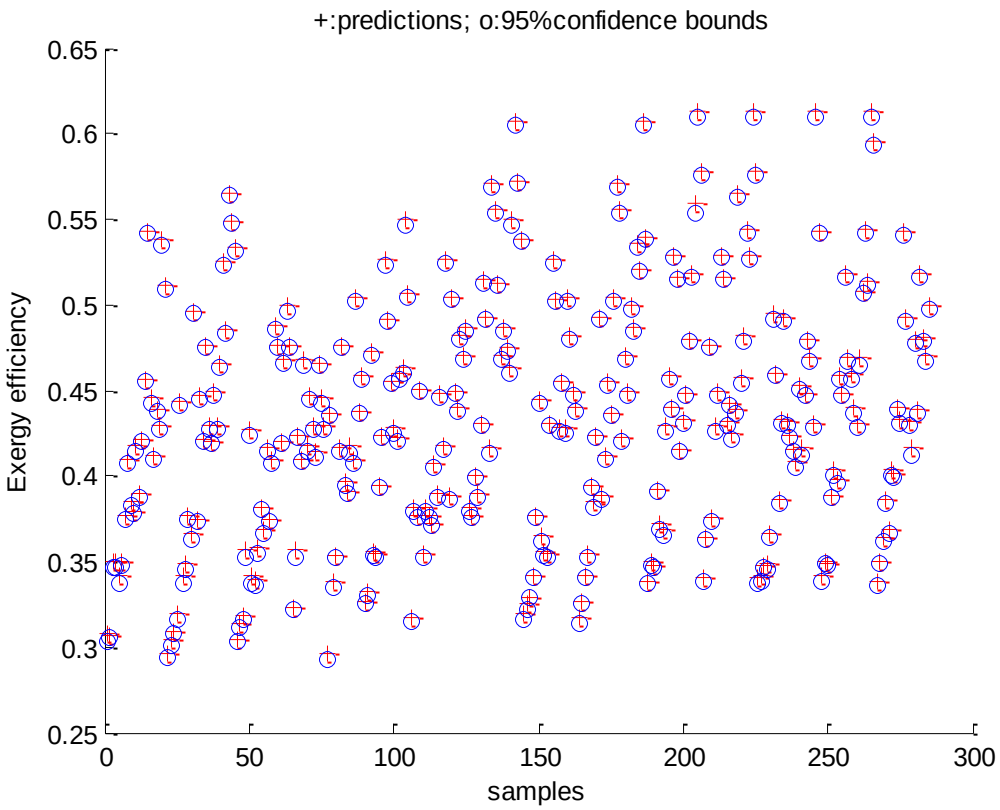

Figure 5.21: Model prediction confidence bounds of the modified multicomponent system

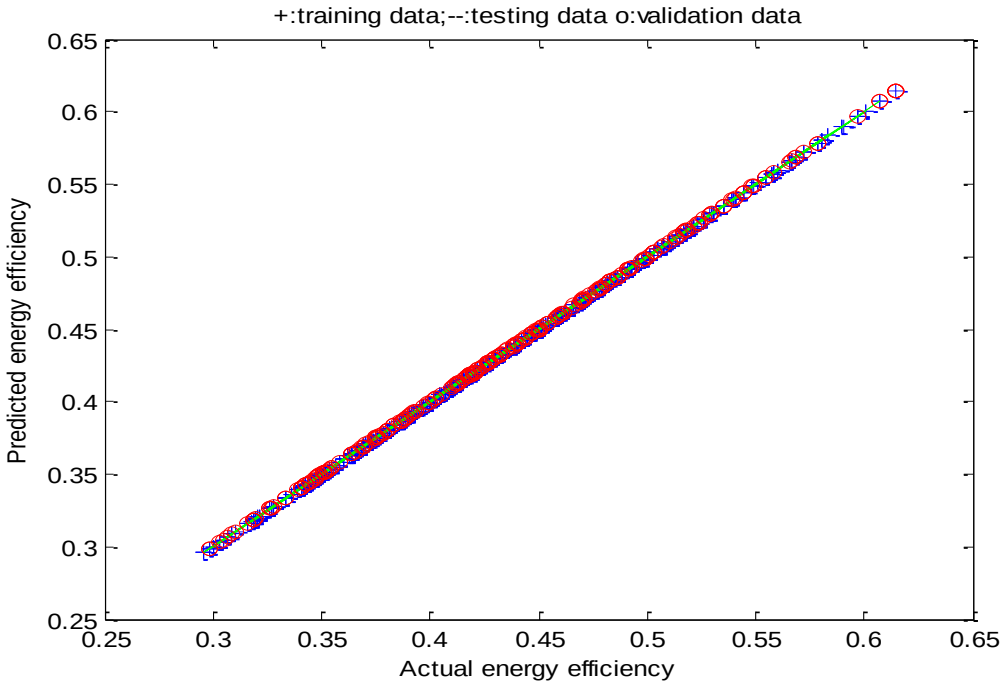

Figure 5.22: Predicted and actual exergy efficiency

5.5.4 Optimization using neural network models

The optimisation objective is to maximise the exergy efficiency of the column subject to product composition constraints. The products are the most volatile in the distillate, side stream and bottom composition.

$$\min_X J = -y \qquad 5.12$$

s.t.

$$\varphi = f(x_1, x_2, x_3, x_4, x_5)$$

$$0.75 \le x_3 \le 0.95$$

$$0.6 \le x_4 \le 0.9$$

$$0.7 \le x_3 \le 0.95$$

In addition to the process operation objective, minimizing the model prediction confidence bounds can be incorporated as an addition optimization objective. To improve the reliability of the optimization strategy, a modified objective function is proposed. The optimization problem can be stated as

$$\min_X J = -(\varphi - \beta\sigma)$$

s.t.

$$\varphi = f(x_1, x_2, x_3, x_4, x_5) \qquad 5.13$$

$$lb \le x_{prod} \le ub$$

where J is the objective function, x=[x_1,x_2,x_3,x_4,x_5] is a vector of decision variables, i.e. neural network model inputs, φ is the exergy efficiency, σ is standard prediction error, and β is weighting factor of σ.

The optimisation problems were solved using the SQP method implemented by the function “fmincon” in MATLAB Optimisation Toolbox. The optimisation framework presented in this work is illustrated in figure 5.23. The optimised operating conditions are further validated on the distillation process and their corresponding exergy analysis are performed.

Table 5.16 shows the optimum results without confidence bounds for the initial system and the modified system. The prediction errors of the optimum results and the HYSYS validated exergy efficiency are 0.00165 and 0.0058 for the initial and modified cases

respectively. The results further confirm the predictability accuracy of BANN. Also without modifying the design, optimum operating conditions that led to 31.4% increase in exergy efficiency of the system were found using the proposed methods. This is without sacrificing the purity of the product specifications. This further justifies the suitability of the method in determining energy efficient operating conditions for the distillation column. However, with the modification, the exergy efficiency has increased from 64.3% to 66.5% this is just about 2% increment in the exergy efficiency as compared to 31.4% from the method presented. This increment for the modified case is at an additional capital cost (increasing number of trays and change in location of feed and side stream). The tools described here can aid in decision making of what trade off should be made in the design and operation of energy efficient column. The modified system is further improved as shown in table 5.16 and there is an increase in its exergy efficiency to 31% of its initial value.

In table 5.17, the results of the optimisation of the base case with model prediction confidence bounds are shown. The effects of some values of the weighting factor of the standard prediction error on exergy efficiency are also investigated. Narrowing the confidence bound to a weighting factor of 0.01 improves the prediction accuracy and reliability of the model. Incorporating confidence bound in the optimisation ensures the reliability and the generalisation of the associated model. Reducing the confidence bound to 0.001 increased the prediction error but not beyond what was obtained for the optimum case. This shows the need for a careful consideration of the weighting factor in order to have a reliable result.

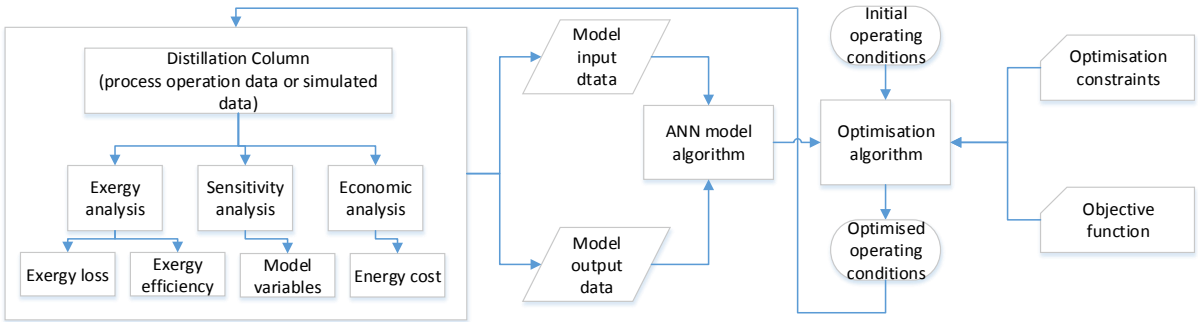

Figure 5.23 : Description of the optimisation procedure.

Table 5.16: Summary of optimization results for multicomponent systems

	Multicomponent System		**Modified System**	
	Base case	Optimum case	Base case	Optimum case
Feed rate (kmol/h)	45.36	45.36	45.36	45.36
Feed temperature(^{o}K)	308.1	308.1	308.1	308.1
Propane in distillate	0.8080	0.85	0.8562	0.85
n Pentane in Bottom	0.6778	0.71	0.7310	0.82
n Butane in sidestream	0.7393	0.85	0.8280	0.92
Exergy efficiency (%)	64.3	96.7	66.8	97.6
ANN predicted exergy efficiency (%)	66	96.5	63.2	97.0

Table 5.17: Summary of optimization results with confidence bounds

Confidence bounds	**Base case**	**0**	**1**	**0.1**	**0.01**
Feed rate (kmol/h)	45.36	45.36	45.36	45.36	45.36
Feed temp (K)	308	308	308	308	308
Propane comp	0.808	0.85	0.85	0.85	0.85
n Pentane comp	0.6778	0.71	0.71	0.71	0.71
n Butane comp	0.7393	0.85	0.85	0.85	0.85
HYSYS validated	64.29	96.67	96.68	96.66	96.66
Optimum efficiency from ANN(%)	66	96.51	95.78	96.44	96.60

Confidence bounds	Base case	0	1	0.1	0.01
Error of prediction	0.0265	0.00165	0.009	0.0022	0.0006

5.6 Conclusions

This chapter shows that ANN can accurately model exergy efficiency in distillation columns. The ANN models are then used in obtaining optimal distillation operation conditions that can maximise the energy performance of distillation systems while maintaining the product quality and throughput. A reliable strategy based on BANN for improved generalisation of the predicted model is also presented. BANN enhances model prediction accuracy and also provides model prediction confidence bounds. Exergy analysis is an effective way of determining the energy efficiency of processes and hence the importance of this study to process and design engineers. Applications to two binary systems and a multicomponent system demonstrate the proposed methods can significantly increase the exergy efficiency of distillation columns. The optimisation resulted in 22.67% increment of the exergy efficiency of methanol water and 33.49% for benzene toluene. This brings about a reduction in the consumption of utility of the systems to 29.4% for methanol water and 66.56% for benzene toluene. The improvement is based on changing the operating conditions of the system and has no additional capital costs. The multi-component system has an improvement in the exergy efficiency to be 31.25%. This is without incurring any additional capital costs as well. The modified multi-component system has an exergy improvement of 47.33%, but the column structure has to be redesigned creating an additional capital costs. The advantage of incurring these further costs can be weighed and informed decisions can then be made. The ANN and BANN model based modelling and optimisation can aid the decision making of energy efficient operations and control of distillation columns.

CHAPTER 6: OPTIMISATION OF ENERGY EFFICIENCY: APPLICATION TO CRUDE DISTILLATION SYSTEM

This chapter is based on the published papers presented at PSE2015/ESCAPE25, 31st May-June 4, 2015; IEEES7, April 27-30, 2015 and two manuscripts in preparation for journal publication

6.1 Introduction

Distillation process has always attracted the interest of researchers and quite a number of work in the literatures are focused on improving its energy consumption either for binary system (Osuolale and Zhang, 2014) or multi-component system (Al-Mutairi and Babaqi, 2014). In recent years optimization of crude distillation system has received considerable research interest. This is because major cost of operation second only to the cost of crude in the refinery is energy and 35% of these is consumed in the crude distillation unit. Optimization is a major quantitative tool in decision making for the process industries. Rather than large scale expansion, most industries will maximize available resources for maximum profitability. Optimization objectives of most chemical engineering processes have complex inter-relationships. This is where multi-objective optimization is useful to find the optimal tradeoffs among two or more conflicting objectives such as economic, energy efficiency, product throughput and carbon emission. And for a crude distillation unit, the combination of the objectives varies (Motlaghi *et al*., 2008). Optimization is a well-developed field in chemical engineering and has been applied on a number of processes (Li *et al.*, 2012). It has also find application in improving the energy efficiency of the crude distillation unit albeit in terms of the utility consumption alone (Ochoa-Estopier *et al*., 2013).

Thermodynamic analysis of the crude distillation unit gives insight into its second law efficiency. Past work on the second law analysis reveals low efficiency of the system. Cornelissen (1997) performed analysis on a crude distillation unit with an efficiency of 0.27 for the ADU, while Al-Muslim and Dincer (2005) came out with a result of 0.43 for the ADU. This could imply that improvement of the efficiency of the column will be better off when it is based on the second law. The challenge therefore is to develop optimization procedures based on second law analysis aimed at minimizing the inefficiencies without compromising the qualities of the products. The crude distillation unit comprises the pre-flash drum, heat exchanger network, atmospheric distillation unit with side strippers and pump arounds and a vacuum distillation unit. In this chapter, a

method of optimizing the atmospheric distillation unit operations on its own and the crude distillation unit as a whole is presented.

The chapter is organized as follows: section 6.2 gives a description of the atmospheric distillation unit, and methods of analysis of the system such as exergy analysis, sensitivity analysis and economic analysis. Section 6.3 deals with BANN modeling of the ADU, single and multi-objective optimization of the ADU with and without product quality constraints. Section 6.4 gives a description of the crude distillation unit, its HYSYS simulation, and exergy analysis. In Section 6.5, simulation of the pre-flash units is considered. Section 6.6 gives the BANN modeling of the CDU with and without the pre-flash units. Section 6.7 presents the optimization of the CDU with and without the pre-flash units and concludes with a multi-objective optimization of the CDU. Some concluding remarks of this chapter are given in Section 6.8.

6.2 Atmospheric distillation unit

6.2.1 Description of Systems

The atmospheric distillation system considered in this study is presented in Figure 6.1. The crude to be processed was Venezuela Tia Juana light crude (Watkins 1973). The crude was characterized using experimental assay that include the bulk crude properties, light end volume percent, ASTM distillation, API gravity and TBP distillation. The assay data was fed into the data bank of the simulator software (HYSYS). The result of the characterization is a set of pseudo-components and a detailed chemical composition of the identified light ends components. The goal is to determine optimal operating conditions to give the maximum exergy efficiency of the process. The column processes 100,000 barrel/day of crude at 25psia and 690 ^{0}F into 6 products: Off gas, Naphtha, Kerosene, Diesel, Atmospheric gas oil (AGO) and Residue.

6.2.2 HYSYS simulation

Process simulators are mathematical tools that model processes with continuous flows of material and energy from one unit operation to another. They are often used to design or select a process from alternatives, in modelling real processes and calculating steady state mass and energy flow, and in evaluating process operations and performance. Crude distillation unit consists of complex mixtures whose compositions and thermodynamic properties vary significantly depending on prevailing conditions. Tables of such properties cannot be easily assessed manually or practically. The process is quite dynamic and it is costly and often impracticable to perform experimental runs.

Hence a simulator software HYSYS is used for its modelling and simulation. The procedure is further highlighted as follows.

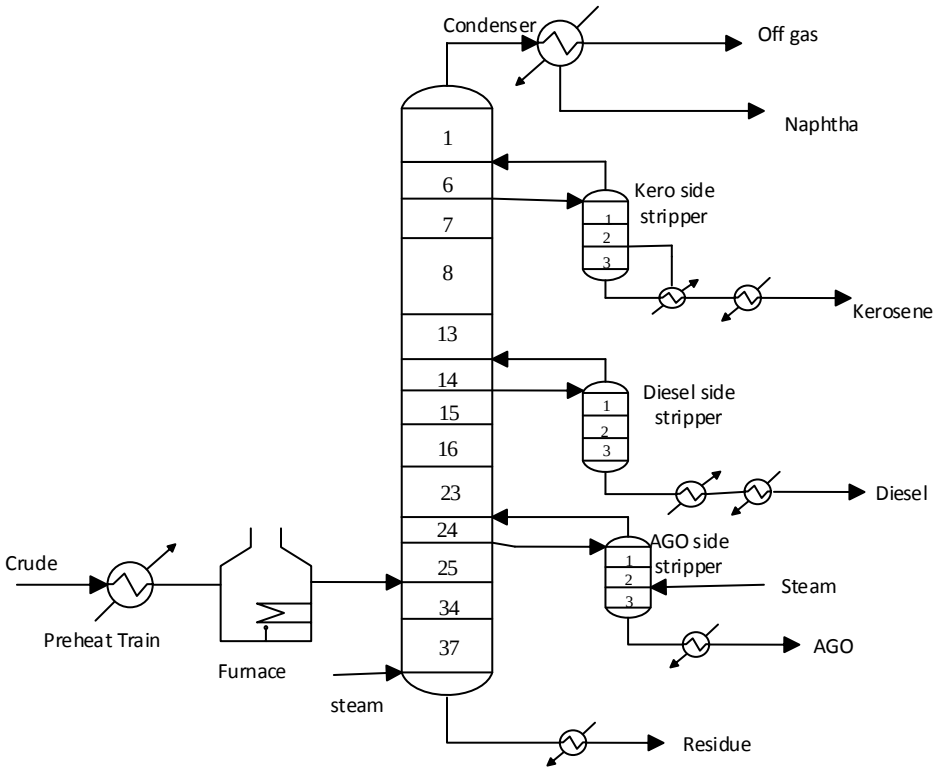

Figure 6.1: Schematic diagram of the atmospheric distillation unit

Component selection

HYSYS contains a number of components in its data bank. The components are well defined with its thermodynamic and physical properties, temperature dependent properties such as enthalpy and critical properties. The light end components of the refineries were inputted here. It should be noted that the given components are from the laboratory analysis of the raw crude. Other unknown components of the crude are determined from the crude characterization in HYSYS.

Thermodynamic property package

The property package in HYSYS includes Equation of states (EOSs), activity models, Chao Seadre models and vapour pressure models. One of the property package in EOS is Peng-Robinson. It was chosen as it properly suited crude oil analysis. The Peng-Robinson method utilises EOS in its enthalpy calculations.

Oil characterisation

Crude oil is a mixture of many identified chemical components and pseudo-components whose chemical identity might be difficult and sometimes impractical to determine.

Hence, there is a need for the characterizations of the crude. The crude was characterized using experimental assay that include the bulk crude properties, light end volume percent, ASTM distillation, API gravity and TBP distillation.

The result of the characterization is detailed chemical compositions of the identified components and the pseudo-components. The complete and definitive analysis of a crude oil is called *crude assay.* This is more detailed than a crude TBP curve.

Building the flow sheet

The modelling of the crude distillation units were done in the HYSYS environment using their operating and design parameters. The simulation was done to be a prototype of the actual process as much as possible in terms of these parameters-the number of trays, feed tray, feed temperature, feed flow rates, heat exchangers supply and target temperatures, product specifications, steam flow rates, pump around flow rates. Data such as entropy, enthalpy, temperatures, pressures, compositions and stream flow rates were extracted from the simulation for exergy analysis.

6.2.3 Exergy analysis

The total exergy of a stream is given as

$$Ex_{total} = Ex_{phy} + Ex_{chem} \quad 6.1$$

The physical exergy is calculated from equation 4.13-4.18.

For the crude stream considered, standard molar chemical exergy Ex_{chem} is calculated from the standard molar chemical exergies of all identified components and pseudo-components as

$$Ex_{chem} = m\left[\sum b_{qi} + \sum b_{chi} + RT_0 \sum lna_i\right] \quad 6.2$$

Where b_{chi} is the chemical exergy for component i, b_{qi} is the chemical exergy for pseudo component and a_i is the activity coefficient of component i. The standard chemical exergy for pseudo-components can be determined for heuristic empirical expression as a function of the elementary composition and their heating values (Szargut *et al*., 1988, Rivero *et al*., 1999)

$$b_{qi} = \vartheta_i C_i \quad 6.3$$

Where ϑ_i is the regression equation to express the ratio H/C, N/C, O/C and S/C for pseudo-component i, C_i is the net calorific heating value of the pseudo-component i. From figure 6.1, the inlet and outlet streams are given as

$$\sum Ex_{out} = Ex_{offgas} + Ex_{naphtha} + Ex_{kero} + Ex_{diesel} + Ex_{AGO} + Ex_{residue} \quad 6.4$$

$$\sum Ex_{in} = Ex_{crude} + Ex_{steam} + Ex_{furnace} + Ex_{kero\ reboiler} + Ex_{diesel\ reboiler} + Ex_{AGO\ steam} \quad 6.5$$

The exergy efficiency and the irreversibility are then calculated as:

$$\varphi = \frac{\sum Ex_{out}}{\sum Ex_{in}} \quad 6.6$$

$$I = \sum Ex_{in} - \sum Ex_{out} \quad 6.7$$

Table 6.1 gives the result of the physical exergy of the ADU.

Table 6.1: Simulated data for exergy analysis

Stream Name	h(kJ/ kmol)	h_0(kJ/hr)	s(kJ/hr K)	s_0(kJ/hr K)	m(kmol/hr)	Ex
Inlet streams						
Crude inlet	-345265	-624086	1084.64	485.72	1910.94	1.92×10^8
Crude Steam	-233887	-286232	181.06	53.66	1200	17256656
Kero Reboil						10386235
Diesel Reb						22617319
AGO steam	-233887	-286232	181.06	53.66	250	3595137
Furnace duty						87342512
TOTAL IN						3.33×10^8
Outlet streams						
Residue	-896119	-1.590087	3157.92	1680.61	259.58	65865065
Naphtha	-342702	-368239	197.57	121.48	374.48	1071996
Off gas	-234440	-282113	182.75	49.93	2022.68	16365119
Kerosene	-384811	-521349	646.14	316.74	266.18	10214893
AGO	-704638	-1110258	2036.66	1130.98	69.59	9445569
Diesel	-467454	-769659	1334.31	672.88	347.89	36562748
TOTAL OUT						1.4×10^8

6.2.4 Economic Analysis

The total operating cost of the column is given as

$$Total\ operating\ cost = Energy\ cost + Capital\ cost \quad 6.8$$

In the above equation,

$$Energy\ cost = \sum Q_x C_x \quad 6.9$$

where Q_x is the duty of utility x and C_x is the unit cost of utility x.

$$Capital\ cost = Heat\ exchanger\ cost = A + B(area)^c \quad 6.10$$

where A is the fixed cost of installation and B is exchanger cost per unit area.
For a stainless steel shell and tube heat exchanger,

$$Heat\ exchanger\ cost = 33422 + 1874(area)^{0.81} \quad 6.11$$

Details of the calculation of the operating costs of a crude distillation system can be found in (Al-Mutairi and Babaqi, 2014).
The method of improvement being proposed here does not include a change in any of the equipment and hence the capital cost remains the same. Basically the economic analysis is based on the operating profit of the column and expressed mathematically as

$$Profit = \sum_{j=1}^{n} M_j C_j - [M_{crude} C_{crude} + M_{steam} C_{steam} + \sum_{x=1}^{n} Q_x C_x\ ] \quad 6.12$$

Where M_j and C_j are the flow rates and costs of products j, M_{steam} and C_{steam} are the flow rate and cost of steam respectively, Q_x and C_x are the heat requirement of utility and the cost of utility respectively. The calculation is based on the assumption of 8600 h per year. In table 6.2, the feed, products and utility prices are shown (Energy information administration, 2014).

Table 6.2: Feed, products and utility prices

Item	Cost	Unit
Crude oil	80	$/bbl
Off gas	44.3	$/bbl
Naphtha	136	$/bbl
Kerosene	122.7	$/bbl

Item	Cost	Unit
Diesel	121.7	$/bbl
Atmospheric gas oil	95.29	$/bbl
Residue	89.71	$/bbl
Fired heating	150	$/kJ
Cooling water	5.25	$/kJ
Stripping steam	0.14	$/kmol

6.2.5 Sensitivity analysis of manipulated variables

In order to evaluate the decision variables, each of the decision variables was changed individually in a range equivalent to 85 % and 115 % of the original value and for some cases, 95 % and 105 %. The variables that significantly affect the objective function were used for the ANN modeling and then optimization. The exergy efficiency (equation. 6.6), energy cost (equation 6.9) and profitability (equation 6.12) of each variables were evaluated. Table 6.3 shows the results of the evaluation. It could be noted that reduction in energy costs translates to improved exergy efficiency. And in all cases, increasing exergy efficiency implies an increase in the profitability of the process.

Table 6.3: Sensitivity analysis of manipulated variables

	Exergy Eff. (%)	Energy cost($/yr)	Profitability ($/yr)	Exergy Eff. (%)	Energy cost($/yr)	Profitability ($/yr)
	% Decrease in initial value			% Increase in initial value		
Kerosene	35.8	8.048×10^{6}	2.279×10^{9}	52.23	5.076×10^{6}	2.442×10^{9}
AGO	35.14	7.74×10^{6}	2.326×10^{9}	50.61	6.088×10^{6}	2.393×10^{9}
Naphtha	40.16	7.185×10^{6}	2.269×10^{9}	46.44	5.915×10^{6}	2.450×10^{9}
Residue	28.68	8.109×10^{6}	2.309×10^{9}	63.79	4.489×10^{6}	2.411×10^{9}
Diesel	35.75	7.788×10^{6}	2.359×10^{9}	52.44	5.171×10^{6}	2.361×10^{9}
PA1 flow rate	42.36	6.939×10^{6}	2.360×10^{9}	41.67	7.261×10^{6}	2.359×10^{9}
PA1 ΔT	42.46	6.889×10^{6}	2.360×10^{9}	41.7	7.224×10^{6}	2.359×10^{9}
PA2 flow rate	42.68	6.790×10^{6}	2.360×10^{9}	41.53	7.319×10^{6}	2.359×10^{9}
PA2 ΔT	42.66	6.8×10^{6}	2.360×10^{9}	41.56	7.307×10^{6}	2.359×10^{9}
PA3 flow rate	42.63	6.820×10^{6}	2.360×10^{9}	41.58	7.289×10^{6}	2.359×10^{9}

PA3 ΔT	42.65	6.811×10^{6}	2.360×10^{9}	41.66	7.256×10^{6}	2.359×10^{9}
Diesel duty	42.14	7.051×10^{6}	2.360×10^{9}	42.06	7.036×10^{6}	2.360×10^{9}
Kerosene duty	42.07	7.095×10^{6}	$2\ 360\times10^{9}$	42.11	7.023×10^{6}	2.360×10^{9}
AGO steam	42.13	7.055×10^{6}	2.360×10^{9}	41.84	7.175×10^{6}	2.359×10^{9}
CDU steam	43.71	6.376×10^{6}	2.360×10^{9}	40.94	7.549×10^{6}	2.359×10^{9}

6.3 Modelling of the Atmospheric distillation unit

In this study, simulated process operational data were generated from HYSYS. Variables selected from sensitivity analysis were varied within their lower and upper bounds in a nested loop. From the simulated data, a bootstrap aggregated neural network (BANN) containing 30 neural networks was developed to model exergy efficiency and products quality. Figure 6.2 shows the BANN model of the crude distillation unit. A single layer network with 30 hidden neurons was used. The number of hidden neurons was determined by building a number of neural networks with different numbers of hidden neurons and testing them on the testing data. The network giving the lowest sum of squared errors (SSE) on the testing data is considered as having the appropriate number of hidden neurons.The Levenberg-Marquardt trainning algorithm was used to train the network. For training each network, bootsrap resampling with replacement was used to generate a replication of the data. 50% of the simulated data was for training, 30% for testing and 20% for unseen validation. Figure 6.3 shows the BANN model performance on the unseen validation data.

Figure 6.4 shows the MSE of the individual networks and BANN containing different number of networks on the training and unseen validation data sets. A network with small training SSE may have quite large SSE on the validation data. This indicate inconsistency and non robust nature of the individual networks. The minimum SSE of individual network on the training and validation data sets are 6×10^{-6} and 1.9×10^{-5} respectively. The SSE for the aggregated network on the training and validation data are 4×10^{-6} and 1.6×10^{-5} respectively. This shows the model accuracy is improved by combining the imperfect models.

It can be seen that individual networks give inconsistent performance on the training and unseen validation data indicating the non-robust nature of single networks. BANNs give consistent and more accurate prediction performance on the training and unseen validation data sets.

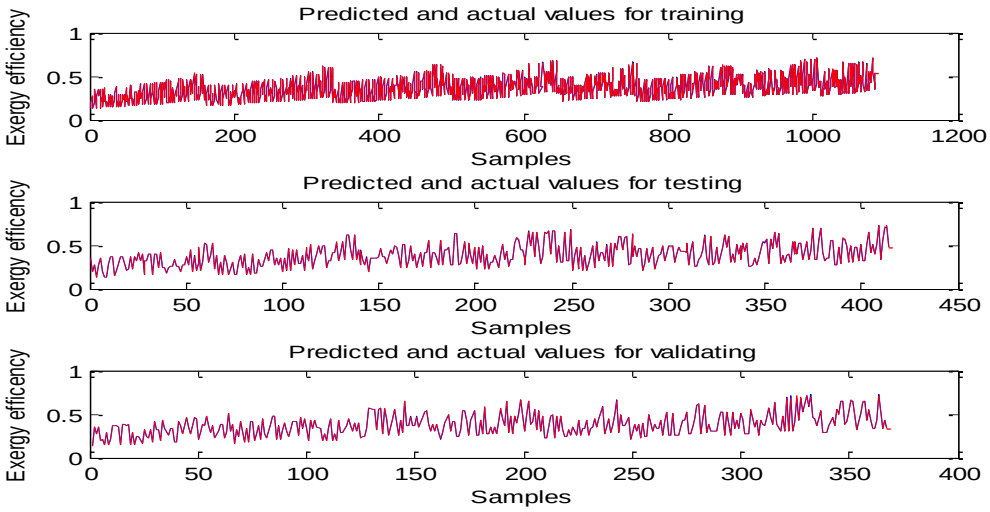

Figure 6.2: BANN model of the ADU

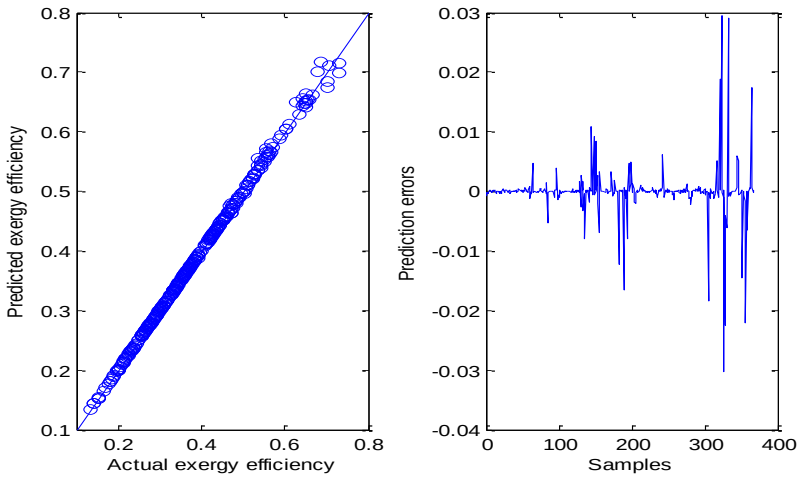

Figure 6.3: BANN predicted vs. actual exergy efficiency (left) and prediction errors (right)

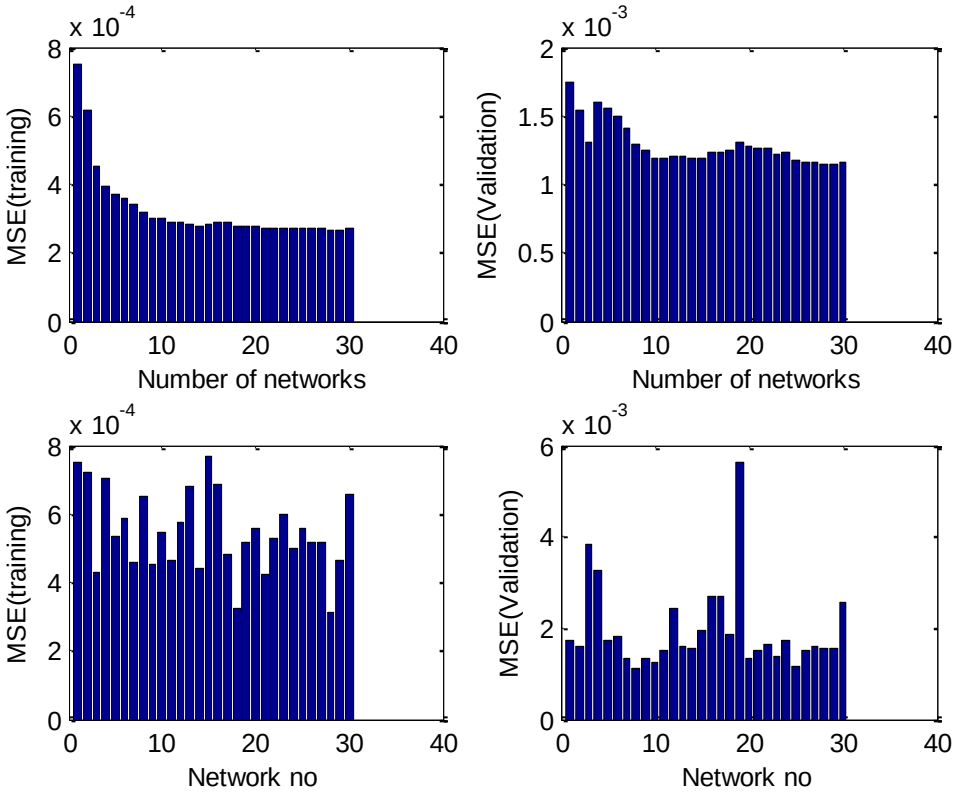

Figure 6.4: Model error of individual networks for the crude distillation unit

6.3.1 ANN model optimization

The objective of the optimization here is to maximize the exergy efficiency of the atmospheric distillation unit. There are a number of decision variables in the ADU where finding their optimal value can significantly improve the exergy efficiency of the ADU. The prediction confidence bound is incorporated in the optimization problem. The optimization formulation is given as

$$\max_{X} J = \varphi - \beta\sigma \qquad 6.13$$

s.t.

$$\varphi = U(x)$$

where J is the objective function, y is the exergy efficiency, U is the knowledge data base model of the ADU, $x_1, x_2, \ldots x_n$ is a vector of decision variables which are the flow rates of heavy naphtha, kerosene, diesel, AGO, residue, PA1, PA2 and PA3, σ is standard prediction error and β is the weighting factor of σ. The optimisation problem was solved using the sequential quadratic programing (SQP) implemented by the function "fmincon" in MATLAB optimisation toolbox. Table 6.4 shows the optimum

and HYSYS validated results with varying weighting factors of the confidence bounds. The approach in this work is to improve model prediction reliability using BANN and to provide a model prediction confidence bounds which is then used in the optimization objective function. The effect of penalization of the wide model prediction confidence bounds during the optimization can be clearly seen in table 6.4. The result of the optimization without including the confidence bounds is included for the purpose of comparison. The relative error is calculated as the difference between BANN and HYSYS validated model divided by the HYSYS validated model. The method results in much less relative error between the BANN model and HYSYS simulated model. This indicates the reliability of the proposed model because the performance of the actual model (HYSYS validated model) is close to that predicted by the neural network model. The accuracy of the predicted model to the simulated model in HYSYS is a function of weightings of the standard prediction error. Hence it can be said that the weighting of 0.001 should be used as it gives the least prediction error.

Table 6.4: Summary of optimization results with confidence bounds

Items	**Base**	**0**	**1**	**0.5**	**0.01**	**0.001**	**LB**	**UB**	**Unit**
Naphtha	517	439	439	439	439	439	439	594	barrel/hr
Kerosene	508	507	557	530	505	508	431	584	barrel/hr
Diesel	952	1000	1000	1000	1000	1000	904	1000	barrel/hr
AGO	267	308	227	266	308	308	226	308	barrel/hr
Residue	1296	1350	1350	1350	1350	1350	1231	1360	barrel/hr
PA1	943	948	947	928	947	885	801	1085	barrel/hr
PA2	1132	1139	945	938	1136	946	800	1085	barrel/hr
PA3	943	958	948	952	957	954	800	1085	barrel/hr
Optimum efficiency		79.8	63.7	72.6	78.9	79.7			%
HYSYS validated	42.1	77.1	64.9	73.2	78	79.1			%
Error		0.0347	0.0183	0.0081	0.011	0.007			

6.3.2 ANN optimisation with product qualities constraints

Crude distillation operations are often bounded by product quality specifications. An optimal efficiency procedure without consideration to the quality specification might not be feasible in practice. For petrochemical system where it is not possible to give a

discrete component specifications as a measure of the product quality, the 95% vol and 5% vol of the ASTM distillation is often use as a guide (Jones, 1999). There are six products from the distillation process as depicted in figure 6.1. BANN models of the 95%vol and 5% vol of the ASTM distillation for each of the product was created. The optimum value and hence the upper and lower bounds were obtained from the models. The exergy efficiency of the ADU is then optimised subject to the product quality specifications constraints as follows.

$$\max_{X} J = \varphi - \beta\sigma$$

s.t. 6.14

$$U(x) = \begin{bmatrix} \varphi \\ m \end{bmatrix}$$

$$m_{lb,k} \ll m_k \ll m_{ub,k} \qquad k = 1, 2, \ldots, 6$$

where m represents the product oil quality (95% vol ASTM distillation for each product), and U is the BANN model of the ADU comprising the flow rates of the products and the pump arounds.

The model error of the individual network and the aggregate network for the 5% vol and 95% vol of each of the products are shown in figures 6.5 to 6.16. The ANN model and BANN models for the training and validation data sets are presented in each figure. Figures 6.5 and 6.6 show the models for 5% vol ASTM distillation and 95% vol ASTM distillation for AGO. As is expected, BANN model errors are much more consistent than the ANN models. In figure 6.6 Model error for 95% vol ASTM distillation seems a bit higher than expected. Figures 6.7 and 6.8 show the model errors for 5% and 95% vol ASTM distillation for diesel product. In Figure 6.7, the model error is between 2×10^{-4} and 6×10^{-4} for ANN training data and between 1.8×10^{-4} and 2.2×10^{-4} for BANN training data respectively. The model error for the 95% vol is slightly higher than for the 5% vol. It ranges from 4.8×10^{-4} to 1×10^{-3} for both ANN and BANN models. Model errors for kerosene product are given in figures 6.9 and 6.10. ANN model error for training data set is from 4×10^{-5} to 2.2×10^{-4} while the BANN model error is from 2×10^{-5} to 1.8×10^{-4}. The BANN training error for 5% Naphtha is between 1.8×10^{-4} and 2.9×10^{-4} as compared to 95% Naphtha which is between 4.2×10^{-4} and 5×10^{-4} as shown in figure 6.11 and 6.12. The model error for most 95% ASTM distillation for most of the product is much higher than for the 5% ASTM distillation. Figures 6.13 and 6.14 give the ANN and BANN model error for off gas. The BANN model error for 5% has a maximum value of 5×10^{-6}while that of 95% is 5.6×10^{-5}. Off gas has the least

model error of all the products. Figures 6.15 and 6.16 are for the residue product. the model error for the 5% behaves similarly to the 95% for AGO. This is quite possible because of the overlap of the two cuts.

The SQP method is very effective for constrained optimization problem. The optimum exergy efficiency obtained here are subject to the constraints imposed by the products quality specifications. In table 6.5, the optimum results obtained with the constraints in effect are given. Without incorporating confidence bounds, the optimum exergy is 74 % in table 6.5. This is about 7.8% decreases in the efficiency as compared to when the quality constraints were not considered in the analysis in table 6.4.

Quite often, optimisation of distillation process is performed subject to one or two distillate qualities (Gadalla *et al*., 2013). The method presented here allows for inclusion of as many product qualities as desired. A number of methods exist in literature for online monitoring of crude distillation process qualities (Shahnovsky *et al*., 2012, Shang *et al*., 2014). The method as proposed here could predict the product qualities and as well predict the optimum operating exergy efficiency of the column. Stringent requirement of petroleum quality demands the need to monitor and control the quality at all times. One approach is to use offline laboratory analysis at periodical intervals. This could result in large time delays and requires additional resources. The other approach of online analyser could be expensive and difficult to predict accurately. These side effects necessitate the need for data driven models for monitoring the product quality. There is a possibility of developing this method further to monitor the product quality with the added advantage of predicting the efficiency of the system. It could have applications in process monitoring, advanced control and fault diagnosis.

Figure 6.17 shows the comparison of the HYSYS validated optimum values obtained for differing weightings with and without the product quality constraints. For all cases, the values obtained without the product quality constraints are higher when compared with quality limitation. Even though there is a reduction in the optimum value, optimisation of the column subject to product quality constraints is preferred as it gives a true indications of what obtains in reality. Distillation operations are not universal for every distillation column. There are many different configurations and different operating objectives that can result in different operational degree of freedom and distinct dynamic behaviours. The methods as described in this thesis can be used to understand and analyse these complexities.

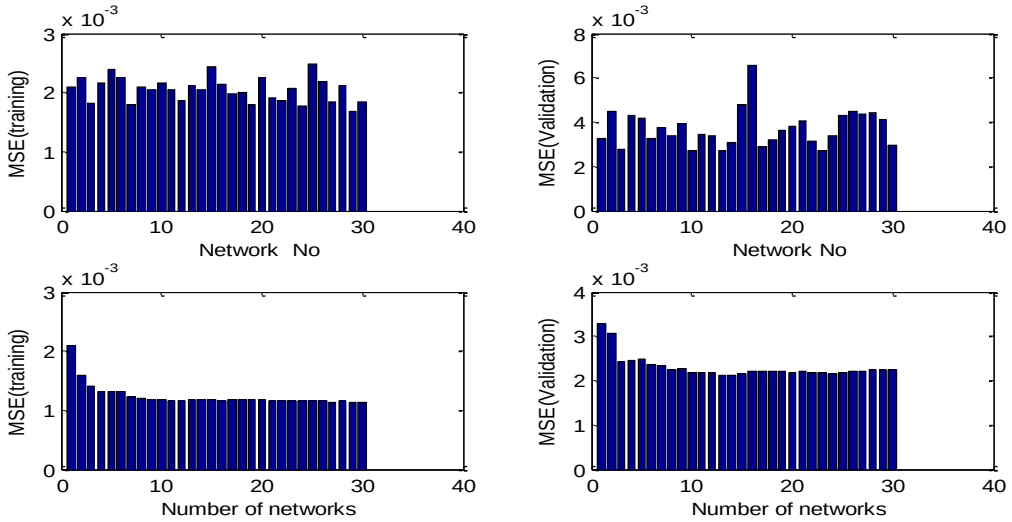

Figure 6.5: Model error for 5%AGO

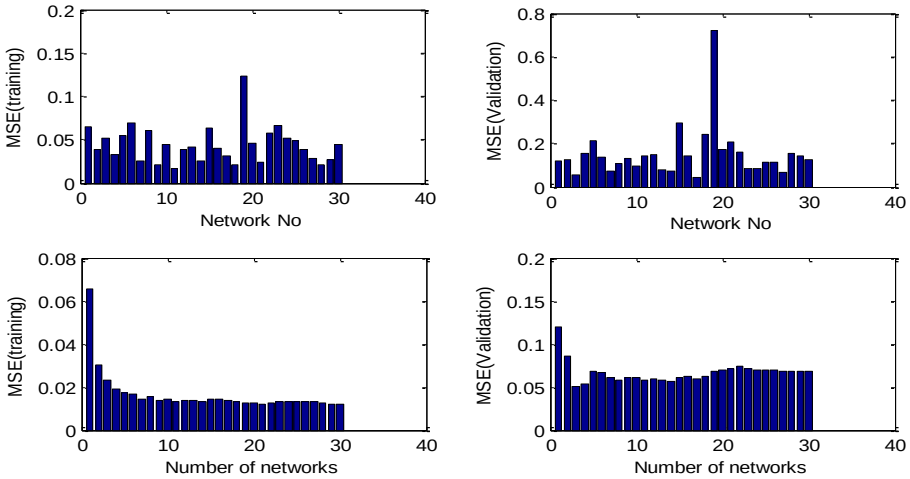

Figure 6.6: Model error for 95%AGO

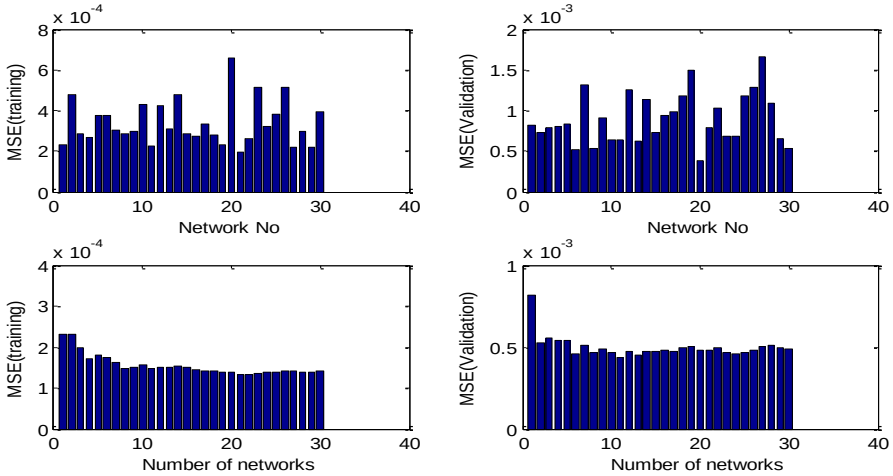

Figure 6.7: Model error for 5% Diesel

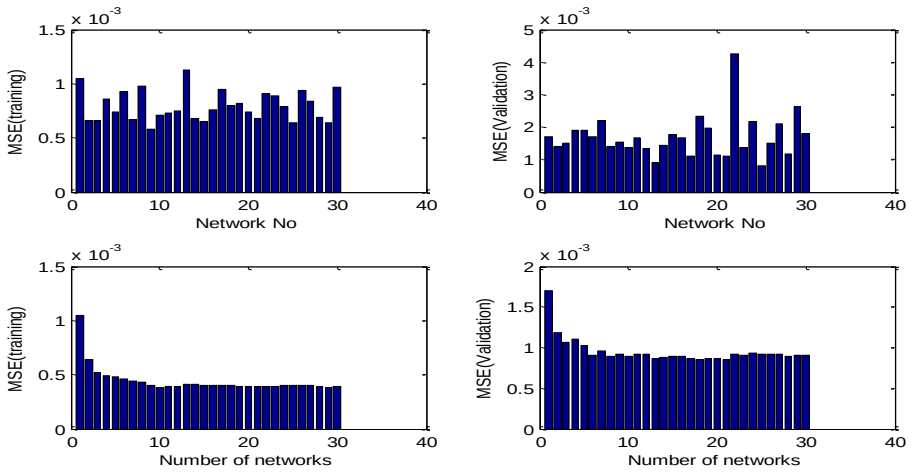

Figure 6.8: Model error for 95% Diesel

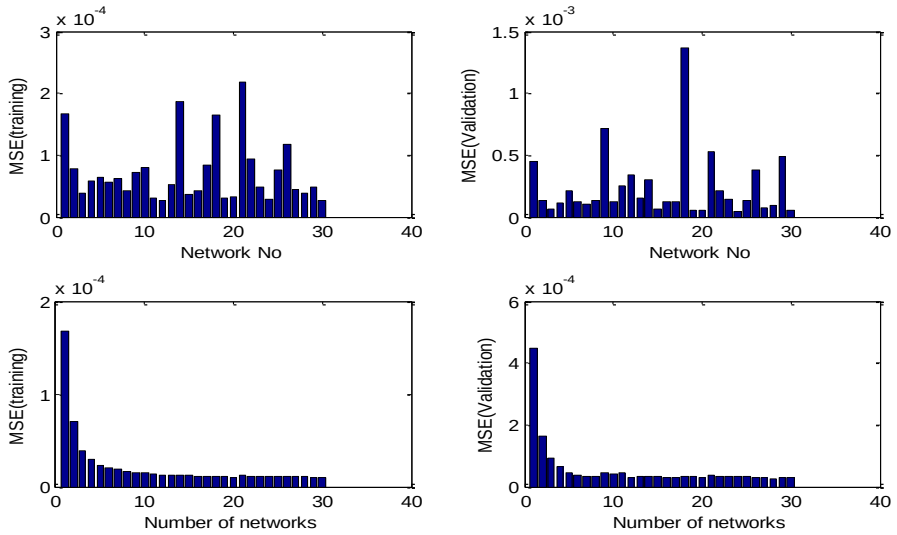

Figure 6.9: Model error for 5% Kero

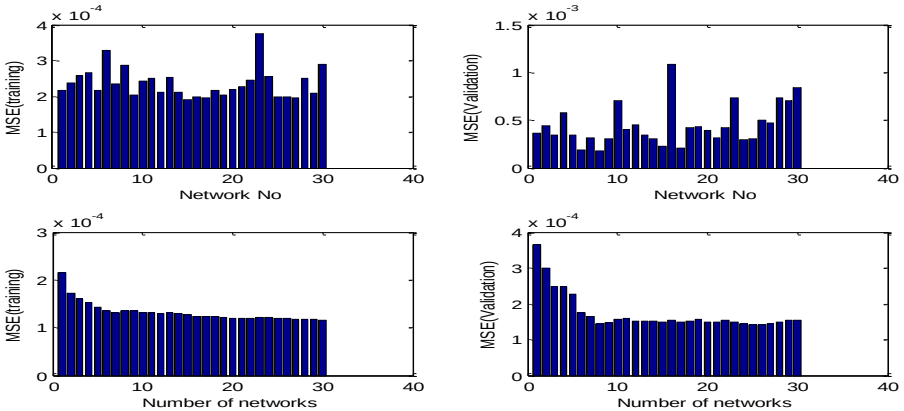

Figure 6.10: Model error for 95% Kero

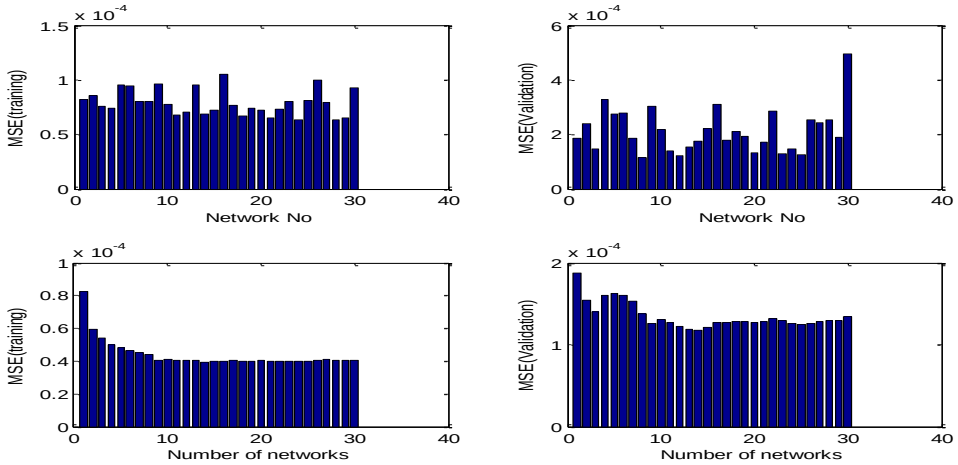

Figure 6.11: Model error for 5% Naphtha

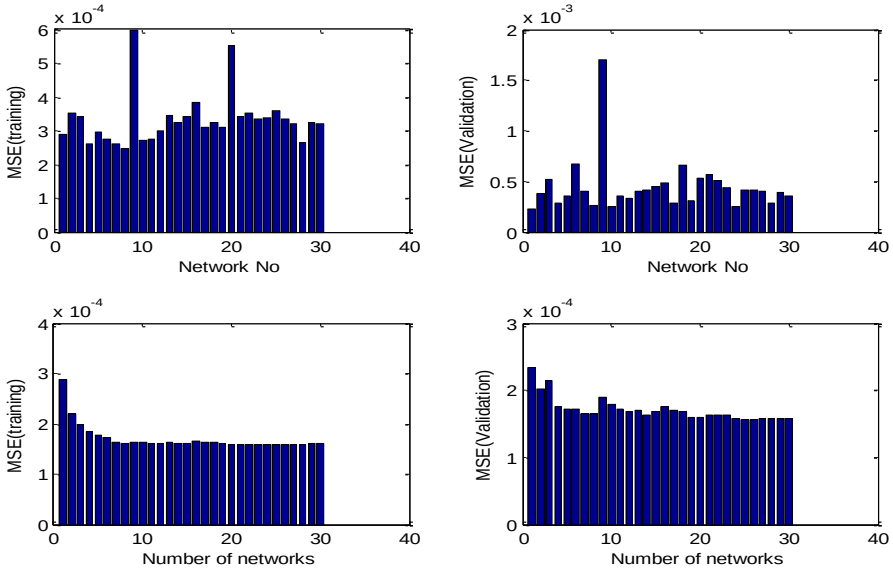

Figure 6.12: Model error for 95% Naphtha

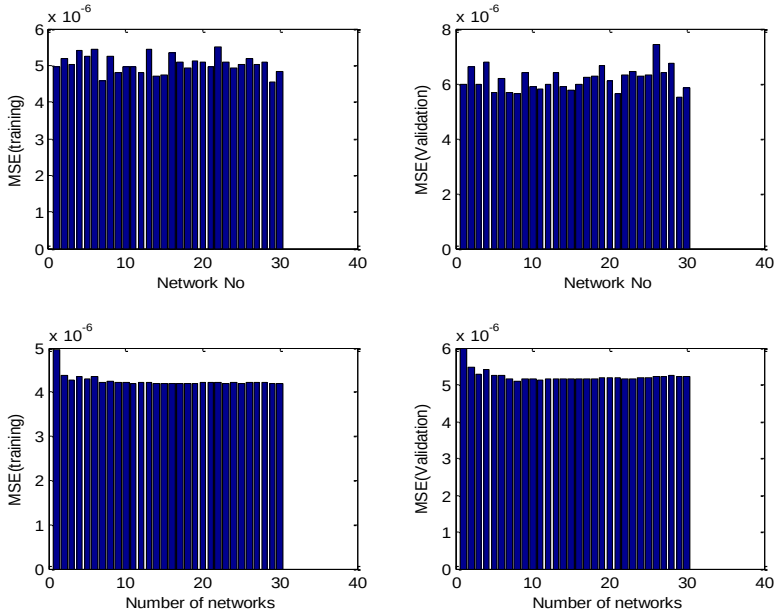

Figure 6.13: Model error for 5% Offgas

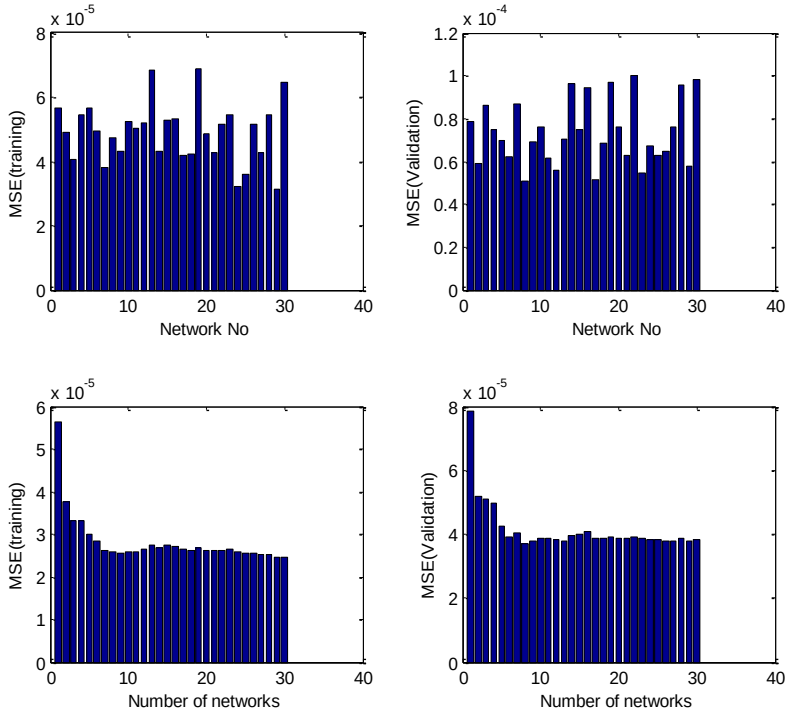

Figure 6.14: Model error for 95% Offgas

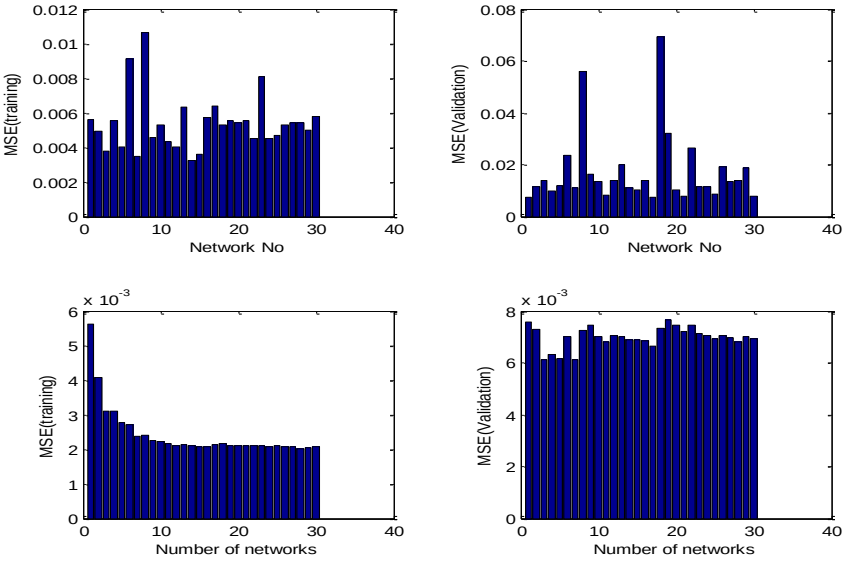

Figure 6.15: Model error for 5% Residue

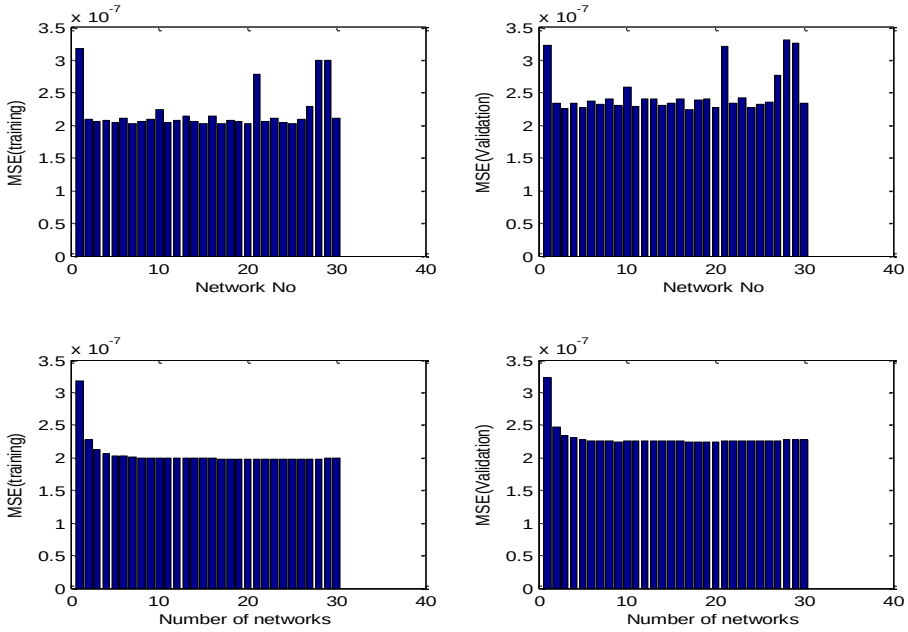

Figure 6.16: Model error for 95% Residue

Table 6.5: Summary of optimization results with confidence bounds and product quality.

	Base case	**0**	**1**	**0.05**	**0.001**	**unit**
Naphtha	517	490	490	490	490	barrel/hr
Kerosene	508	490	490	490	490	barrel/hr

	Base case	**0**	**1**	**0.05**	**0.001**	**unit**
Diesel	952	1000	1000	1000	1000	barrel/hr
AGO	267	275	261	275	275	barrel/hr
Residue	1296	1350	1350	1350	1350	barrel/hr
PA1	943	943	944.6	943.5	943.5	barrel/hr
PA2	1132	1130	1133	1130	1130	barrel/hr
PA3	943	940	941	940	940	barrel/hr
Optimum Efficiency		74	29.43	69.3	73.91	%
HYSYS validated	42.1	69.37	64.73	70.19	69.37	%
Relative Error		0.067	0.506	0.013	0.062	

6.3.3 Multi-objective optimisation

Optimisation of chemical process operations is often a multi-criteria optimization problem with conflicting objectives. Optimization objectives of most chemical engineering processes have complex inter-relationships and improvements in a particular objective in most cases lead to a decline in the other (Bortz *et al.*, 2014). This is especially true for crude distillation column where diverse objectives such as economic and product quality (Yu *et al*., 2008), energy efficiency and production rate (Zhu *et al*., 2014) and economic and environment (Alcántara-Avila *et al.*, 2012) and some other combinations have been considered.

In this section, an additional objective of minimising the standard error of individual network predictions was introduced and formulated using the goal attainment multi-objective optimization procedure. This is to improve the reliability of the optimum solution found. Equation (6.14) is then modified as

$$J = \begin{bmatrix} -\varphi \\ \sigma \end{bmatrix} \qquad 6.15$$

$$\min_{x,\delta} \delta$$

s.t. $J(\varphi) - W_i\delta \leq F$

$U(x) = \begin{bmatrix} \varphi \\ m \end{bmatrix}$

$$m_{lb,k} \ll m_k \ll m_{ub,k} \qquad k = 1, 2, \ldots, 12$$

where J is the objective function, φ is the exergy efficiency, U is the BANN model of the ADU, $x = [x_1, x_2, \ldots x_8]$ is a vector of decision variables containing 5 product flow rates and 3 pump around flow rates, m is a vector of the product oil quality, σ is a vector of standard prediction errors, F is a vector of the desired goals, and W is a vector of weighting parameters which controls the degree of goal achievement and introduces a measure of flexibility that allows for trade off the conflicts among objectives.

If the quality constraints are not considered, equation (6.15) becomes

$$J = \begin{bmatrix} -\varphi \\ \sigma \end{bmatrix} \qquad 6.16$$

$$\min_{x,\delta} \delta$$

s.t. $J(\varphi) - W_i\delta \leq F$

$\varphi = U(x)$

Table 6.6 shows the results of the multi-objective optimisation without including the quality constraints. The effect of incorporating the confidence bounds in the multi-objective optimization can be revealed in that the exergy efficiency of the HYSYS validated process is close to that predicted by the model.

Table 6.6: Multi objective optimisation results without product quality constraints

Hysys validated	**Optimum 1 (Eff)**	**Optimum 2 (cb)**	**Goal 1 (Eff)**	**Goal 2 (cb)**	**Weight 1 (Eff)**	**Weight 2 (cb)**	**Relative error**
73.86	79.62	0.3883	0.8	0.01	0.01	1	0.07798
71.90	78.12	0.1982	0.8	0.01	0.1	1	0.08650
71.68	75.34	0.0566	0.8	0.01	1	1	0.05106
61.62	65.56	0.0244	0.8	0.01	1	0.1	0.06394
50.84	53.18	0.0127	0.8	0.01	1	0.01	0.0458

Table 6.7 shows the base case and the optimum results of the decision variables with no consideration for the product qualities.

The multi-objective optimization method as described here allows for trade off between minimizing the prediction error and the exergy efficiency of the column. The decision influences the weighting factor of choice. If the decision is to minimize the prediction

error, weighting factor of [1, 0.01] might be appropriate for the system if however the optimum efficiency is preferred, the weighting factor might be [0.01, 1].

Table 6.7: Optimisation results (decision variables)

	HN	**Kero sene**	**Diesel**	**AGO**	**Residue**	**PA1**	**PA2**	**PA3**	**Unit**
Base case	517	508	952	267	1296	943	1132	943	**Barrel / hr**
Optimum	511	511	1000	267	1348	946	1127	940	**Barrel / hr**

Table 6.8: Optimisation results (efficiency and profit)

	Exergy (%)	**Irreversibility (kJ/hr)**	**Energy cost ($/yr)**	**Profit ($/yr)**
Base case	42.10	1.913×10^{8}	7.655×10^{6}	2.360×10^{9}
Optimum	71.68	6.085×10^{7}	4.095×10^{6}	2.398×10^{9}

Taking the case of using an equal weighting for the two objective functions, in table 6.8, the optimization resulted in 29.5 % increment of the exergy efficiency. This translates to 68 % decrease in irreversibility loss in the column and 46.5 % reduction in energy costs of the column with reference to their initial values. Every real process has an element of irreversibility and often the performance of engineering system is degraded by their presence. With the methodology presented from this study ways of considerably decreasing the irreversibility of the system as well as determining the efficiency of the process is made easy. This will be a good tool in the hand of process and design engineers for the operation of energy efficient column. It could equally find relevance in the control of the column for improve efficiency.

The total profit is increased by $\$38\times10^{6}$/year. The increment is majorly due to the optimum operating conditions from the exergy based analysis of the column. The reduction in the cost of energy contributed to about 10% in the total profit. The results show that considerable economic benefit of the column can be achieved at no additional cost of equipments.

In Table 6.9, multi-objective optimization with the quality constraints results is shown. With the added constraints of product quality to the optimization problem, the complexities of the system increases. This explains why the relative errors are considerably higher for some of the cases considered. Considering the case of the weighting factor [1,1], the relative error of the predicted and validated exergy efficiency of the system is 0.156 as compared to 0.05 when the product quality constraint was not included in the optimization problem.

Table 6.9: Multi-objective optimisation results with product quality constraints

Hysys validated	**Optimum 1 (Eff)**	**Optimum 2 (cb)**	**Goal 1 (Eff)**	**Goal 2 (cb)**	**Weight 1 (Eff)**	**Weight 2 (cb)**	**Relative error**
75.24	74.67	0.9557	0.8	0.01	0.01	1	0.007575
75.24	73.05	0.7947	0.8	0.1	0.1	1	0.029239
75.24	65.31	0.3938	0.8	0.1	0.5	1	0.1319
71.95	60.7	0.2930	0.8	0.1	1	1	0.15636
52.37	54.11	0.2294	0.8	0.1	1	0.5	0.03322
45.44	33.48	0.1465	0.8	0.1	1	0.1	0.2632

6.3.4 Summary

The BANN models were found to predict optimum operating conditions of the ADU. The proposed technique can significantly improve the second law efficiency of the system with an additional economic advantage. The method can aid in the operation and design of an energy efficient column. Product quality constraints introduce a measure of penalization on the optimization result to give as close as possible to what obtains in reality. Multi-objective optimization gives a degree of freedom in the design and optimization of the unit.

6.4 Application to crude distillation unit

Generally, the crude distillation unit (CDU) contains a pre-flash column, an atmospheric distillation unit (ADU) and a vacuum distillation unit (VDU). With the demand for a reduction in chemical process energy consumption due to high energy costs and regulations on strict greenhouse gas emission, CDU has always been the target for improved energy usage. Energy analysis and optimisation of CDU has been widely investigated, especially the atmospheric distillation unit (Arjmand *et al*., 2011) and the vacuum distillation unit. (Gu *et al*., 2014). Recently, the research focus has been on the

pre-flash unit and its effect on the energy efficiency of the CDU (Al-Mayyahi *et al.*, 2014). Past studies on the second law analysis of the crude distillation unit gave some considerable insight. It has been observed that the crude distillation unit has as low as 20% reduction in exergy efficiency compared to the atmospheric distillation unit and vacuum distillation unit (Al-Muslim and Dincer, 2005). This informs the need for the search light on improving the efficiency of the unit to be focused on the CDU as a whole.

6.4.1 Description of the system

Crude at its raw state is a relatively low value material but when refined could yield products whose value is many times that of the original crude. Refining of crude is in two stages of distillation: the atmospheric distillation unit and the vacuum distillation unit. The crude distillation unit under consideration is diagrammatically represented in figure 6.17 (García-Herreros and Gómez, 2013, Kaes, 2000). A pre-flash unit is later incorporated into the system. Preheated crude at 343^{o}C and 344kPa is introduced at its flash point to the ADU. Superheated steam is injected at the bottom to enhance vaporisation and separation of the crude. Light Naphtha, Heavy Naphtha, Kerosene, Diesel and AGO are drawn from the column. Three side stream products are taken from the side strippers. The ADU is equipped with three pump arounds that recover heat for the preheat trains. The bottom product (residue) is the residual liquid material which could not be vaporised under the existing operating conditions of temperature and pressure in the tower. It is further fed to another tower which operates at subatmospheric pressure; the vacuum tower. The side products of the VDU are Light vacuum gas oil (LVGO), Heavy vacuum gas oil (HVGO). The overhead product and the bottom product could serve as inlets to other processing units such as stabilisation and catalytic cracking unit respectively.

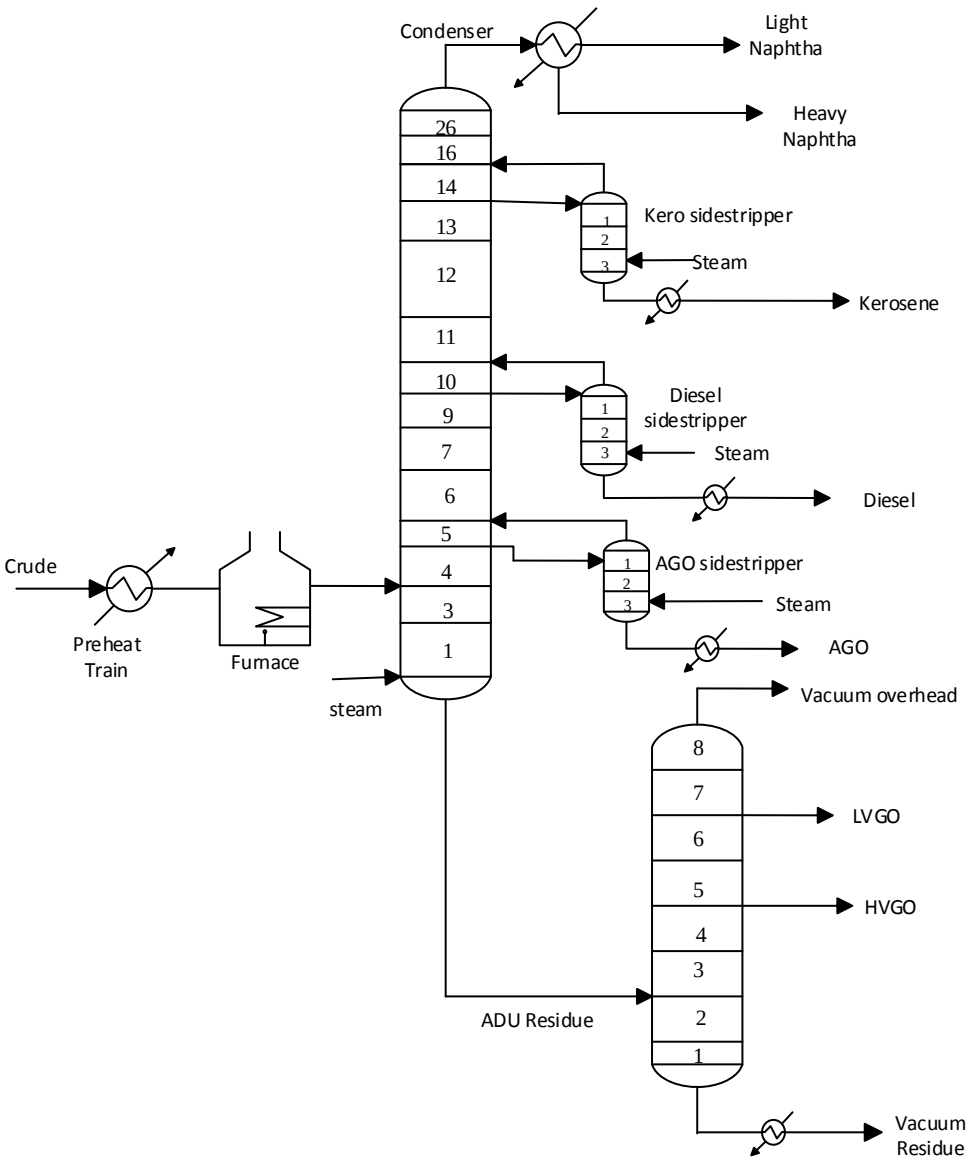

Figure 6.17: A diagrammatic representation of the crude distillation unit (with ADU and VDU)

6.4.2 HYSYS Simulation

Atmospheric distillation (ADU)

The crude distillation system described in figure 6.17 was simulated in HYSYS. The simulation of the ADU is as described in Section 6.2.2. The crude is described by the TBP distillation curve given in table 6.10 and the light ends properties in table 6.11. The light ends basis in the assay is 16.8%. The specifications of the products are added to the streams as given in table 6.12. The crude is fed to the main column at tray 3 and steam is fed at tray 1 with bottom up numbering. The main objective is to improve the overall efficiency of the crude distillation unit by seeking out the optimum operating conditions. The large number of variables involved in the operation of the crude

distillation unit allows a great variety of operating conditions which can lead to different amount and quality of products. Hence in the HYSYS simulation, the quality of the ADU product is maintained by ensuring the temperature difference between the 95% vol. and the 5% vol. of the ASTM D86 of two consecutive products is within the acceptable limit (Jones *et al*., 1999). The ASTM curve for the product of ADU is shown in figure 6. 18

Table 6.10: TBP distillation curve

Assay Percent	**Temperature(K)**
2.68	309
7.2	366.5
15	422
24.5	477.6
33.31	533.1
44.70	588.7
49.60	616.5
59.14	672
75.22	783
84.46	866.5
95.81	1023

Table 6.11: Light ends assay

Light ends	**Composition (mass%)**
Propane	0.7595
i-Butane	0.5622
n-Butane	0.1567
i-Pentane	1.173
n-Hexane	4.203
n-Heptane	1.308
n-Octane	5.475
n-Nonane	2.939
n-Pentane	0.2167

Table 6.12: ADU products specifications

Product	**Specifications(K)**
Light Naphtha	ASTM D86 95% =384
Heavy Naphtha	ASTM D86 95% =458
Kerosene	ASTM D86 95% =544
Diesel	ASTM D86 95% =608
AGO	ASTM D86 95% =730

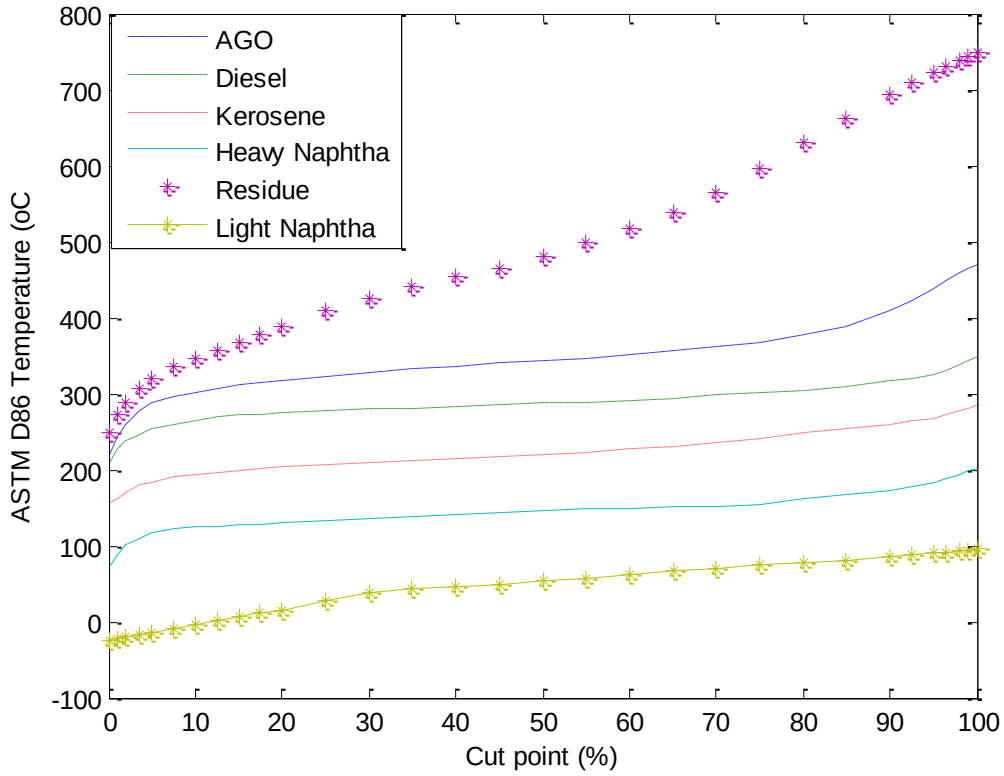

Figure 6.18: ASTM D86 of end products of the ADU

Vacuum distillation unit

After converging the simulation of the ADU, the residue is used as feed to the vacuum distillation unit. The VDU is simulated with 8 theoretical trays. The feed is introduced on the 2nd tray. There are three pump arounds between trays 7 and 8, 4 and 5, 1 and the bottom. The product specifications are LVGO D1160 95% (volume %) = 556K and HVGO D1160 95% (volume %) = 634K.

6.4.3 Exergy analysis of the CDU

Exergy analysis of the ADU, VDU and the overall system was performed as described in Section 6.2.3. The chemical exergy at reference conditions for the known components are as given in Table 6.13 (Szargut *et al*., 1988).

The exergy efficiency and irreversibility is calculated from the total exergy inlets and exergy outlets of the ADU as

$$\sum Ex_{out} = Ex_{L\ Naptha} + Ex_{H\ Naptha} + Ex_{kerosene} + Ex_{diesel} + Ex_{AGO} + Ex_{residue} \quad 6.17$$

$$\sum Ex_{in} = Ex_{crude} + Ex_{steam} + Ex_{furnace} + Ex_{kero\ steam} + Ex_{diesel\ steam} + Ex_{AGO\ steam} \quad \mathbf{6.18}$$

The total exergy inlets and outlets for the VDU is given as

$$\sum Ex_{out} = Ex_{vacuum\ overhead} + Ex_{LVGO} + Ex_{HGVO} + Ex_{vacuum\ residue} \quad 6.19$$

$$\sum Ex_{in} = Ex_{residue} + Ex_{vacuum\ steam} \quad 6.20$$

The overall exergy efficiency and irreversibility of the CDU is calculated from

$$\sum Ex_{in} = Ex_{crude} + Ex_{steam} + Ex_{furnace} + Ex_{kero\ steam} + Ex_{diesel\ steam} + Ex_{AGO\ steam} + Ex_{vacuum\ steam} \quad 6.21$$

$$\sum Ex_{out} = Ex_{L\ Naptha} + Ex_{H\ Naptha} + Ex_{kerosene} + Ex_{diesel} + Ex_{AGO} + Ex_{vacuum\ overhead} + Ex_{LVGO} + Ex_{HGVO} + Ex_{vacuum\ residue} \quad \mathbf{6.22}$$

Table 6.13: Reference chemical exergy of known components

Light ends	**Enthalpy (kJ/kmol)**	**Standard chemical exergy(kJ/kmol)**
Propane	2045.4	2154
*i-Butane	2658.4	2805.8
n-Butane	2658.4	2805.8
*i-Pentane	3274.3	3463.3
n-Hexane	3889.3	4118.5
n-Heptane	4464.7	4761.7
n-Octane	5074.4	5413.1
n-Nonane	5684.2	6064.9

Light ends	Enthalpy (kJ/kmol)	Standard chemical exergy(kJ/kmol)
n-Pentane	3274.3	3463.3

In table 6.14, the simulated exergy of the streams in and out of the CDU is shown. The calculated exergy efficiency and irreversibility of the ADU, VDU and CDU is also given. The overall efficiency and irreversibility are calculated from equations 6.6 and 6.7. The results show the overall efficiency to be 23.9% and the irreversibility to be 2.43×10^{8}kJ/hr. This clearly shows the need to improve the overall efficiency of the CDU.

Table 6.14 Exergy data of the CDU

Stream	h(kJ/ kmol)	h_0(kJ/ kmol)	s(kJ/kmolK)	s_0(kJ/ kmol/K)	m(kmol/hr)	Ex(kJ/hr)
Inlet streams						
Crude Steam	-230833	-286232	186.45	53.66	125.89	1992669
Kero Steam	-230833	-286232	186.45	53.66	88.12	1394869
Diesel Steam	-230833	-286232	186.45	53.66	62.95	996334.7
AGO steam	-230833	-286232	186.45	53.66	18.88	298900.4
VDU steam	-230832	-286232	186.45	53.66	41.96	664242.9
Preheat crude	-353010	-463267	583.04	309.37	2227.05	63925386
Furnace						2.5×10^{8}
TOTAL IN						3.2×10^{8}
Outlet streams						
H Naphtha L	-219225	-261920	218.22	103.10	504.00	4228307
Naphtha	-162826	-194813	187.17	96.83	594.99	3013674

Stream	h(kJ/ kmol)	h_o(kJ/ kmol)	s(kJ/kmolK)	s_o(kJ/ kmol/K)	m(kmol/hr)	Ex(kJ/hr)
Kerosene	-286630	-356746	338.36	158.68	423.00	7009952
AGO	-386922	-599476	871.94	396.66	184.00	13049405
Diesel	-346030	-476299	578.42	267.78	177.00	6673343
Vacuum ovhd	-347679	-477346	604.73	264.38	150.00	4236643
LVGO	-618226	-790376	1014.91	581.94	120.00	5175037
HVGO	-683722	-954754	1392.17	749.98	70.003	5576618
Vacuum Residue	-931454	-1402873	2296.19	1227.59	181.22	27723741
TOTAL OUT						76686720

6.4.4 Selection of decision variables

Several operating variables such as flow, temperature and pressure of the streams in ADU and VDU were varied within their upper and lower bounds. The variables that have independent influence on the objective function were then used as the decisions variables. These were used to generate the data for the training of the neural network. The variables are the flow rates of H Naphtha, AGO, Diesel, PA1, PA2, PA3, LVGO, HVGO and vacuum residue.

6.5 Pre-flash units

Two main approaches of the effect of pre-flash implementation that has been considered in the literatures are the impact on the heat exchanger network and on the column (Ji and Bagajewicz, 2002). In this section, the addition of pre-flash unit to the column is being considered on the assumption that it will give a further reduction on the energy consumption of the column. Crude oil is made up of light and heavy components which are continuously being vaporised. The installation of pre-flash unit ensures separation of the vaporised portion and avoids unnecessary heating. This should offer a considerable potential in reducing the energy consumption in the furnace. In this work, the focus is to study the influence of the pre-flash device (column or drum) on the overall exergy efficiency of the column. In doing this, the temperature profile of the column, the furnace duty and the product quality are kept identical to the reference (Benali *et al*.,

2012). This is to prevent as much deviation as possible of the modified cases from the reference. It is also to allow a fair base level for the comparison of the exergy efficiency of the modified cases and the reference. The ADU products flow rates are however adjusted (see table 6.17 and figure 6.19).

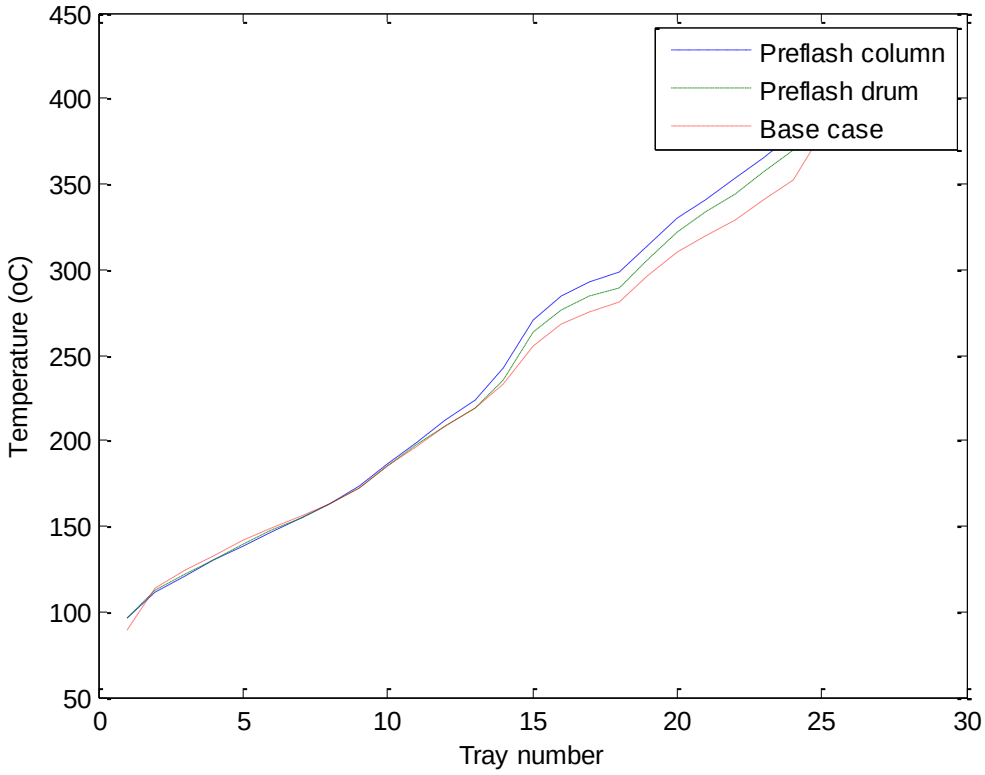

Figure 6.19: Temperature profile of the base case and modified cases

6.5.1 CDU with pre-flash column

The pre-flash column considered here is an 11 stage column with a pre-flash furnace that operates at 200^{o}F and 44.7 psia. The crude is heated to 450^{o}F and introduced to the column at the base. Stripping steam is also added at the base. A study on the optimised design of such a column has been carried out (Luyben; 2011). A diagrammatic representation of the pre-flash column is as shown in figure 6.20. The main design optimization variables in the pre-flash column are reflux drum pressure, reflux drum temperature, pre-flash furnace inlet temperature and the number of trays. The number of trays is not considered here because reducing the tray number further might not be practically possible. The reflux rate is fixed and hence the reflux temperature is not considered as a design variable. The furnace outlet temperature and the reflux drum pressure were considered.

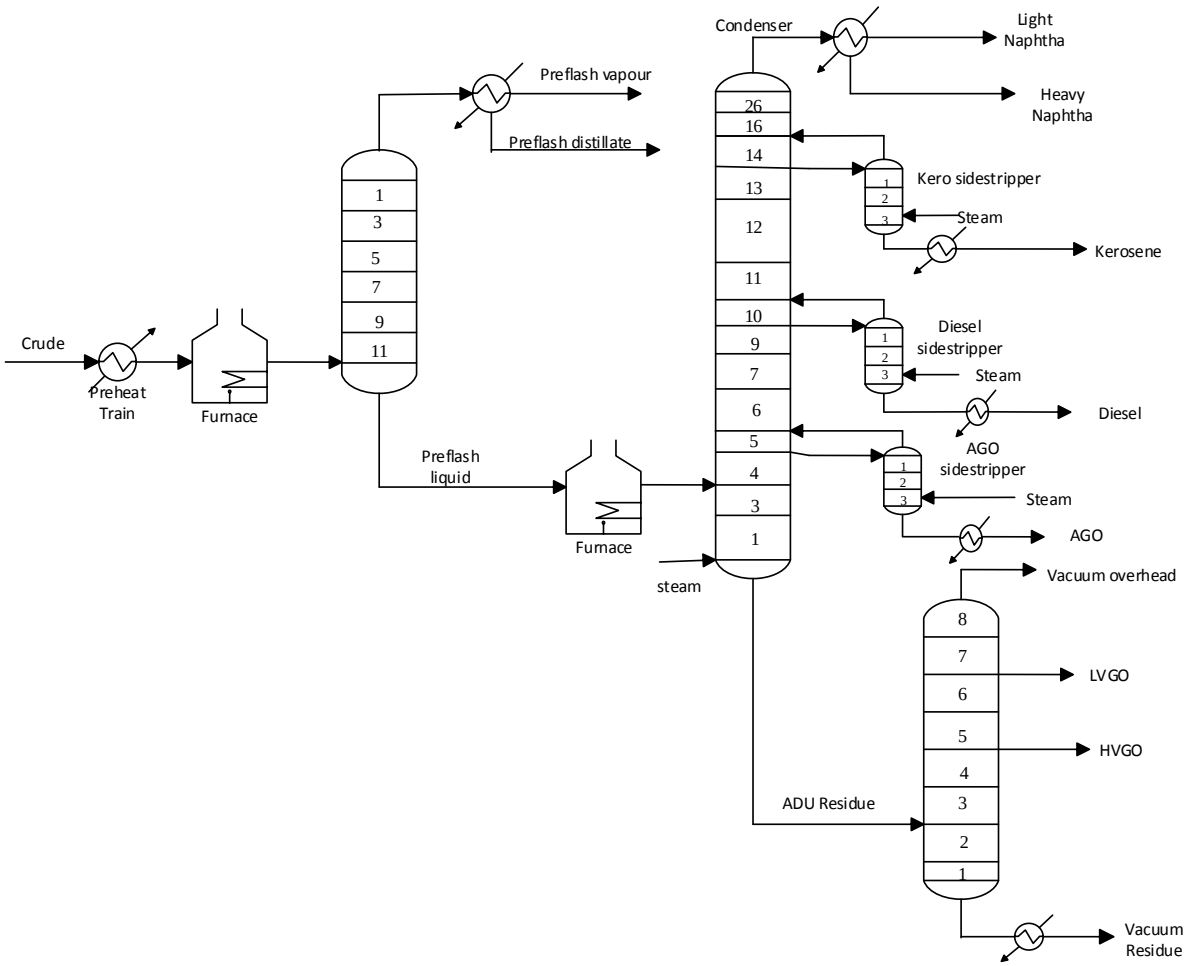

Figure 6.20: Diagrammatic representation of the CDU with pre-flash column

The total exergy streams in and out of the CDU with a pre-flash column is given as

$$\sum Ex_{in} = Ex_{crude} + Ex_{steam} + Ex_{furnace} + Ex_{kero\ steam} + Ex_{diesel\ steam} + Ex_{AGO\ steam} + Ex_{vacuum\ steam} + Ex_{preflash\ steam} \quad 6.23$$

$$\sum Ex_{out} = Ex_{L\ Naptha} + Ex_{H\ Naptha} + Ex_{kerosene} + Ex_{diesel} + Ex_{AGO} + Ex_{vacuum\ ovhd} + Ex_{LVGO} + Ex_{HGVO} + Ex_{vacuum\ residue} + Ex_{preflash\ vapour} + Ex_{preflash\ distillate} \quad 6.24$$

The exergy of the streams in and out of the CDU with pre-flash column is given in Table 6.15. The efficiency and irreversibility of the system is calculated from equations 6.6 and 6.7. The system has an overall efficiency of 16.6% and exergy loss of 3.9165×10^{8}kJ/hr.

Table 6.15: Thermodynamic properties of streams in and out of the ADU with pre-flash column

Stream	h(kJ/ kmol)	h_0(kJ/ kmol)	s(kJ/ kmolK)	s_0(kJ/ kmolK)	m(kmol/ hr)	Ex(kJ/hr)
Inlet streams						
Crude inlet	-365195	-604915	949.00	425.39	1412.01	1.18E+08
Crude Steam	-230833	-286232	186.45	53.66	125.89	1992669
Kero Steam	-230833	-286232	186.45	53.66	88.12	1394869
Diesel Steam	-230833	-286232	186.45	53.66	62.94	996334.7
AGO steam	-230833	-286232	186.45	53.66	18.88	298900.4
Preflash steam	-235870	-286232	177.82	53.66	277.54	3708808
VDU steam	-230832	-286232	186.45	53.66	41.96	664242.9
Furnace 1						1.55×10^8
Furnace 2						1.84×10^8
TOTAL IN						4.7×10^8
Outlet streams						
Naphtha	-222232	-265885	225.68	108.09	156.43	1347188
Off gas	-175083	-216382	191.64	74.96	66.47	434180.4
Kerosene	-287217	-360428	347.10	160.47	371.32	6533229
AGO	-372176	-603173	905.78	399.75	191.99	15397792
Diesel	-338154	-474843	588.04	265.83	187.14	7611091
Vacuum ovhd	-357481	-495941	640.51	282.35	150.00	4759110
LVGO	-628738	-815398	1070.24	606.78	120.00	5825977
HVGO	-687561	-976865	1451.37	774.19	70.01	6126277
Vacuum Residue	-922889	-1437124	2407.57	1262.51	166.67	28835946
Preflash vapour	-139657	-151707	178.22	147.97	100.95	306477
Preflash distillate	-216657	-227484	132.09	98.54	734.52	609178.5
TOTAL OUT						77857486

6.5.2 CDU with pre-flash drum

The pre-flash drum is located just before the furnace (see figure 6.21) and the temperature is at the temperature of the heat exchanger network. The feed to the pre-

flash drum is at the tray where the end points of the flashed vapour and internal liquid are equal. The total exergy of the inlet streams to the pre-flash drum is given in equation 6.25. The inlet streams for this system is similar to that of the CDU without pre-flash. However the outlet streams differs and that may account for the increase in efficiency of the CDU with pre-flash drum when compared. The presence of pre-flash drum allows the vaporisation of the volatile components from the drum and thus reduces the quantity of crude to be heated up for the ADU separation. This will be a viable option for crude stream with a sizable quantity of low boiling components.

$$\sum Ex_{in} = Ex_{crude} + Ex_{steam} + Ex_{furnace} + Ex_{kero\ steam} + Ex_{diesel\ steam} + Ex_{AGO\ steam} + Ex_{vacuum\ steam} \quad \textbf{6.25}$$

The total outlet streams is given as

$$\sum Ex_{out} = Ex_{L\ Naptha} + Ex_{H\ Naptha} + Ex_{kerosene} + Ex_{diesel} + Ex_{AGO} + Ex_{LVGO} + Ex_{vacuum\ overhead} + Ex_{vacuum\ residue} + Ex_{preflash\ vapour} \quad 6.26$$

The exergy efficiency and irreversibility of the system is calculated from equations 6.6 and 6.7. The thermodynamic properties of the inlet and outlet streams are given in table 6.16. The efficiency and irreversibility of the systems are 26.7% and 2.369×10^8

Table 6.16: Thermodynamic properties of streams in and out of the ADU with pre-flash drum

Stream	h(kJ/kmol)	h_0(kJ/kmol)	s(kJ/kmolK)	s_0(kJ/kmolK)	m(kmol/hr)	Ex(kJ/kmol)
Inlet streams						
Preheat crude	-353010	-463267	583.04	309.37	2227.05	63925386
Crude Steam	-230833	-286232	186.45	53.66	125.89	1992669
Kero Steam	-230833	-286232	186.45	53.66	88.12	1394869
Diesel Steam	-230833	-286232	186.45	53.66	62.94	996334.7
AGO steam	-230833	-286232	186.45	53.66	18.88	298900.4
VDU steam	-230832	-286232	186.45	53.66	41.96	664242.9
Furnace						2.54×10^8
TOTAL IN						3.23×10^8
Outlet Streams						
Naphtha	-221324	-264544	222.48	105.96	255.74	2173286

Off gas	-173617	-214030	191.03	76.63	138.64	876680.2
Kerosene	-286090	-355784	337.24	158.22	370.82	6062014
AGO	-376487	-598858	886.67	395.47	170.17	12931957
Diesel	-341339	-474296	581.07	265.67	178.21	6944848
Vacuum ovhd	-350618	-481068	609.25	267.52	150.00	4292175
LVGO	-610355	-778286	991.87	569.63	119.99	5052397
HVGO	-673674	-938164	1357.06	730.64	69.99	5446686
Vacuum Residue	-916394	-1389778	2282.20	1214.13	188.95	29306389
Preflash vapour	-146318	-220483	290.60	108.12	675.98	13374267
TOTAL OUT						8.65×10^{7}

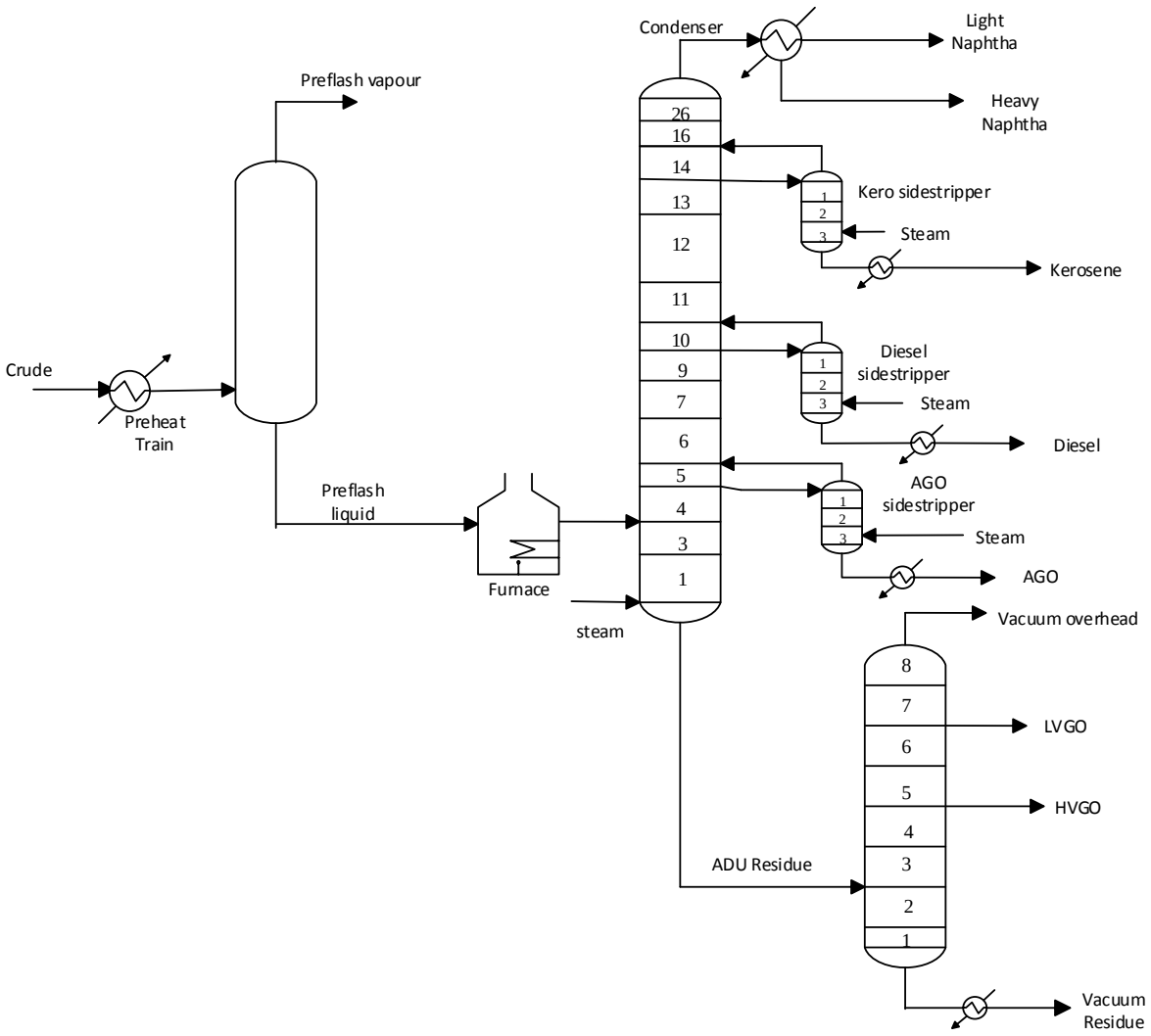

Figure 6.21: Diagrammatic representation of the CDU with preflash drum

In Table 6.17, the exergy efficiency of the ADU, VDU and overall unit before and after the addition of the pre-flash unit is shown. It can be seen that pre-flash drum improves the exergy efficiency of the ADU. This is in line with what is obtained in the literature (Errico *et al*., 2009) and significantly improves the overall efficiency of the CDU. Pre-flash column also improves the efficiency of the ADU but has a significant reduction on the overall exergy.

Table 6.17: Exergy analysis and flow rates of ADU for the base case and improved cases

	Base case	**With preflash drum**	**With preflash column**	**Unit**
Light Naphtha	595	139	156	kgmol/hr

	Base case	With preflash drum	With preflash column	Unit
Heavy Naphtha	504	256	66.5	kgmol/hr
Kerosene	423	371	371	kgmol/hr
AGO	184	170	192	kgmol/hr
Diesel	177	178	187	kgmol/hr
Residue	479	487	465	kgmol/hr
ADU Efficiency	46.98	47.62	47.38	%
VDU Efficiency	62.42	57.42	57.59	%
Overall Efficiency	23.99	26.73	16.58	%
Furnace duty	2.5×10^8	2.54×10^8	3.39×10^8	kJ/hr

6.6 Modelling of the crude distillation unit

The BANN model developed here is an aggregation of 30 individual neural networks. Each network has a single hidden layer with 30 hidden neurons and is used to model exergy efficiency. The data for model building were divided into training data (50%), testing data (30%), and unseen validation data (20%). Levenberg-Marquardt training algorithm was used to train the networks. The number of hidden neurons was determined by building a number of neural networks with different numbers of hidden neurons and testing them on the testing data. The network giving the lowest sum of squared errors (SSE) on the testing data is considered as having the appropriate number of hidden neurons.

Figure 6.22 shows the BANN model performance in predicting the overall exergy efficiency of the crude distillation unit on the training, testing, and unseen validation data. It can be seen that the model accurately depicts the crude distillation unit with the error of prediction as shown in figure 6.23 between -0.01 and 0.01. In Figure 6.24, the predicted and actual value of the exergy efficiency for the training, testing and validation data is shown. It can be seen that the prediction and actual values are well correlated. This shows the accuracy of the model. BANN model allows assigning measure of reliability to sample estimates in terms of confidence intervals and prediction errors. Confidence intervals are used to bound the mean and standard deviation of the sample. It indicates 95% confidence that the mean for the entire population falls within the given range.

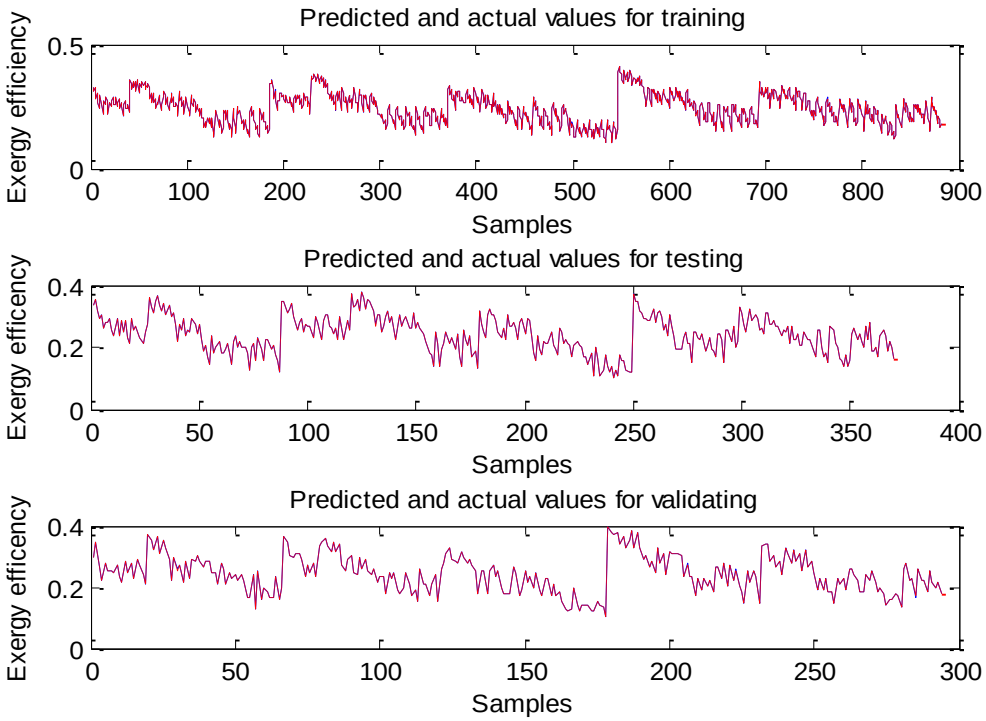

Figure 6.22: BANN model of the CDU

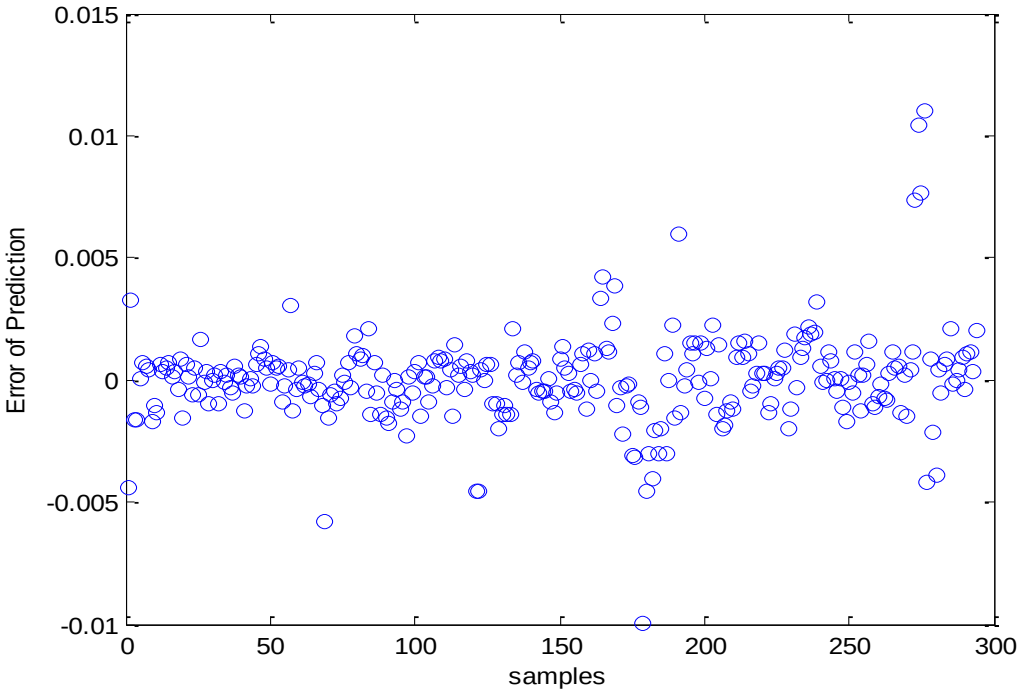

Figure 6.23: Error of prediction of the CDU model

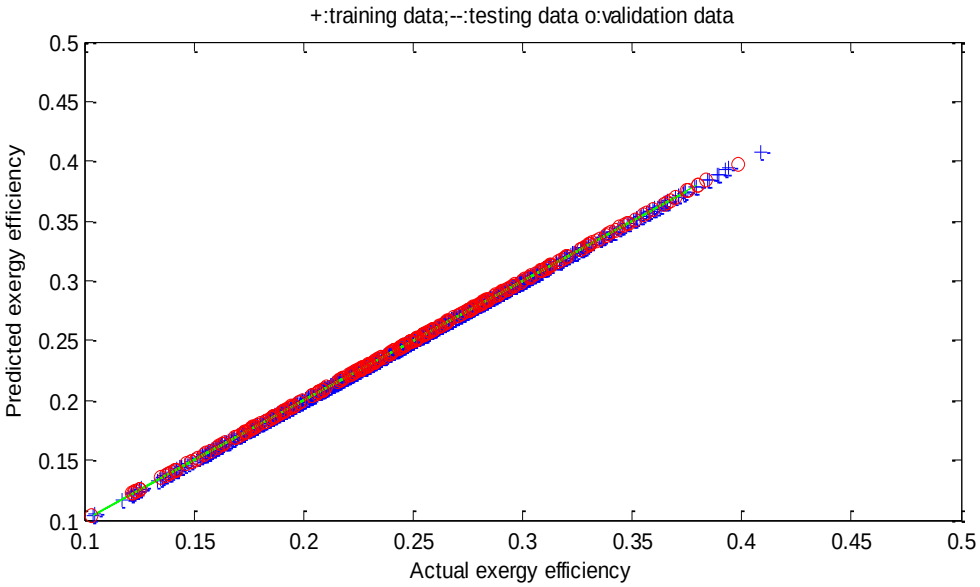

Figure 6.24: Predicted and actual efficiency of the CDU model

Bootstrap resampling ensures that different individual networks are obtained by using different training data for the network. This enhances the model accuracy because that combination of several imperfect models can improve model reliability and accuracy. If only a single network is used, the model accuracy will be significantly impaired. Figure 6.25 shows the mean square error of the individual networks on training, testing and validation data sets and figure 6.26 shows those for the aggregated neural network. The performances of the individual networks are inconsistent in that a network that gives small errors on the training data set may not give small error on the validation set and vice versa. The MSE for the aggregated network on the training, testing and validation data are given in table 6.18. In comparison with the minimum values for single network, the aggregated network shows a significant improvement on the model accuracy.

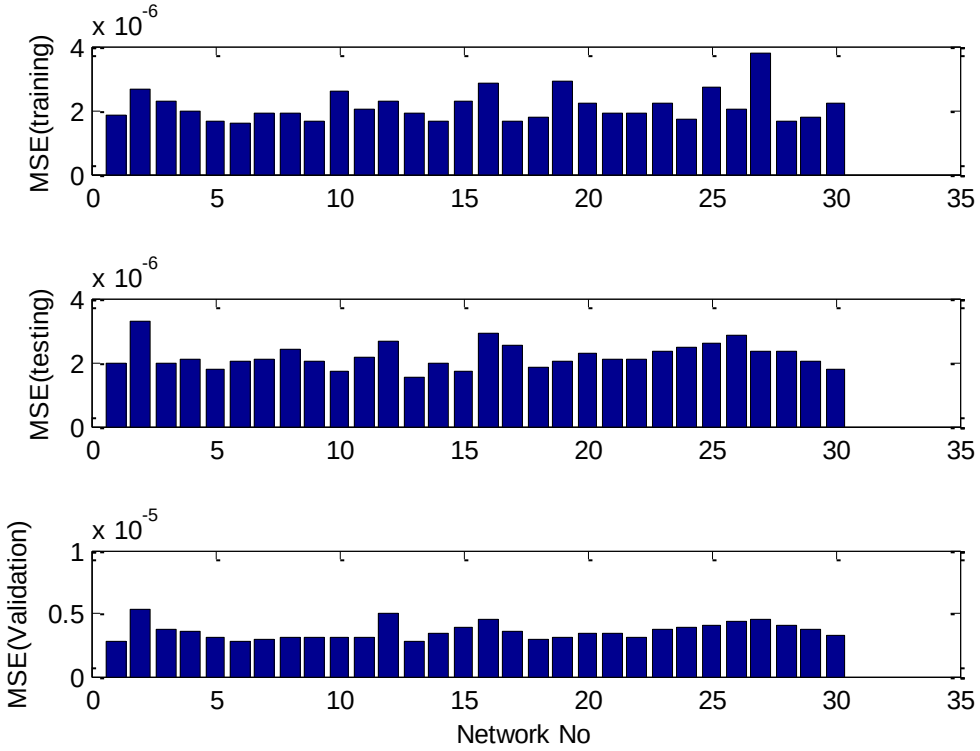

Figure 6.25: Model error of the single neural networks

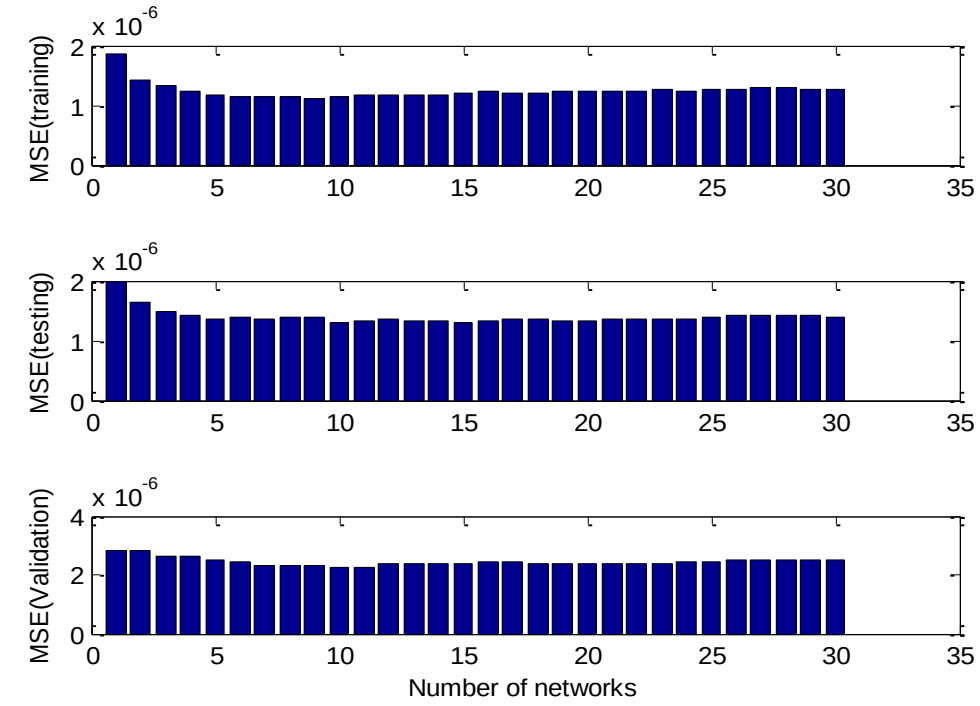

Figure 6.26: Model error of the aggregated neural networks of the CDU

Table 6.18: Model error of single and aggregated neural network

	MSE Testing	MSE Training	MSE Validation
Aggregated network	1.110×10^{-6}	1.301×10^{-6}	$2.264\times\times10^{-6}$
Individual network	1.652×10^{-6}	1.528×10^{-6}	2.78×10^{-6}

6.6.1 BANN model of CDU with pre-flash column

Figure 6.27 shows the performance of BANN model of the CDU with the addition of the pre-flash column. Figures 6.28 and 6.29 show the model error of the single networks and the aggregated network.

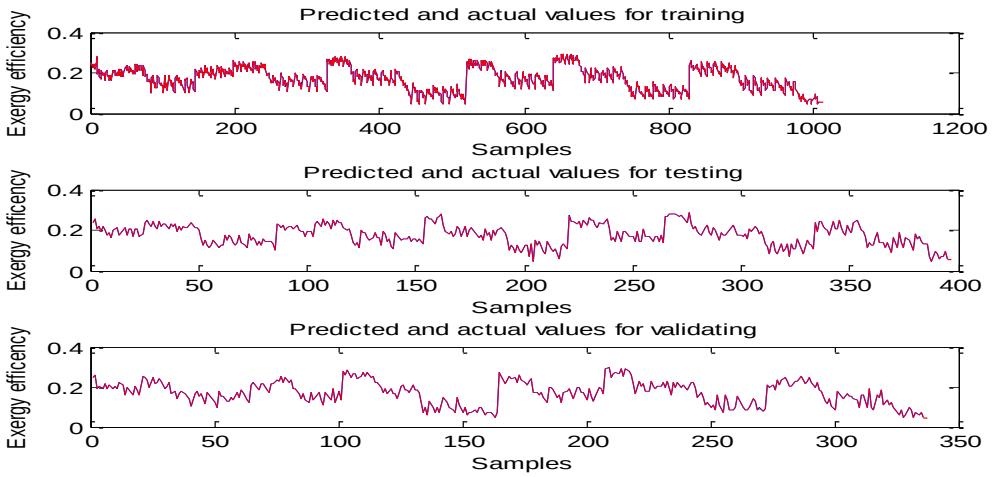

Figure 6.27: BANN model of CDU with pre-flash column

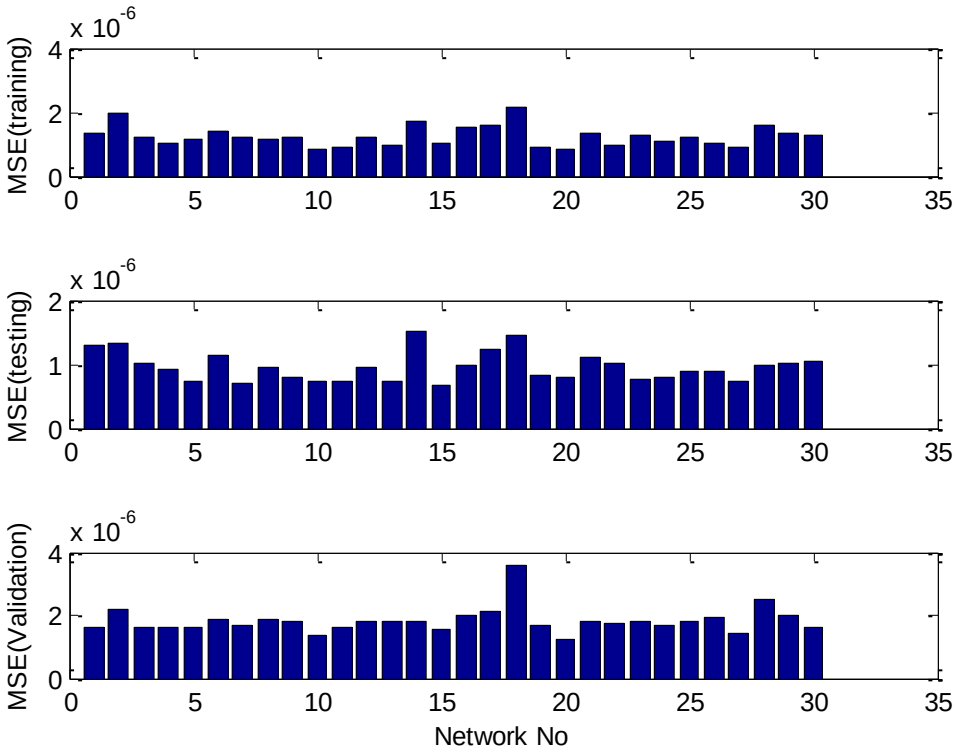

Figure 6.28: Model error of the single network for CDU with pre-flash column

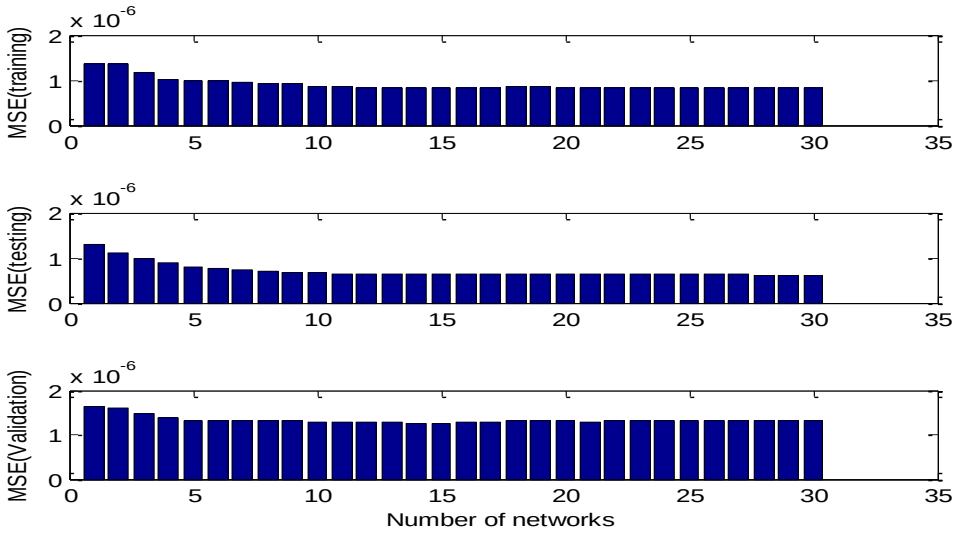

Figure 6.29: Model error of the aggregated network for CDU with pre-flash column

6.6.2 BANN model of CDU with pre-flash drum

The overall exergy efficiency of the CDU with pre-flash drum was also modelled using BANN. Figure 6.30 shows the BANN model with the training, testing and validation data sets for the CDU with pre-flash drum. The model can be seen to actually represent the system. In figure 6.31, the mean square error (MSE) of the aggregated neural network for the CDU with pre-flash drum is shown. As compared to the single network in figure 6.32, the combinations of 30 models culminate in the production of a single perfect and more robust model.

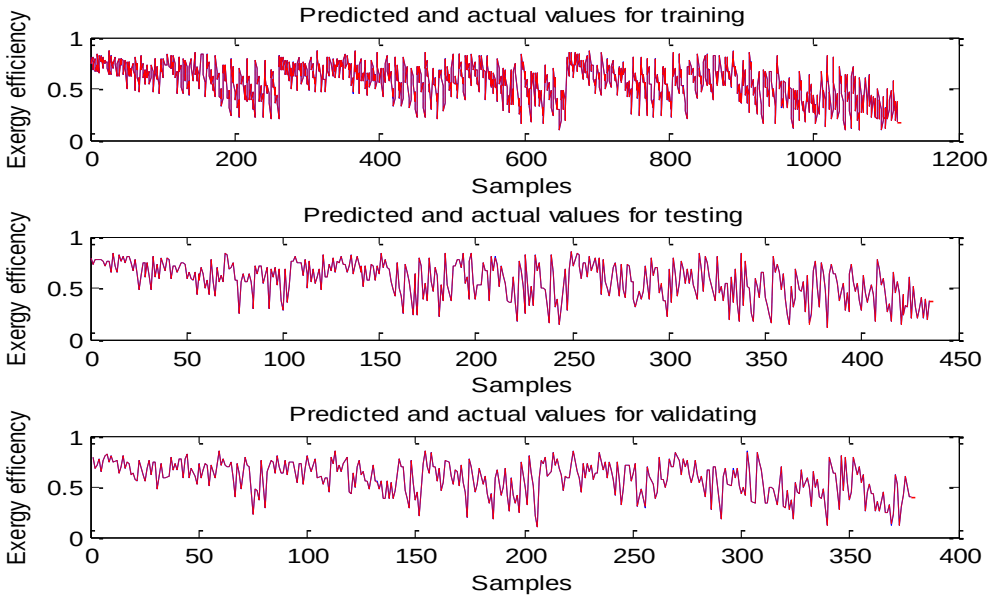

Figure 6.30: BANN model of CDU with pre-flash drum

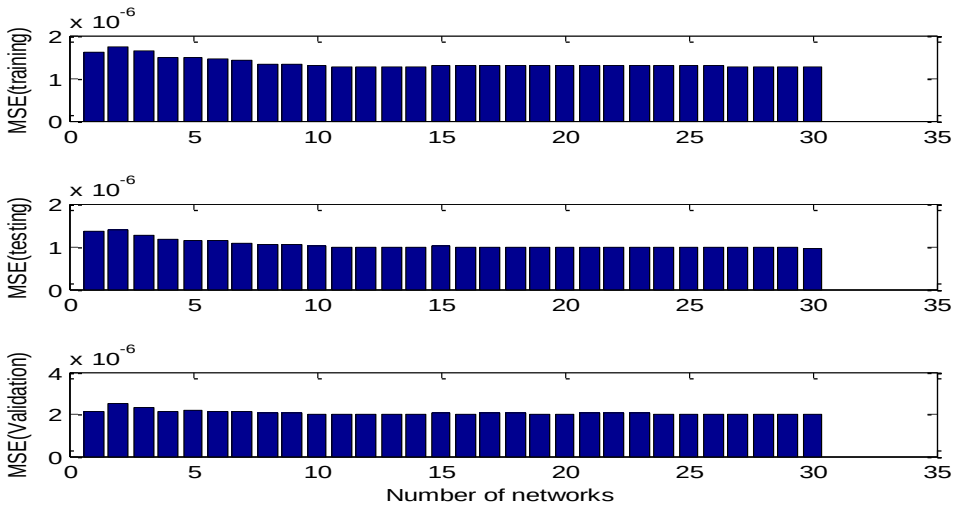

Figure 6.31: Model error of the single network for CDU with pre-flash drum

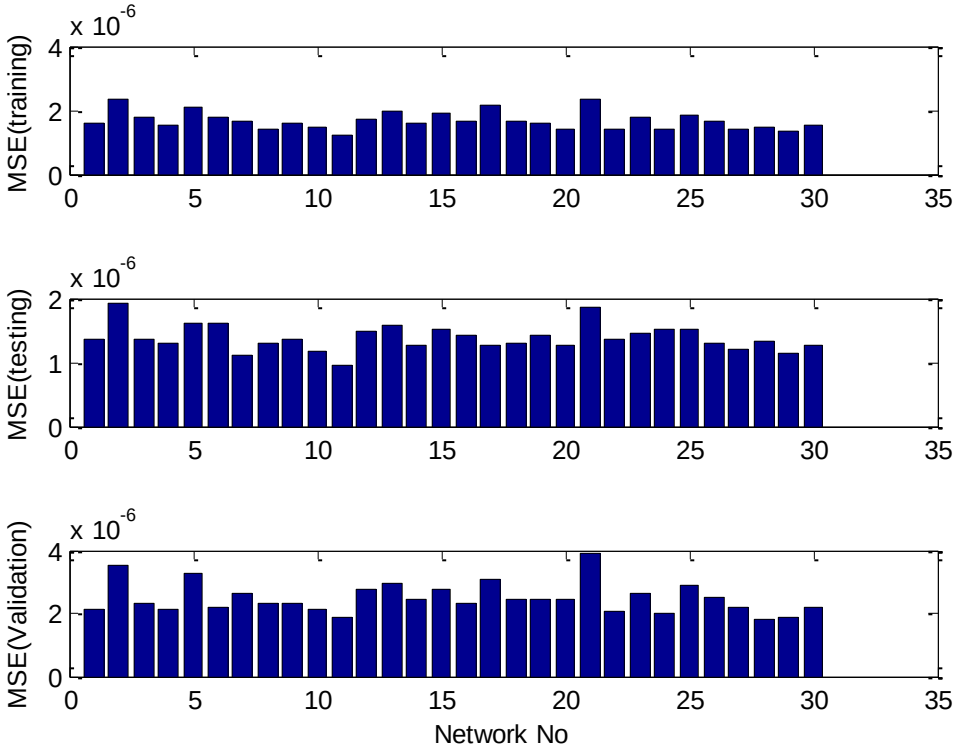

Figure 6.32: Model error of the aggregated network for CDU with pre-flash drum

6.7 Exergetic Optimisation of the CDU

The optimization problem can be stated as

$$\min_{X} J = -(\varphi - \beta\sigma)$$

s.t. 6.27

$$\varphi = \mathrm{f}(x_1, x_2, x_3, x_4, x_5, x_6, x_7, x_8, x_9)$$

$$lb \leq \mathrm{x}_{prod} \leq ub$$

where J is the objective function, $x = [x_1, x_2, x_3, x_4, x_5, x_6, x_7, x_8, x_9]$ is a vector of decision variables, i.e. neural network model inputs, φ is the exergy efficiency, σ is standard prediction error, and β is the weighting factor for σ.

In addition to the process operation objective, minimising the model prediction confidence bounds is incorporated as an addition optimisation objective. The optimisation problem was solved using the SQP method implemented by the function "fmincon" in MATLAB Optimisation Toolbox.

The objective is to maximise the overall exergy efficiency of the CDU. The results of the optimisation for the base case and the pre-flash units' cases are shown in Table 6.19. The values of the decision variables for the base case and the optimum cases are also shown. The optimisation results clearly show improvement in the overall exergy efficiency of all the cases considered. This shows that the method being proposed here can effectively give an improvement in the exergy efficiency of the CDU with or without the addition of the pre-flash unit.

Table 6.19: Optimisation results of the base case and modified cases

Decision variables	**Base case optimum**	**pre-flash drum optimum**	**pre-flash column optimum**	**Base case lower bound**	**Base case upper bound**	**unit**
AGO	150	150	150	150	203	kmol/hr
Diesel	150	150	150	140	212	kmol/hr
H Naphtha	478	220	150	470	529	kmol/hr
PA1	1587.6	1587.6	1587.6	1348	1826	kmol/hr
PA2	997	997	997	848	1147	kmol/hr
PA3	450	450	450	383	518	kmol/hr
LGVO	102	102	102	100	138	kmol/hr
HVGO	60	60	60	60	80	kmol/hr
Vacuum overhead	142	142	142	135	158	kmol/hr
Overall Eff	57.22	60.30	46.89			%
HYSYS validated	65.18	67.33	43.57			%
Relative error	0.122	0.104	0.076			

The results are further validated with HYSYS simulation. The relative error of the validated efficiency was calculated as the absolute difference between the neural network and HYSYS model predictions divided by the HYSYS model prediction. The large relative errors clearly signify the need to minimise the standard prediction error (model prediction confidence bound) in the optimisation.

The model prediction confidence bound is then incorporated in the optimisation procedure. The result for the base case is presented in table 6.20. The effect of penalization of the wide model prediction confidence bounds can be seen. For all the considered cases, the model prediction confidence bounds become narrower and the predicted value of the model move towards the HYSYS validated value. The weighting factor of 0.01might be the most appropriate here as it gives the lowest relative error. The result presented here shows another good advantage of using BANN for the modelling and subsequent optimisation of the CDU. This also indicates that the proposed method is reliable in the sense that the performance on the actual model is close to that predicted by the neural network model.

Table 6.20: Optimisation results with confidence bounds

β	**0.01**	**0.05**	**0.5**	**1**	**unit**
AGO	150	150	161.8	162.2	kmol/hr
Diesel	150	150	150.6	150	kmol/hr
Naphtha	478	478	478	478	kmol/hr
PA1	1587.6	1587.9	1587.9	1585.5	kmol/hr
PA2	997	997.7	997.7	998.5	kmol/hr
PA3	450	450	450	449	kmol/hr
LGVO	120	120	120	120	kmol/hr
HVGO	60	60	60	80	kmol/hr
Vacuum overhead	142	142	142	142	kmol/hr
Overall Eff (%)	57.09	56.57	50.71	46.42	%
HYSYS validated (%)	60.83	60.83	57.21	53.49	%
Relative error	0.061	0.07	0.1136	0.1321	

6.7.1 Multi-objective optimisation

As discussed in Section 6.3.3, an additional objective of minimising the standard error of individual network predictions was introduced and formulated using the goal attainment multi-objective optimization procedure. The objective functions are optimised simultaneously.

Equation 6.27 becomes

$$J = \begin{bmatrix} -\varphi \\ \sigma \end{bmatrix}$$

$$\min_{x,\delta} \delta \qquad 6.28$$

s.t. $J(\varphi) - W_i\delta \leq F$

$\varphi = U(x)$

where J is the objective function, φ is the exergy efficiency, U is the BANN model of the ADU, $x = [x_1, x_2, \ldots x_9]$ is a vector of decision variables for the ADU and VDU. These are flow rates AGO, diesel, Heavy Naphtha, PA1, PA2, PA3, LGVO, HGVO and vacuum overhead. σ is standard prediction error, F is the desired goal, and W is a vector of weighting parameters.

The focus is to improve the optimum results from the optimisation and introduce another degree of freedom that may enhance operating and design choices. Often in practical process performance are measured with respect to multi-objectives (Bamufleh *et al.*, 2013). It might then be possible to quantify the tradeoffs in satisfying the objectives or find a single solution that satisfies the objectives.

The results of the optimisation for the case of the CDU without pre-flash units are given in tables 6.21 and 6.22. Then objectives functions can be said to be conflicting. This is because improving the exergy efficiency degrades the other objective values and vice versa. Minimising the standard error of prediction is at the cost of trading off the exergy efficiency of the system. The efficiency is at the lowest when the standard error is 0.01. The exergy loss at this value is the highest too as given in table 6.22. Depending on the design and operation objectives, the technique as described here can aid in making choices amongst several alternatives. The confidence in the design of processes is that the process as designed can be replicated in practical. Minimising the confidence bounds error while keeping an eye on the goal of efficiency as presented here could be of great value. In addition, the exergy efficiency of the CDU is the focus here. While optimising it, invariably the ADU and VDU efficiencies are optimised as well. The HYSYS validated results of the ADU efficiency are presented in table 6.22. Optimising the CDU as a whole is a much effective way of optimising the crude distillation system.

Table 6.21: Multi-objective optimisation results without pre-flash units

Hysys validated	**Optimum 1 (Eff)**	**Optimum 2 (cb)**	**Goal 1 (Eff)**	**Goal 2 (cb)**	**Weight 1 (Eff)**	**Weight 2 (cb)**	**Relative error**
48.99	48.24	0.0218	0.6	0.01	1	0.1	0.015
44.88	44.69	0.0115	0.6	0.01	1	0.01	0.005
57.19	54.36	0.0664	0.6	0.01	1	1	0.049
64.21	58.71	0.1391	0.6	0.01	0.1	1	0.085
66.18	59.81	0.1850	0.6	0.01	0.01	1	0.096

Table 6.22: Multi-objective optimisation results of decision variables without pre-flash units

β	**1,0.1**	**1,0.01**	**1,1**	**0.1,1**	**0.1,1**	**unit**
AGO	176.4	175	150	150	150	kmol/hr
Diesel	150	150	150	150	150	kmol/hr
H Naphtha	478	478	478	478	478	kmol/hr
PA1	1431.2	1698.7	1507	1609.8	1460.5	kmol/hr
PA2	1066.1	1037.1	1147	1147	1065.6	kmol/hr
PA3	383	383	383	383	383	kmol/hr
LGVO	110.9	138	119.8	102	102	kmol/hr
HVGO	80	80	80	60	60	kmol/hr
Vacuum overhead	150.7	142	142	142	142	kmol/hr
Overall Eff	48.24	44.69	54.36	58.71	59.81	%
HYSYS validated	48.99	44.88	57.19	64.21	66.18	%
ADU efficiency	71.11	69.71	75.91	74.99	77.64	%
Exergy loss	1.561×10^{8}	1.726×10^{8}	1.335×10^{8}	1.125×10^{8}	1.034×10^{8}	kJ/hr

6.8 Conclusions

This study shows that BANN models result in greater model accuracy and more robust models. They have an additional advantage of providing model prediction confidence bounds indicating the reliability of model predictions. Incorporating model prediction confidence bounds in the optimisation objective function can enhance the reliability of optimisation results. Thermodynamic analysis offers a much better way of process system analysis. Method of incorporating it in the analysis of process system is a valuable tool for design and operation of process systems. The complexity of the process greatly influences the prediction accuracy of the process. This is reflected in the prediction error of the CDU in comparisons with the case of ADU discussed in the previous section. Effect of the pre-flash unit on the overall exergy efficiency of the CDU shows a preference of the pre-flash drum to the pre-flash column. Though both increases the exergy efficiency of the ADU, having an overall view of their effect gives a much more informed decision. Rather than opting for localised improvement of the ADU as is common in most research, improving the overall efficiency of the CDU is a more realistic way of reducing the energy consumption of the refinery as a whole.

CHAPTER 7: CONCLUSIONS AND RECOMMENDATIONS

7.1 Conclusions

Distillation processes have been vital for chemical and petrochemical industries. They have always been a prime target for energy efficiency improvement. In previous research, thermodynamic analysis of distillation processes has been presented mostly as an analytical tool for quantifying the energy efficiency of processes in terms of useful work. It has often been used for locating points of inefficiency and quantifying recoverable energy of the process. In this research, thermodynamic analysis has been presented not only as an analytical tool but as well as a design tool for improving the efficiency of a distillation process. There is a great need for concerted efforts to be targeted by means of using the available analytical and simulation tools for energy consumption reduction. In the first part of this thesis, an integrated approach of process design and control with the aim of enhancing energy efficiency was presented with particular application to distillation columns. And in the second part, optimisation techniques embedding thermodynamic analysis for energy efficient operation of distillation columns was presented.

With the wake of energy crises and environmental implications of unutilised energy, control loop configuration should not focus on control loop stability and quality of the controller variable alone but also need to include energy efficiency. Control structure selection for distillation column should be supplemented with relative exergy array (REA) for energy efficiency consideration in addition to the traditional relative gain array (RGA) for operability analysis. REA was developed from analysing the exergy efficiency of the control configuration. It gives an indication of the control loop interaction on the exergy efficiency of the control loop. REA gives an additional consideration for control structure selection in terms of exergy efficiency and hence can help in deciding the final control structure selection. The tools when combined can aid in the selection of optimum control structure for a distillation column and could possibly find application in determining optimum operating conditions of the column.

REA and RGA were performed based on steady state matrix. The steady state selection of the control structure based on REA and RGA should be confirmed with dynamic simulation. This is to demonstrate the effectiveness of the selection and in case of several options, to assist in the choice of a probable one. Also since real processes are mostly in the dynamic domain, there is a strong need to validate the steady state

selection in the dynamic state. The steady state results obtained from the application to binary distillation columns in this study were further confirmed with dynamic simulation. It should be stressed that the steady state REA and RGA choices should be validated for informed decision.

In an attempt to model the exergy efficiency of the distillation column a number of data driven models were explored. Artificial neural network (ANN) was found to accurately model the exergy efficiency of a distillation column irrespective of the complexity of the column. To improve the generalisation capability of the model, Bootstrap aggregated neural network (BANN) were introduced. BANN is a combination of several neural networks modelling different faces of the data input space. This makes BANN more robust than a single neural network. BANN enhances model prediction accuracy and also provides model prediction confidence bounds. Model prediction confidence bounds give a measure of the reliability of the model. It gives a sense of confidence that the model can replicate the actual plant data. BANN is advised for better prediction accuracy of the exergy efficiency and product composition modelling in distillation columns especially for complex columns such as crude distillation unit.

Often in the exergy analysis of chemical processes, every change in the design and operating conditions necessitate a re-calculation of the exergy efficiency to determine the impacts of such changes on the system. Developing a model for the exergy efficiency as given in this thesis might minimise such rigours. This might be quite handy in the preliminary design of processes. It could also be of great use in deciding on the combination of operating conditions to improve the exergy efficiency of the process.

The exergy efficiency model as developed was further employed to improve the exergy efficiency of the column. With maximising the exergy efficiency of the column as the optimisation objective, optimum operating conditions of the columns were found. Optimisation technique for distillation process based on BANN model is thus presented in this work. Model prediction confidence bounds could be incorporated in the objective function or formulated as a multi-objective optimisation problem. In either case, the weighting factor of choice greatly influences the optimisation results and should be carefully considered. Inclusion of model prediction confidence bounds introduces a measure of penalization of the optimisation results and improves the reliability of the results. The optimisation technique as applied to a number of distillation columns in this research shows a marked improvement in the exergy efficiency of the column as compared to their initial values. The efficiency improvement has an added advantage of

improved economic cost without having to incur an additional capital cost. The performance on the actual process (represented by HYSYS model) is close to that predicted by BANN model. The technique as presented will be of great advantage at addressing energy and economy issues of distillation processes.

A reliable modelling and optimisation strategy based on BANN for improved generalisation of the predicted model is also presented. The method could predict optimum operating conditions of the column. Simulation based optimisation as presented in this thesis treats simulation as black box model. Hence, it does not require mathematical details of the model making it easy to implement. It also does not require simplification of the process model making it a high fidelity model and it can be readily adapted for parallel computing with reduced computational time. These advantages suggest the possibility of the versatility of the technique.

Every distillation process is often tailored to a particular product specification depending on demands and objectives of the process. Products quality constraints were introduced in the optimisation objectives. Products quality constraints introduce a measure of penalisation on the optimisation result to give as close as possible to what is obtained in reality. Where there are product specification constraints, the technique still holds true. The exergy efficiency may however be reduced as compared to what it will ordinarily be without the constraints. This is mainly due to the restricted optimum search area as a result of the limitations imposed by having to satisfy the constraints.

Also, the complexity of the process greatly influences the prediction accuracy of the process. For instance, the lowest prediction errors between the models and HYSYS validated cases are 0.0006, 0.007 and 0.061 for the multi-component system, the atmospheric distillation unit (ADU) and the crude distillation unit (CDU) respectively. This suggests the need for caution in using the simulation based optimisation. All the variables that greatly influence the objective function should be well factored in the model. It might not be well suited for problems with many variables such as heat exchanger network integration.

The effect of the pre-flash units on the overall exergy efficiency of the CDU shows a preference of the pre-flash drum to the pre-flash column. Though both increases the exergy efficiency of the ADU, having an overall view of their effect gives a much more informed decision. Rather than opting for localised improvement of the ADU as much

common in most researches, improving the overall efficiency of the CDU is a more realistic way of reducing the energy consumption of the refinery as a whole.

7.2 Recommendations

The quest for reducing the energy consumption of distillation process has led to the evolution of columns such as heat integrated columns, petyluk column and thermally coupled dividing wall; all targeted at reducing the energy consumption of distillation processes. The application of the techniques developed in this work has been limited to the conventional distillation units. It would be interesting to study what further improvement this techniques can have on the energy efficiency of heat efficient distillation columns.

The main focus has been on the operating parameters of the column. Further work could be focused on design parameters and possible consideration of other optimisation objectives such as feed tray location, type of feed and heat exchanger networks.

Furthermore, distillation unit is often a part of a whole process. The techniques as developed here have been targeted to distillation units. The next step ahead would be to apply these techniques to the whole plant. The increased complexity of the process will require for detailed preliminary studies to determine the variables to be considered in the model as well as setting their upper and lower boundaries. In addition, there are a number of unit operations that though may not consume as much energy as a distillation process but will probably benefit much more from the application of the techniques.

A detailed step wise procedure of the techniques developed in this thesis has been presented. This can be further developed into software. The software could possibly be for the selection of energy efficient control structure or it might be for the optimisation procedure. Perhaps it might be possible to actually have the two combined in single software. At the moment, software that incorporates these techniques has not been developed.

The method as presented could be further developed for real time optimisation and or model predictive control of the column. This should find application in the operational control and optimisation of the column.

REFERENCES

ABDULLAH, Z., AHMAD, Z. & AZIZ, N. Year. Multiple Input-Single Output (MISO) Feedforward Artificial Neural Network (FANN) Models for Pilot Plant Binary Distillation Column. *In:* Bio-Inspired Computing: Theories and Applications (BIC-TA), 27-29 Sept. 2011. 157-160.

ADETOLA, V. & GUAY, M. 2010. Integration of real-time optimization and model predictive control. *Journal of Process Control,* 20**,** 125-133.

AGUIRRE, P., ESPINOSA, J., TARIFA, E. & SCENNA, N. 1997. Optimal Thermodynamic Approximation to Reversible Distillation by Means of Interheaters and Intercoolers. *Industrial & Engineering Chemistry Research,* 36**,** 4882-4893.

AL-MAYYAHI, M. A., HOADLEY, A. F. A. & RANGAIAH, G. P. 2014. Energy optimization of crude oil distillation using different designs of pre-flash drums. *Applied Thermal Engineering,* 73**,** 1204-1210.

AL-MUSLIM, H. & DINCER, I. 2005. Thermodynamic analysis of crude oil distillation systems. *International Journal of Energy Research,* 29**,** 637-655.

AL-MUSLIM, H., DINCER, I. & ZUBAIR, S. M. 2003. Exergy analysis of single- and two-stage crude oil distillation units. *Journal of Energy Resources Technology-Transactions of the Asme,* 125**,** 199-207.

AL-MUTAIRI, E. M. & BABAQI, B. S. 2014. Energy optimization of integrated atmospheric and vacuum crude distillation units in oil refinery with light crude. *Asia-Pacific Journal of Chemical Engineering,* 9**,** 181-195.

AL SEYAB, R. K. & CAO, Y. 2008. Differential recurrent neural network based predictive control. *Computers & Chemical Engineering,* 32**,** 1533-1545.

ALATTAS, A. M., GROSSMANN, I. E. & PALOU-RIVERA, I. 2011. Integration of nonlinear crude distillation unit models in refinery planning optimization. *Industrial and Engineering Chemistry Research,* 50**,** 6860-6870.

ALCÁNTARA-AVILA, J., KANO, M. & HASEBE, S. 2012. Environmental and economic optimization of distillation structures to produce anhydrous ethanol. *Computer Aided Chemical Engineering.*

ALMEHAIDEB, R. A., ABDULKARIM, M. A. & AL-KHANBASHI, A. S. 2001. Improved K-values correlation for UAE crude oil components at low pressures using PVT laboratory data. *Fuel,* 80**,** 117-124.

ALMEHAIDEB, R. A., ASHOUR, I. & EL-FATTAH, K. A. 2003. Improved K-value correlation for UAE crude oil components at high pressures using PVT laboratory data *Fuel,* 82**,** 1057-1065.

AMIT, K. S., BARJEEV, T. & VISHAL, K. 2013. Application of Feed Forward and Recurrent Neural Network Topologies for the Modeling and Identification of Binary Distillation Column. *IETE Journal of Research,* 59**,** 167-175.

AMIYA, K. J. 2010. Heat integrated distillation operation. *Applied Energy,* 87**,** 1477-1494.

AMMINUDIN, K. A., SMITH, R., THONG, D. Y. C. & TOWLER, G. P. 2001. Design and Optimization of Fully Thermally Coupled Distillation Columns: Part 1: Preliminary Design and Optimization Methodology. *Chemical Engineering Research and Design,* 79**,** 701-715.

ANITHA, K., SHUWANA, T. & KUMAR, V. R. 2011. Simulation of Atmospheric and Vacuum Crude Units Using Aspen Plus. *Petroleum Science and Technology,* 29**,** 1885-1894.

ANITHA, K. S., T.; AND KUMAR, V.R 2011. Simulation of atmospheric and vacuum crude units using aspen plus. *Petroleum Science and Technology,* 29**,** 1885-1894.

ANOZIE, A. N., OSUOLALE, F. N. & OSUNLEKE, A. S. 2009. Exergy analysis of binary plate distillation column operations. *International Journal of Exergy,* 6**,** 715-728.

ARJMAND, M., MORENO, L. & LIU, L. 2011. Energy Saving in Crude Oil Atmospheric Distillation Columns by Modifying the Vapor Feed Inlet Tray. *Chemical Engineering & Technology,* 34**,** 1359-1367.

ASADA, H. & BOELMAN, E. C. 2004. Exergy analysis of a low temperature radiant heating system. *Building Services Engineering Research & Technology,* 25**,** 197-209.

ASSALI, W. A. & MCAVOY, T. 2010. Optimal Selection of Dominant Measurements and Manipulated Variables for Production Control. *Industrial & Engineering Chemistry Research,* 49**,** 7832-7842.

BACHNAS, A. A., TÓTH, R., LUDLAGE, J. H. A. & MESBAH, A. 2014. A review on data-driven linear parameter-varying modeling approaches: A high-purity distillation column case study. *Journal of Process Control,* 24**,** 272-285.

BAHAR, A., ÖZGEN, C., LEBLEBICIOĞLU, K. & HALıCı, U. 2004. Artificial Neural Network Estimator Design for the Inferential Model Predictive Control

of an Industrial Distillation Column. *Industrial & Engineering Chemistry Research,* 43**,** 6102-6111.

BAMUFLEH, H., PONCE-ORTEGA, J. & EL-HALWAGI, M. 2013. Multi-objective optimization of process cogeneration systems with economic, environmental, and social tradeoffs. *Clean Technologies and Environmental Policy,* 15**,** 185-197.

BANDYOPADHYAY, S. 2007. Thermal Integration of a Distillation Column Through Side-Exchangers. *Chemical Engineering Research and Design,* 85**,** 155-166.

BANSAL, V., PERKINS, J. D., PISTIKOPOULOS, E. N., ROSS, R. & VAN SCHIJNDEL, J. M. G. 2000. Simultaneous design and control optimisation under uncertainty. *Computers & Chemical Engineering,* 24**,** 261-266.

BASAK, K., ABHILASH, K. S., GANGULY, S. & SARAF, D. N. 2002. On-Line Optimization of a Crude Distillation Unit with Constraints on Product Properties. *Industrial & Engineering Chemistry Research,* 41**,** 1557-1568.

BENALI, T., TONDEUR, D. & JAUBERT, J. N. 2012. An improved crude oil atmospheric distillation process for energy integration: Part I: Energy and exergy analyses of the process when a flash is installed in the preheating train. *Applied Thermal Engineering,* 32**,** 125-131.

BOGGS, P. T. & TOLLE, J. W. 1995. Sequential Quadratic Programming. *Acta Numerica,* 4**,** 1-51.

BOLF, N., GALINEC, G. & BAKSA, T. 2010. Development of Soft Sensor for Diesel Fuel Quality Estimation. *Chemical Engineering & Technology,* 33**,** 405-413.

BORTZ, M., BURGER, J., ASPRION, N., BLAGOV, S., BÖTTCHER, R., NOWAK, U., SCHEITHAUER, A., WELKE, R., KÜFER, K. H. & HASSE, H. 2014. Multi-criteria optimization in chemical process design and decision support by navigation on Pareto sets. *Computers & Chemical Engineering,* 60**,** 354-363.

BOX, G. E. P. & NORMAN, R. D. 1987. *Empirical model-building and response surfaces*, Wiley, pg 424.

BRISTOL, E. 1966. On a new measure of interaction for multivariable process control. *Automatic Control, IEEE Transactions on,* 11**,** 133-134.

BURNHAM, K. P. & ANDERSON, D. R. 2002. *Model selection and multimodel inference: A practical information-theoretic approach,* Springer-Verlag.

CAO, Y. 2005. A formulation of nonlinear model predictive control using automatic differentiation. *Journal of Process Control,* 15**,** 851-858.

CAO, Y., JIN, Y., KOWALCZYKIEWICZ, M. & SENDHOFF, B. Year. Prediction of convergence dynamics of design performance using differential recurrent neural networks. *In:* Neural Networks, 2008. IJCNN 2008. (IEEE World Congress on Computational Intelligence). IEEE International Joint Conference on Neural Networks, 1-8 June 2008 2008 Hong Kong. 528-533.

CHEN, Z., HENSON, M. A., BELANGER, P. & MEGAN, L. 2010. Nonlinear Model Predictive Control of High Purity Distillation Columns for Cryogenic Air Separation. *IEEE Transactions on Control Systems Technology,* 18**,** 811-821.

CHUN, H. & KIM, Y. 2013. Application of a divided wall column for gas separation in floating liquefied natural gas plant. *Korean Journal of Chemical Engineering***,** 1-7.

COELLO COELLO, C. 1999. A Comprehensive Survey of Evolutionary-Based Multiobjective Optimization Techniques. *Knowledge and Information Systems,* 1**,** 269-308.

CORNELISSEN, R. L. 1997. *Thermodynamics and sustainable development, the use of exergy analysis and the reduction of irreversibility.* PhD, University of Twente.

COUGHANOWR, D. R. & LEBLANC, S. E. 2009. *Process systems analysis and control,* New York, McGraw Hill.

DARBY, M. L. & NIKOLAOU, M. 2012. MPC: Current practice and challenges. *Control Engineering Practice,* 20**,** 328-342.

DARTT, S. R. 1985. A Survey on process-control application needs. *Chemical Engineering Progress,* 81**,** 11-14.

DAVE, D. J., DABHIYA, M. Z., SATYADEV, S. V. K., GANGULY, S. & SARAF, D. N. 2003. Online tuning of a steady state crude distillation unit model for real time applications. *J. Process Control,* 13**,** 267-282.

DAVE, D. J., DABHIYA, M. Z., SATYADEV, S. V. K., GANGULY, S. & SARAF, D. N. 2004. Online tuning procedures for crude distillation unit model. American Institute of Chemical Engineers.

DE KOEIJER, G. M., KJELSTRUP, S., SALAMON, P., SIRAGUSA, G., SCHALLER, M. & HOFFMANN, K. H. 2002. Comparison of Entropy Production Rate Minimization Methods for Binary Diabatic Distillation. *Industrial & Engineering Chemistry Research,* 41**,** 5826-5834.

DEB, K. 2001. *Multi-objective optimization using evolutionary algorithms,* John Wiley & Sons.

DEMIREL, Y. 2004. Thermodynamic analysis of separation system. *Separation Science and Technology,* 39**,** 3897-3942.

DHOLE, V. R. & LINNHOFF, B. 1993. Distillation column targets. *Computers & Chemical Engineering,* 17**,** 549-560.

DIEHL, M., BOCK, H. G., SCHLÖDER, J. P., FINDEISEN, R., NAGY, Z. & ALLGÖWER, F. 2002. Real-time optimization and nonlinear model predictive control of processes governed by differential-algebraic equations. *Journal of Process Control,* 12**,** 577-585.

DINCER, I. 1998. Energy and Environmental Impacts: Present and Future Perspectives. *Energy Sources,* 20**,** 427-453.

DINCER, I. & AL-MUSLIM, H. 2001. Thermodynamic analysis of reheat cycle steam power plants. *International Journal of Energy Research,* 25**,** 727-739.

DINCER, I. & CENGEL, Y. 2001. Energy, Entropy and Exergy Concepts and Their Roles in Thermal Engineering. *Entropy,* 3**,** 116.

DINCER, I. & ROSEN, M. A. 1998. A worldwide perspective on energy, environment and sustainable development. *International Journal of Energy Research,* 22**,** 1305-1321.

DINCER, I. & ROSEN, M. A. 2012. *Exergy:energy, environment and sustainable development,* Great Britain, Oxford, Elsevier.

DOE 1998. Energy and enviromental profile of the U.S. petroleum refining industry. *In:* ENERGY, U. S. D. O. (ed.).

DOE 2000. Technology roadmap for the petroleum industry. *In:* ENERGY, U. S. D. O. (ed.).

DOLDERSUM, A. 1998. Exergy analysis proves viability of process modifications. *Energy Conversion and Management,* 39**,** 1781-1789.

DUA, P., KOURAMAS, K., DUA, V. & PISTIKOPOULOS, E. N. 2008. MPC on a chip-Recent advances on the application of multi-parametric model-based control. *Computers and Chemical Engineering,* 32**,** 754-765.

EDGAR, T. F., HIMMELBLAU, D. M., LASDON, L.S. 2001. *Optimisation of chemical processes,* New York, McGraw Hill.

EDMISTER, W. C. 1938. Thermodynamic Properties of Hydrocarbons. *Industrial & Engineering Chemistry,* 30**,** 352-358.

ERRICO, M., TOLA, G. & MASCIA, M. 2009. Energy saving in a crude distillation unit by a preflash implementation. *Applied Thermal Engineering,* 29**,** 1642-1647.

FESANGHARY, M., MAHDAVI, M., MINARY-JOLANDAN, M. & ALIZADEH, Y. 2008. Hybridizing harmony search algorithm with sequential quadratic programming for engineering optimization problems. *Computer Methods in Applied Mechanics and Engineering,* 197**,** 3080-3091.

FITZMORRIS, R. E. & MAH, R. S. H. 1980. Improving distillation column design using thermodynamic availability analysis. *Aiche Journal,* 26**,** 265-273.

FORTUNA, L., GRAZIANI, S. & XIBILIA, M. G. 2005. Soft sensors for product quality monitoring in debutanizer distillation columns. *Control Engineering Practice,* 13**,** 499-508.

GADALLA, M., KAMEL, D., ASHOUR, F. & EL DIN, H. N. Year. A new optimisation based retrofit approach for revamping an Egyptian crude oil distillation unit. *In:* Energy Procedia, 2013. 454-464.

GARCÍA-HERREROS, P. & GÓMEZ, J. M. 2013. Modeling and optimization of a crude distillation unit: A case study for undergraduate students. *Computer Applications in Engineering Education,* 21**,** 276-286.

GEDDES, D. & KUBERA, T. 2000. Integration of planning and real-time optimization in olefins production. *Computers & Chemical Engineering,* 24**,** 1645-1649.

GELADI, P. & KOWALSKI, B. R. 1986. Partial least-squares regression: a tutorial. *Analytica Chimica Acta,* 185**,** 1-17.

GMEHLING, J. & ONKEN, U. 1991. *Vapor-liquid equilibrium data collection,* Dechema.

GONCALVES, D. D., MARTINS, F. G. & FEYO, D. A. S. 2010. Dynamic simulation and control: application to Atmospheric Distillation Unit of crude oil refinery. *Comput.-Aided Chem. Eng.,* 28**,** 1593-1598.

GONZÁLEZ, J., AGUILAR, R., ALVAREZ-RAMíREZ, J., FERNÁNDEZ, G. & BARRÓN, M. 1999. Linearizing control of a binary distillation column based on a neuro-estimator. *Artificial Intelligence in Engineering,* 13**,** 405-412.

GRANET, I. & BLUESTEIN, M. 2014. *Thermodynamics and Heat Power, Eighth Edition* [Online]. Hoboken: CRC Press. Available: http://public.eblib.com/choice/PublicFullRecord.aspx?p=1702488 [Accessed].

GREEN, D. W. & PERRY, R. H. (eds.) 2006. *Perry's chemical engineering handbook,* China: McGraw Hill.

GROENENDIJK, A. J., DIMIAN, ALEXANDRE C., IEDEMA, PIET D. 2000. Systems approach for evaluating dynamics and plantwide control of complex plants. *Aiche Journal,* 46**,** 133-145.

GU, W., HUANG, Y., WANG, K., ZHANG, B., CHEN, Q. & HUI, C.-W. 2014. Comparative analysis and evaluation of three crude oil vacuum distillation processes for process selection. *Energy,* 76**,** 559-571.

HAYDARY, J. A. P., TOMAS 2009. Steady state and dynamic simulation of crude oil distillation using ASPEN plus and ASPEN dynamics. *Petroleum and coal,* 51**,** 100-109.

HE, M.-J., CAI, W.-J., NI, W. & XIE, L.-H. 2009. RNGA based control system configuration for multivariable processes. *Journal of Process Control,* 19**,** 1036-1042.

HINDERINK, A. P., KERKHOF, F. P. J. M., LIE, A. B. K., DE SWAAN ARONS, J. & VAN DER KOOI, H. J. 1996. Exergy analysis with a flowsheeting simulator—I. Theory; calculating exergies of material streams. *Chemical Engineering Science,* 51**,** 4693-4700.

HOLMAN, J. P. 1980. *Thermodynamics,* Japan, McGraw Hill.

HOSEN, M. A., HUSSAIN, M. A. & MJALLI, F. S. 2011. Control of polystyrene batch reactors using neural network based model predictive control (NNMPC): An experimental investigation. *Control Engineering Practice,* 19**,** 454-467.

HUANG, H. P., OHSHIMA, M. & HASHIMOTO, I. 1994. Dynamic interaction and multiloop control system design. *Journal of Process Control,* 4**,** 15-27.

HULTMANN AYALA, H. V. & DOS SANTOS COELHO, L. 2012. Tuning of PID controller based on a multiobjective genetic algorithm applied to a robotic manipulator. *Expert Systems with Applications,* 39**,** 8968-8974.

HUMPHREY, J. L. & SIEBERT, A. F. 1992. Separation technologies; An opportunity for energy savings. *Journal Name: Chemical Engineering Progress; (United States); Journal Volume: 88:3***,** Medium: X; Size: Pages: 32-42.

INAMDAR, S. V., GUPTA, S. K. & SARAF, D. N. 2004. Multi-objective optimization of an industrial crude distillation unit using the elitist non-dominated sorting genetic algorithm. *Chem. Eng. Res. Des.,* 82**,** 611-623.

JAIN, A. & BABU, B. V. 2012. Analysis of process interactions in dynamic system using frequency dependent RGA. *Advanced Materials Research.*

JI, S. & BAGAJEWICZ, M. 2002. Design of Crude Fractionation Units with Preflashing or Prefractionation: Energy Targeting. *Industrial & Engineering Chemistry Research,* 41**,** 3003-3011.

JIN, H., ISHIDA, M., KOBAYASHI, M. & NUNOKAWA, M. 1997. Exergy Evaluation of Two Current Advanced Power Plants: Supercritical Steam Turbine and Combined Cycle. *Journal of Energy Resources Technology,* 119**,** 250-256.

JONES, A., O'DONNELL, M. & TERNDRUP, H. 1999. Crude unit control and optimisation at Grangemouth refinery. *Computing & Control Engineering Journal,* 10**,** 209-213.

JONES, D. S. J. 1999. *Elements of Petroleum Processing,* Wiley.

JORGE, J. M. & SORENSEN, D. C. 1983. Computing a Trust Region Step. *SIAM Journal on Scientific and Statistical Computing,* 4**,** 553-572.

KAES, G. L. 2000. *Refinery Process Modeling: A Practical Guide to Steady State Modeling of Petroleum Processes : Using Commercial Simulators,* Athens Printing Company.

KAMELA, D., GADALLAA, M. & ASHOURB, F. 2013. New Retrofit Approach for Optimisation and Modification for a Crude Oil Distillation System. *Chemical Engineering,* 35.

KANSHA, Y., KISHIMOTO, A. & TSUTSUMI, A. 2012. Application of the self-heat recuperation technology to crude oil distillation. *Applied Thermal Engineering,* 43**,** 153-157.

KIM, J., LIM, W., LEE, Y., KIM, S., PARK, S.-R., SUH, S.-K. & MOON, I. 2011. Development of Corrosion Control Document Database System in Crude Distillation Unit. *Industrial & Engineering Chemistry Research,* 50**,** 8272-8277.

KIM, Y. 2012. Energy saving and thermodynamic efficiency of a double-effect distillation column using internal heat integration. *Korean Journal of Chemical Engineering,* 29**,** 1680-1687.

KISS, A. A., FLORES LANDAETA, S. J. & INFANTE FERREIRA, C. A. 2012. Towards energy efficient distillation technologies – Making the right choice. *Energy,* 47**,** 531-542.

KOOKOS, I. K. 2005. Real-Time Regulatory Control Structure Selection Based on Economics. *Industrial & Engineering Chemistry Research,* 44**,** 3993-4000.

KREUL, L. U., GÓRAK, A. & BARTON, P. I. 1999. Dynamic rate-based model for multicomponent batch distillation. *Aiche Journal,* 45**,** 1953-1962.

KRISHNAMURTHY, R. & TAYLOR, R. 1985. A nonequilibrium stage model of multicomponent separation processes. Part II: Comparison with experiment. *Aiche Journal,* 31**,** 456-465.

KUMANA, J. D., POLLEY, G. T., PUGH, S. J. & ISHIYAMA, E. M. Year. Improved energy efficiency in CDUs through fouling control. *In:* 10AIChE - 2010 AIChE Spring Meeting and 6th Global Congress on Process Safety 2010 San Antonio.

KUMAR, A. S. & AHMAD, Z. 2012. Model predictive control (MPC) and its current issues in Chemical Engineering. *Chemical Engineering Communications,* 199**,** 472-511.

KUMAR, V., SHARMA, A., CHOWDHURY, I. R., GANGULY, S. & SARAF, D. N. 2001. A crude distillation unit model suitable for online applications. *Fuel Processing Technology,* 73**,** 1-21.

LARSSON, T. & SKOGESTAD, S. 2000. Plantwide control- A review and a new design procedure. *Modeling, identification and control,* 21**,** 209-240.

LETCHER, T. M., SCOTT, J. L., PATTERSON, D. A. (ed.) 2015. *Chemical processes for a sustainable future,* United Kingdom: Royal society of chemistry.

LI, J., MISENER, R. & FLOUDAS, C. A. 2012. Continuous-time modeling and global optimization approach for scheduling of crude oil operations. *Aiche Journal,* 58**,** 205-226.

LIANG, Y.-C., ZHOU, Z., WU, Y.-T., GENG, J. & ZHANG, Z.-B. 2006. A nonequilibrium model for distillation processes. *Aiche Journal,* 52**,** 4229-4239.

LIAU, L. C.-K., YANG, T. C.-K. & TSAI, M.-T. 2004. Expert system of a crude oil distillation unit for process optimization using neural networks. *Expert Systems with Applications,* 26**,** 247-255.

LIPTAK, B. G. (ed.) 2006. *Instrument Engineers' Handbook,* USA: CRC Press.

LOVE, J. 2007. *Process automation handbook: a guide to theory and practice,* London, Springer.

LUYBEN, M. L., TYREUS, B. D. & LUYBEN, W. L. 1997. Plantwide control design procedure. *Aiche Journal,* 43**,** 3161-3174.

LUYBEN, W. L. 1990. *Process modeling, simulation and control for chemical engineers,* Singapore, McGraw Hill.

LUYBEN, W. L. (ed.) 1992. *Practical distillation control,* New York: Van Nostrand Reinhold.

LUYBEN, W. L. 2006. *Distillation design and control using ASPEN simulation.* New Jersey: Wiley-Interscience.

LUYBEN, W. L. 2012. Rigorous dynamic models for distillation safety analysis. *Computers & Chemical Engineering,* 40**,** 110-116.

LUYBEN, W. L., TYREUS, B. D., LUYBEN, M. L. 1998. *Plant wide process control,* New York, McGraw Hill.

MAHALEC, V. & SANCHEZ, Y. 2012. Inferential monitoring and optimization of crude separation units via hybrid models. *Computers & Chemical Engineering,* 45**,** 15-26.

MARTIN, T. H. H., B. DEMUTH; MARK, H. BEALE; ORLANDO, DE JESUS 2014. Neural network design. 2nd ed.

MASCIA, M., FERRARA, F., VACCA, A., TOLA, G. & ERRICO, M. 2007. Design of heat integrated distillation systems for a light ends separation plant. *Applied Thermal Engineering,* 27**,** 1205-1211.

MATSUDA, K., KAWAZUISHI, K., KANSHA, Y., FUSHIMI, C., NAGAO, M., KUNIKIYO, H., MASUDA, F. & TSUTSUMI, A. 2011. Advanced energy saving in distillation process with self-heat recuperation technology. *Energy,* 36**,** 4640-4645.

MC AVOY, T., ARKUN, Y., CHEN, R., ROBINSON, D. & SCHNELLE, P. D. 2003. A new approach to defining a dynamic relative gain. *Control Engineering Practice,* 11**,** 907-914.

MCCABE, W. L. & SMITH, J. C. 2005. *Unit operations of chemical engineering,* Dubuque, Iowa, McGraw-Hill.

MINGJIAN, S., YUDE, S., NAIZHANG, F. & CHENG, M. Year. Advanced RMPCT control strategy in CDU. *In:* Robotics and Biomimetics, 2007. ROBIO 2007. IEEE International Conference on, 15-18 Dec. 2007 2007. 2273-2277.

MITTAL, V., ZHANG, J., YANG, X. & XU, Q. 2011. E3 Analysis for crude and vacuum distillation system. *Chemical Engineering and Technology,* 34**,** 1854-1863.

MIZOGUCHI, A., MARLIN, T. E. & HRYMAK, A. N. 1995. Operations optimization and control design for a petroleum distillation process. *Canadian Journal of Chemical Engineering,* 73**,** 896-907.

MODELL, M. & REED, R. C. 1974. *Thermodynamics and its applications,* Englewood Cliff, New Jersey, Prentice Hall.

MONEDERO, I., BISCARRI, F., LEÓN, C., I. GUERRERO, J., GONZÁLEZ, R. & PÉREZ-LOMBARD, L. 2012. Decision system based on neural networks to optimize the energy efficiency of a petrochemical plant. *Expert Systems with Applications,* 39**,** 9860-9867.

MONTELONGO-LUNA, J. M., SVRCEK, W. Y. & YOUNG, B. R. 2011. The relative exergy array—a new measure for interactions in process design and control. *The Canadian Journal of Chemical Engineering,* 89**,** 545-549.

MOTLAGHI, S., JALALI, F. & AHMADABADI, M. N. 2008. An expert system design for a crude oil distillation column with the neural networks model and the process optimization using genetic algorithm framework. *Expert Systems with Applications,* 35**,** 1540-1545.

MUKHERJEE, A. & ZHANG, J. 2008. A reliable multi-objective control strategy for batch processes based on bootstrap aggregated neural network models. *Journal of Process Control,* 18**,** 720-734.

MULLINS, O. C. & BERRY, R. S. 1984. Minimization of entropy production in distillation. *The Journal of Physical Chemistry,* 88**,** 723-728.

MUNIR, M., YU, W. & YOUNG, B. 2013a. Eco-efficiency and control loop configuration for recycle systems. *Korean Journal of Chemical Engineering***,** 1-11.

MUNIR, M. T., YU, W. & YOUNG, B. R. Year. Eco-efficiency of control configurations using exergy. *In,* 2012a Cardiff. 160-165.

MUNIR, M. T., YU, W. & YOUNG, B. R. 2012b. Recycle effect on the relative exergy array. *chemical engineering research and design,* 90**,** 110-118.

MUNIR, M. T., YU, W. & YOUNG, B. R. Year. The relative exergy destroyed: A new tool for process design and control. *In,* 2012c Singapore. 292-297.

MUNIR, M. T., YU, W. & YOUNG, B. R. 2012d. A software algorithm/package for control loop configuration and eco-efficiency. *ISA Transactions,* 51**,** 827-833.

MUNIR, M. T., YU, W. & YOUNG, B. R. 2013b. Plant-wide control: Eco-efficiency and control loop configuration. *ISA Transactions,* 52**,** 162-169.

MUNIR, M. T., YU, W. & YOUNG, B. R. 2013c. The relative exergy-destroyed array: A new tool for control structure design. *The Canadian Journal of Chemical Engineering***,** n/a-n/a.

NAKAIWA, M., HUANG, K., ENDO, A., OHMORI, T., AKIYA, T. & TAKAMATSU, T. 2003. Internally Heat-Integrated Distillation Columns: A Review. *chemical engineering research and design,* 81**,** 162-177.

NAKKASH, N. B. & DHIAA, N. 2011. Energy conservation on multicomponent non ideal distillation using heat pump and split tower technique. *AIChE* Chicago, United States.

NAPHTALI, L. M. & SANDHOLM, D. P. 1971. Multicomponent separation calculations by linearization. *Aiche Journal,* 17**,** 148-153.

OCHOA-ESTOPIER, L. M. & JOBSON, M. 2015. Optimization of Heat-Integrated Crude Oil Distillation Systems. Part III: Optimization Framework. *Industrial & Engineering Chemistry Research,* 54**,** 5018-5036.

OCHOA-ESTOPIER, L. M., JOBSON, M. & SMITH, R. 2013. Operational optimization of crude oil distillation systems using artificial neural networks. *Computers & Chemical Engineering,* 59**,** 178-185.

OCHOA-ESTOPIER, L. M., JOBSON, M. & SMITH, R. 2014. The use of reduced models for design and optimisation of heat-integrated crude oil distillation systems. *Energy,* 75**,** 5-13.

OGUNNAIKE, B. A. & RAY, W. H. 1994. *Process dynamics, modeling and control,* New York, Oxford University press inc.,.

ONI, A. O. & WAHEED, M. A. 2015. Methodology for the thermoeconomic and environmental assessment of crude oil distillation units. *International Journal of Exergy,* 16**,** 504-532.

OSMAN, M. & RAMASAMY, M. 2010. Neural Network based Soft Sensor for Inferential Control of a Binary Distillation Column. *Journal of Applied Sciences,* 10**,** 2558-2564.

OSUOLALE, F. N. & ZHANG, J. 2014. Energy Efficient Control and Optimisation of Distillation Column Using Artificial Neural Network. *Chemical Engineering Transactions,* 39**,** 37- 42.

PARASCHIV, N., BAIESU, A. & STAMATESCU, G. Year. Using an advanced control technique for controlling a distillation column. *In:* Control and Automation, 2009. ICCA 2009. IEEE International Conference on, 9-11 Dec. 2009 2009. 581-584.

PERRY, D. W. G. R. H. (ed.) 2008. *Perry's chemical engineers handbook,* New York: McGraw-Hill.

PLESU, V., BUMBAC, G., IANCU, P., IVANESCU, I. & CORNELIU POPESCU, D. 2003. Thermal coupling between crude distillation and delayed coking units. *Applied Thermal Engineering,* 23**,** 1857-1869.

PORFíRIO, C. R., ALMEIDA NETO, E. & ODLOAK, D. 2003. Multi-model predictive control of an industrial C3/C4 splitter. *Control Engineering Practice,* 11**,** 765-779.

PORFÍRIO, C. R. & ODLOAK, D. 2011. Optimizing model predictive control of an industrial distillation column. *Control Engineering Practice,* 19**,** 1137-1146.

PRICE, R. M., LYMAN, P. R. & GEORGAKIS, C. 1994. Throughput Manipulation in Plantwide Control Structures. *Industrial & Engineering Chemistry Research,* 33**,** 1197-1207.

QIN, S. J. & BADGWELL, T. A. 2003. A survey of industrial model predictive control technology. *Control Engineering Practice,* 11**,** 733-764.

RATKJE, S. K., SAUAR, E., HANSEN, E. M., LIEN, K. M. & HAFSKJOLD, B. 1995. Analysis of Entropy Production Rates for Design of Distillation Columns. *Industrial & Engineering Chemistry Research,* 34**,** 3001-3007.

REWAGAD, R. R. & KISS, A. A. 2012. Dynamic optimization of a dividing-wall column using model predictive control. *Chemical Engineering Science,* 68**,** 132-142.

RIAZI, M. R. & DAUBERT, T. E. 1987. Characterization parameters for petroleum fractions. *Industrial & Engineering Chemistry Research,* 26**,** 755-759.

RIVERO, R. 2001. Exergy simulation and optimization of adiabatic and diabatic binary distillation. *Energy,* 26**,** 561-593.

RIVERO, R., RENDON, C. & GALLEGOS, S. 2004. Exergy and exergoeconomic analysis of a crude oil combined distillation unit. *Energy,* 29**,** 1909-1927.

RIVERO, R., RENDON, C. & MONROY, L. 1999. The Exergy of Crude Oil Mixtures and Petroleum Fractions: Calculation and Application. *International Journal of Thermodynamics,* 2**,** 115-123.

RIVOTTI, P., LAMBERT, R. S. C. & PISTIKOPOULOS, E. N. 2012. Combined model approximation techniques and multiparametric programming for explicit nonlinear model predictive control. *Computers & Chemical Engineering,* 42**,** 277-287.

ROBBINS, L. 2011. Distillation Control, Optimization, and Tuning : Fundamentals and Strategies. CRC Press.

ROGINA, A., ŠIŠKO, I., MOHLER, I., UJEVIĆ, Ž. & BOLF, N. 2011. Soft sensor for continuous product quality estimation (in crude distillation unit). *chemical engineering research and design,* 89**,** 2070-2077.

ROSEN, M. A. & DINCER, I. 1997. ON EXERGY AND ENVIRONMENTAL IMPACT. *International Journal of Energy Research,* 21**,** 643-654.

SANKARANARAYANAN, K., ARONS, J. D. S. & KOOI, H. J. V. D. 2010. *Efficiency and Sustainability in the Energy and Chemical Industries,* United states, CRC Press, Taylor and Francis group.

SCHITTKOWSKI, K. 1983. On the convergence of a sequential quadratic programming method with an augmented lagrangian line search function. *Mathematische Operationsforschung und Statistik. Series Optimization,* 14**,** 197-216.

SCHITTKOWSKI, K. 1986. NLPQL: A fortran subroutine solving constrained nonlinear programming problems. *Annals of Operations Research,* 5**,** 485-500.

SCIUBBA, E. & WALL, G. 2007. A brief commented history of exergy from the beginnings to 2004. *International Journal of Thermodynamics,* 10**,** 1-26.

SEBORG, D. E., EDGAR, D. F., MELLICHAMP, D. A. 1989. *Process dynamics and control,* New York, Wiley.

SENGUPTA, S., DATTA, A. & DUTTAGUPTA, S. 2007. Exergy analysis of a coal-based 210 MW thermal power plant. *International Journal of Energy Research,* 31**,** 14-28.

SHAHNOVSKY, G., COHEN, T. & MCMURRAY, R. 2012. Integrated monitoring for optimising crude distillation. *Petroleum Technology Quarterly,* 17.

SHANG, C., YANG, F., HUANG, D. & LYU, W. 2014. Data-driven soft sensor development based on deep learning technique. *Journal of Process Control,* 24**,** 223-233.

SHARIFZADEH, M. & THORNHILL, N. F. 2012. Optimal selection of control structure using a steady-state inversely controlled process model. *Computers & Chemical Engineering,* 38**,** 126-138.

SHINSKEY, F. G. 1988. *Process control systems,* New York, McGraw Hill.

SIMPSON, M. B., RYBAR, I., KESTER, M. & SZAKALL, T. 2010. Optimized crude distillation unit (CDU) operations with advanced process control. *Proc. Annu. ISA Anal. Div. Symp.,* 55th**,** simpson1/1-simpson1/18.

SKOGESTAD, S. 1997. Dynamics and Control of Distillation Columns - A Critical Survey. *Modeling, identification and control,* 18**,** 177-217.

SKOGESTAD, S. 2000. Plantwide control: the search for the self-optimizing control structure. *Journal of Process Control,* 10**,** 487-507.

SKOGESTAD, S. 2007. The Dos and Don'ts of Distillation Column Control. *chemical engineering research and design,* 85**,** 13-23.

SKOGESTAD, S., LUNDSTRÖM, P. & JACOBSEN, E. W. 1990. Selecting the best distillation control configuration. *Aiche Journal,* 36**,** 753-764.

SKOGESTAD, S. & MORARI, M. 1987. CONTROL CONFIGURATION SELECTION FOR DISTILLATION COLUMNS. *Aiche Journal,* 33**,** 1620-1635.

SMITH, J. M., VAN NESS, H. C. & ABBOTT, M. M. 2005. *Introduction to chemical engineering thermodynamics,* Boston ; Montreal, McGraw-Hill.

SZARGUT, J., MORRIS, D. R. & STEWARD, F. R. 1988. *Exergy analysis of thermal, chemical and metallurgical processes. ,* New York, Hemisphere Publishing Corporation.

TARIGHALESLAMI, A. H., OMIDKHAH, M. R. & SINAKI, S. Y. 2011. An Exergy Analysis on a Crude Oil Atmospheric Distillation Column. *In:* KLEMES, J. J. V. P. S. L. H. L. (ed.) *Pres 2011: 14th International Conference on Process Integration, Modelling and Optimisation for Energy Saving and Pollution Reduction, Pts 1 and 2.*

TOMICH, J. F. 1970. A new simulation method for equilibrium stage processes. *Aiche Journal,* 16**,** 229-232.

TREYBAL, R. E. 1980. *Mass-transfer operations,* New York, McGraw-Hill.

UJEVIĆ, Ž., MOHLER, I. & BOLF, N. 2011. Soft sensors for splitter product propertyestimation in CDU. *Chemical Engineering Communications,* 198**,** 1566-1578.

UMAR, L. M., CAO, Y. & KARIWALA, V. 2014. Incorporating feedforward action into self-optimising control policies. *The Canadian Journal of Chemical Engineering,* 92**,** 90-96.

UZLU, E., KANKAL, M., AKPıNAR, A. & DEDE, T. 2014. Estimates of energy consumption in Turkey using neural networks with the teaching–learning-based optimization algorithm. *Energy,* 75**,** 295-303.

VAN DE WAL, M. & DE JAGER, B. 2001. Review of methods for input/output selection. *Automatica,* 37**,** 487-510.

VAN WIJK, R. A. & POPE, M. R. 1992. Advanced process control and on-line optimisation in shell refineries. *Computers & Chemical Engineering,* 16, Supplement 1**,** S69-S80.

VAZQUEZ–CASTILLO, J. A., VENEGAS–SÁNCHEZ, J. A., SEGOVIA–HERNÁNDEZ, J. G., HERNÁNDEZ-ESCOTO, H., HERNÁNDEZ, S., GUTIÉRREZ–ANTONIO, C. & BRIONES–RAMÍREZ, A. 2009. Design and

optimization, using genetic algorithms, of intensified distillation systems for a class of quaternary mixtures. *Computers & Chemical Engineering,* 33**,** 1841-1850.

VIJAYAN, V. & PANDA, R. C. 2012. Design of PID controllers in double feedback loops for SISO systems with set-point filters. *ISA Transactions,* 51**,** 514-521.

WALL, G. 2009. Exergetics. www.exergy.se/ftp/exergetics.pdf.

WHITE, D. C. 2012. Optimize energy use in distillation. *Chemical Engineering Progress,* 108**,** 35-41.

WHITSON, C. H. & TORP, S. B. 1983. Evaluating constant volumn depletion data. *Journal of Petroleum Technology***,** 610-620.

WILSON, G. A. 1968. A modified Redlich-Kwong EOS, application to physical data calculation. *Annual AICHE National Meeting.* Cleveland, Ohio.

WITTGENS, B. & SKOGESTAD, S. 2000. Evaluation of Dynamic Models of Distillation Columns with Emphasis on the Initial Response. *Modeling, identification and control,* 21**,** 83-103.

XIAOOU, L. & WEN, Y. Year. Modeling and neuro control for multicomponent nonideal distillation column. *In:* Control and Automation (ICCA), 2011 9th IEEE International Conference on, 19-21 Dec. 2011 2011. 979-984.

XIONG, Q., CAI, W.-J. & HE, M.-J. 2005. A practical loop pairing criterion for multivariable processes. *Journal of Process Control,* 15**,** 741-747.

XU, Q., YANG, X., ZHANG, J. & MITTAL, V. 2011. E3 Analysis for crude and vacuum distillation system. *Chemical Engineering and Technology,* 34**,** 1854-1863.

YELCHURU, R. & SKOGESTAD, S. 2012. Convex formulations for optimal selection of controlled variables and measurements using Mixed Integer Quadratic Programming. *Journal of Process Control,* 22**,** 995-1007.

YING, C. M. & JOSEPH, B. 1999. Performance and stability analysis of LP-MPC and QP-MPC cascade control systems. *Aiche Journal,* 45**,** 1521-1534.

YU, X., LU, W., HUANG, D. & JIN, Y. 2008. Multi-objective optimization of industrial crude distillation unit based on HYSYS and NSGA-II. *Huagong Xuebao/Journal of Chemical Industry and Engineering (China),* 59**,** 1646-1649.

YU, X. H. Year. A neuromorphic controller for a distillation column. *In:* Fourth International Conference on Control and Automation, 10 June 2003 through 12 June 2003 2003 Montreal, Que.; Canada. 679-682.

ZHANG, J. 1999. Developing robust non-linear models through bootstrap aggregated neural networks. *Neurocomputing,* 25**,** 93-113.

ZHANG, J. 2004. A Reliable Neural Network Model Based Optimal Control Strategy for a Batch Polymerization Reactor. *Industrial & Engineering Chemistry Research,* 43**,** 1030-1038.

ZHOU, C., LIU, Q., HUANG, D. & ZHANG, J. 2012. Inferential estimation of kerosene dry point in refineries with varying crudes. *Journal of Process Control,* 22**,** 1122-1126.

ZHU, L., SU, H., LU, S., WANG, Y. & ZHANG, Q. 2014. Coordinating and evaluating of multiple key performance indicators for manufacturing equipment: Case study of distillation column. *Chinese Journal of Chemical Engineering,* 22**,** 805-811.

APPENDIX A

- Perform a closed loop tuning based on Ziegler-Nichols method to obtain the ultimate gain μ_u and the ultimate period P_u
- Subtitute the values obtained to get the relevant controller parameter as given in the table below

Controller type	Gain(K_{ZN})	Reset(τ_{ZN})	Derivative
P	$\frac{\mu_u}{2}$		
PI	$\frac{\mu_u}{2.2}$	$\frac{P_u}{1.2}$	
PID	$\frac{\mu_u}{1.7}$	$\frac{P_u}{2}$	$\frac{P_u}{1.8}$

- Assume a factor F usually between 2-5

  The Gain K_c and the period τ_i are calculated as

$$K_c = \frac{K_{ZN}}{F}$$

$$\tau_i = F * \tau_{ZN}$$

- Make a plot of $W_{iw} = -1 + Det\left(1 + G_{m(iw)}B_{iw}\right)$

  Where $B_{iw} = K_c\left(1 + \frac{1}{\tau_i}\right)$

  $G_{m(iw)}$ is the open loop transfer relating controlled variable to manipulated variable

- Make a plot of Lcm. This is the closed loop log modulus which is the magnitude of the closed loop servo function. For a choosen controller, the maximum value of Lc is determined, if is less than dB, the gain is increased.

$$L_c = 20log\left|\frac{GB}{1 + GB}\right|$$

An example code for calculating this in MATLAB is given as follows

```
%BLT method
ku1 = 10;% Ultimate gain from Ziegler nichols method
ku2 = 3;
pu1 = 5;
pu2 = 3.5;
```

```
wu1 =2*pi/pu1%Ultimate frequency from Ziegler nichols method (note
period pu =2*pi/wu
wu2 =2*pi/pu2

f =4.45; %BLT assumed factor
j = sqrt(-1)
k1 = ku1/(2.2*f); % Gains of feedback controller
k2 = ku2/(2.2*f);
t1 = f*2*pi/(1.2*wu1); % Reset time fo controller
t2 = f*2*pi/(1.2*wu2);


y = logspace(-3,1,80);
for i =1:80
    x =y(i);
    c =[k1*(1+1/(j*x*t1)) 0; 0 k2*(1+1/(j*x*t2))]; % transfer function
for feedback controller
    g =[-1.49/(1+1.216*j*x) -1.1/(1+5.766*j*x); -5.43/(1+1.016*j*x)
7.04e-1/(1+4.333*j*x)];
    w(i) = -1+det(eye(2)+g*c);
    l(i) = 20*log10(abs(w(i)/(1+w(i))))
end
semilogx(y,l)
```

APPENDIX B

```
%Code for BANN modelling
clear all
load input_data.txt
load output_data.txt
plot(output_data(:,1),output_data(:,2))
  [sx,mex,stdx]=autosc(input_data(:,[2:5])); %calculates the mean,
standard deviation and scales the data but excludes the time
[sy,mey,stdy]=autosc(output_data(:,2));
  x = sx(:,[1:4]);
     y = sy(:,1);

rand('seed',0)
[xt,yt,xv,yv] = select(x,y,0.8);
[xtr,ytr,xts,yts]=select(xt,yt,0.7);
NNTWARN OFF

%STACKED NEURAL NETWORK
nm = 30;
 for i=1:nm
      av = bootsr([xt yt],i);
[xtr2,ytr2,xts2,yts2]=select(av(:,1:4),av(:,5),0.7);

ess = 1e30;

sse=[];

for nh=5:30;
  rand('seed',0)
  w1=0.2*(rand(nh,4)-0.5);
  b1=0.2*(rand(nh,1)-0.5);
  w2=0.2*(rand(1,nh)-0.5);
  b2=0.2*(rand(1,1)-0.5);

[w1,b1,w2,b2,tre,tse]=nntrlm(w1,b1,'logsig1',w2,b2,'purelin1',xtr2,ytr
2,xts2,yts2,[100;0.0001]);
   ytrp=simuff(xtr2',w1,b1,'logsig1',w2,b2,'purelin1')';
   ytsp=simuff(xts2',w1,b1,'logsig1',w2,b2,'purelin1')';
  yvp=simuff(xv',w1,b1,'logsig1',w2,b2,'purelin1')';
   ErrorPred=yvp-yv;
%   %sse2=[sse;(yv-yvp)'*(yv-yvp) ];
%
   sse=[sse;(ytr2-ytrp)'*(ytr2-ytrp) (yts2-ytsp)'*(yts2-ytsp) (yv-
yvp)'*(yv-yvp)];

 [ii1,ii2]=min(sse(:,2));
 nh=ii2+4;
   tse = sumsqr(yts2-simuff(xts2', w1,
b1,'logsig1',w2,b2,'purelin1')');
  if(tse < ess)
      ess=tse;
      ws1=w1;
      bs1=b1;
      ws2=w2;
      bs2=b2;
      is(i,1)=nh;
  end
end
 sw1(1:is(i,1)*6+1,i) = [reshape(ws1,is(i,1)*4,1);bs1;ws2';bs2];
  ytrp1(:,i) = simuff(xtr', ws1,bs1,'logsig1',ws2,bs2,'purelin1')';
  ytsp1(:,i) = simuff(xts', ws1,bs1,'logsig1',ws2,bs2,'purelin1')';
  yvp1(:,i) = simuff(xv', ws1,bs1,'logsig1',ws2,bs2,'purelin1')';
```

```
 end
ypln = mean(ytrp1')';
ytspln = mean(ytsp1')';
yvpln = mean(yvp1')';
sse1 = [sse; (ytr-ypln)'*(ytr-ypln) (yts-ytspln)'*(yts-ytspln) (yv-
yvpln)'*(yv-yvpln)];
sse2(i,1) = (ytr-ytrp1(:,i))'*(ytr-ytrp1(:,i)) ;
sse2(i,2) = (yts-ytsp1(:,i))'*(yts-ytsp1(:,i));
sse2(i,3) = (yv-yvp1(:,i))'*(yv-yvp1(:,i));
ypln_lp = ypln-1.96*std((ytrp1-ypln*ones(1,30))')';
ypln_up = ypln+1.96*std((ytrp1-ypln*ones(1,30))')';
ytspln_lp = ytspln-1.96*std((ytsp1-ytspln*ones(1,30))')';
ytspln_up = ytspln+1.96*std((ytsp1-ytspln*ones(1,30))')';
yvpln_lp = yvpln-1.96*std((yvp1-yvpln*ones(1,30))')';
yvpln_up = yvpln+1.96*std((yvp1-yvpln*ones(1,30))')';
sseb = [sse; (ytr-ypln)'*(ytr-ypln) (yts-ytspln)'*(yts-ytspln) (yv-
yvpln)'*(yv-yvpln)];
for i = 1:nm;
    mse(i,1) = (ytr-ytrp1(:,i))'*(ytr-ytrp1(:,i))/length(ytr);
    mse(i,2) = (yts-ytsp1(:,i))'*(yts-ytsp1(:,i))/length(yts);
    mse(i,3) = (yv-yvp1(:,i))'*(yv-yvp1(:,i))/length(yv);
    ytpp = mean(ytrp1(:,1:i)',1)';
    ytspp = mean(ytsp1(:,1:i)',1)';
    yvpp = mean(yvp1(:,1:i)',1)';
    mse(1,4) = (ytr-ytpp)'*(ytr-ytpp)/length(ytr);
     mse(1,5) = (yts-ytspp)'*(yts-ytspp)/length(yts);
    mse(1,6) = (yv-yvpp)'*(yv-yvpp)/length(yv);
end
save 'model_ref3b_newest2' sw1 is nm ws1 bs1 ws2 bs2 mex stdx mey
stdy ;
 figure
subplot(311)
plot(ytr,'-')
hold
plot(ytrp1,'r--','LineWidth',1)
title('Predicted and actual values for training')
 xlabel('Samples')
 ylabel('Exergy efficiency')
subplot(312)
plot(yts,'-')
hold
plot(ytsp1,'r--','LineWidth',1)
title('Predicted and actual values for testing')
 xlabel('Samples')
 ylabel('Exergy efficency')
subplot(313)
plot(yv,'-')
hold
plot(yvp1,'r--','LineWidth',1)
title('Predicted and actual values for validating')
 xlabel('Samples')
 ylabel('Exergy efficency')

 figure
 plot(ytr*stdy+mey, ypln*stdy+mey, 'b+')
 hold
plot(yts*stdy+mey, ytspln*stdy+mey, 'g--')
plot(yv*stdy+mey, yvpln*stdy+mey, 'ro')
xlabel('Actual energy efficiency')
ylabel('Predicted energy efficiency')
title('+:training data;--:testing data o:validation data')

figure
```

```
plot(yv*stdy+mey,'o')
hold
plot(yvpln*stdy+mey,'r+')
plot(yvpln_lp*stdy+mey,'g--')
plot(yvpln_up*stdy+mey,'g--')
xlabel('samples')
ylabel('Exergy efficiency')
title('o:actual values; +:predictions; --:95%confidence bounds')
%plot MSE of single networks
figure
subplot(311)
bar(mse(:,1))
ylabel('MSE(training)')
subplot(312)
bar(mse(:,2))
ylabel('MSE(testing)')
subplot(313)
bar(mse(:,3))
ylabel('MSE(Validation)')
xlabel('Network No')

%plot MSE of stacked networks
figure
subplot(311)
bar(mse(:,4))
ylabel('MSE(training)')
subplot(312)
bar(mse(:,5))
ylabel('MSE(testing)')
subplot(313)
bar(mse(:,6))
ylabel('MSE(Validation)')
xlabel('Network No')
```